

Investigation of Neurexin 2 as a Candidate for Parkinson's Disease

by
Katelyn Cuttler

*Dissertation presented for the degree Doctor of Philosophy in Science (Human
Genetics) in the Faculty of Medicine and Health Sciences at Stellenbosch*



University

Supervisor: Prof. Soraya Bardien
Co-Supervisor: Dr. Ruben Cloete
Co-Supervisor: Prof. Matthew Farrer

December 2022

Declaration

By submitting this dissertation electronically, I declare that the entirety of the work contained therein is my own, original work, that I am the sole author thereof (save to the extent explicitly otherwise stated), that reproduction and publication thereof by Stellenbosch University will not infringe any third-party rights and that I have not previously in its entirety or in part submitted it for obtaining any qualification.

This dissertation includes 2 original papers published in peer-reviewed journals, 2 submitted papers, and 1 unpublished (submission-ready) publication. The development and writing of the papers (published and unpublished) were the principal responsibility of myself and, for each of the cases where this is not the case, a declaration is included in the dissertation before each article indicating the nature and extent of the contributions of co-authors.

Signature:

Date: 28/09/2022

Abstract

Parkinson's disease (PD) is a neurodegenerative disorder which primarily affects movement and is characterized by the loss of dopaminergic neurons in the substantia nigra pars compacta (SNpc). There is no cure for the disorder and current drug treatments often have severe side effects. Several pathogenic variants have been implicated in PD, in various genes including *SNCA*, *LRRK2*, *PRKN*, and *PINK1*. However, these variants have mainly been found in individuals of European ancestry. In Sub-Saharan Africa (SSA), studies done on the genetic aetiology of PD have shown that these known pathogenic variants are only minor contributors to the aetiology. Since SSA is expected to face a surge in age-related disorders, such as PD, due to the gradual improvement in quality of life and increased life expectancy, it is important to study the disorder in these populations.

To this end, we have recruited individuals with PD from the South African population for genetic studies. One of the probands recruited had a family history of PD and also had several PD affected and unaffected family members. This family was designated ZA253. Therefore, we decided to perform whole exome sequencing on three of the affected individuals in an attempt to elucidate the genetic aetiology of their disorder. Variants that were novel or rare (MAF < 1%), non-synonymous, heterozygous, and shared amongst the three individuals were prioritised. These were found in the *CCNF*, *CFAP65*, *NRXN2*, *RTF1*, and *TEP1* genes. After screening unaffected members and ethnic-matched controls, as well as performing pathway and expression analysis and functional predictions of the effect of the variant on the translated protein, the p.G849D variant in *NRXN2* (neurexin 2) was prioritised for further study.

First, we performed molecular dynamic (MD) simulations after constructing a homologous model of the human NRXN2 α protein. These simulations showed that the variant had a destabilizing effect on the protein structure and resulted in an extended conformation of the laminin/neurexin/sex-hormone binding domain 6 (LNS6), which is responsible for binding to other proteins. Thereafter, we performed a literature search on the neurexin gene family to determine if they are good candidate genes for PD. We found that there is a well-established role of neurexins in neuropsychiatric disorders, such as autism spectrum disorders and schizophrenia, as well as evidence of a role for neurexins in neurodegenerative disorders, such as Alzheimer's disease and PD. Therefore, we concluded that *NRXN2* is a good candidate gene for further examination using functional studies.

Functional studies were then performed using a cDNA overexpression model in SH-SY5Y neuroblastoma cells to analyze the effect of the variant in an *in vitro* model of PD. First, we used assays to examine the effect of the mutant NRXN2 α protein on cell death, mitochondrial function, and reactive oxygen species (ROS) production. We found that overexpression of the mutant protein had a negative effect on all of these aspects and therefore concluded that the mutant NRXN2 α could induce a toxic feedback loop of mitochondrial dysfunction, increased ROS generation and increased neuronal cell death.

Consequently, we performed proteomics analysis on the same model to determine how overexpression of NRXN2 α affects cellular pathways. Interestingly, overexpression of the wild-type protein led to the enrichment of proteins involved in neurodegenerative pathways, providing preliminary evidence that NRXN2 α could be involved in these pathways. Overexpression of the mutant protein led to the decline in proteins involved in ribosomal functioning. Since NRXN2 α is a synaptic protein, it is possible that the variant affects synaptic translation. Indeed, dysregulated synaptic translation has been linked to altered mitochondrial physiology. Therefore, we hypothesized that dysregulated synaptic translation and mitochondrial dysfunction are linked and act together to result in neuronal death.

The last part of the study examined the effect of the variant on the synaptic function of NRXN2 α . We first used MD simulations to examine the variant's effect on the binding of NRXN2 α to a known binding partner, neuroligin 1 (NLGN1). In synapses, neurexins bind to neuroligins to facilitate synaptic transmission and maintenance. The results of the simulations suggest that the variant may be able to disrupt this interaction. Thereafter, we stained synaptic markers *in vitro*, in differentiated SH-SY5Y cells, to determine whether overexpression of the mutant protein affects synapse formation and synaptic transmission. We found an increase in the levels of both markers possibly indicating that there is increased synapse formation resulting in increased transmission between synapses. Since the MD simulations showed that the variant could disrupt neurexin-neuroligin signalling, we propose that this increase in transmission is a compensatory mechanism and suggest that, over time, this response would strain the synaptic maintenance systems and eventually lead to neurodegeneration.

In conclusion, our findings have indicated that a variant in NRXN2 α may be linked to mitochondrial and synaptic dysfunction that may eventually lead to neurodegeneration. However, further targeted experiments in other PD models are required in order to prove these findings. Nevertheless, it is important to look at the genetics of PD in understudied populations as this may lead to the discovery of new genes and disease mechanisms underlying this disorder. Therefore, studies such as these can help to shed light on this debilitating disorder.

Opsomming

Parkinson se siekte (PS) is 'n neurodegeneratiewe versteuring wat hoofsaaklik beweging beïnvloed en word gekenmerk deur die verlies van dopaminergiese neurone in die substantia nigra pars compacta (SNpc). Daar is geen geneesmiddel vir die siekte nie en huidige dwelmbehandelings het dikwels ernstige newe-effekte. Verskeie patogene variante is in PS geïmpliseer, in verskeie gene, waaronder *SNCA*, *LRRK2*, *PRKN* en *PINK1*. Hierdie variante is egter hoofsaaklik gevind in individue van Europese afkoms. In Afrika suid van die Sahara (SSA) het studies wat oor die genetiese etiologie van PS gedoen is, getoon dat hierdie bekende patogene variante slegs geringe bydraers tot die etiologie is. Aangesien SSA na verwagting 'n toename in ouderdomsverwante afwykings, soos PS, in die gesig staar as gevolg van die geleidelike verbetering in lewensgehalte en verhoogde lewensverwagting, is dit belangrik om die wanorde in hierdie bevolking te bestudeer.

Vir hierdie doel het ons individue met PS van die Suid-Afrikaanse bevolking gewerf vir genetiese studies. Een van die probande wat gewerf is, het 'n familiegeskiedenis van PS gehad en het ook verskeie PS geïmpasseerde en onaangeraakte familieledede gehad. Hierdie familie is as ZA253 aangewys. Daarom het ons besluit om volledige eksome volgordebepaling op drie van die geïmpasseerde individue uit te voer in 'n poging om die genetiese etiologie van hul wanorde te verduidelik. Variante wat nuut of skaars was (MAF < 1%), nie-sinoniem, heterosies en gedeel onder die drie individue is geprioritiseer. Dit is gevind in die *CCNF*, *CFAP65*, *NRXN2*, *RTF1* en *TEP1* gene. Na die sifting van onaangeraakte lede en etnies-ooreenstemmende kontroles, sowel as die uitvoering van pad- en uitdrukingsanalise en funksionele voorspellings van die effek van die variant op die vertaalde proteïene, is die p.G849D variant in *NRXN2* (neurexin 2) geprioritiseer vir verdere studie.

Eerstens het ons molekulêre dinamiese (MD) simulaties uitgevoer nadat ons 'n homoloë model van die menslike *NRXN2α* proteïen gebou het. Hierdie simulaties het getoon dat die variant 'n destabiliserende effek op die proteïenstruktuur gehad het en gelei het tot 'n uitgebreide konformasie van die laminin / neurexin / sex hormone bindende domein 6 (LNS6), wat verantwoordelik is vir die binding van ander proteïene. Daarna het ons 'n literatuursoektog op die neurexin-geenfamilie gedoen om vas te stel of dit goeie kandidaatgene vir PS is. Ons het bevind dat daar 'n gevestigde rol van neurexins in neuropsigiatriese afwykings is, soos outisme spektrumversteurings en skisofrenie, asook bewyse van 'n rol vir neurexins in neurodegeneratiewe afwykings, soos Alzheimer se siekte en PS. Daarom het ons tot die gevolgtrekking gekom dat *NRXN2* 'n goeie kandidaat is vir verdere ondersoek met behulp van funksionele studies.

Funksionele studies is dan uitgevoer met behulp van 'n cDNA oordrukingsmodel in SH-SY5Y neuroblastoma selle om die effek van die variant in 'n *in vitro* model van PD te analiseer. Eerstens het ons toetsings gebruik om die effek van die mutant *NRXN2α* proteïen op seldood, mitochondriale funksie en reaktiewe suurstofspesies (ROS) produksie te ondersoek. Ons het

bevind dat ooruitdrukking van die mutant proteïen 'n negatiewe uitwerking op al hierdie aspekte gehad het en daarom tot die gevolgtrekking gekom het dat die mutant NRXN2 α 'n giftige terugvoerlus van mitochondriale disfunksie, verhoogde ROS generasie en verhoogde neuronale seldood kan veroorsaak.

Gevolglik het ons proteomiese analise op dieselfde model uitgevoer om te bepaal hoe ooruitdrukking van NRXN2 α sellulêre paaie beïnvloed. Interessant genoeg, ooruitdrukking van die wilde-tipe proteïen het gelei tot die verryking van proteïene wat betrokke is by neurodegeneratiewe paaie, bied voorlopige bewyse dat NRXN2 α by hierdie paaie betrokke kan wees. Ooruitdrukking van die mutant proteïen het gelei tot die afname in proteïene wat betrokke is by ribosomale funksionering. Aangesien NRXN2 α 'n sinaptiese proteïen is, is dit moontlik dat die variant sinaptiese vertaling beïnvloed. Inderdaad, disreguleerde sinaptiese vertaling is gekoppel aan veranderde mitochondriale fisiologie. Daarom het ons veronderstel dat gedisreguleerde sinaptiese vertaling en mitochondriale disfunksie gekoppel is en saamwerk om neuronale dood tot gevolg te hê.

Die laaste deel van die studie het die effek van die variant op die sinaptiese funksie van NRXN2 α ondersoek. Ons het eers MD simulaties gebruik om die variant se effek op die binding van NRXN2 α aan 'n bekende bindende vennoot, neuroligin 1 (NLGN1) te ondersoek. In sinapse bind neurexins aan neuroligins om sinaptiese oordrag en instandhouding te vergemaklik. Die resultate van die simulaties dui daarop dat die variant hierdie interaksie kan ontwig. Daarna het ons sinaptiese merkers *in vitro*, in gedifferensieerde SH-SY5Y selle, gevlek om te bepaal of ooruitdrukking van die mutant proteïen sinapsevorming en sinaptiese oordrag beïnvloed. Ons het 'n toename in die vlakke van beide merkers gevind wat moontlik aandui dat daar verhoogde sinapsevorming is wat verhoogde oordrag tussen sinapse tot gevolg het. Aangesien die MD simulaties getoon het dat die variant neurexin-neuroligien sein kan ontwig, stel ons voor dat hierdie toename in oordrag 'n kompenserende meganisme is en stel voor dat hierdie reaksie mettertyd die sinaptiese instandhoudingstelsels sal spanning en uiteindelik tot neurodegenerasie sal lei.

Ten slotte het ons bevindings aangedui dat 'n variant in NRXN2 α gekoppel kan word aan mitochondriale en sinaptiese disfunksie wat uiteindelik tot neurodegenerasie kan lei. Verdere geteikende eksperimente in ander PD-modelle is egter nodig om hierdie bevindings te bewys. Nietemin is dit belangrik om na die genetica van PD in onderstudeerde bevolkings te kyk, aangesien dit kan lei tot die ontdekking van nuwe gene en siekteteganismes onderliggend aan hierdie versteuring. Daarom kan studies soos hierdie help om lig te werp op hierdie aftakelende versteuring.

Dedicated to my mother

Jean Lynch

1959-2017

Acknowledgements

This work is based on research supported in part by the **National Research Foundation of South Africa (NRF, Grant Numbers: 129249 and 146254)**, the **South African Medical Research Council (SAMRC)**, and the **Harry Crossley Foundation**. I would also like to acknowledge the **Stellenbosch University Postgraduate Scholarship Programme**, the **NRF**, the **Ernst & Ethel Eriksen Trust**, and the **Department of Biomedical Sciences** for their assistance with personal bursaries.

I would also like to acknowledge those individuals who contributed to this PhD and express my gratitude to them.

To my supervisor, **Prof. Soraya Bardien**, for being the best mentor I could ask for. Your kindness and understanding, as well as your willingness to push me have had a huge impact on my life. As I have expressed before, I hope to be like you when I grow up!

To my co-supervisor, **Dr. Ruben Cloete**, thank you for your patience in teaching someone with absolutely no bioinformatics experience. Because of you, I have learnt so much during this PhD. Thank you for always being willing to help and give feedback.

To my co-supervisor, **Prof. Matthew Farrer**, thank you for the whole exome sequencing that started this study and for all your insight.

Thank you, **Prof. Jonathan Carr**, for recruiting the family for this study and for all the other recruitment work you do.

A special thank you to all our **study participants**. The work we do would not be possible without you.

A special thank you to **Ms. Boiketlo Sebate** and **Ms. Maryam Hassan**. Thank you, Bibi, for allowing me to take your project so much further, and thank you, Maryam, for all the assistance. I would have been lost without you!

Thank you to all my **collaborators** for all your assistance. Thank you for working with me, helping me, and teaching me.

To all the members of the **PD Research Group**, thank you for all the laughs and support. You made the past three years so enjoyable. A special thank you to **Amica** and **Zuné** for always listening to my complaints and being great friends.

Thank you so much to my dad, **Mark Cuttler**. Thank you for allowing me to follow my dream and supporting me throughout. Thank you for listening to my problems and trying to offer solutions even though you have no idea what I do! And thank you for telling everyone (I mean everyone) how proud you are of me. You have no idea how much better it makes me feel about myself! You are the best!

A special thank you to my dogs, **Marty** and **Maya**, for all the support they did not even know they were giving! I love being your mom!

“And All’s well as ends Better!” – Gaffer Gamgee

The Lord of the Rings: The Return of the King (J.R.R. Tolkien)

Table of Contents

Declaration.....	i
Abstract.....	ii
Opsomming.....	iv
Acknowledgements	vii
Table of Contents	viii
List of Abbreviations	xii
List of Figures.....	xxii
List of Movies	xxvi
List of Tables	xxvii
Dissertation Outline	xxix
CHAPTER 1	1
Introduction.....	1
1.1 Parkinson’s Disease	1
1.1.1 Neuropathology of Parkinson’s Disease	2
1.1.2 Treatment of Parkinson’s Disease	3
1.2 Aetiology and Risk Factors for Parkinson’s Disease.....	4
1.2.1 Genetic Risk Factors	6
1.3 Parkinson’s Disease Genetic Studies in Sub-Saharan Africa	11
1.4 South African Parkinson’s Disease Study Collection.....	11
1.5 Family ZA253.....	12
1.6 The Neurexin Protein Family.....	13
1.6.1 Functions of Neurexins	15
1.6.2 NRXN2 α	15

1.7 The Present Study	16
1.7.1 The Problem Statement.....	16
1.7.2 Hypothesis.....	17
1.7.3 Aims and Objectives	17
CHAPTER 2.....	19
Overview of Methodology	19
CHAPTER 3.....	23
Identification of a Novel Variant	23
Published Article: Prioritization of candidate genes for a South African family with Parkinson’s disease using <i>in-silico</i> tools.....	23
Declarations	24
Supplementary Figures	47
Supplementary Tables.....	53
CHAPTER 4.....	58
Review of Neurexins in Neurodegenerative and Neuropsychiatric Disorders	58
Published Article: Emerging evidence implicating a role for neurexins in neurodegenerative and neuropsychiatric disorders	58
Declarations	59
CHAPTER 5.....	81
Functional Analysis of the <i>NRXN2</i> p.G849D Variant	81
Submitted Article: Neurexin 2 p.G849D variant, implicated in Parkinson’s disease, increases reactive oxygen species, and reduces cell viability and mitochondrial membrane potential in SH-SY5Y cells.....	81
Declarations	82
Supplementary Figures	110
Supplementary Methods	114

CHAPTER 6.....	117
Proteomics Analysis of the <i>NRXN2</i> p.G849D Variant	117
Submitted Article: Proteomics analysis of the p.G849D variant in neurexin 2 alpha may reveal insight into Parkinson’s disease pathobiology	117
Declarations	118
Supplementary Figures	135
Supplementary Methods	139
CHAPTER 7.....	143
Analysis of the Effect of the <i>NRXN2</i> p.G849D Variant on its Synaptic Function	143
Submission-Ready Article: p.G849D mutant neurexin 2 alpha disrupts the neurexin-neuroigin system <i>in silico</i> and synapse formation in SH-SY5Y cells.....	143
Declarations	144
Supplementary Figures	176
CHAPTER 8.....	179
Discussion and Conclusion	179
8.1 Identification of a Novel Variant in Neurexin 2	182
8.2 Toxic Feedback Loop Hypothesis	183
8.3 Dysregulation of Pathways	184
8.4 Interaction with Neuroigin.....	185
8.5 Dysregulation of Synaptic Function	186
8.6 Overall Hypothesis.....	187
8.7 Study Limitations.....	189
8.8 Future Work	190
8.9 Conclusion	191
References.....	192

Appendices.....	206
Appendix I: Standard Operating Procedures	206
Appendix II: Chapter 6 Supplementary Tables	243
Appendix III: American College of Medical Genetics (ACMG) Variant Characterization...	297
Appendix IV: Ethical Approvals	298

List of Abbreviations

°C:	Degrees Celsius
µg:	Microgram
µl:	Microlitre
µm:	Micrometre
µM:	Micromolar
2D:	Two-dimensional
3D:	Three-dimensional
6-OHDA:	6-hydroxydopamine
Aβ:	Amyloid beta
AAO:	Age at onset
AAV:	Adeno-associated virus
ACMG:	American College of Medical Genetics
ACP-RT PCR:	Annealing control primer reverse transcriptase PCR
ACTN3:	Actinin alpha 3
AD:	Alzheimer's disease
ADL:	Activities of Daily Living
ADNI:	Alzheimer's Disease Neuroimaging Initiative
AFDN:	Afadin
AGC:	Automatic gain control
AGRE:	Autism Genetic Resource Exchange
ALS:	Amyotrophic lateral sclerosis
AMPA4:	GluA4-containing glutamate
ANNOVAR:	Annotate variation
ANOVA:	Analysis of variance
AP2A1:	AP-2 complex subunit alpha-1
Arg:	Arginine
ARHGAP10:	Rho GTPase activating protein 10

Array-CGH:	Array Comparative Genomic Hybridization
ASD:	Autism spectrum disorder
Asn:	Asparagine
Asp:	Aspartic acid
ATP:	Adenine triphosphate
ATPD:	ATP synthase subunit delta, mitochondrial
BD:	Bipolar disorder
BLAST:	Basic Local Alignment Search Tool
BPD:	Borderline personality disorder
BSA:	Bovine serum albumin
BWA:	Burrows-Wheeler Aligner
Ca ²⁺ :	Calcium ion
CADD:	Combined Annotation Dependent Depletion
CAF:	Stellenbosch University Central Analytical Facilities
CASK:	Calmodulin-dependent serine protein kinase
CBDB:	Clinical Brain Disorders Branch
CBLN1:	Cerebellin 1
CCCP:	Carbonyl cyanide m-chlorophenyl hydrazone
CCNF:	Cyclin F
CDC27:	Cell division cycle protein 27
cDNA:	Complementary DNA
CFAP65:	Cilia and flagella associated protein 65
CFP:	Cyan fluorescent protein
CHARMM:	Chemistry at Harvard Macromolecular Mechanics
CHCHD2:	Coiled-coil-helix-coiled-coil-helix domain containing 2 protein
CHPC:	Centre for High Performance Computing
CIBERSAM:	Centro de Investigación Biomédica en Red de Salud Mental
cm:	Centimetre
CNS:	Central nervous system
CNV:	Copy number variation

CO ₂ :	Carbon dioxide
COMT:	Catechol O-methyltransferase
CSF:	Cerebrospinal fluid
CT:	Computerized tomography
Cy3:	Cyanine 3
D-PBS:	Dulbecco's phosphate buffered saline
DA:	Dopamine
DAG1:	Dystroglycan
DALYs:	Disability-adjusted life years
dbSNP:	Single Nucleotide Polymorphism database
DJ-1:	Deglycase 1
DLG4:	Discs large homologue 4
DMEM:	Dulbecco's Modified Eagle Medium
DMSO:	Dimethyl sulfoxide
DNM1L:	Dynamin-1-like protein
dNTP:	Deoxyribose nucleotide triphosphate
E. coli:	Escherichia coli
EAE:	Experimental autoimmune encephalomyelitis
EBI:	European Bioinformatics Institute
EDTA:	Ethylenediaminetetraacetic acid
EGF:	Epidermal growth factor
EIF4G1:	Eukaryotic translation initiation factor 4 gamma 1
ELISA:	Enzyme-linked immunosorbent assay
EMAS:	Epilepsy with myoclonic-atonic seizures
EMBL:	European Molecular Biology Laboratory
EV:	Empty vector
EXAC:	Exome Aggregation Consortium
FA:	Formic acid
FBS:	Foetal bovine serum
FBXO7:	F-box only protein 7

FDR:	False discovery rate
FES:	Free energy surface
FITC:	Fluorescein isothiocyanate
FTD:	Frontotemporal dementia
FTD-GWAS:	Frontotemporal dementia genome-wide association study
FUS:	RNA-binding protein FUS
g:	Gram
GaASP:	Gallium arsenide phosphide
GABA:	γ -Aminobutyric acid
GAPDH:	Glyceraldehyde-3-phosphate dehydrogenase
GATK:	Genome Analysis Toolkit
GBA:	Glucocerebrosidase
GEO:	Gene expression omnibus
Gln:	Glutamine
Glu:	Glutamic acid
GluR δ :	δ -type glutamate receptor
GMQE:	Global Mean Quality Estimation
gnomAD:	Genome Aggregation Database
GO:	Gene ontology
GRCh:	Genome Reference Consortium Human Build
GRCm:	Genome Reference Consortium Mouse Build
GROMACS:	Groningen Machine for Chemical Simulation
GWAS:	Genome-wide association study
H-bond:	Hydrogen bond
H ₂ O ₂ :	Hydrogen peroxide
HBSS:	Hank's Balanced Salt Solution
HCD:	Higher-energy C-trap dissociation
HD:	Huntington's disease
HEK-293:	Human embryonic kidney cells
hESC:	Human embryonic stem cell

HILIC:	Hydrophilic interaction chromatography
HIV:	Human immunodeficiency virus
HRM:	High resolution melt
HRP:	Horse radish peroxidase
HYPERGENES:	European Network for Genetic-Epidemiological Studies
IgG:	Immunoglobulin G
iN:	Induced neuron
iPSC:	Induced pluripotent stem cell
JC-1:	5,5',6,6'-tetrachloro-1,1',3,3'-tetraethylbenzimidazolylcarbocyanine iodide
K:	Kelvin
KEGG:	Kyoto Encyclopaedia of Genes and Genomes
kJ/mol:	Kilojoule per Mole
KO:	Knockout
l:	Litre
LB:	Luria Bertani
LC-MS/ MS:	Liquid chromatography mass spectrometry/ mass spectrometry
LC-SRM:	Liquid chromatography single reaction monitoring
L-DOPA:	Levodopa
LNS:	Laminin/neurexin/sex-hormone binding domain
LRP10:	Low density lipoprotein receptor related protein 10
LRRK2:	Leucine-rich repeat kinase 2
LRRTM:	Leucine-rich repeat transmembrane neuronal protein
MACF1:	Microtubule actin cross-linking factor 1
MAF:	Minor allele frequency
MAO-B:	Monoamine oxidase B
MAP:	Rush Memory and Aging Project
MAPP:	Multivariate Analysis of Protein Polymorphism
MCI:	Mild cognitive impairment
mCSM:	Mutation Cutoff Scanning Matrix
MD:	Molecular dynamic

mESC:	Mouse embryonic stem cell
MgCl ₂ :	Magnesium chloride
mGluR5:	Metabolic glutamate receptor 5
min:	Minute
miRNA:	MicroRNA
mg:	Milligram
ml:	Millilitre
mm:	Millimetre
mM:	Millimolar
MMP:	Mitochondrial membrane potential
MOCA:	Montreal Cognitive Assessment
MR:	Magnetic resonance
MRI:	Magnetic resonance imaging
mRNA:	Messenger RNA
MRPL4:	39S ribosomal protein L4, mitochondrial
MRPL43:	39S ribosomal protein L43, mitochondrial
MRPS34:	28S ribosomal protein S34, mitochondrial
MS:	Multiple sclerosis
mTLE:	Mesial temporal lobe epilepsy
MTT:	3-(4,5-dimethylthiazol-2-yl)-2,5-diphenyltetrazolium bromide
MUT:	Mutant
N/A:	Not applicable
N-Cadherin:	Neural cadherin
N-CAM:	Neural cell adhesion molecule
NaCl:	Sodium chloride
NADPH:	Nicotinamide adenine dinucleotide phosphate
NAG:	N-acetyl-D-glucosamine
NES:	Normalized enrichment score
NGS:	Next generation sequencing
NH ₄ HCO ₃ :	Ammonium bicarbonate

NIMH:	National Institute of Mental Health
NLGN:	Neuroigin
nm:	Nanometre
nM:	Nanomolar
NMDAR:	N-methyl-D-aspartate receptor
NPT:	Constant number of particles, pressure, and temperature
NPTX2:	Neuronal pentraxin 2
NRF:	National Research Foundation
NRXN:	Neurexin
ns:	Nanosecond
NT:	Non-transfected
NVT:	Constant number of particles, volume, and temperature
ODPB:	Pyruvate dehydrogenase E1 component subunit beta, mitochondrial
ONIND:	Other noninflammatory neurological disease
OR:	Odds ratio
PBD:	Protein databank
PBS:	Phosphate buffered saline
PC:	Principal component
PCA:	Principal component analysis
PCDH8:	Protocadherin-8
PCR:	Polymerase chain reaction
PD:	Parkinson's disease
PDZ:	PSD-95, DLG1, ZO-1 domain
PDZD2:	PDZ domain-containing protein 2
PE:	Phycoerythrin
PGM1:	Phosphoglucomutase-1
PHAX:	Phosphorylated adapter RNA export protein
PINK1:	PTEN induced kinase 1
PLP1:	Proteolipid protein 1
PNN:	Pinin

POU2FI:	POU class 1 homeobox 1
PP1B:	Serine/threonine-protein phosphatase PP1-beta catalytic subunit
PPMI:	Parkinson's Progression Markers Initiative
PRKN:	Parkin
PRP4:	U4/U6 small nuclear ribonucleoprotein Prp4
ps:	Picosecond
PSD-95:	Post-synaptic density protein 95
PSI-BLAST:	Position Specific Iterative BLAST
PSM:	Peptide-spectrum match
PUR9:	Bifunctional purine biosynthesis protein ATIC
PVDF:	Polyvinylidene fluoride
QCR:	Cytochrome b-c1 complex subunit
QMEAN:	Quantitative Model Energy Analysis
qRT-PCR:	Quantitative real-time PCR
RAP-PCR:	Reverse arbitrarily primed PCR
RBD:	REM Sleep Behaviour Disorder
RBMX:	RNA-binding motif protein, X chromosome
REM:	Rapid eye movement
Rg:	Radius of gyration
rMOG:	Rat myelin oligodendrocyte glycoprotein
RMSD:	Root mean square deviation
RMSF:	Root mean square fluctuation
ROS:	Reactive oxygen species
RPB2:	DNA-directed RNA polymerase II subunit RPB2
RPL8:	60S ribosomal protein L8
rpm:	Revolutions per minute
RPS6:	40S ribosomal protein S6
RPS21:	40S ribosomal protein S21
RPS25:	40S ribosomal protein S25
RRMS:	Relapsing remitting MS

RSLC:	Rapid separation liquid chromatography
RTF1:	Requiring fifty-three 1 protein
RT-PCR:	Reverse transcriptase PCR
SA:	South Africa
SALM:	Synaptic adhesion-like molecule
SAMRC:	South African Medical Research Council
SASA:	Solvent accessible surface area
SCZ:	Schizophrenia
SDCBP:	Syndecan binding protein
SDHB:	Succinate dehydrogenase [ubiquinone] iron-sulfur subunit, mitochondrial
SDS:	Sodium dodecylsulfate
SFM:	Serum-free media
SH3GL2:	SH3 domain-containing GRB2-like protein 2
SHANK:	SH3 and multiple ankyrin repeat domains protein
SH-SY5Y:	Neuroblastoma cells
SIFT:	Sorting Intolerant From Tolerant
SIPA1L1:	Signal-induced proliferation-associated 1-like protein 1
SMA:	Spinal muscular atrophy
SNCA:	α -synuclein
SNP:	Single nucleotide polymorphism
SNpc:	Substantia nigra pars compacta
SOP:	Standard Operating Procedure
SP:	Signal peptide
SPSY:	Spermine synthase
SSA:	Sub-Saharan Africa
SSC:	Simons Simplex Collection
STEP-BD:	Systematic Treatment Enhancement Program for Bipolar Disorder
STRING:	Search Tool for the Retrieval of Interacting Genes/ Proteins
synCAM:	Synaptic cell adhesion molecule
SYNJ1:	Synaptojanin 1

SYT13:	Synaptotagmin-13
TAFA1:	TAFA chemokine-like family member 1
TBS:	Tris-buffered saline
TBST:	Tris-buffered saline with 0.1% Tween-20
TCEP:	Tris(carboxyethyl) phosphine
TEP1:	Telomerase associated protein
TFA:	Trifluoroacetic acid
Thr:	Threonine
TM:	Transmembrane
TMEM30:	Transmembrane protein 30
tRNA:	Transfer RNA
TUBB6:	Tubulin beta 6 class V
TULP1:	TUBB-like protein 1
UK:	United Kingdom
UPDRS:	Unified Parkinson's Disease Rating Scale
UPS:	Ubiquitin-proteasome system
UTR:	Untranslated region
UV:	Ultraviolet
UV-CLIP:	Ultraviolet crosslinking and immunoprecipitation
V:	Volt
VMD:	Visual Molecular Dynamics
VPS13C:	Vacuolar protein sorting 13 homolog C
VPS35:	Vacuolar protein sorting ortholog 35
WebGestalt:	Web-based Gene Set Analysis Toolkit
WES:	Whole exome sequencing
WGS:	Whole genome sequencing
WT:	Wild-type
XKR4:	XK-related protein 4
XPO2:	Exportin-2

List of Figures

		Page No.
	Chapter 1	
Figure 1.1	The neuropathology of Parkinson's disease	2
Figure 1.2	Simplified schematic of the molecular mechanisms implicated in Parkinson's disease	5
Figure 1.3	Simplified pedigree of the South African family ZA253	13
Figure 1.4	Location and structure of neurexins	14
	Chapter 2	
Figure 2.1	Outline of the current PhD study	22
	Chapter 3	
Figure 1	Pedigree of the South African family ZA253	33
Figure 2	Swissmodel predicted 3-dimensional (3D) structure for human NRXN2 with mutation p.G849D (p.G889D) in complex with N-acetyl-D-glucosamine	37
Figure 3	Trajectory analysis of wild type (WT) NRXN2 and mutant (MUT) NRXN2, both with and without NAG	38
Figure 4	Two-dimensional (2D) projections of the first and second principal components for the WT NRXN2, MUT NRXN2 without NAG and WT NRXN2, MUT NRXN2 with NAG systems	39
Figure 5	Two-dimensional (2D) free energy landscapes plotted for NRXN2 along two order parameters root mean square deviation (RMSD) to average structure and Rg	40
Figure S1	Total energy of the four systems of NRXN2 (WT_noNAG, MUT_noNAG, WT_NAG and MUT_NAG) over 100 ns	47
Figure S2	Potential energy of the four systems of NRXN2 (WT_noNAG, MUT_noNAG, WT_NAG and MUT_NAG) over 100 ns	47
Figure S3	The average temperature of the four systems of NRXN2 (WT_noNAG, MUT_noNAG, WT_NAG and MUT_NAG) over 100 ns	48
Figure S4	2D interaction diagram showing polar contacts formed between NRXN2 residues and sugar moiety NAG	48
Figure S5	Total energy of the four systems of the repeat 1 of NRXN2 (WT_noNAG, MUT_noNAG, WT_NAG and MUT_NAG) over 100 ns	49

Figure S6	Potential energy of the four systems of repeat 1 of NRXN2 (WT_noNAG, MUT_noNAG, WT_NAG and MUT_NAG) over 100 ns	49
Figure S7	The average temperature of the four systems of repeat 1 NRXN2 (WT_noNAG, MUT_noNAG, WT_NAG and MUT_NAG) over 100 ns	50
Figure S8	RMSD deviation of the backbone atoms for the four systems of repeat 1 NRXN2	50
Figure S9	Total energy of the four systems of the repeat 2 of NRXN2 (WT_noNAG, MUT_noNAG, WT_NAG and MUT_NAG) over 100 ns	51
Figure S10	Potential energy of the four systems of repeat 2 of NRXN2 (WT_noNAG, MUT_noNAG, WT_NAG and MUT_NAG) over 100 ns	51
Figure S11	The average temperature of the four systems of repeat 2 NRXN2 (WT_noNAG, MUT_noNAG, WT_NAG and MUT_NAG) over 100 ns	52
Figure S12	RMSD deviation of the backbone atoms for the four systems of repeat 2 NRXN2	52
Chapter 4		
Figure 1	Location of neurexins and their binding partners, neuroligins, in the synapse	62
Figure 2	Structural domain organization of the α and β forms of neurexin	62
Figure 3	A summary of GO terms associated with neurexins 1–3	63
Figure 4	Protein interacting partners of neurexins 1–3	64
Chapter 5		
Figure 1	Overexpression of wild-type and mutant NRXN2 α in SH-SY5Y cells increases NRXN2 α protein levels	93
Figure 2	Overexpression of wild-type and mutant NRXN2 α in SH-SY5Y cells decreases metabolic activity and cell viability	95
Figure 3	Overexpression of wild-type and mutant NRXN2 α in SH-SY5Y cells decreases mitochondrial membrane potential (MMP)	97
Figure 4	Overexpression of wild-type and mutant NRXN2 α in SH-SY5Y cells induces ROS	99
Figure S1	Generation of the p.D882 mutant construct	110
Figure S2	Transfection efficiency examined by CFP fluorescence in SH-SY5Y cells	111

Figure S3	Caspase 8 and 9 levels in wild-type and mutant NRXN2 α overexpressing SH-SY5Y cells	112
Figure S4	Mitochondrial network analysis of wild-type and mutant NRXN2 α overexpressing SH-SY5Y cells	113
Chapter 6		
Figure 1	Differentially abundant proteins present when comparing several treatment groups to each other	126
Figure S1	Overexpression of wild-type and mutant NRXN2 α in SH-SY5Y cells increases NRXN2 α protein levels	135
Figure S2	Scatterplot of the standard deviation (log ₁₀) vs mean (log ₁₀) shows good clustering of all samples along the linear regression line	136
Figure S3	Venn diagram of the total proteins identified in each treatment group shows the distribution of shared proteins and numbers of proteins unique to each group	136
Figure S4	Gene set enrichment analysis performed using WebGestalt (http://www.webgestalt.org)	137
Figure S5	Normalized expression scores obtained from WebGestalt (http://www.webgestalt.org) for the GO term “ribosome” in each analysis.	138
Chapter 7		
Figure 1	The 3D structure predicted for NRXN2 α in complex with NLGN1	154
Figure 2	Trajectory analysis of WT and MUT systems for the total protein	156
Figure 3	Trajectory analysis of WT and MUT systems for the NRXN2 α LNS6 domain and NLGN1	158
Figure 4	Two-dimensional (2D) projections of the first and second principal components for the WT and MUT systems	160
Figure 5	Free Energy Surface (FES) analysis of the WT and MUT systems	161
Figure 6	Representative images of SH-SY5Y cells show successful differentiation after 7 days in the differentiation medium	163
Figure 7	Overexpression of wild-type and mutant NRXN2 α in differentiated SH-SY5Y cells increases synapsin I and PSD-95 levels	165
Figure S1	Thermodynamic and kinetic properties of the WT and MUT systems over the 200 ns simulation	176
Figure S2	Thermodynamic and kinetic properties of the WT and MUT systems (repeat 1) over the 200 ns simulation	177
Figure S3	Thermodynamic and kinetic properties of the WT and MUT systems (repeat 2) over the 200 ns simulation	178

	Chapter 8	
Figure 8.1	Schematic diagram summarizing the different parts of the doctoral study and the main findings	180
Figure 8.2	Proposed schema of how the p.G849D variant in <i>NRXN2</i> can lead to Parkinson's disease	188

List of Movies

		Page No.	URL
	Chapter 3		
Movie S1	Change in secondary structure simulation movie for wild-type NRNX2 noNAG last 50ns	39	URL
Movie S2	Change in secondary structure simulation movie for mutant NRNX2 noNAG last 50ns.	39	URL
	Chapter 7		
Movie S1	Change in secondary structure simulation movie for wild-type NRXN2 LNS6 domain-NLGN1 last 10ns	157	URL
Movie S2	Change in secondary structure simulation movie for mutant NRXN2 LNS6 domain-NLGN1 last 10ns	157	URL

List of Tables

		Page No.
	Chapter 1	
Table 1.1	Main functions of the genes conclusively implicated in Parkinson's disease	7
	Chapter 3	
Table 1	Rare and novel exonic missense variants shared between the three affected individuals after variant filtering	34
Table 2	<i>In-silico</i> functional tool scores and predictions for the five variants validated with Sanger sequencing	34
Table S1	Clinical and demographic information on members of South African family ZA253 with Parkinson's disease	53
Table S2	Summary of whole exome sequencing metrics in the three affected individuals	57
	Chapter 4	
Table 1	List of studies that have implicated neurexin genes in neuropsychiatric disorders	66
Table 2	List of studies that have implicated neurexin genes in neurodegenerative disorders and ageing	71
	Chapter 5	
Table 1	Primer sequences used to generate the novel <i>NRXN2</i> p.D889 construct	88
Table 2	Transfection of SH-SY5Y cells with Lipofectamine3000 transfection reagent	89
Table S1	Antibodies used for this study	115
	Chapter 6	
Table 1	Enrichment terms obtained from the STRING online tool for the unique proteins in each treatment group	125
Table 2	The number of differentially abundant proteins found for each comparison	125
Table 3	Enrichment terms obtained from the KEGG and STRING online tools for each protein set	127
Table S1	List of unique proteins in wild-type transfected cells	243
Table S2	List of unique proteins in mutant transfected cells	246
Table S3	List of unique proteins in non-transfected cells	254
Table S4	List of unique proteins in empty vector transfected cells	259

Table S5	List of proteins differentially abundant between wild-type transfected and non-transfected cells	263
Table S6	List of proteins differentially abundant between mutant transfected and non-transfected cells	274
Table S7	List of proteins differentially abundant between mutant transfected and wild-type transfected cells	285
Table S8	List of proteins differentially abundant between empty vector transfected and non-transfected cells	291
 Chapter 7		
Table 1	Antibodies used for confocal microscopy	153
Table 2	Residues potentially involved in hydrogen bonding between NLGN1 and the LNS6 domain of NRXN2 α	155

Dissertation Outline

This dissertation is presented in 8 Chapters that include a general introduction section, an overview of the methodology section, a published research article, a published review article, three submission-ready articles, and an overall discussion section. This constitutes a “hybrid” dissertation format, which is an acceptable format at Stellenbosch University.

Chapter 1 is the Introduction which briefly introduces Parkinson’s disease (PD), gives an overview of PD genetic research in Sub-Saharan Africa (SSA) and introduces the candidate gene and its transcribed protein discovered during the course of this study. It also highlights the knowledge gap the study aimed to address and the novelty of the study.

Chapter 2 is an Overview of the Methodology used throughout the study. It highlights the main methods used for each of the subsequent chapters.

Chapter 3 consists of a published article that reports on a novel genetic variant in the gene *NRXN2* that may be implicated in PD.

Chapter 4 consists of a published review article that provides further evidence that the neurexin gene and protein family may be implicated in neuropsychiatric and neurodegenerative disorders.

Chapter 5 consists of an article currently under review with the Journal of Neural Transmission. It describes functional work done to determine the effect of the variant in a cell culture model of PD.

Chapter 6 consists of an article currently under review with Frontiers in Aging Neuroscience that reports on the proteomics analysis of the effect of the variant in a cell culture model of PD.

Chapter 7 is a submission-ready manuscript that reports on the effect of the variant on its synaptic functioning.

Chapter 8 is the overall Discussion chapter which brings all the sections together. It summarizes the PhD study, highlights the limitations and strengths of the study, provides recommendations for future studies, and draws a final conclusion of the study.

References for the published articles (Chapters 3 and 4), the submitted articles (Chapter 5 and 6), as well as the submission-ready article (Chapter 7) follow directly after the chapter in the format required by the respective journals. All other references used in this dissertation are included in the **References** section.

British English is used throughout this dissertation, except in Chapters 3 and 7, whereby American English was required by the publisher.

CHAPTER 1

Introduction

1.1 Parkinson's Disease

Parkinson's disease (PD) is the most common neurodegenerative disorder of movement and the second most common neurodegenerative disorder after Alzheimer's disease (AD). It affects 1 – 2% of the global population over the age of 65 (Antony et al., 2013). However, the prevalence of PD has increased by 118% between 1990 and 2015, and it is the fastest growing neurological disorder globally (Feigin et al., 2017), affecting over 6 million people (Dorsey et al., 2018). Indeed, Feigin et al., (2017) found that PD was the only neurological disorder with increasing age-standardised rates of deaths, prevalence, and disability-adjusted life years (DALYs) between 1990 and 2015, while all other neurological disorders examined showed overall decreases. The disorder does not have a cure and only limited treatments are available.

The disease was named after Dr. James Parkinson, a British surgeon who was the first one to clearly describe the disorder and its cardinal symptoms in his 1817 treatise, “An Essay on the Shaking Palsy” (Parkinson, 2002). However, PD-like symptoms have been recorded as far back as 2500 years ago in ancient Indian and Chinese medical literature (Zhang et al., 2006; Ovallath and Deepa, 2013).

The classic symptoms of PD as described by Dr. Parkinson are resting tremor, rigidity, bradykinesia, and postural instability (Jankovic, 2008). Additionally, other motor symptoms are common in PD, such as speech disturbances, problems with swallowing, problems showing facial expressions, and involuntary muscle contractions (Mazzoni et al., 2012). There are also multiple non-motor symptoms present in PD, the most common of which include constipation and other gut problems, sleep disturbances, impaired olfaction, and neuropsychiatric dysfunction (e.g. apathy, depression, anxiety, hallucinations) (Poewe, 2008; Bernal-Pacheco et al., 2012). These non-motor symptoms severely impact the quality of life for those with PD and in some cases can have more of a detrimental effect than the motor symptoms (Gökçal et al., 2017).

1.1.1 Neuropathology of Parkinson's Disease

There are two neuropathological hallmarks of PD. The first is the loss of the dopamine (DA) producing neurons of the substantia nigra pars compacta (SNpc) (**Figure 1.1**), and the second is the aggregation of misfolded α -synuclein into cytoplasmic inclusions called Lewy bodies (Dauer and Przedborski, 2003).

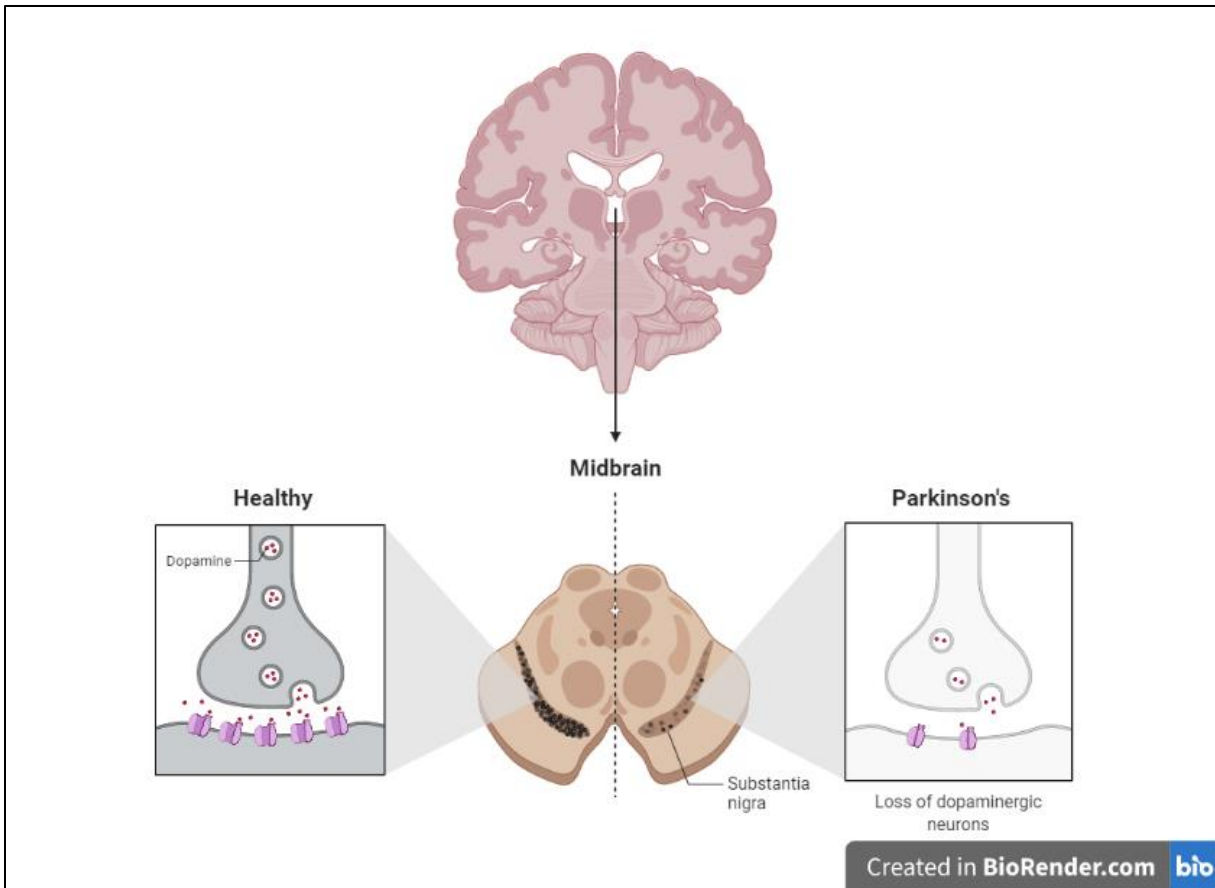


Figure 1.1: The neuropathology of Parkinson's disease. Cross sections of the substantia nigra in the midbrain of healthy individuals and individuals with PD. The brains of healthy individuals are rich in the pigmented dopaminergic neurons and dopaminergic signalling functions normally. Individuals with PD have a loss of pigmented dopaminergic neurons and decreased dopaminergic signalling. (Image created in BioRender.com)

The SNpc is a component of the midbrain and forms part of the basal ganglia (**Figure 1.1**). The DA neurons in the SNpc are involved in the nigrostriatal pathway which helps control voluntary and involuntary movements (Galvan and Wichmann, 2008). Briefly, the nigrostriatal pathway is able to excite the direct pathway to facilitate voluntary movements and is able to inhibit the indirect pathway to stop unwanted involuntary movements (Galvan and Wichmann, 2008). Therefore, the progressive loss of these neurons is what gives rise to the motor symptoms observed in PD.

However, the non-motor symptoms observed in PD are also caused by neuronal loss (Lim et al., 2009). Several other peripheral and central neuronal populations are also lost in PD (Grosch et al., 2016) as they are physiologically similar to the DA neurons of the SNpc (Sulzer and Surmeier, 2013). These include neurons in the dorsal motor nucleus of the vagus, the pedunculopontine nuclei, the medullary reticular formation, the locus ceruleus, the raphe nuclei, and to a lesser extent, the retrorubral area and the ventral tegmental area of the brainstem (Sulzer and Surmeier, 2013). These neurons have also been shown to degenerate and give rise to the non-motor symptoms of PD (Lim et al., 2009).

1.1.2 Treatment of Parkinson's Disease

The available therapies for PD are palliative in nature since they only focus on treating the symptoms of the disorder. Therefore, the basis of most PD therapies is replacing the lost DA (Connolly and Lang, 2014). This is achieved by administering the DA precursor, Levodopa (L-3,4-dihydroxyphenylalanine; L-DOPA) and/or DA agonists (Connolly and Lang, 2014).

L-DOPA is a precursor to DA in the DA-producing pathway; therefore, its administration increases the amount of DA present in the brain. DA agonists mimic the action of DA by binding to and activating DA receptors, allowing for better functioning of the nigrostriatal pathway. They are more commonly used to treat the symptoms in early disease. Most therapies for PD, however, are adjuncts in order to improve their effectiveness and limit their side effects. For instance, DA agonists and L-DOPA can be used in conjunction. L-DOPA is also generally coupled with a peripheral DOPA decarboxylase inhibitor and may also be coupled with monoamine oxidase B

(MAO-B) and catechol O-methyltransferase (COMT) inhibitors. MAO-B and COMT metabolize DA in the brain, so inhibiting them can improve the efficiency of the treatment (Finberg, 2019).

Surgical treatments are also another option. Deep brain stimulation and targeted brain lesions can be used when the pharmacological interventions are ineffective. However surgical treatments are very expensive and only effective for a select group of individuals (Mitchell and Ostrem, 2020). Unfortunately, physicians cannot yet accurately predict which individuals will benefit from surgical interventions (Mitchell and Ostrem, 2020).

There are also multiple therapies for the non-motor symptoms of PD. Antipsychotics and antidepressants can be used to treat the neuropsychiatric symptoms, while cholinesterase inhibitors can be used for PD patients with dementia (Connolly and Lang, 2014; Seppi et al., 2019; Armstrong and Okun, 2020). Medication is also available to assist with gut problems and sleep disturbances (Seppi et al., 2019).

Many of the therapies for PD patients have severe side effects (Suchowersky, 2002). Additionally, as PD progresses these medications become less effective and can, in some cases, exacerbate PD symptoms, particularly the dyskinesia (Suchowersky, 2002; Connolly and Lang, 2014). Therefore, there is an urgent need for more effective, non-palliative therapies with fewer side effects.

1.2 Aetiology and Risk Factors for Parkinson's Disease

PD is a complex disorder that can present as either sporadic or familial PD. Sporadic forms constitute up to 90% of the cases (Yasuda and Mochizuki, 2010), whereas only approximately 10% of patients report a positive family history (Klein and Westenberger, 2012). In sporadic PD, ~90 associated loci have been implicated through genome-wide association studies (GWAS) (Blauwendraat et al., 2019). These polymorphisms contribute only marginally to disease susceptibility (odds ratios (ORs) <1.5, with the majority <1.1).

Sporadic PD is thought to result from the complex interplay of genetic factors, environmental toxins and oxidative stress, which ultimately results in the loss of neurons (Lesage and Brice, 2009). There are several mechanisms believed to be involved in the development of sporadic PD

and these include the aggregation of abnormal protein (Langston, 2006), damage to cellular membranes, mitochondrial dysfunction (Winklhofer and Haass, 2010), impaired transportation in neural synaptic clefts (Belin and Westerlund, 2008), and apoptosis (Perier et al., 2011). Environmental risk factors such as exposure to pesticides, old age and male gender also play important roles in the development of sporadic PD (Di Monte et al., 2002).

Variants consistent with a Mendelian pattern of inheritance are rare and globally account for <1% PD. In total, there are ~30-40 genes ‘linked’ to disease (in genes such as *LRRK2* and *SNCA*), with mutant alleles of major effect (ORs >10) (Lill, 2016; Puschmann, 2017). Currently, the aetiology of familial PD is still better understood than sporadic PD, and has provided clues to the molecular pathogenesis of the disorder (Klein and Westenberger, 2012). A summary of these pathways is shown in **Figure 1.2**.

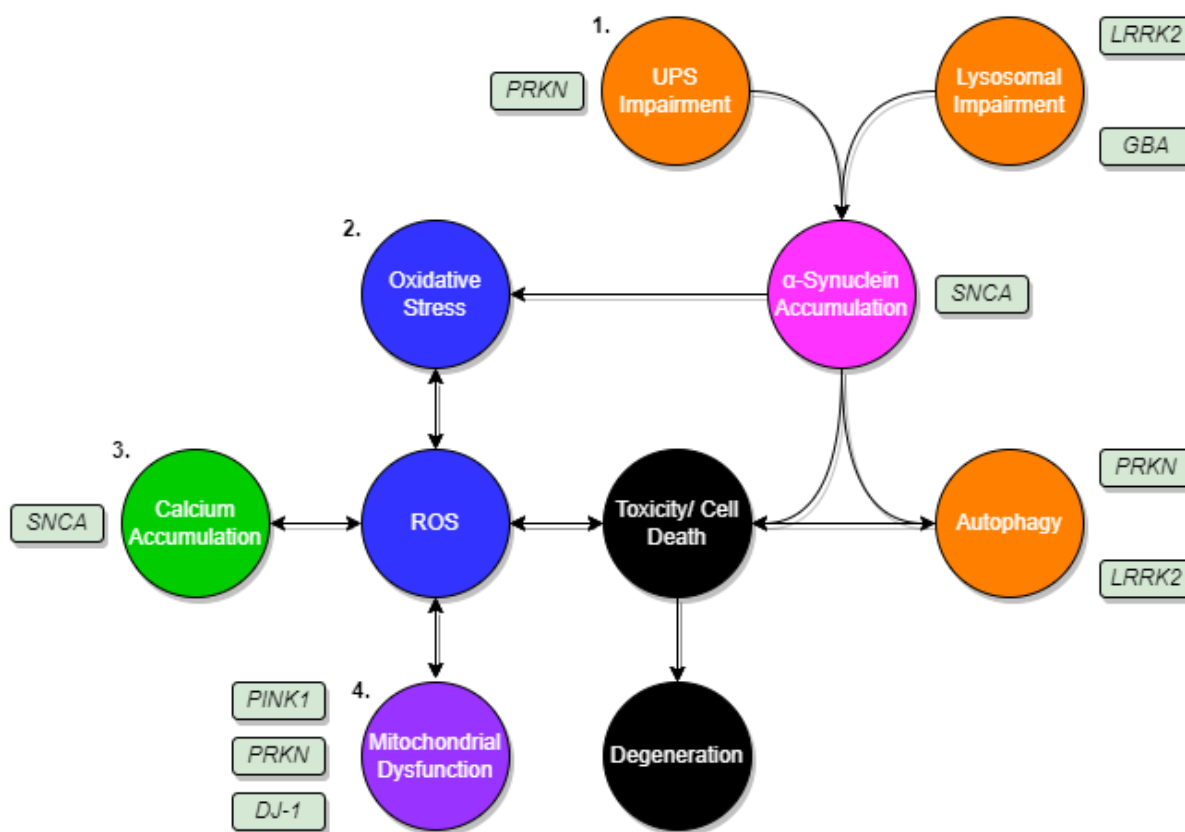


Figure 1.2: Simplified schematic of the molecular mechanisms implicated in Parkinson's disease. 1) dysregulated proteolysis (UPS, lysosome, and autophagy), 2) oxidative stress, 3) calcium accumulation, 4) mitochondrial dysfunction. Gene symbols shown in light green boxes

next to a process represent known PD-associated genes that are involved in that particular process. Abbreviations: UPS: ubiquitin-proteasome system. (Image created in draw.io)

In addition, the main functions of the genes conclusively implicated in PD, obtained from UniProt (<https://www.uniprot.org>) (The UniProt Consortium, 2021), are shown in **Table 1.1**.

1.2.1 Genetic Risk Factors

Research on the genetic aetiology of PD has led to the discovery of “established” PD genes with variants that are proven to be pathogenic. These include *SNCA*, *PRKN*, *PINK1*, *DJ-1*, *EIF4G1*, and *VPS35* (**Table 1.1**) (Lill, 2016; Puschmann, 2017). Autosomal dominant PD genes usually result in typical late-onset PD, while autosomal recessive genes generally result in early disease onset (≤ 50 years).

More recently, next generation sequencing (NGS) technologies have contributed to the discovery of novel genes in large multiplex families, such as *VPS35* (Vilariño-Güell et al., 2011; Zimprich et al., 2011), *CHCHD2* (Funayama et al., 2015), *VPS13C* (Lesage et al., 2016), *TMEM230* (Deng et al., 2016) and *LRP10* (Quadri et al., 2018), as reviewed in (Pillay et al., 2022). Therefore, NGS approaches have advanced the global understanding of the genetics of PD.

Table 1.1: Main functions of the genes conclusively implicated in Parkinson's disease

Gene Symbol	Original Reference	Main Function	Gene Ontology (GO) Terms	
			Molecular Function:	Biological Process:
Autosomal Dominant				
<i>EIF4G1</i>	(Chartier-Harlin et al., 2011)	Component of the protein complex eIF4F, which is involved in the recognition of the mRNA cap, ATP-dependent unwinding of 5'-terminal secondary structure and recruitment of mRNA to the ribosome.	<ul style="list-style-type: none"> • initiation factor • RNA-binding • translational shunt 	<ul style="list-style-type: none"> • host-virus interaction • protein biosynthesis • translation regulation
<i>GBA</i>	(Sidransky et al., 2009)	Glucosylceramidase that catalyses, within the lysosomal compartment, the hydrolysis of glucosylceramide/GlcCer into free ceramide and glucose	<ul style="list-style-type: none"> • glycosidase • glycosyltransferase • hydrolase • transferase 	<ul style="list-style-type: none"> • cholesterol metabolism • lipid metabolism • sphingolipid metabolism • steroid metabolism • sterol metabolism
<i>LRP10</i>	(Quadri et al., 2018)	Probable receptor, which is involved in the internalization of lipophilic molecules and/or signal transduction.	<ul style="list-style-type: none"> • receptor 	<ul style="list-style-type: none"> • endocytosis
<i>LRRK2</i>	(Zimprich et al., 2004)	Serine/threonine-protein kinase which phosphorylates a broad range of proteins involved in multiple processes	<ul style="list-style-type: none"> • GTPase activation • hydrolase • kinase 	<ul style="list-style-type: none"> • autophagy • differentiation

		such as neuronal plasticity, autophagy, and vesicle trafficking.	<ul style="list-style-type: none"> • serine/ threonine protein kinase • transferase 	
<i>SNCA</i>	(Polymeropoulos et al., 1997)	Neuronal protein that plays several roles in synaptic activity such as regulation of synaptic vesicle trafficking and subsequent neurotransmitter release.	<ul style="list-style-type: none"> • ion binding • metal binding • protein binding • synaptic vesicle trafficking 	<ul style="list-style-type: none"> • acyl-CoA biosynthesis • dopamine biosynthesis • long-term neuronal synaptic plasticity • long-term synaptic potentiation
<i>VPS35</i>	(Vilariño-Güell et al., 2011)	Acts as component of the retromer cargo-selective complex (CSC). The CSC is believed to be the core functional component of retromer or respective retromer complex variants acting to prevent missorting of selected transmembrane cargo proteins into the lysosomal degradation pathway.	<ul style="list-style-type: none"> • dopamine receptor binding 	<ul style="list-style-type: none"> • host-virus interaction • protein transport • transport
Autosomal Recessive				
<i>DJ-1</i>	(Bonifati et al., 2003)	Multifunctional protein which plays an important role in cell protection against oxidative stress and cell death acting as	<ul style="list-style-type: none"> • Chaperone • hydrolase • protease 	<ul style="list-style-type: none"> • autophagy • DNA damage • DNA repair

		oxidative stress sensor and redox-sensitive chaperone and protease.	<ul style="list-style-type: none"> • RNA-binding 	<ul style="list-style-type: none"> • fertilization • inflammatory response • stress response
<i>FBXO7</i>	(Fonzo et al., 2009)	Substrate recognition component of a SCF (SKP1-CUL1-F-box protein) E3 ubiquitin-protein ligase complex which mediates the ubiquitination and subsequent proteasomal degradation of target proteins. Plays a role downstream of PINK1 in the clearance of damaged mitochondria via selective autophagy (mitophagy) by targeting PRKN to dysfunctional depolarized mitochondria.	<ul style="list-style-type: none"> • protein kinase binding • ubiquitin binding 	<ul style="list-style-type: none"> • ubiquitin-ligase conjugation pathway
<i>PINK1</i>	(Valente et al., 2004)	Serine/threonine-protein kinase which protects against mitochondrial dysfunction during cellular stress by phosphorylating mitochondrial proteins such as PRKN and DNMI1L, to coordinate mitochondrial quality control mechanisms that remove and	<ul style="list-style-type: none"> • kinase • serine/ threonine-protein kinase • transferase 	<ul style="list-style-type: none"> • autophagy

		replace dysfunctional mitochondrial components.		
<i>PRKN</i>	(Kitada et al., 1998)	Functions within a multiprotein E3 ubiquitin ligase complex, catalysing the covalent attachment of ubiquitin moieties onto substrate proteins.	<ul style="list-style-type: none"> • transferase 	<ul style="list-style-type: none"> • autophagy • transcription • transcription regulation • ubiquitin-ligase conjugation pathway
<i>SYNJ1</i>	(Krebs et al., 2013)	Phosphatase that acts on various phosphoinositides, including phosphatidylinositol 4-phosphate, phosphatidylinositol (4,5)-bisphosphate and phosphatidylinositol (3,4,5)-trisphosphate.	<ul style="list-style-type: none"> • hydrolase • RNA binding 	<ul style="list-style-type: none"> • endocytosis • lipid metabolism

Functional and gene ontology information was obtained from UniProt (<https://www.uniprot.org>) (The UniProt Consortium, 2021).

Abbreviations: DJ-1: deglycase 1; DNM1L: dynamin-1-like protein; EIF4G1:eukaryotic translation initiation factor 4 gamma 1; FBXO7: F-box only protein 7; GBA: glucocerebrosidase; GO: gene ontology; LRP10: low density lipoprotein receptor related protein 10; LRRK2: leucine-rich repeat kinase 2; PINK1: PTEN induced kinase 1; PRKN: parkin; SNCA: α -synuclein; SYNJ1: synaptojanin 1; VPS35: vacuolar protein sorting ortholog 35

1.3 Parkinson's Disease Genetic Studies in Sub-Saharan Africa

While the prevalence of PD in Sub-Saharan Africa (SSA) has been reported to be low ranging from 7/100 000 in Ethiopia to 67/100 000 in Nigeria (Williams et al., 2018), SSA is expected to face a future surge in age-related disorders, including PD, due to the gradual improvement in quality of life and increased life expectancy (Velkoff and Kowal, 2006; Lekoubou et al., 2014; Bower, 2017). Therefore, it is important to better understand the aetiology of PD in SSA including the genetic factors, in order to manage this impending health care burden.

However, in contrast to the global advances in the understanding of PD genetics, studies in SSA populations are scarce (Schumacher-Schuh et al., 2022). Most genetic PD research in this region is conducted in South Africa and has involved the screening of known candidate genes (Dekker et al., 2020). These, and other studies, have shown that known PD mutations appear to be only minor contributors to the aetiology of PD in SSA populations (Okubadejo et al., 2008; Bardien et al., 2009, 2010; Keyser et al., 2009, 2010; Cilia et al., 2012; Yonova-Doing et al., 2012; Blanckenberg et al., 2013, 2014; van der Merwe et al., 2016). Therefore, there is an urgent need to bridge the knowledge gap on the genetics of PD in SSA populations.

1.4 South African Parkinson's Disease Study Collection

As a step towards helping to bridge this knowledge gap, our research group is recruiting individuals with PD from the South African (SA) population for genetic studies. We recruited 687 unrelated individuals from different ancestral groups across SA. A summary of this study collection is provided in Jansen van Rensburg et al., (2022). The ancestral breakdown is as follows: European (30%), Afrikaner European (28.1%), Mixed (26.2%), African (14.8%), and Indian (0.9%). We found that more men had PD than women, similar to global studies on PD. Interestingly, we also found that Afrikaner Europeans had more cases of early onset PD compared to the other ancestral groups.

One of our Afrikaner European probands has a family history of PD and we were able to recruit other family members for further studies. This family was the two hundred and fifty third family to be recruited and is denoted as ZA253. This family, and the whole exome sequencing (WES) approach used in an attempt to identify a possible novel PD-causing genes, forms the basis of the present study.

1.5 Family ZA253

The complete pedigree of family ZA253, contains 57 individuals, and in total, eight members were reported to have PD. Five individuals affected with PD and four unaffected family members consented to be recruited for this study. A simplified version of the pedigree indicating the family members who took part in this study is shown in **Figure 1.3**. The patient labelled as individual III-8 (proband) was the first individual to be diagnosed with PD and his age at onset (AAO) was 48 years. His siblings were subsequently assessed, and his brother (III-7) was also confirmed as having PD, with an AAO of 42 years. Patient IV-2, the nephew of the two affected siblings, was diagnosed with early-onset PD at the age of 37 years. Individual III-6 was diagnosed with mild generalized bradykinesia at age 70. Individual III-2 was the most recent individual in the family to be diagnosed with PD, in 2017. However, she presented as typical idiopathic PD, with AAO of 75 years. Further clinical information on these family members is present in **Chapter 3** of this dissertation.

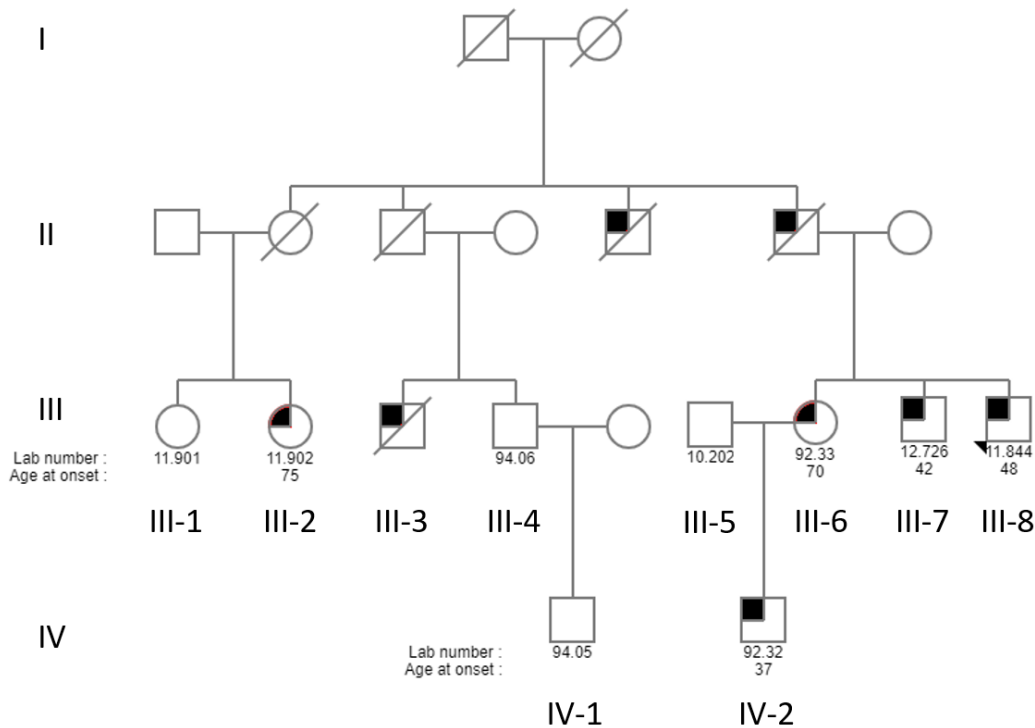


Figure 1.3. Simplified pedigree of the South African family ZA253. Circles denote females and squares depict males. The filled in symbols indicate affected individuals. A diagonal line indicates that the person is deceased, and the arrow indicates the proband. The numbers below each individual represent the laboratory ID number and the age at onset. (Image obtained from Sebate, Cuttler et al., 2021))

1.6 The Neurexin Protein Family

Since a variant in the neurexin 2 (*NRXN2*) gene was identified in our study, a brief overview of this protein family will be provided. Neurexins (*NRXNs*) are a family of highly polymorphic transmembrane proteins that are highly expressed in the brain (Schreiner et al., 2014, 2015). They were first identified as calcium-dependent α -latrotoxins present at the synapse (Ushkaryov et al., 1992). Thousands of isoforms of the three neurexin genes (*NRXN 1*, *2* and *3*) can be generated since each gene has multiple promoters and alternative splicing is common (Missler and Südhof, 1998). Though these isoforms co-express, they each have different mRNA sequences and are

therefore differentially expressed in different brain regions according to their specific function (Ullrich et al., 1995; Schreiner et al., 2014, 2015).

An α and β transcript is produced by each *NRXN* gene (**Figure 1.4**). The α forms are composed of six large extracellular laminin/neurexin/sex-hormone binding (LNS) globulin domains with three interspersed epidermal growth factor (EGF)-like regions. The β forms are shorter and only have the sixth extracellular LNS domain and no EGF-like regions (Missler and Südhof, 1998; Rudenko et al., 1999, 2001). Intracellularly, all neurexins contain a transmembrane region, carboxy terminus and short tail.

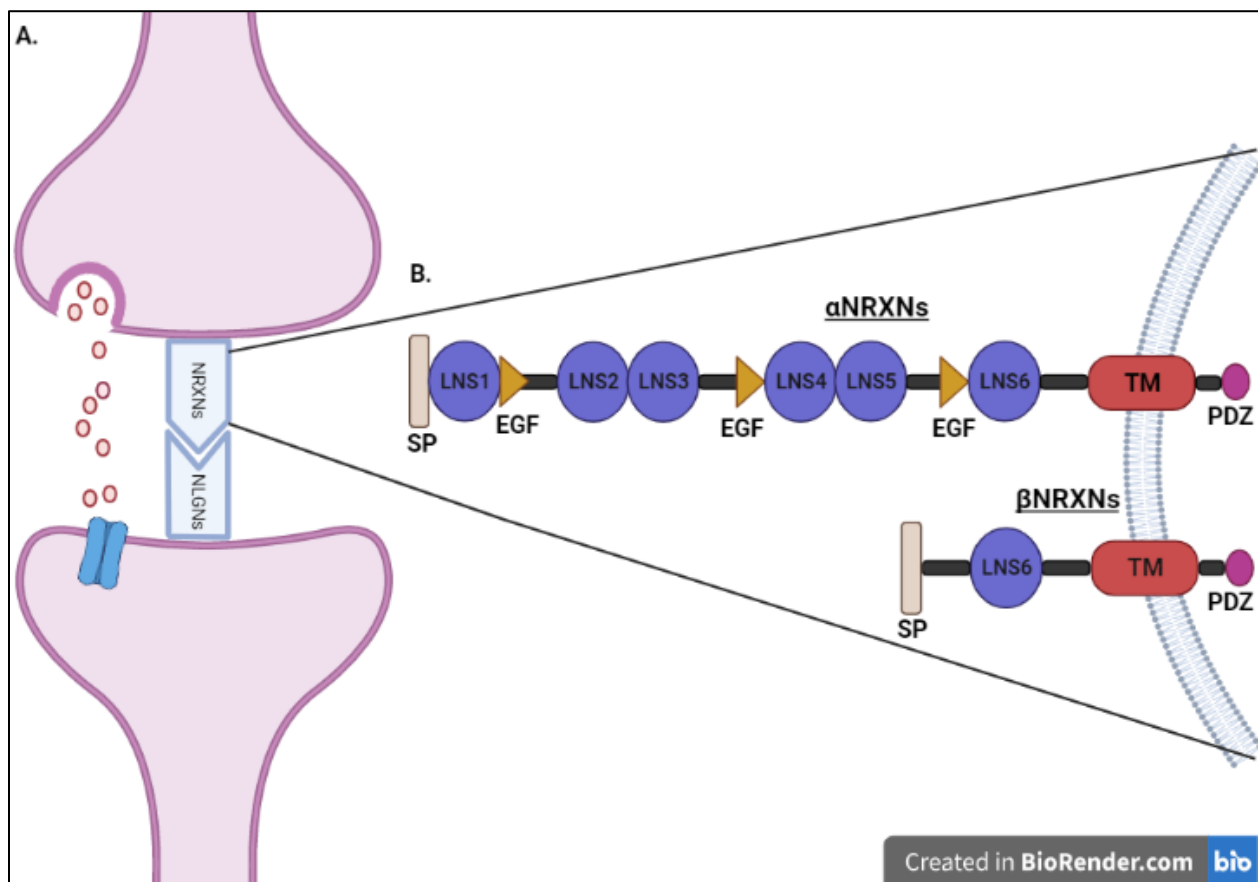


Figure 1.4: Location and structure of neurexins. A) Neurexins are located in the pre-synaptic membrane and commonly bind with post-synaptic neuroligins. B) Each *NRXN* gene encodes both a long α transcript and a short β transcript. Abbreviations: NRXN: neurexin; NLGN: neuroligin; SP: signalling peptide; LNS: laminin/neurexin/sex-hormone binding domain; EGF: epidermal growth factor like region; TM: transmembrane region; PDZ: domain binding site. (Image created in BioRender.com)

1.6.1 Functions of Neurexins

Neurexins are embedded in the presynaptic membrane and interact with key postsynaptic surface proteins (**Figure 1.4**), such as neuroligins (NLGNs) (Craig and Kang, 2007; Mukherjee et al., 2008), cerebellin-1 precursor (CBLN1), δ -type glutamate receptor (GluR δ) (Uemura et al., 2010) and leucine-rich repeat transmembrane neuronal proteins (LRRTMs) (de Wit et al., 2009; Ko et al., 2009; Siddiqui et al., 2010). However, it must be noted that these binding partners may be specific to different neurexins. In general, neurexins are thus considered an important family of synaptic regulation proteins. A more in-depth examination of neurexin binding partners is provided in **Chapter 4**.

Inactivation of *NRXN1* is associated with multiple neurodevelopmental disorders, such as schizophrenia, epilepsy and autism spectrum disorders (Schaaf et al., 2012; Møller et al., 2013; Dachtler et al., 2014, 2015; Yangngam et al., 2014; Chen et al., 2017). Research into *NRXN3* is more limited, however it has also been implicated in autism spectrum disorder (Vaags et al., 2012) and is associated with genetic vulnerability to addictive behaviours, such as smoking (Docampo et al., 2012). Interestingly, a recent longitudinal study on the blood transcriptome of PD patients has revealed neurexin-neuroligin signalling to be an important pathway in the disorder (Koks et al., 2022). They found that nascent transcription of introns causes substantial changes in cellular pathways and that this may underpin the molecular pathology of PD (Koks et al., 2022). The link between *NRXN2* and human disease is elaborated on in the following section.

1.6.2 *NRXN2* α

The protein of interest for this study, *NRXN2* α , is known to be involved in calcium channel regulation, synaptic organization, neuronal cell adhesion, transmembrane signaling and neuroligin family protein binding (Craig and Kang, 2007). It is also highly expressed in the SNpc, the main region of the brain affected by PD. Studies on *NRXN2* α in disease are limited, but they implicate the protein in neuronal and synaptic disorders. A study on synaptic impairment in mice observed the dysregulation of neurotransmitter release and synaptic trafficking when both *NRXN1* and

NRXN2 were inactivated (Dachtler et al., 2015). In an animal study, *NRXN2α* knockout mice displayed a dramatic impairment in synaptic transmission, likely due to the loss in presynaptic Ca^{2+} influx (Missler et al., 2003). In another animal study, mutated mouse *NRXN2α* cDNA resulted in a loss of synaptic activity and failure to cluster glutamatergic components, namely *LRRTM2*, *PSD-95*, *NLGN2* and *gephyrin*, at the dendrite contact sites (Tabuchi and Südhof, 2002). The mutation was present at the end of the fourth LNS domain and resulted in the loss of approximately half of the *NRXN2α* protein, including the binding sites for *NLGNs* and *LRRTMs* (Tabuchi and Südhof, 2002).

More recently, Naito et al., (2017) investigated whether neurexins play a role in AD. They observed an interaction between amyloid beta ($A\beta$) oligomers and *NRXN1/2* that diminished presynaptic organization (Naito et al., 2017). In addition, Brito-Moreira et al., (2017) found that $A\beta$ oligomers interact specifically with *NRXN2α* and *neuroigin 1 (NLGN1)* to mediate synapse damage and memory loss in mice. Thus, it was hypothesized that these interactions could result in the synaptic pathology that is present in AD (Naito et al., 2017).

Taken together, these previous studies show that the loss of or dysregulated function of *NRXN2α* causes an impairment in synaptic activity and have implicated the protein in AD aetiology. Thus, it is this possible that neurexins may play a similar role in the synaptology of PD.

1.7 The Present Study

1.7.1 The Problem Statement

There is a large knowledge gap regarding the genetics of PD in SSA (Schumacher-Schuh et al., 2022). Studies have shown that the known PD pathogenic variants may be minor contributors to these populations. Also, the genetic architecture of the people of SSA appears to be different from that of other populations outside Africa and in parts of Africa outside SSA (Gomez et al., 2014; Lekoubou et al., 2014). It is therefore speculated that due to the rich genetic heterogeneity present in the region, there are unique genotypes, environmental factors, and cultural influences which

may affect the disease phenotypes displayed in the region (Gomez et al., 2014; Lekoubou et al., 2014). As a result, it is plausible to speculate that the treatment strategies that are effective in the widely studied European ancestry populations may not be as efficacious in SSA. Therefore, it is important to study SSA populations to identify novel genetic contributors to the disorder in order to improve our understanding of PD in these populations and potentially develop better treatment strategies for these populations.

In order to add to the limited studies on genetic studies on SSA individuals with PD, in the present study we recruited a multiplex SA family of Afrikaner European ancestry with early onset PD in order to investigate the genetic aetiology of the disorder. However, it is not sufficient to only identify candidate genes, it is also important to perform functional studies to validate them. These functional studies will hopefully aid in improving our understanding of the pathways involved in PD. Ultimately, this knowledge could lead to a better understanding of the disorder and potentially assist in the development of improved therapeutic modalities.

1.7.2 Hypothesis

We hypothesize that due to the unique ancestry of the South African population that we will find a novel PD-causing gene in our multiplex family, and that this gene will provide new insights into the pathobiology of PD.

1.7.3 Aims and Objectives

The aims of this study were thus to identify the genetic cause underlying PD in a SA multiplex PD family. Thereafter, to use a range of wet-lab and *in-silico* approaches to study its effect on various aspects of cellular and mitochondrial function as well as protein structure.

In order to achieve this, the following objectives were set:

- 1) Perform whole exome sequencing (WES) and bioinformatic analysis to identify the causal genetic factor in the South African family
- 2) Write a literature review about evidence for the involvement of the protein of interest in neurodegenerative and neuropsychiatric disorders
- 3) Generate a mutant plasmid from the wild-type plasmid using site-directed mutagenesis and transfect SH-SY5Y neuroblastoma cells, as a cellular model to study the effect of the variant
- 4) Measure the effects of the variant on cell viability, cytotoxicity and apoptosis using functional assays
- 5) Measure the effects of the variant on various features of mitochondrial function including membrane potential, the mitochondrial network and oxidative stress using fluorescent probe-based assays
- 6) Investigate evidence for dysregulated biological pathways caused by the variant using proteomics analysis
- 7) Perform molecular dynamics simulations of the wild-type and mutant protein in complex with a known interactor to determine changes in protein stability, as well as determine the effect of the variant on protein-protein binding using GROMACS
- 8) Perform an *in vitro* assay to better understand how the variant affects one of the main functions of the protein of interest

CHAPTER 2

Overview of Methodology

This chapter provides a broad overview of all the Methods used in this dissertation in Chapters 3 to 7. An outline of the experimental approach is provided in **Figure 2.1**. The Standard Operating Procedures (SOPs) referred to are in **Appendix I**.

Chapter 3:

A multiplex SA family with familial PD was recruited for genetic analysis in an attempt to determine the genetic aetiology of the disease. This family comprises five affected individuals who were examined by a movement disorder specialist and diagnosed according to the United Kingdom (UK) Parkinson's Disease Society Brain Bank Research criteria. Peripheral blood samples were collected from the study participants and genomic DNA was extracted according to the procedure for the phenol-chloroform DNA extraction (**Appendix I: SOP LM-018**). WES was performed on three affected individuals using an Illumina HiSeq 2000 and variants were annotated to the GRCh37/human genome 19. After exclusion of synonymous, common, non-co-segregating and homozygous variants, the remaining variants were validated using Sanger sequencing. We then utilized functional prediction tools, pathway and expression analysis, and examined the frequency of these variants in control populations. One variant was prioritised for further study. Thereafter, we created a homology model of the protein of interest, NRXN2 α , using Swissmodel with the *Bos taurus* crystal structure of neurexin 1 alpha (PDBID: 3R05) as the template. We then performed molecular dynamics simulations using GROMACS to analyze the effect of the variant on the structure of the protein.

Chapter 4:

After prioritizing a variant in *NRXN2* as a possible candidate gene in our multiplex family, we wanted to investigate the potential roles of neurexins in disease. First, we examined the biological pathways and interacting partners of neurexins using STRING (<https://string-db.org>) (Szklarczyk et al., 2019) and GeneMANIA (<https://genemania.org>) (Warde-Farley et al., 2010) to understand the broader pathways that neurexins are involved in. Thereafter, we performed a literature search on neurexins in both neurodegenerative disorders (such as AD, Huntington's disease (HD), and PD) as well as neuropsychiatric disorders (such as autism spectrum disorders and schizophrenia). The main findings of the studies were then summarized and discussed.

Chapter 5:

Next, we wanted to perform functional studies on the prioritised variant to better understand its potential role in PD. To this end, we obtained the NRXN2 α -ECFP-N1 plasmid from Prof. Ann Marie Craig (University of British Columbia, Canada), which expresses mouse NRXN2 α . We used site-directed mutagenesis to generate the mutant plasmid (p.G882D in our mouse model) (**Appendix I: SOP LM-030**). The plasmids were transfected into SH-SY5Y neuroblastoma cells (**Appendix I: SOP TC_LM-002**). General cell culture was performed as per the SOP TC_LM-001 (**Appendix I**). After transfection, functional assays were performed to evaluate the effect of the variant on cellular viability and apoptosis, mitochondrial membrane potential and mitochondrial fragmentation, as well as H₂O₂ levels as a proxy for oxidative stress.

Chapter 6:

Additionally, in order to obtain a better understanding of the pathways affected by *NRXN2*, we wanted to analyze our cells using proteomics. As before, we used the wild-type NRXN2 α -ECFP-N1 plasmid and our generated mutant plasmid and transfected them into SH-SY5Y cells. Total

protein was then isolated from these cells and prepared for mass spectrometry. A Thermo Scientific Fusion mass spectrometer equipped with a Nanospray Flex ionization source was used. The data was interrogated against the UniProt *H. sapiens* database (The UniProt Consortium, 2021). Unique proteins were detected, and significantly differentially abundant proteins were determined using a student's *t*-test. Data was then uploaded to WebGestalt (<http://www.webgestalt.org>) (Liao et al., 2019), KEGG (<https://www.kegg.jp>) (Kanehisa et al., 2021) and STRING (<https://string-db.org>) (Szkłarczyk et al., 2019) to perform enrichment and pathway analysis.

Chapter 7:

Since NRXN2 α functions mainly as a synaptic protein, we wanted to evaluate the effect of the prioritised variant on synapse function. To this end, we created a homology model of NRXN2 α bound to a known interactor at the synapse, neuroligin 1 (NLGN1). We utilized our previous homology model of NRXN2 α from Sebaste et al., (2021) and NLGN1 extracted from PDBID: 3BIW [Neuroligin-1/Neurexin-1beta synaptic adhesion complex, *Rattus norvegicus* (rat)]. Structures were superimposed together using PyMol (DeLano, 2002). NRXN2 α is located in the pre-synapse and commonly binds to NLGN1, which is located in the post-synapse. We then performed molecular dynamic simulations using GROMACS (Van Der Spoel et al., 2005) to analyze the effect of the variant on NRXN2 α -NLGN1 binding. Thereafter, we wanted to examine synapse formation. To this end, we differentiated SH-SY5Y cells with retinoic acid, as per the SOP TC_LM-004 (**Appendix I**). Thereafter, we transfected these cells with the wild-type NRXN2 α -ECFP-N1 and mutant plasmids. We then stained for synaptic markers using immunofluorescence (**Appendix I: SOP LM-048**) and evaluated synapse formation microscopically.

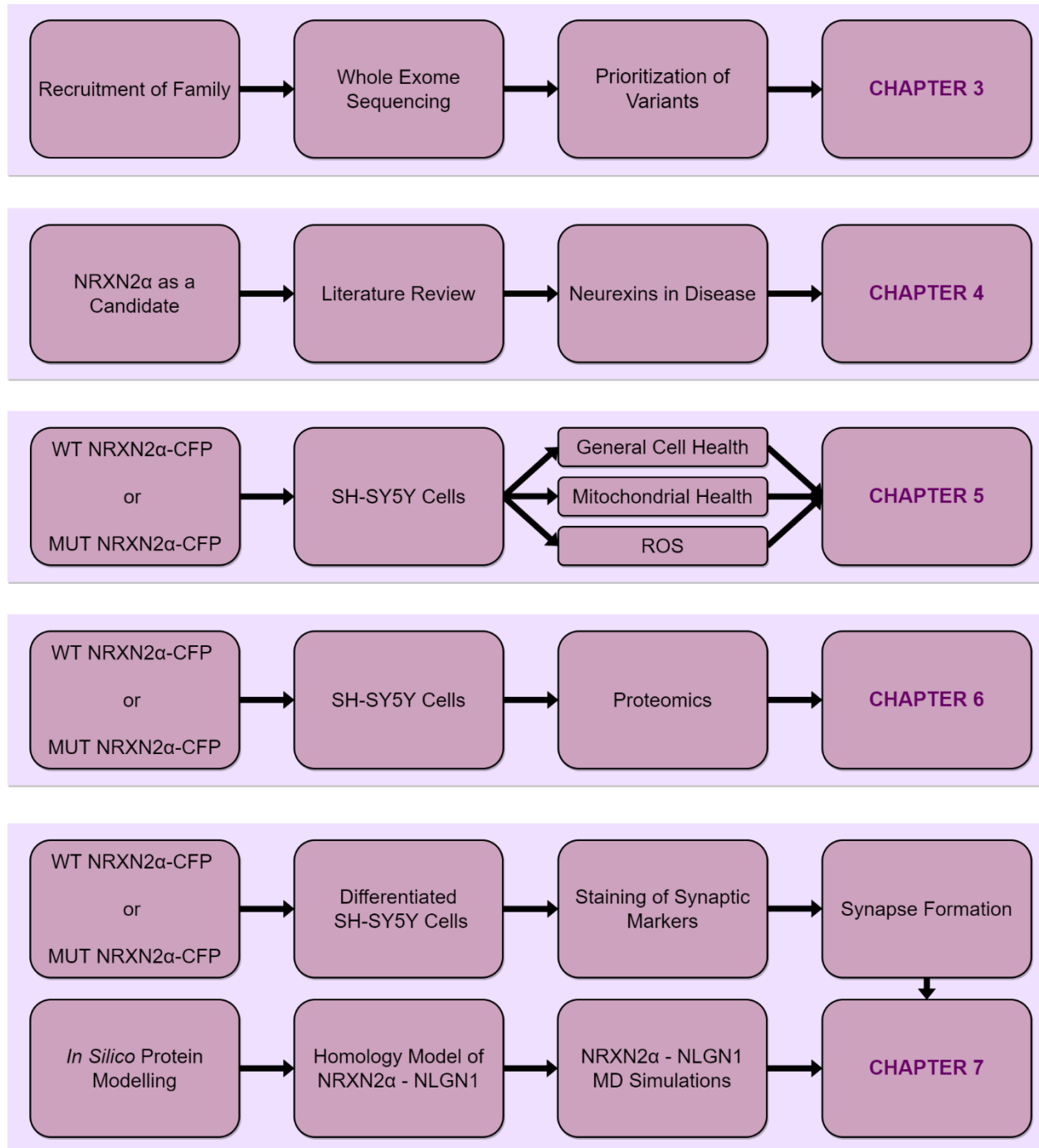


Figure 2.1: Outline of the current PhD study. Each block corresponds to one chapter of the dissertation. The individual boxes within the block represents the overarching methodology used in that chapter. Abbreviations: CFP: cyan fluorescent protein; MD: molecular dynamic; MUT: mutant; NLGN1: neuroligin 1; NRXN2 α : neurexin 2 α ; ROS: reactive oxygen species; SH-SY5Y: neuroblastoma cells; WT: wild-type

CHAPTER 3

Identification of a Novel Variant

This chapter consists of a peer-reviewed published article that addressed **Objective 1** of this study. In this chapter, members of family ZA253 were whole exome sequenced to identify a possible pathogenic variant. Molecular dynamic simulations were then performed to analyse the effect prioritised variant on the protein's structure.

Published Article: Prioritization of candidate genes for a South African family with Parkinson's disease using *in-silico* tools

Authors: Sebate, B.[◦], Cuttler, K.[◦], Cloete, R., Britz, M., Christoffels, A., Williams, M., Carr, J. and Bardien, S.

[◦]These authors contributed equally to this work

Journal: PLoS ONE (Impact Factor: 3.240)

DOI: <https://doi.org/10.1371/journal.pone.0249324>

Supplementary Material: This follows directly after the published article, in text, but can also be found in the [online version](#) of the article. However, Supplementary Table S3, an Excel spreadsheet which lists all the variants found, has not been included in text.

Declarations

Declaration by the candidate

With regard to the published original research article (DOI: <https://doi.org/10.1371/journal.pone.0249324>) constituting Chapter 3 of the dissertation, the nature and scope of my contributions were as follows:

Screened controls for identified variants, revised and edited first draft to conform with journal requirements and submitted to co-authors, collated all supplementary material of the article, reviewed, and edited the manuscript, and made reviewers' corrections (extent of contribution = 40%).

Disclaimer: This article was published under an Open Access CC-BY license. Therefore, this article is permitted to be included in full or in part in a thesis or dissertation for non-commercial purposes without the need to request permission from the publisher (PLoS).

The following co-authors have contributed to Chapter 3:

Name	E-mail Address	Nature of Contribution	Extent of Contribution (%)
Boiketlo Sebate	Miss.sebate@gmail.com	<ul style="list-style-type: none"> Performed experiments and analyzed data. Wrote the first draft of the manuscript. 	40
Ruben Cloete	ruben@sanbi.ac.za	<ul style="list-style-type: none"> Modelled NRXN2 structure and performed molecular dynamic simulations. Manuscript review and editing. 	5
Marcell Britz	marcellb@mweb.co.za	<ul style="list-style-type: none"> Family recruitment and clinical expertise. Manuscript review and editing. 	2
Alan Christoffels	alan@sanbi.ac.za	<ul style="list-style-type: none"> Manuscript review and editing. 	2
Monique Williams	monique.williams@uct.ac.za	<ul style="list-style-type: none"> Manuscript review and editing. 	2
Jonathan Carr	jcarr@sun.ac.za	<ul style="list-style-type: none"> Family recruitment and clinical expertise. Manuscript review and editing. 	4

Soraya Bardien	sbardien@sun.ac.za	<ul style="list-style-type: none"> • Research project conception and organization. • Manuscript review and editing. 	5
----------------	--	---	---

Signature of candidate:

Date: 10/03/2022

Declaration by co-authors

The undersigned hereby confirm that

1. the declaration above accurately reflects the nature and extent of the contributions of the candidate and the co-authors to Chapter 3,
2. no other authors contributed to Chapter 3, besides those specified above, and
3. potential conflicts of interest have been revealed to all interested parties and that the necessary arrangements have been made to use the material in Chapter 3 of this dissertation.

Name	Signature	Affiliation	Date
Boiketlo Sebate		Stellenbosch University, Cape Town, South Africa	23/02/2022
Ruben Cloete		South African National Bioinformatics Institute (SANBI), University of the Western Cape, Cape Town, South Africa	24/02/2022
Marcell Britz		Greenacres Medical Centre, Port Elizabeth, South Africa	23/02/2022
Alan Christoffels		South African National Bioinformatics Institute (SANBI), University of the Western Cape, Cape Town, South Africa	08/03/2022

Monique Williams		University of Cape Town, Cape Town, South Africa	24/02/2022
Jonathan Carr		Stellenbosch University, Cape Town, South Africa	22/02/2022
Soraya Bardien		Stellenbosch University, Cape Town, South Africa	10/03/2022


RESEARCH ARTICLE

Prioritization of candidate genes for a South African family with Parkinson's disease using *in-silico* tools

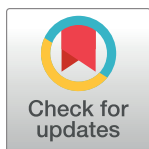
Boiketlo Sebate¹ , Katelyn Cuttler¹ , Ruben Cloete^{1,2*} , Marcell Britz³, Alan Christoffels², Monique Williams^{4#}, Jonathan Carr⁵, Soraya Bardien^{1*} 

1 Division of Molecular Biology and Human Genetics, Department of Biomedical Sciences, Faculty of Medicine and Health Sciences, Stellenbosch University, Cape Town, South Africa, **2** South African Medical Research Council Bioinformatics Unit, South African National Bioinformatics Institute, University of the Western Cape, Cape Town, South Africa, **3** Greenacres Medical Centre, Port Elizabeth, South Africa, **4** Division of Molecular Biology and Human Genetics, Department of Biomedical Sciences, NRF/DST Centre of Excellence for Biomedical Tuberculosis Research, South African Medical Research Council Centre for Tuberculosis Research, Faculty of Medicine and Health Sciences, Stellenbosch University, Cape Town, South Africa, **5** Division of Neurology, Department of Medicine, Stellenbosch University, Cape Town, South Africa

 These authors contributed equally to this work.

 Current address: Department of Molecular and Cell Biology, University of Cape Town, Cape Town, South Africa

* sbardien@sun.ac.za (SB); ruben@sanbi.ac.za (RC)



OPEN ACCESS

Citation: Sebate B, Cuttler K, Cloete R, Britz M, Christoffels A, Williams M, et al. (2021) Prioritization of candidate genes for a South African family with Parkinson's disease using *in-silico* tools. PLoS ONE 16(3): e0249324. <https://doi.org/10.1371/journal.pone.0249324>

Editor: Yona Levites, University of Florida, UNITED STATES

Received: September 23, 2020

Accepted: March 15, 2021

Published: March 26, 2021

Peer Review History: PLOS recognizes the benefits of transparency in the peer review process; therefore, we enable the publication of all of the content of peer review and author responses alongside final, published articles. The editorial history of this article is available here: <https://doi.org/10.1371/journal.pone.0249324>

Copyright: © 2021 Sebate et al. This is an open access article distributed under the terms of the [Creative Commons Attribution License](https://creativecommons.org/licenses/by/4.0/), which permits unrestricted use, distribution, and reproduction in any medium, provided the original author and source are credited.

Data Availability Statement: All single nucleotide variants identified using whole exome sequencing in three affected family members are available in [S3 Table](#).

Abstract

Parkinson's disease (PD) is a neurodegenerative disorder exhibiting Mendelian inheritance in some families. Next-generation sequencing approaches, including whole exome sequencing (WES), have revolutionized the field of Mendelian disorders and have identified a number of PD genes. We recruited a South African family with autosomal dominant PD and used WES to identify a possible pathogenic mutation. After filtration and prioritization, we found five potential causative variants in *CFAP65*, *RTF1*, *NRXN2*, *TEP1* and *CCNF*. The variant in *NRXN2* was selected for further analysis based on consistent prediction of deleteriousness across computational tools, not being present in unaffected family members, ethnic-matched controls or public databases, and its expression in the substantia nigra. A protein model for NRXN2 was created which provided a three-dimensional (3D) structure that satisfied qualitative mean and global model quality assessment scores. Trajectory analysis showed destabilizing effects of the variant on protein structure, indicated by high flexibility of the LNS-6 domain adopting an extended conformation. We also found that the known substrate N-acetyl-D-glucosamine (NAG) contributed to restoration of the structural stability of mutant NRXN2. If *NRXN2* is indeed found to be the causal gene, this could reveal a new mechanism for the pathobiology of PD.

Funding: SB and JC received support from the National Research Foundation of South Africa (Grant Number: 106052) and the South African Medical Research Council (Self-Initiated Research Grant). RC and AC were supported by the South African Research Chairs Initiative of the Department of Science and Technology and National Research Foundation (NRF) of South Africa (award number UID 64751). The funders had no role in study design, data collection and analysis, decision to publish, or preparation of the manuscript.

Competing interests: The authors have declared that no competing interests exist.

Introduction

Parkinson's disease (PD), the most common neurodegenerative movement disorder, is characterized by loss of dopaminergic neurons in the substantia nigra. PD affects motor, autonomic and cognitive functioning, as well as overall mood and behavior [1]. Research on PD has firmly established the role of genetic factors in its etiology. To date, several PD-associated genes have been identified through linkage analysis including *LRRK2*, *SNCA*, *DJ-1*, *PRKN*, *PINK1* and *SYNJ1* [2, 3]. More recently, next-generation sequencing (NGS) has contributed to the discovery of novel genes including *VPS35* [4, 5], *CHCHD2* [6], *VPS13C* [7], *TMEM230* [8] and *LRP10* [9]. These NGS technologies, namely whole exome sequencing (WES) and whole genome sequencing (WGS), provide the entire exome or genome of an individual at an affordable cost [10]. WES generates 20,000 to 30,000 variants, per individual [11], far less compared to WGS. However, it still requires filtration and prioritization analysis of variants into a workable list of candidates because it is not feasible to determine the effect of all variants, with functional experiments.

Currently, there is no standard filtration protocol, and it is a lengthy and complicated task that requires the use of several bioinformatic platforms [12]. These computational prediction tools allow prioritization of potentially deleterious variants over other variants. Sequence-based tools use computational algorithms based on amino acid physicochemical properties, protein structure and cross-species conservation. These include SIFT [13], PolyPhen-2 [14], MutationTaster [15], MAPP [16] and Panther [17]. Studies have compared multiple tools concluding that the algorithms were informative and valuable in determining the impact of the variant, although they had high rates of both false-positive and false-negative predictions [18, 19]. To address this shortfall, new meta-tools were developed such as CADD (Combined Annotation Dependent Depletion) [20, 21]. CADD achieves better performance by combining the predictive scores of multiple prediction tools into one unified score of potential deleteriousness, and for all 8.6 billion possible human mutations, it compares variants that survived natural selection with simulated mutations.

Assessing the frequency of genetic variants in population databases such as the Genome Aggregation Database (gnomAD) [22], the 1000 Genomes Project [23] and dbSNP [24] can also be used to prioritize variants. A minor allele frequency (MAF) threshold of $\leq 1\%$ is typically used to select potential pathogenic mutations by filtering out polymorphisms, based on the premise that risk alleles occur at low frequencies due to negative selection against deleterious mutations [25]. Furthermore, co-segregation analysis of the variant within families is invaluable for interpreting the variant's significance. However, phenocopies (present at relatively high levels in PD [26]) as well as non-manifesting mutation carriers need to be taken into account in family studies.

In the present study, a multiplex South African family with PD was recruited for genetic analysis. WES variants were filtered and prioritized using various computational tools, and additionally structural methods (DUET webserver) and molecular dynamic simulation analysis were performed. Using this approach, we excluded all known PD-associated mutations and identified a novel variant in a gene, not previously implicated in PD, for further functional studies.

Materials and methods

Ethical considerations

Ethical approval was obtained from the Health Research Ethics Committee of Stellenbosch University, Cape Town, South Africa (Protocol number 2002/C059). The research was

performed in accordance with the relevant guidelines and regulations. Written informed consent was obtained from all study participants.

Study participants

Initially, we selected 11 multiplex South African families from our PD study collection for WES. These families were selected on the basis of having DNA available of at least two affected second degree relatives, PD had been diagnosed by a neurologist, and at least one individual had young-onset PD. WES was performed on a total of 24 affected individuals from these families. One of these families self-identified as Afrikaner and is the subject of the present study. The Afrikaner is a group that is unique to South Africa, and whose ancestry can be traced to people of predominantly Dutch but also German and French ancestry [27]. The family (ZA 253) comprises five PD affected individuals who were examined by a movement disorder specialist and diagnosed according to the UK Parkinson's Disease Society Brain Bank Research criteria [28]. A total of 218 unrelated ethnic-matched individuals were recruited as controls from the Western Province Blood Transfusion Service in Cape Town. These individuals were not clinically assessed for PD. Peripheral blood samples were collected from the study participants and genomic DNA was extracted according to the procedure for the phenol-chloroform DNA extraction, as previously described [29].

Whole exome sequencing

WES was performed on three affected individuals using an Illumina HiSeq 2000, enrichment for exonic regions was performed according to the Agilent SureSelect Custom Enrichment Kit protocol. Burrows-Wheeler Aligner (BWA-MEM) [30] was used to align sequence reads or assembly contigs against a large reference, duplicate removal, SNP calling and indel detection. ANNOVAR software [31] was used to annotate the variants using GRCh37/human genome 19 as the reference genome. The Genome Analysis Toolkit (GATK) was used for variant calling and described variants as either exonic, intronic, in the UTR or splice-site region by comparison with a reference sequence [31]. To provide a summary of the coverage of mapped reads on a reference sequence at a single base pair resolution, SAMtools mpileup and the Minimum variant QUAL score of 30 was used.

Validation using Sanger sequencing

Oligonucleotide primers were designed using sequence data obtained from the Ensembl Genome Browser database (<http://www.ensembl.org>). *In silico* verification of primers was conducted on Primer3 software version 4.0.0 (<http://primer3.ut.ee>) [32], as well as on Basic Local Alignment Search Tool (BLAST) (<http://www.ncbi.nlm.nih.gov/BLAST>). Forward and reverse PCR primers sequences, annealing temperatures and the sizes of the PCR products are available upon request.

Polymerase chain reaction (PCR)

To amplify the fragments of interest for Sanger sequencing, 25 μ l PCR reactions containing template genomic DNA, 20 μ moles of each of the forward and reverse primers, 2.5 μ M dNTPs (Promega, Madison, Wisconsin, USA), 1.5 mM MgCl₂, 1X Green GoTaq[®] Reaction Buffer (Promega, Madison, Wisconsin, USA) and 0.01U GoTaq[®] G2 Flexi DNA Polymerase (Promega, Madison, Wisconsin, USA) was used. Amplification was performed in an ABI 2720 Thermal Cycler (Applied Biosystems Inc., Foster City, California, USA). To visualize the PCR amplicons and to investigate if non-specific primer binding or contamination was present,

agarose gel electrophoresis was used. PCR amplicons were visualized using a SynGene UV gel documentation system (Synoptics Ltd., Cambridge, UK) with GeneTools software version 3.0.6 (Synoptics Ltd., Cambridge, UK).

Screening of controls

HRM analysis detects the shift in fluorescence as a double-stranded PCR product dissociates to single-stranded DNA with increasing temperature. For this analysis, PCR was performed with the inclusion of 1% SYTO9 fluorescent dye (Invitrogen, USA). The melting temperature conditions ranged from 75°C to 95°C rising by 0.1°C increments on a Rotor-Gene 6000 analyzer (Corbett Life Science, Australia). The resulting thermal denaturation profile is unique to that specific PCR product, because DNA strand melting depends on sequence length, bases and GC content (HRM Assay Design and Analysis Booklet; http://www.corbettlifescience.com/shared/Rotor-Gene%206000/hrm_corprotocol.pdf). Samples with known variants were included as positive controls, for comparison. A negative control was included in each run to monitor contamination.

In-silico functional prediction tools

To investigate the variants identified, computational analysis was performed. Public mutation databases were searched to determine the frequency of the variants, these included EXAC Database (<http://exac.broadinstitute.org/>), gnomAD (<https://gnomad.broadinstitute.org/>), the 1000 Genomes Project (<http://browser.1000genomes.org/index.html>) and dbSNP (<https://www.ncbi.nlm.nih.gov/snp>). Functional predictions were determined from sequence homology-based programs namely Sorting Intolerant From Tolerant (SIFT; <http://sift.jcvi.org/>), PolyPhen-2 (<http://genetics.bwh.harvard.edu/pph2/>), MutationTaster (<http://www.mutationtaster.org/>) and Combined Annotation Dependent Depletion (CADD; <http://cadd.gs.washington.edu/>). To determine evolutionary constraint acting on genomic sites GERP++ was used (<http://mendel.stanford.edu/SidowLab/downloads/gerp/>).

SIFT and PolyPhen-2 both report results in terms of pathogenic scores accompanied by the prediction (Benign, Tolerated or Deleterious). MutationTaster scores the amino acid change then reports one of two predictions based on its disease-causing threshold (Disease causing or Neutral). CADD integrates 63 predictive features in total which includes the scores of SIFT, GERP++, PolyPhen-2 as well as CpG distance (a short stretch of DNA in which the frequency of the CG sequence is higher than other regions), and total GC content. It reports phred-like scores ("scaled C-scores") ranging from zero to 50, the variant that is predicted to be among the 10% most deleterious substitutions that can occur in the human genome at that specific base position, is assigned a score of 10 or greater. While variants in the 1% most deleterious substitutions are assigned values of 20 or greater and those within 0.1% of the highest possible substitutions at that specific locus are assigned values of 30 or greater. Thus, the higher the CADD score the more likely it is that the variant is highly pathogenic. GERP++ uses maximum likelihood evolutionary rate estimation for position-specific scoring, the score ranges from -12.3 to 6.17. The closer the score is to 6.17, a value that represents the most conserved a region can be, the greater the level of evolutionary constraint inferred to be acting on that site.

Pathway and expression analysis

To prioritize the variants, pathway analysis was performed using KEGG Pathways Analysis (<http://www.genome.jp/kegg/pathway.html>) and Pathway Analysis (<http://www.pantherdb.org/pathway/>). The publicly available expression databases accessed were the Allen Brain Atlas (www.brain-map.org/) and Human Protein Atlas (<https://www.proteinatlas.org/>). Both

database record human mRNA expression data but Allen brain Atlas gives only brain regional whole-transcriptome gene expression data.

NRXN2 protein structure modelling

The three dimensional (3D) structure for human NRXN2 has not yet been resolved experimentally and was predicted using the online Swissmodel Webserver [33]. Prior to modelling, Swissmodel constructs an alignment between the target amino acid sequence of NRXN2 and potential homologous templates by performing a position specific iterative (PSI-BLAST) against the non-redundant protein databank (PDB) sequences [34]. Once a suitable template was identified then the actual modelling step was invoked by submitting the alignment to the Swissmodel webserver. Subsequent, to the modelling of NRXN2 the quality of the protein model was assessed using Swissmodel inbuilt assessment methods Global Model Quality Estimation (GMQE) and QMEAN6 composite score as well as performing a structural alignment of atoms between the NRXN2 protein structure and the homologous template using the Pymol align command to calculate the RMSD [35]. Usually models with a lower RMSD value suggest very little deviation between the backbone atoms of the protein model and the homologous template.

Molecular dynamic simulation

We prepared in total four simulation systems for NRXN2, each consisting of the wild type (WT) NRXN2 with and without sugar moiety N-acetyl-D-glucosamine (NAG) and mutant (MUT) structures NRXN2 with and without NAG, for simulation studies. The sugar moiety NAG was extracted from the homologous template PDBID: 3R05 (NEUREXIN-1-ALPHA; BOS TAURUS) by superimposition using PyMol. The NAG was included because it is important for glycosylation of membrane proteins whereby glycans are attached to proteins necessary for protein-protein interactions. All the simulations were carried out using the GROMACS-5.1 package [36] along with the CHARMM36 all-atom force field [37]. The accurate topologies for NAG was generated using SwissParam tool [38]. All four systems were solvated with TIP3 water molecules in a cubic box of at least 18 Å of water between the protein and edges of the box. To neutralize the negative charge of the WT and MUT systems without NAG, WT and variant with NAG systems, 14, 15, 14 and 15 sodium ions were added to each system, respectively.

Each system underwent 50,000 steps of steepest descents energy minimization to remove close van der Waals force contacts. Subsequently, all systems were subjected to a two-step equilibration phase namely; NVT (constant number of particles, Volume and Temperature) for 500 ps to stabilize the temperature of the system and a short position restraint NPT (constant number of particles, Pressure and Temperature) for 500 ps to stabilize the pressure of the system by relaxing the system and keeping the protein restrained. For the NVT simulation the system was gradually heated by switching on the water bath and the V-rescale temperature-coupling method [39] was used, with constant coupling of 0.1 ps at 300 K under a random sampling seed. While for NPT the Parrinello-Rahman pressure coupling [40] was turned on with constant coupling of 0.1 ps at 300 K under conditions of position restraints (all-bonds). For both NVT and NPT electrostatic forces were calculated using Particle Mesh Ewald method [41]. All systems were subjected to a full 100 ns simulation and these were repeated twice for 100 ns to validate reproducibility of results. The analysis of the trajectory files was done using GROMACS utilities. The root mean square deviation (RMSD) for backbone atoms was calculated using `gmx rmsd`, RMSF average per-residue analysis using `gmx rmsf`. The change in the solvent accessibility surface area (SASA) for protein atoms was calculated using `gmx sasa` and

the radius of gyration for the backbone atoms was calculated using `gmx gyrate` to determine if the system reached stability and compactness over the 100 ns simulation. VMD [42] was used to visually inspect changes in secondary structural elements and motion of domains along the trajectory.

Principal component analysis

Principal component analysis (PCA) is a statistical technique that reduces the complexity of a data set and was used here to extract biologically relevant movements of protein domains from irrelevant localized motions of atoms. For PCA analysis the translational and rotational movements were removed from the system using `g_covar` from GROMACS to construct a covariance matrix. Next, the eigenvectors and eigenvalues were calculated by diagonalizing the matrix. The eigenvectors that correspond to the largest eigenvalues are called “principal components”, as they represent the largest-amplitude collective motions. We filtered the original trajectory and project out the part along the most important eigenvectors namely: vector 1 and 2 using `g_anaeig` from GROMACS utilities. Furthermore, we visualized the sampled conformations in the subspace along the first two eigenvectors using `g_anaeig` in a two-dimensional projection. The two-dimensional projection of the first two principal components was plotted using Gnuplot version 4.4 [43]. Afterwards, we calculated the free energy surface (FES) using the program `g_sham` and plotted it using `xpm2mat.py` script and Gnuplot in a 3n matrix along the two order parameters, Rg and RMSD. The FES represents all the possible different conformations a protein can adopt during a simulation and are typically reported as Gibbs free energy. The molecule free energy was calculated with the formula $\Delta G(r) = -k_B T \ln P(x,y)/P_{min}$, where P is the probability distribution of the two variables Rg and RMSD, P_{min} is the maximum probability density function, k_B is the Boltzmann constant and T is the temperature of the simulation. Conformations sampled during the simulation are projected on a two dimensional plane to visualize the reduced free energy surface. The clustering of points in a specific cell represents a possible metastable conformation. All simulations were carried out using the GROMACS-5.1 package [36] along with the CHARMM36 all-atom force field [37].

NRXN2 variant structure stability predictions

The mCSM webserver was used to assess the effect of the mutation on the stability of the protein structure of NRXN2 [44]. First, we extracted six structures (every 10ns) in total over the last 50ns of the simulation trajectory. Next, each WT structure without NAG was uploaded to the webserver and the position of the variant was specified as G889D on the webpage. mCSM calculates a Delta-delta G stability score and provides a phenotypic assessment of the score with destabilizing scores being negative, while stabilizing scores are positive [45].

Results

Description of the family

The complete pedigree of this family, which is denoted as family ZA253, contains 57 individuals, and in total, eight members were reported to have PD. A simplified version of the pedigree indicating the family members, who took part in this study, is shown in Fig 1. The patient labelled as individual III-8 (proband) was the first individual to be diagnosed with PD and his age at onset (AAO) was 48 years. He initially presented with anxiety and difficulty with the use of his leg following a general anesthetic. He later developed moderate to high amplitude rest tremor. Levodopa improved his condition markedly, but he developed dystonia of the left leg within weeks of starting medication. His siblings were subsequently assessed, and his brother

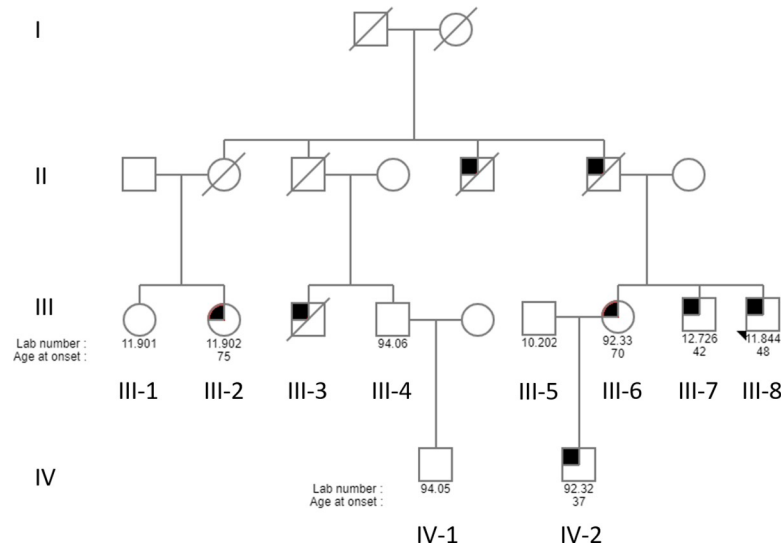


Fig 1. Pedigree of the South African family ZA253. For readability and confidentiality, the pedigree is greatly simplified. Circles denote females and squares depict males. The filled in symbols indicate affected individuals. The diagonal line indicates that the person is deceased, and the arrow indicates the proband. The numbers below each individual is the laboratory ID number and age at onset of disease. Branches without clinically confirmed PD or without DNA samples were omitted, but all known living family members with PD diagnoses are included.

<https://doi.org/10.1371/journal.pone.0249324.g001>

(III-7) was also confirmed as having PD. His AAO was 42 years, at which time he developed difficulties with concentration together with weakness of the legs and gait disturbances. On examination, he had marked dystonia of the left arm, and very asymmetrical bradykinesia and rigidity. Patient IV-2, the nephew of the two affected siblings, was diagnosed with early-onset PD at the age of 37 years. Examination revealed facial dystonia, rigidity at the right wrist, mild generalized bradykinesia, and slowness of gait [Unified Parkinson's Disease Rating Scale (UPDRS) motor score 16]. Furthermore, his mother (individual III-6) was examined at the age of 67 years; at that time her examination was normal. Repeat examination three years later (aged 70 years) showed mild generalized bradykinesia (UPDRS motor score 11), although she had no complaints. Individual III-2 was the most recent individual in the family to be diagnosed with PD, in 2017. However, she presented as typical idiopathic PD, with AAO of 75 years. The symptoms at the time of diagnosis were tremor and rapid eye movement sleep behavior disorder, with no evidence of dystonia. A summary of the family's clinical characteristics is provided in [S1 Table](#).

Whole exome sequencing

WES was performed on three of the affected family members (III-7, III-8 and IV-2). These three patients all appear to have young onset PD, with prominent dystonia, resembling similar cases with *PRKN* and *PINK1* mutations. Moreover, all three cases are characterized by a long duration of illness, mild autonomic impairment, and delayed and mild impairment of cognition, with absence of REM sleep behavior disorder. DNA of individual III-2 was not available at the time that the WES was performed.

The WES metrics ([S2 Table](#)), revealed good overall coverage of the target regions in all three individuals. For the data analysis, we assumed that the three affected individuals have the same genetic cause of disease and that the mode of inheritance is autosomal dominant. Importantly, none of the known PD mutations were found in any of the affected individuals which suggests that there is likely a novel PD-causing mutation in this family.

Table 1. Rare and novel exonic missense variants shared between the three affected individuals after variant filtering.

		<i>CFAP65</i>	<i>RFT1</i>	<i>NRXN2</i>	<i>TEP1</i>	<i>CCNF</i>
		p.T1023A	p.A463G	p.G849D	p.Y412C	p.C363S
Affected individuals	III-8 (proband)	Present	Present	Present	Present	Present
	III-7	Present	Present	Present	Present	Present
	IV-2	Present	Present	Present	Present	Present
	III-6	Present	Present	Present	Present	Present
	III-2	Present	Absent	Absent	Absent	Absent
Unaffected individuals	III-4	Absent	Absent	Absent	Absent	Present
	IV-1	Absent	Absent	Absent	Absent	Present
	III-1	Absent	Absent	Absent	Absent	Present
	III-5	Absent	Absent	Absent	Absent	Absent

Present, variant present; Absent, variant absent

<https://doi.org/10.1371/journal.pone.0249324.t001>

After exclusion of synonymous, common, non-co-segregating and homozygous variants, a total of nine novel or rare non-synonymous heterozygous variants were shared between the three affected individuals. These variants are in nine genes, *ACTN3* (Actinin Alpha 3), *CCNF* (Cyclin F), *CDC27* (Cell Division Cycle 27), *CFAP65* (Cilia and Flagella Associated Protein 65), *RFT1* (Requiring Fifty-Three 1), *NRXN2* (Neurexin 2), *POU2F1* (POU Class 1 Homeobox 1), *TEP1* (Telomerase Associated Protein 1) and *TUBB6* (Tubulin Beta 6 Class V).

Sanger sequencing of variants and co-segregation in family

Sanger sequencing validation was performed to ensure that the variants are not NGS artefacts, and five variants in *CCNF*, *CFAP65*, *RFT1*, *NRXN2* and *TEP1* were validated. Thereafter, we performed genotyping of the family and these results are summarized in Table 1. The most recently diagnosed patient III-2 had only one of the five validated variants, p.T1023A in *CFAP65*. The unaffected family members shared only one variant, p.C363S in *CCNF*, with the affected individuals, which indicates that it may be a polymorphism.

Analysis using functional prediction tools

Various functional prediction tools were used to identify and prioritize variants that are predicted to have a major impact on the protein. Notably, none of the codon changes occurred in the interchangeable third base position (wobble base). The results are summarized in Table 2 with the functional scores and predictions from SIFT, PolyPhen-2, MutationTaster, GERP++,

Table 2. In-silico functional tool scores and predictions for the five variants validated with Sanger sequencing.

Gene	cDNA position	Amino acid and codon change	SIFT prediction	PolyPhen-2 prediction	Mutation Taster prediction	GERP prediction	CADD prediction	Condel prediction
<i>CFAP65</i>	c.A3151G	p.T1023A ACC⇒GCC	0; Deleterious	0.124; Benign	1; Disease causing	2,38; Conserved	18,70; Deleterious	0.763 Deleterious
<i>RFT1</i>	c.C1450G	p.A463G GCT⇒GGT	0.49; Tolerated	0.001; Benign	0; Neutral	2,53; Conserved	4,96; Benign	0.042 Neutral
<i>NRXN2</i>	c.G3008A	p.G849D GGC⇒GAC	0; Deleterious	0.973; Probably damaging	1; Disease causing	4,93; Conserved	29,50; Deleterious	0.831 Deleterious
<i>TEP1</i>	c.A1276G	p.Y412C TAC⇒TGC	0.51; Tolerated	0; Benign	0; Neutral	-8,29; Not conserved	0,00; Benign	0.050 Neutral
<i>CCNF</i>	c.G1176C	p.C363S TGC⇒TCC	0.06; Tolerated	0.939; Probably damaging	1; Disease causing	5,43; Conserved	27,30; Deleterious	0.707 Deleterious

<https://doi.org/10.1371/journal.pone.0249324.t002>

CADD and Condel. The *TEP1* p.Y412C variant was predicted to be benign across all of the different prediction tools with a CADD score of zero and with a GERP++ score of -8.29 . The conservation score implies that in the region of the genome where this variant occurs, there are more substitutions than the average neutral site and thus indicates that this region may not be under evolutionary constraint. The p.A463G variant in *RFT1* was also predicted to be benign by all of the tools though its conservation score (of 2,53) implies that it occurs in a region that is evolutionarily-conserved. The p.T1023A variant in *CFAP65* and the p.C363S variant in *CCNF* are predicted to be pathogenic by most of the tools, and both have positive scores indicating that they are found in conserved regions of the genome. The only variant that was predicted to be pathogenic across all of the functional prediction tools was p.G849D in *NRXN2*, which had a CADD score of 29,50 and a conservation score of 4,93 showing that the level of evolutionary constraint inferred to be acting on this position is relatively high.

Frequency of variants in control populations

To determine the frequency of the five variants in controls, a search was performed of publicly available databases including the 1000 Genomes Project, dbSNP and gnomAD. This revealed that four of the variants are either extremely rare or are novel according to data available on African American, American, East Asian, South Asian, Finnish and Non-Finnish European populations. *CFAP65* p.T1023A was found in gnomAD with a MAF frequency of $8.88e-5$ (25 out of 281690 alleles) (https://gnomad.broadinstitute.org/variant/2-219886565-T-C?dataset=gnomad_r2_1).

When assessing the frequency of these variants, it is important to consider not just the publicly available online databases but also to screen ethnically matched controls. Therefore, we screened South African ethnic-matched controls, but none of the variants was present in these individuals. The *TEP1* p.Y412C, *RFT1* p.A463G and *CCNF* p.C363S variants were screened in 192 individuals, and the *CFAP65* p.T1023A and *NRXN2* p.G849D variants were screened in 218 and 216 individuals, respectively.

Pathway and expression analysis

To add further information about the possible causal role of the variants, gene expression profiles were assessed using publicly available databases, namely the Allen Brain Atlas [46] and the Human Protein Atlas [47]. Pathway analysis was also performed using KEGG Pathways Analysis [48] and Panther Pathway Analysis [49] to determine if any of the five candidates are co-expressed, co-regulated or co-localize with each other or any of the known PD genes. This analysis also shows if the variants and any of the known PD genes are functionally related or impact a pathway of interest or even a trait of interest such as neuronal development, regulation and functioning. The results show that none of the five proteins are co-expressed, co-regulated or co-localize with each other or any of the proteins encoded by the known PD genes. Notably, *NRXN2* was found to be highly expressed in the brain including the substantia nigra (<https://www.proteinatlas.org/ENSG00000110076-NRXN2/tissue>). This is the region of the brain predominantly involved in PD pathogenesis and also thought to be involved in pathways that regulate synaptic functioning, neurotransmitter secretion and neuronal cell-to-cell adhesion. *RFT1* is also expressed in the brain, however not particularly defined to any specific region. *RFT1* was implicated in pathways of protein metabolism and the endoplasmic reticulum membrane network. *CFAP65* was associated with the motile cilia pathway, *TEP1* is reported to be involved in apoptotic pathways and in assembling telomerase components in cell signaling and *CCNF* was associated with pathways of ubiquitination and cell cycle regulation.

Selection of NRXN2

After the above analyses, we prioritized one candidate gene (*NRXN2*) for further study. As mentioned previously, even though the *CCNF* p.C363S variant was predicted to be deleterious by most of the prediction tools, it was excluded at this stage as it was found in unaffected family members. The variants in *TEP1* (p.Y412C) and *RTF1* (p.A463G) were predicted to be benign across all the prediction tools used, therefore they were also excluded. Although the p.T1023A variant in *CFAP65* was predicted to be deleterious by the majority of the prediction tools, it functions specifically in ciliac processes, and thus is unlikely to be involved in PD pathobiology. Importantly, while affected individual III-2 has the *CFAP65* variant, we suspect that she is a phenocopy. Evidence for this is that her phenotype is typical late-onset PD that is unlike the other affected family members. Consequently, the p.G849D variant in *NRXN2* is considered to be the strongest candidate of the five variants. All of the computational algorithms predicted the G849D substitution as being potentially deleterious. The position where this variant occurs was reported to be highly conserved by GERP++ and it resulted in a codon change from a small, non-polar amino acid to a larger, negatively charged, polar one. None of the controls obtained from the online databases or in the local population had the variant. The *NRXN2* variant was also not present in exomes of 600 probands of French, North African and Turkish origins with predominantly early-onset PD (Suzanne Lesage, personal communication). *NRXN2* was reported by two expression databases to be expressed in the brain and specifically in the substantia nigra, a key brain region involved in PD pathogenesis. *NRXN2* was therefore selected for further studies involving protein structure modelling and simulation analysis.

NRXN2 protein model

The Swissmodel webserver [33] search, identified homologous template PDBID: 3R05 crystal structure of neurexin 1 alpha [Laminin neurexin sex hormone binding globulin domains (LNS1-LNS6), with splice insert SS3, Bos taurus (cow)] as a highly similar protein to human NRXN2. The template 3R05 was chosen to construct a three-dimensional (3D) structure for NRXN2 because it shared 71% sequence identity and over 50% structural similarity with our target protein. The 3D structure built for human NRXN2 is structurally similar to template 3R05 displaying the five LNS2-6 and two EGF-like repeats excluding LNS domain 1 and one EGF-like domain (Fig 2). The protein model predicted for human NRXN2 had a GMQE score of 0.51 [value between 0 and 1] and a QMEAN Z-score of -1.67 that are close to zero and higher than -4, suggesting high reliability in the quality of the predicted protein model. Superimposition of the predicted model onto the homologous template structure indicated a root mean square deviation (RMSD) value of 0.226Å, which is less than 2Å, suggesting very little deviation in the main chain backbone atoms of the protein model and the template. Furthermore, the Glycine residue (G849) in the template and homology model is conserved and has a positive phi and psi dihedral angle conformation and therefore any amino acid substitution at this position will have a significant effect on the protein structure.

NRXN2 molecular dynamic simulation analysis and stability predictions

Four simulation systems were prepared for NRXN2 analysis. These are wild type (WT) NRXN2 with and without the sugar moiety, N-acetyl-D-glucosamine (NAG), and mutant (MUT) NRXN2 with and without NAG. NAG was used in this analysis as it is important for the glycosylation of NRXN2 and it was extracted from the homologous template. The kinetic energy and thermodynamic properties were found to fluctuate around stable values with the potential and total energies values fluctuating at negative 1×10^{-6} values and the temperature fluctuating around 300K for the four NRXN2 systems (S1–S3 Figs).

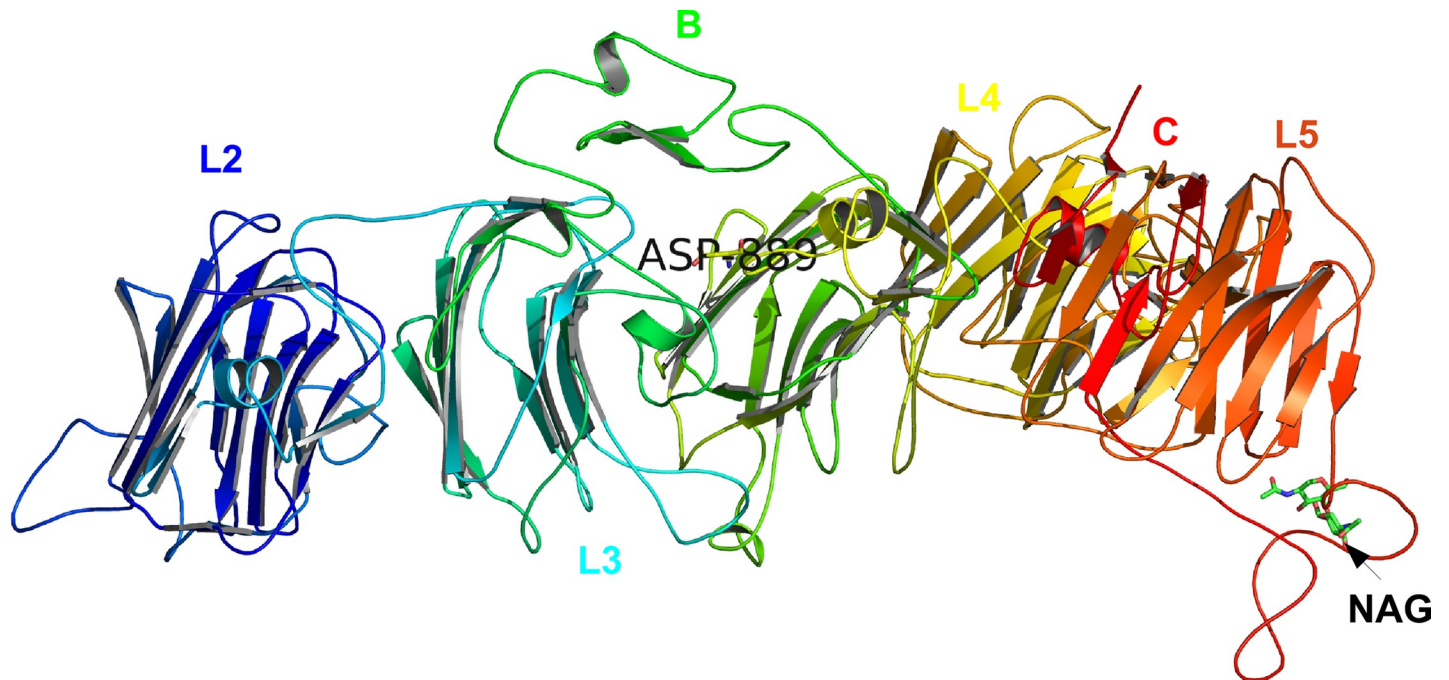


Fig 2. Swissmodel predicted 3-dimensional (3D) structure for human NRXN2 with mutation p.G849D (p.G889D) in complex with N-acetyl-D-glucosamine (NAG). Each domain is colour coded, EGF-like domains are labelled B and C, substrate NAG are labelled as well as the mutation, p.G889D in our protein model.

<https://doi.org/10.1371/journal.pone.0249324.g002>

Measuring the mean and standard deviation of the RMSD values for the four systems indicated lower values of $1.61 \text{ nm} \pm 0.26$ for the WT system without NAG compared to the MUT system without NAG of $2.16 \text{ nm} \pm 0.60$ (Fig 3A). However, for the WT system with NAG, a higher RMSD value ($2.25 \text{ nm} \pm 0.52$) was observed compared to the MUT system with NAG ($1.54 \text{ nm} \pm 0.55$) (Fig 3A). The RMSD showed that the MUT systems with and without NAG reached equilibrium after 50ns, therefore subsequent analysis considered only the last 50ns of the simulation trajectories. The average root mean square fluctuation (RMSF) per-residue values for the four systems indicated lower fluctuation values for the WT system without NAG ($0.32 \text{ nm} \pm 0.14$) compared to the MUT system without NAG ($0.53 \text{ nm} \pm 0.24$) (Fig 3B). Furthermore, the RMSF fluctuation per-residue values for the other two systems with NAG indicated slightly lower values of $0.37 \text{ nm} \pm 0.18$ for the WT system compared to $0.40 \text{ nm} \pm 0.16$ for the MUT system (Fig 3B). Similarly, the radius of gyration values and the solvent accessible surface area values for the WT NRXN2 without NAG were significantly lower than that of the other three systems. The calculated Rg values for the backbone atoms for WT NRXN2 without NAG was lower ($3.90 \text{ nm} \pm 0.03$) compared to MUT NRXN2 without NAG, WT and MUT NRXN2 with NAG, ($5.01 \text{ nm} \pm 0.10$; $4.76 \text{ nm} \pm 0.11$; $5.13 \text{ nm} \pm 0.08$, respectively) (Fig 3C). The solvent accessible surface area values of the protein for WT and MUT NRXN2 in absence of NAG were lower ($480.84 \text{ nm} \pm 5.43$; $490.59 \text{ nm} \pm 4.46$) compared to the WT and MUT NRXN2 in the presence of NAG ($507.63 \text{ nm} \pm 4.26$; $495.76 \text{ nm} \pm 4.78$) (Fig 3D).

Calculation of the contribution of each of the top ten principal components (PCs) indicated that the first two PCs contributed significantly to the movement of the protein. For each system, PC1 contributed to 70%, 46%, 60% and 37% to WT no NAG, WT with NAG, MUT no NAG, and MUT with NAG for NRXN2, respectively. While, PC2 contributed 8%, 19%, 15% and 29% to WT no NAG, WT with NAG, MUT no NAG, and MUT with NAG for NRXN2, respectively. Therefore, 2D projections of the first and second principal components for all

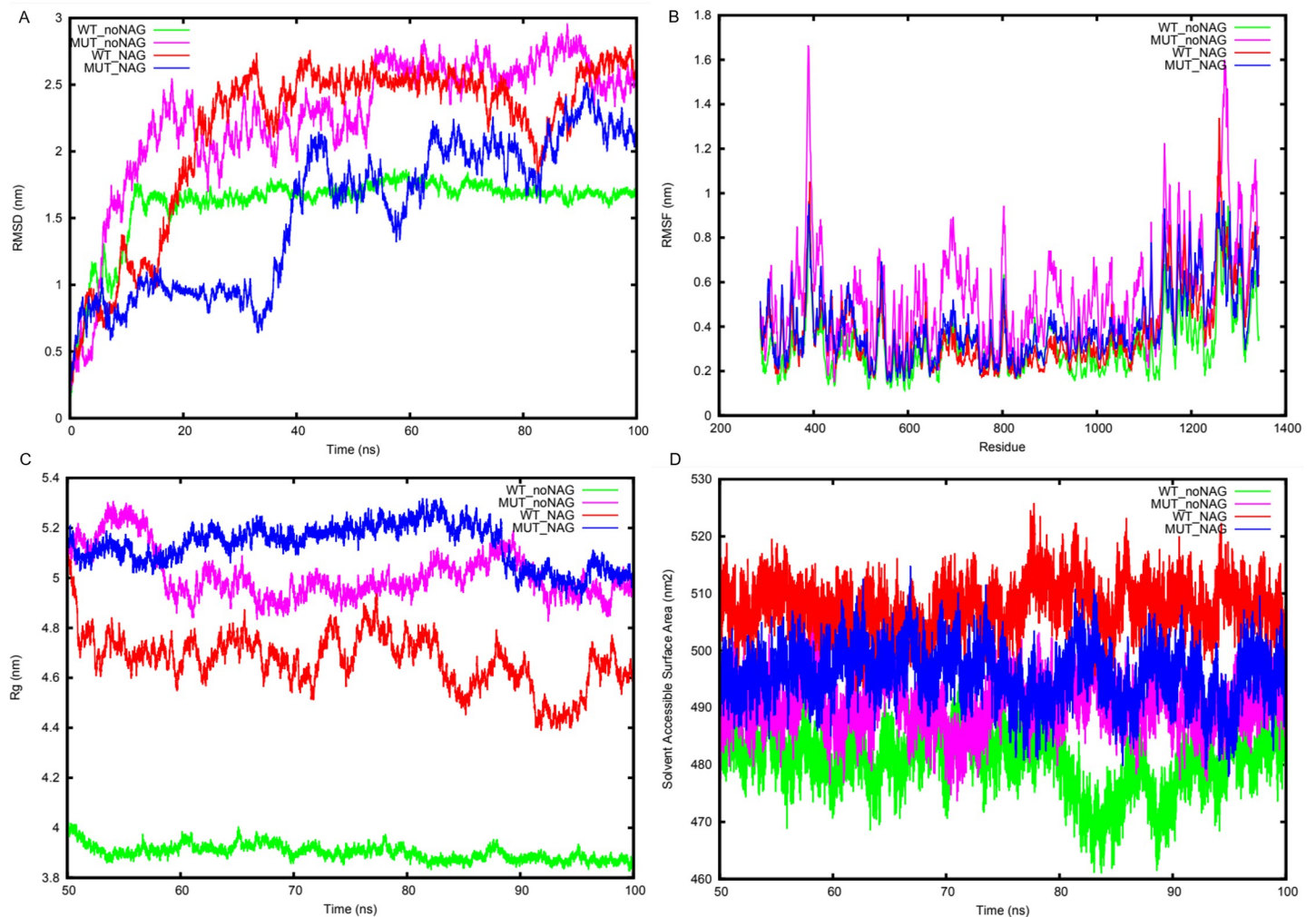


Fig 3. Trajectory analysis of wild type (WT) NRNX2 and mutant (MUT) NRNX2, both with and without NAG. (A) root mean square deviation (RMSD) deviation of the backbone atoms. MEAN + STDEV (1.61mm \pm 0.26, 2.26mm \pm 0.52, 2.16mm \pm 0.60 and 1.54mm \pm 0.55). (B) The average RMSF fluctuation per-residue. MEAN + STDEV (0.31mm \pm 0.14, 0.54mm \pm 0.24, 0.37mm \pm 0.18 and 0.40mm \pm 0.19). (C) Radius of gyration of the backbone atoms. MEAN + STDEV (3.90mm \pm 0.03, 5.01mm \pm 0.10, 4.67mm \pm 0.11 and 5.13mm \pm 0.08). (D) Solvent accessible surface area of the protein. MEAN + STDEV (3.90mm \pm 0.03, 5.01mm \pm 0.10, 4.67mm \pm 0.11 and 5.13mm \pm 0.08). Line colors: WT_noNAG = green, MUT_noNAG = light magenta, WT_NAG = red and MUT_NAG = blue.

<https://doi.org/10.1371/journal.pone.0249324.g003>

four systems were plotted and shown in Fig 4. Calculation of the covariance matrix values after diagonalization showed a significant decrease for the WT NRNX2 without NAG (237.82 nm) system compared to the other three systems MUT without NAG, WT and MUT with NAG (612.38 nm; 508.19 nm; 554.72 nm, respectively) (Fig 4).

We performed interaction analysis to determine which residues played a role in the binding of NAG to the protein in the WT NRNX2 and identified one conserved hydrogen bond interaction with Arg1266 (in our model) as an important anchor point that could be exploited for drug design (S4 Fig). The first repeat of the four simulation systems showed similar results to the first run for thermodynamic and kinetic energy parameters (S5–S7 Figs). Additionally, equilibrium is reached after 50ns of the simulation run and the WT system without NAG had higher stability values based on RMSD analysis compared to the MUT system without NAG (S8 Fig). Similarly, the repeat 2 showed convergence of energy and temperature terms (S9–S11

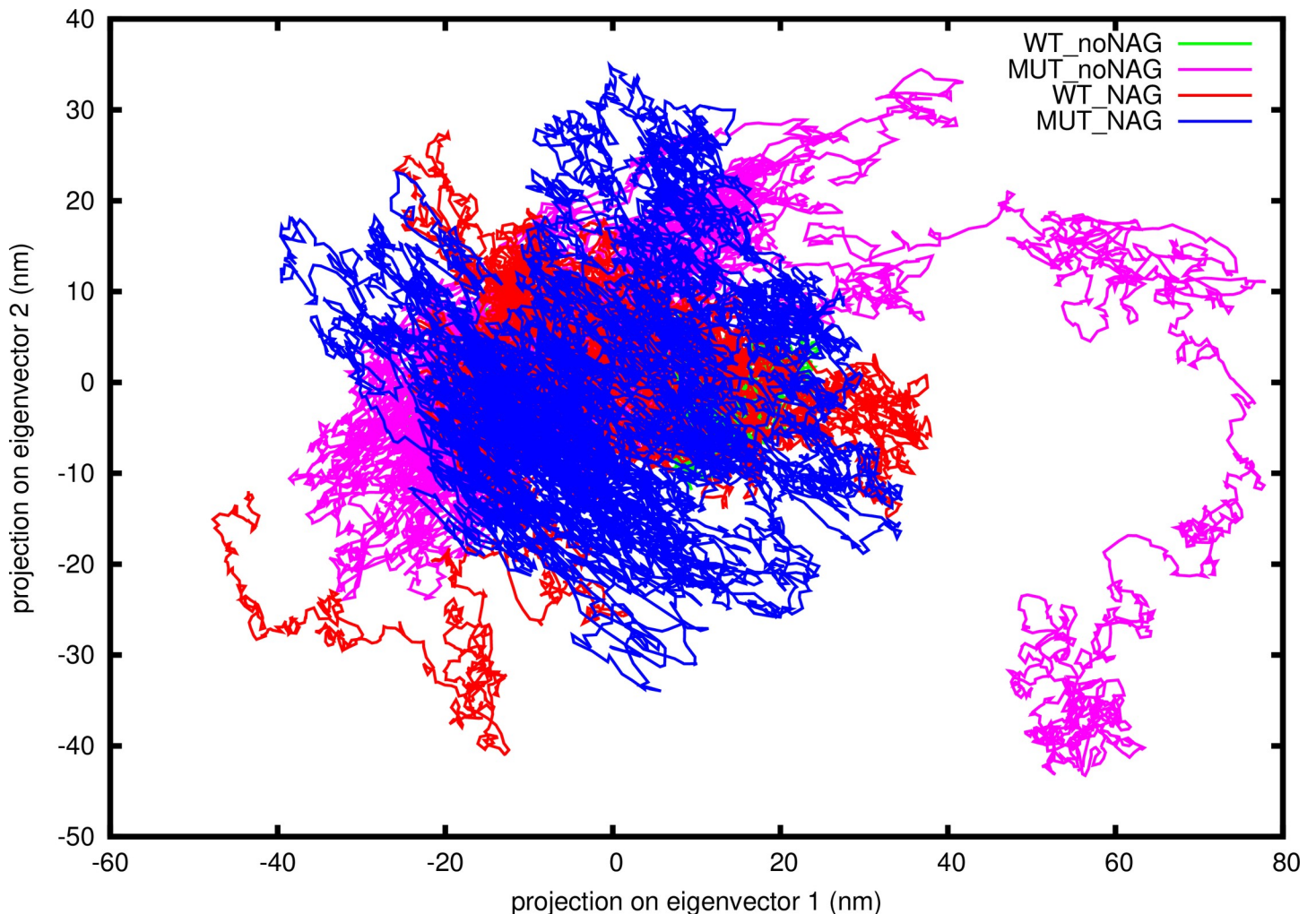


Fig 4. Two-dimensional (2D) projections of the first and second principal components for the WT NRNX2, MUT NRNX2 without NAG and WT NRNX2, MUT NRNX2 with NAG systems. Covariance matrix after diagonalization values for each system; 237.82 nm, 612.38 nm, 508.19 nm and 554.72 nm. Line colors: WT_noNAG = green, MUT_noNAG = light magenta, WT_NAG = red and MUT_NAG = blue.

<https://doi.org/10.1371/journal.pone.0249324.g004>

Figs), this is in agreement with repeat 1, while the RMSD analysis for repeat 2 confirmed stability values of repeat 1 (S12 Fig).

The change in secondary structure for the NRNX2 WT and MUT without NAG is visually shown in a short simulation movie over the last 50ns for the simulation trajectory (S1 and S2 File). In these movies, the LNS6 domain undergoes large transitions between flexed and extended conformations for the mutant structure without NAG while the LNS6 domain for the WT without NAG remains in a stable flexed conformation. FES analysis of the four systems identified several (up to 6) metastable conformations for the WT system without NAG, while the MUT without NAG showed only one energy minima state. In contrast, the other two systems with NAG adopted at least one metastable state for the MUT structure and none for the WT structure (Fig 5A–5D). The WT system without NAG seems to be more stable than the MUT without NAG due to the six energy minima states. The opposite is found for the systems with NAG, as the MUT with NAG becomes more stable while the WT with NAG becomes more flexible. Furthermore, stability predictions using the mCSM webserver was performed to determine the effect of the novel variant p.G849D (in our model p.G889D) on the NRNX2

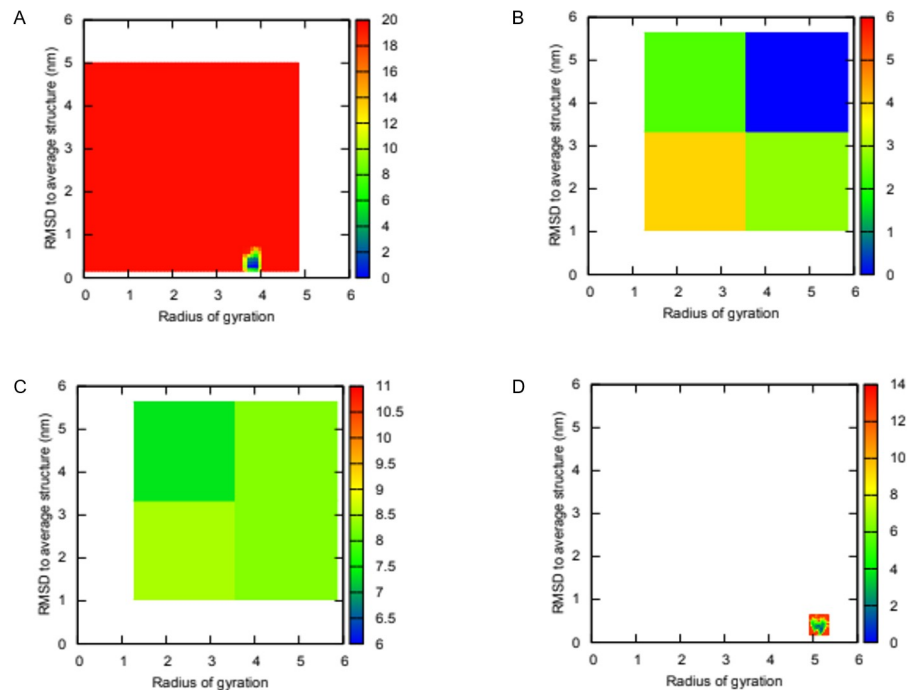


Fig 5. Two-dimensional (2D) free energy landscapes plotted for NRXN2 along two order parameters root mean square deviation (RMSD) to average structure and Rg. (A) WT without NAG (B) MUT without NAG (C) WT with NAG (D) MUT with NAG. Blue regions represent low energy conformational states while red indicate high energy states.

<https://doi.org/10.1371/journal.pone.0249324.g005>

protein structure. The results were in concordance for all six structures extracted over the last 50 ns indicating destabilizing $\Delta\Delta G$ scores of -1.389, -1.131, -1.573, -1.183, -1.298 and -1.596 for 50, 60, 70, 80, 90 and 100 ns frames, respectively.

Discussion

The absence of known PD mutations in this South African family led to the conclusion that a novel mutation could be responsible for the disease phenotype. Four variants in *CFAP65*, *RFT1*, *NRXN2* and *TEP1* are shared by four of the affected family members and are not in the unaffected family members or the controls. It is possible that the variants in any of these genes or even in another gene is responsible for the disease in this family, however, at this stage, the *NRXN2* p.G849D variant was selected for further study. It is the top candidate even though patient III-2 does not share this variant, as this patient may be a phenocopy, known to occur in PD families [26, 50], since she has typical, late-onset sporadic PD unlike the other four affected individuals. This highlights the complexity of interpreting familial co-segregation in disorders where the genetic disease can be indistinguishable from idiopathic forms.

The *NRXN2* p.G849D change is from glycine a small, non-polar, side chain free amino acid, to aspartic acid a larger, negatively charged amino acid with a carboxyl group side chain. The 3D structure predicted for *NRXN2* provided deeper insight into the structural implications of G849D on *NRXN2* protein structure. The overall structure of *NRXN2* is similar to that of the homologous template 3r05, and adopts a similar fold. Using molecular dynamic simulations to understand the overall movement of the protein structure added support to the destabilizing effect of the variant p.G849D on the mobility of the LNS6 domain (residues 1137–1343 in our model). Trajectory analysis confirmed the destabilizing effect of the variant

on the protein structure and the predicted increase in the flexibility of the LNS6 domain might prevent the binding of neuroligins and synaptic organization. Additionally, we showed that adding NAG to the mutant 'system' restored some stability to the NRXN2 protein. From these findings, we hypothesize that the novel variant p.G849D (in our model p.G889D) is destabilizing to NRXN2's protein structure, and that adding NAG to the mutated structure might reduce flexibility and restore its ability to interact with its known interactors such as neuroligin.

NRXN2 has been linked to pathways associated with neuronal and synaptic functioning, and expression analysis showed that it is expressed in the pars reticulata of the substantia nigra, the main region of the brain affected in PD. Its predicted functions range from neuronal cell-cell adhesion, neurotransmitter secretion regulation to synaptic regulation. Indeed, NRXN2 is known to mediate synaptic organization and differentiation [51, 52]. Recently, Naito et al. [51] investigated whether neurexins plays a role in Alzheimer's disease (AD), and observed an interaction between amyloid beta (A β) oligomers and NRXN1/2 that diminished presynaptic organization [51]. Additionally, A β oligomers were found to interact specifically with NRXN2 α and neuroligin 1 to mediate synapse damage and memory loss in mice [53].

Limitations of this study are the limited sequencing scope of WES, which includes its inability to accurately detect copy number [54, 55] and non-coding variants [56], and the fact that each of the functional prediction tools used relies on their own in-built algorithm, which can produce inaccurate results. Another limitation is that the LNS-1 domain of the protein could not be modelled due to the lack of sequence coverage between the target sequence and homologous template structure. Also, the short simulation times (100ns) used may not allow NRXN2 to sample enough of the protein's energy minima landscape or phase space thereby missing important energetic conformations.

In conclusion, we identified a novel candidate gene, *NRXN2*, for PD thereby potentially implicating synaptic dysfunction in neuronal cell death. Future studies will involve wet-laboratory functional studies in relevant disease models to determine the biological significance of the variant identified.

Supporting information

S1 Table. Clinical and demographic information on members of South African family ZA253 with Parkinson's disease.

(PDF)

S2 Table. Summary of whole exome sequencing metrics in the three affected individuals.

(PDF)

S3 Table. Single nucleotide variants identified in three Parkinson's disease-affected individuals using whole exome sequencing.

(XLSX)

S1 Fig. Total energy of the four systems of NRXN2 (WT_noNAG, MUT_noNAG, WT_NAG and MUT_NAG) over 100 ns.

(PDF)

S2 Fig. Potential energy of the four systems of NRXN2 (WT_noNAG, MUT_noNAG, WT_NAG and MUT_NAG) over 100 ns.

(PDF)

S3 Fig. The average temperature of the four systems of NRXN2 (WT_noNAG, MUT_noNAG, WT_NAG and MUT_NAG) over 100 ns.

(PDF)

S4 Fig. 2D interaction diagram showing polar contacts formed between NRXN2 residues and sugar moiety NAG. Figure generated using PoseView. Dashed lines show hydrogen bond contacts formed NAG and NRXN2 residues.

(PDF)

S5 Fig. Total energy of the four systems of the repeat 1 of NRXN2 (WT_noNAG, MUT_noNAG, WT_NAG and MUT_NAG) over 100 ns.

(PDF)

S6 Fig. Potential energy of the four systems of repeat 1 of NRXN2 (WT_noNAG, MUT_noNAG, WT_NAG and MUT_NAG) over 100 ns.

(PDF)

S7 Fig. The average temperature of the four systems of repeat 1 NRXN2 (WT_noNAG, MUT_noNAG, WT_NAG and MUT_NAG) over 100 ns.

(PDF)

S8 Fig. RMSD deviation of the backbone atoms for the four systems of repeat 1 NRXN2. MEAN + STDEV (1.71mm ± 0.52, 2.26mm ± 0.52, 1.27mm ± 0.46 and 2.14mm ± 0.79). Line colours: WT_noNAG = green, MUT_noNAG = light magenta, WT_NAG = red and MUT_NAG = blue.

(PDF)

S9 Fig. Total energy of the four systems of the repeat 2 of NRXN2 (WT_noNAG, MUT_noNAG, WT_NAG and MUT_NAG) over 100 ns.

(PDF)

S10 Fig. Potential energy of the four systems of repeat 2 of NRXN2 (WT_noNAG, MUT_noNAG, WT_NAG and MUT_NAG) over 100 ns.

(PDF)

S11 Fig. The average temperature of the four systems of repeat 2 NRXN2 (WT_noNAG, MUT_noNAG, WT_NAG and MUT_NAG) over 100 ns.

(PDF)

S12 Fig. RMSD deviation of the backbone atoms for the four systems of repeat 2 NRXN2, (1.40mm ± 0.33, 1.98mm ± 0.45, 2.15mm ± 0.51 and 1.29mm ± 0.29). Line colours: WT_noNAG = green, MUT_noNAG = light magenta, WT_NAG = red and MUT_NAG = blue.

(PDF)

S1 File. Change in secondary structure simulation movie for wild-type NRXN2 noNAG last 50ns. Also available at: <https://www.dropbox.com/s/ucb8bosmaq2tqw2/WT.mp4?dl=0>.

(MP4)

S2 File. Change in secondary structure simulation movie for mutant NRXN2 noNAG last 50ns. Also available at: <https://www.dropbox.com/s/wkdmvyrvrqummi/MUT.mp4?dl=0>.

(MP4)

Acknowledgments

We thank the study participants for their participation in and contribution to this study. We also gratefully acknowledge the Western Province Blood Transfusion Service for providing the control samples. We thank Prof. Matthew Farrer and his research group at the Djavad Mowafagian Centre for Brain Health, University of British Columbia, Canada for performing the whole exome sequencing. Prof. Chandra Verma is acknowledged for providing constructive input into the simulation methods and interpretation of the results. We would like to thank Drs Suzanne Lesage and Christelle Tesson for screening for the presence of *NRXN2* p.G849D and *CFAP65* p.T1023A in their exome datasets. We would like to acknowledge the Centre for High Performance Computing (CHPC), Rondebosch, South Africa for allowing us to run our molecular dynamics simulations on their cluster.

Author Contributions

Conceptualization: Ruben Cloete, Soraya Bardien.

Data curation: Ruben Cloete.

Formal analysis: Boiketlo Sebate, Ruben Cloete.

Funding acquisition: Alan Christoffels, Soraya Bardien.

Investigation: Boiketlo Sebate, Katelyn Cuttler, Ruben Cloete, Marcell Britz, Alan Christoffels, Monique Williams, Jonathan Carr, Soraya Bardien.

Methodology: Boiketlo Sebate, Katelyn Cuttler, Ruben Cloete, Soraya Bardien.

Resources: Alan Christoffels, Jonathan Carr, Soraya Bardien.

Supervision: Ruben Cloete, Monique Williams, Soraya Bardien.

Writing – original draft: Boiketlo Sebate, Ruben Cloete.

Writing – review & editing: Boiketlo Sebate, Katelyn Cuttler, Ruben Cloete, Marcell Britz, Alan Christoffels, Monique Williams, Jonathan Carr, Soraya Bardien.

References

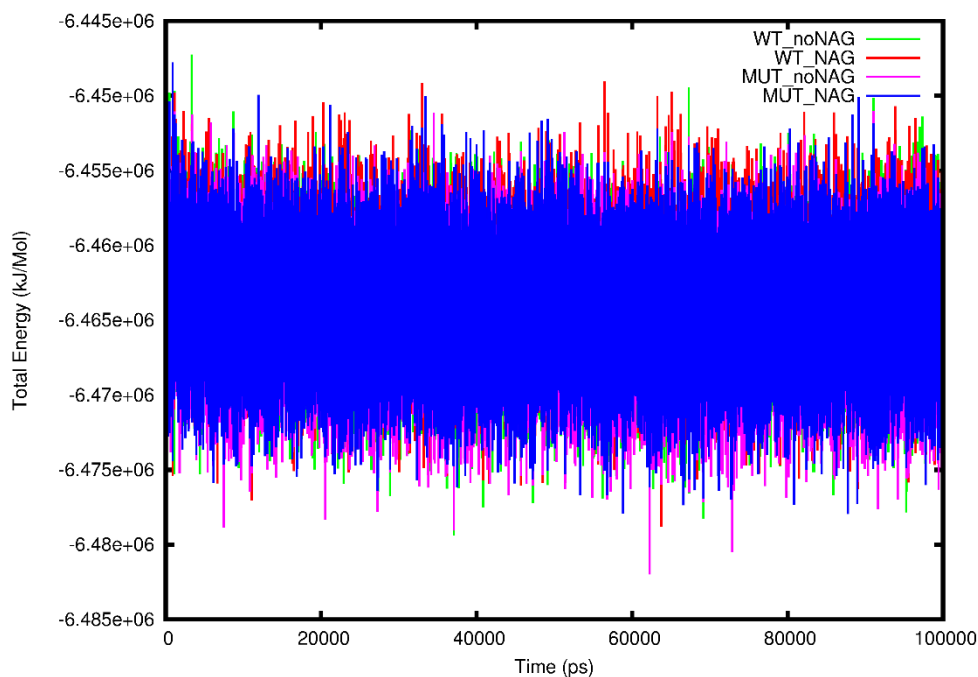
1. Barone P, Antonini A, Colosimo C, Marconi R, Morgante L, Avarello TP, et al. The PRIAMO study: A multicenter assessment of nonmotor symptoms and their impact on quality of life in Parkinson's disease. *Mov Disord.* 2009; 24: 1641–1649. <https://doi.org/10.1002/mds.22643> PMID: 19514014
2. Lill CM. Genetics of Parkinson's disease. *Mol Cell Probes.* 2016; 3: 386–396. <https://doi.org/10.1016/j.mcp.2016.11.001> PMID: 27818248
3. Puschmann A. New Genes Causing Hereditary Parkinson's Disease or Parkinsonism. *Curr Neurol Neurosci Rep.* 2017; 17: 66. <https://doi.org/10.1007/s11910-017-0780-8> PMID: 28733970
4. Zimprich A, Benet-Pagès A, Struhal W, Graf E, Eck SH, Offman MN, et al. A mutation in *VPS35*, encoding a subunit of the retromer complex, causes late-onset parkinson disease. *Am J Hum Genet.* 2011; 89: 168–175. <https://doi.org/10.1016/j.ajhg.2011.06.008> PMID: 21763483
5. Vilariño-Güell C, Wider C, Ross OA, Dachsel JC, Kachergus JM, Lincoln SJ, et al. *VPS35* mutations in parkinson disease. *Am J Hum Genet.* 2011; 89: 162–167. <https://doi.org/10.1016/j.ajhg.2011.06.001> PMID: 21763482
6. Funayama M, Ohe K, Amo T, Furuya N, Yamaguchi J, Saiki S, et al. *CHCHD2* mutations in autosomal dominant late-onset Parkinson's disease: A genome-wide linkage and sequencing study. *Lancet Neurol.* 2015; 14: 274–282. [https://doi.org/10.1016/S1474-4422\(14\)70266-2](https://doi.org/10.1016/S1474-4422(14)70266-2) PMID: 25662902
7. Lesage S, Drouet V, Majounie E, Deramecourt V, Jacoupy M, Nicolas A, et al. Loss of *VPS13C* Function in Autosomal-Recessive Parkinsonism Causes Mitochondrial Dysfunction and Increases *PINK1*/Parkin-Dependent Mitophagy. *Am J Hum Genet.* 2016; 98: 500–513. <https://doi.org/10.1016/j.ajhg.2016.01.014> PMID: 26942284

8. Deng HXH, Shi Y, Yang Y, Ahmeti KB, Miller N, Huang C, et al. Identification of TMEM230 mutations in familial Parkinson's disease. *Nat Genet.* 2016; 48: 733–739. <https://doi.org/10.1038/ng.3589> PMID: [27270108](https://pubmed.ncbi.nlm.nih.gov/27270108/)
9. Quadri M, Mandemakers W, Grochowska MM, Masius R, Geut H, Fabrizio E, et al. LRP10 genetic variants in familial Parkinson's disease and dementia with Lewy bodies: a genome-wide linkage and sequencing study. *Lancet Neurol.* 2018; 17: 597–608. [https://doi.org/10.1016/S1474-4422\(18\)30179-0](https://doi.org/10.1016/S1474-4422(18)30179-0) PMID: [29887161](https://pubmed.ncbi.nlm.nih.gov/29887161/)
10. Christensen KD, Dukhovny D, Siebert U, Green RC. Assessing the costs and cost-effectiveness of genomic sequencing. *J Pers Med.* 2015; 5: 470–486. <https://doi.org/10.3390/jpm5040470> PMID: [26690481](https://pubmed.ncbi.nlm.nih.gov/26690481/)
11. Robinson P, Krawitz P, Mundlos S. Strategies for exome and genome sequence data analysis in disease-gene discovery projects. *Clin Genet.* 2011; 80: 127–132. <https://doi.org/10.1111/j.1399-0004.2011.01713.x> PMID: [21615730](https://pubmed.ncbi.nlm.nih.gov/21615730/)
12. Cooper GM, Shendure J. Needles in stacks of needles: finding disease-causal variants in a wealth of genomic data. *Nat Rev Genet.* 2011; 12: 628–640. <https://doi.org/10.1038/nrg3046> PMID: [21850043](https://pubmed.ncbi.nlm.nih.gov/21850043/)
13. Ng PC, Henikoff S. SIFT: Predicting amino acid changes that affect protein function. *Nucleic Acids Res.* 2003; 31: 3812–3814. <https://doi.org/10.1093/nar/gkg509> PMID: [12824425](https://pubmed.ncbi.nlm.nih.gov/12824425/)
14. Adzhubei I, Jordan DM, Sunyaev SR. Predicting functional effect of human missense mutations using PolyPhen-2. *Curr Protoc Hum Genet.* 2013; 76: 7–20. <https://doi.org/10.1002/0471142905.hg0720s76> PMID: [23315928](https://pubmed.ncbi.nlm.nih.gov/23315928/)
15. Schwarz JM, Cooper DN, Schuelke M, Seelow D. Mutationtaster2: Mutation prediction for the deep-sequencing age. *Nat Methods.* 2014; 11: 361–362. <https://doi.org/10.1038/nmeth.2890> PMID: [24681721](https://pubmed.ncbi.nlm.nih.gov/24681721/)
16. Stone EA, Sidow A. Physicochemical constraint violation by missense substitutions mediates impairment of protein function and disease severity. *Genome Res.* 2005; 15: 978–986. <https://doi.org/10.1101/gr.3804205> PMID: [15965030](https://pubmed.ncbi.nlm.nih.gov/15965030/)
17. Mi H, Huang X, Muruganujan A, Tang H, Mills C, Kang D, et al. PANTHER version 11: Expanded annotation data from Gene Ontology and Reactome pathways, and data analysis tool enhancements. *Nucleic Acids Res.* 2017; 45: D183–D189. <https://doi.org/10.1093/nar/gkw1138> PMID: [27899595](https://pubmed.ncbi.nlm.nih.gov/27899595/)
18. Mathe E, Olivier M, Kato S, Ishioka C, Hainaut P, Tavtigian S V. Computational approaches for predicting the biological effect of p53 missense mutations: A comparison of three sequence analysis based methods. *Nucleic Acids Res.* 2006; 34: 1317–1325. <https://doi.org/10.1093/nar/gkj518> PMID: [16522644](https://pubmed.ncbi.nlm.nih.gov/16522644/)
19. Wei Q, Wang L, Wang Q, Kruger WD, Dunbrack RL. Testing computational prediction of missense mutation phenotypes: Functional characterization of 204 mutations of human cystathionine beta synthase. *Proteins Struct Funct Bioinforma.* 2010; 78: 2058–2074. <https://doi.org/10.1002/prot.22722> PMID: [20455263](https://pubmed.ncbi.nlm.nih.gov/20455263/)
20. Kircher M, Witten DM, Jain P, O'roak BJ, Cooper GM, Shendure J. A general framework for estimating the relative pathogenicity of human genetic variants. *Nat Genet.* 2014; 46: 310–315. <https://doi.org/10.1038/ng.2892> PMID: [24487276](https://pubmed.ncbi.nlm.nih.gov/24487276/)
21. Tang H, Thomas PD. Tools for predicting the functional impact of nonsynonymous genetic variation. *Genetics.* 2016; 203: 635–647. <https://doi.org/10.1534/genetics.116.190033> PMID: [27270698](https://pubmed.ncbi.nlm.nih.gov/27270698/)
22. Karczewski KJ, Francioli LC, Tiao G, Cummings BB, Alföldi J, Wang Q, et al. The mutational constraint spectrum quantified from variation in 141,456 humans. *Nature.* 2020; 581: 434–443. <https://doi.org/10.1038/s41586-020-2308-7> PMID: [32461654](https://pubmed.ncbi.nlm.nih.gov/32461654/)
23. The 1000 Genomes Project Consortium. A global reference for human genetic variation. *Nature.* 2015; 526: 68–74. <https://doi.org/10.1038/nature15393> PMID: [26432245](https://pubmed.ncbi.nlm.nih.gov/26432245/)
24. Sherry ST. dbSNP: the NCBI database of genetic variation. *Nucleic Acids Res.* 2001; 29: 308–311. <https://doi.org/10.1093/nar/29.1.308> PMID: [11125122](https://pubmed.ncbi.nlm.nih.gov/11125122/)
25. Wong GKS, Yang Z, Passey DA, Kibukawa M, Paddock M, Liu CR, et al. A population threshold for functional polymorphisms. *Genome Res.* 2003; 13: 1873–1879. <https://doi.org/10.1101/gr.1324303> PMID: [12902381](https://pubmed.ncbi.nlm.nih.gov/12902381/)
26. Klein C, Chuang R, Marras C, Lang AE. The curious case of phenocopies in families with genetic Parkinson's disease. *Mov Disord.* 2011; 26: 1793–1802. <https://doi.org/10.1002/mds.23853> PMID: [21735483](https://pubmed.ncbi.nlm.nih.gov/21735483/)
27. Greeff JM. Deconstructing Jaco: Genetic heritage of an Afrikaner. *Ann Hum Genet.* 2007; 71: 674–688. <https://doi.org/10.1111/j.1469-1809.2007.00363.x> PMID: [17521310](https://pubmed.ncbi.nlm.nih.gov/17521310/)

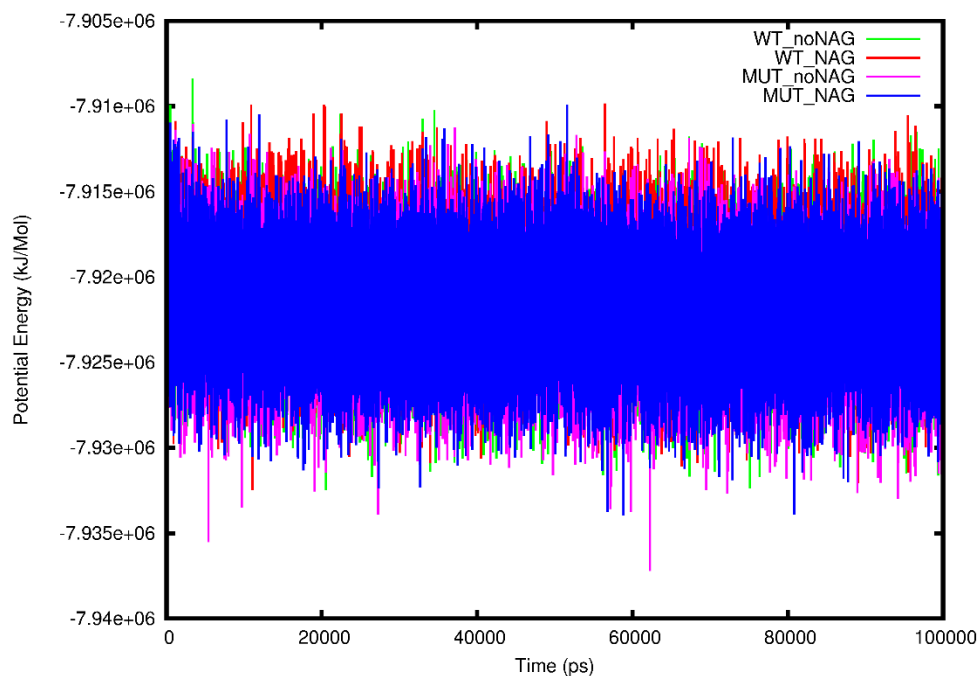
28. Gibb WRG, Lees AJ. The relevance of the Lewy body to the pathogenesis of idiopathic Parkinson's disease. *J. Neurol. Neurosurg. Psychiatry*. 1988; pp. 745–752. <https://doi.org/10.1136/jnnp.51.6.745> PMID: 2841426
29. Sambrook J, Russell DW. Rapid Isolation of Mammalian DNA. *Cold Spring Harb Protoc*. 2006; 2006: pdb.prot3514. <https://doi.org/10.1101/pdb.prot3514> PMID: 22485273
30. Li H. Aligning sequence reads, clone sequences and assembly contigs with BWA-MEM. *arXiv Prepr*. 2013; arXiv:1303.3997.
31. Wang K, Li M, Hakonarson H. ANNOVAR: Functional annotation of genetic variants from high-throughput sequencing data. *Nucleic Acids Res*. 2010; 38: e164. <https://doi.org/10.1093/nar/gkq603> PMID: 20601685
32. Koressaar T, Remm M. Enhancements and modifications of primer design program Primer3. *Bioinformatics*. 2007; 23: 1289–1291. <https://doi.org/10.1093/bioinformatics/btm091> PMID: 17379693
33. Schwede T, Kopp J, Guex N, Peitsch MC. SWISS-MODEL: An automated protein homology-modeling server. *Nucleic Acids Res*. 2003; 31: 3381–3385. <https://doi.org/10.1093/nar/gkg520> PMID: 12824332
34. Deshpande N, Address KJ, Bluhm WF, Merino-Ott JC, Townsend-Merino W, Zhang Q, et al. The RCSB Protein Databank: A redesigned query system and relational database based on the mmCIF schema. *Nucleic Acids Res*. 2005; 33: D233–D237. <https://doi.org/10.1093/nar/gki057> PMID: 15608185
35. DeLano W. Pymol: An open-source molecular graphics tool. *CCP4 Newsl Protein Crystallogr*. 2002; 40: 82–92.
36. Van Der Spoel D, Lindahl E, Hess B, Groenhof G, Mark AE, Berendsen HJC. GROMACS: Fast, flexible, and free. *J Comput Chem*. 2005; 26: 1701–1718. <https://doi.org/10.1002/jcc.20291> PMID: 16211538
37. Huang J, Mackerell AD. CHARMM36 all-atom additive protein force field: Validation based on comparison to NMR data. *J Comput Chem*. 2013; 34: 2135–2145. <https://doi.org/10.1002/jcc.23354> PMID: 23832629
38. Zoete V, Cuendet MA, Grosdidier A, Michielin O. SwissParam: A fast force field generation tool for small organic molecules. *J Comput Chem*. 2011; 32: 2359–2368. <https://doi.org/10.1002/jcc.21816> PMID: 21541964
39. Bussi G, Donadio D, Parrinello M. Canonical sampling through velocity rescaling. *J Chem Phys*. 2007; 126: 014101. <https://doi.org/10.1063/1.2408420> PMID: 17212484
40. Parrinello M, Rahman A. Polymorphic transitions in single crystals: A new molecular dynamics method. *J Appl Phys*. 1981; 52: 7182–7190. <https://doi.org/10.1063/1.328693>
41. Essmann U, Perera L, Berkowitz ML, Darden T, Lee H, Pedersen LG. A smooth particle mesh Ewald method. *J Chem Phys*. 1995; 103: 8577–8593. <https://doi.org/10.1063/1.470117>
42. Humphrey W, Dalke A, Schulten K. VMD: Visual molecular dynamics. *J Mol Graph*. 1996; 14: 33–38. [https://doi.org/10.1016/0263-7855\(96\)00018-5](https://doi.org/10.1016/0263-7855(96)00018-5) PMID: 8744570
43. Williams T, Kelley C. gnuplot 4.4 An Interactive Plotting Program. 2011.
44. Pires DEV, Ascher DB, Blundell TL. DUET: A server for predicting effects of mutations on protein stability using an integrated computational approach. *Nucleic Acids Res*. 2014; 42: W314–W319. <https://doi.org/10.1093/nar/gku411> PMID: 24829462
45. Worth CL, Preissner R, Blundell TL. SDM: A server for predicting effects of mutations on protein stability. *Nucleic Acids Res*. 2011; 39: W215–W222. <https://doi.org/10.1093/nar/gkr363> PMID: 21593128
46. Sunkin SM, Ng L, Lau C, Dolbeare T, Gilbert TL, Thompson CL, et al. Allen Brain Atlas: An integrated spatio-temporal portal for exploring the central nervous system. *Nucleic Acids Res*. 2012; 41: D996–D1008. <https://doi.org/10.1093/nar/gks1042> PMID: 23193282
47. Pontén FK, Schwenk JM, Asplund A, Edqvist PHD. The Human Protein Atlas as a proteomic resource for biomarker discovery. *J Intern Med*. 2011; 270: 428–446. <https://doi.org/10.1111/j.1365-2796.2011.02427.x> PMID: 21752111
48. Kanehisa M, Goto S. Yeast Biochemical Pathways. KEGG: Kyoto encyclopedia of genes and genomes. *Nucleic Acids Res*. 2000; 28: 27–30. <https://doi.org/10.1093/nar/28.1.27> PMID: 10592173
49. Mi H, Thomas P. PANTHER pathway: an ontology-based pathway database coupled with data analysis tools. In: Nikolsky Y, Bryant J, editors. *Protein Networks and Pathway Analysis Methods in Molecular Biology (Methods and Protocols)*. Humana Press; 2009. pp. 123–140. https://doi.org/10.1007/978-1-60761-175-2_7
50. Nichols WC, Pankratz N, Hernandez D, Paisán-Ruiz C, Jain S, Halter CA, et al. Genetic screening for a single common LRRK2 mutation in familial Parkinson's disease. *Lancet*. 2005; 365: 410–412. [https://doi.org/10.1016/S0140-6736\(05\)17828-3](https://doi.org/10.1016/S0140-6736(05)17828-3) PMID: 15680455

51. Naito Y, Tanabe Y, Lee AK, Hamel E, Takahashi H. Amyloid- β Oligomers Interact with Neurexin and Diminish Neurexin-mediated Excitatory Presynaptic Organization. *Sci Rep*. 2017; 7. <https://doi.org/10.1038/srep42548> PMID: 28211900
52. Tanabe Y, Naito Y, Vasuta C, Lee AK, Soumounou Y, Linhoff MW, et al. IgSF21 promotes differentiation of inhibitory synapses via binding to neurexin2 α . *Nat Commun*. 2017; 8. <https://doi.org/10.1038/s41467-017-00333-w> PMID: 28864826
53. Brito-Moreira J, Lourenco M V, Oliveira MM, Ribeiro FC, Ledo JH, Diniz LP, et al. Interaction of amyloid- β (A β) oligomers with neurexin 2 α and neuroligin 1 mediates synapse damage and memory loss in mice. *J Biol Chem*. 2017; 292: 7327–7337. <https://doi.org/10.1074/jbc.M116.761189> PMID: 28283575
54. Botstein D, Risch N. Discovering genotypes underlying human phenotypes: Past successes for mendelian disease, future approaches for complex disease. *Nat Genet*. 2003; 33: 228–237. <https://doi.org/10.1038/ng1090> PMID: 12610532
55. Krumm N, Sudmant PH, Ko A, O’Roak BJ, Malig M, Coe BP, et al. Copy number variation detection and genotyping from exome sequence data. *Genome Res*. 2012; 22: 1525–1532. <https://doi.org/10.1101/gr.138115.112> PMID: 22585873
56. Fromer M, Moran JL, Chambert K, Banks E, Bergen SE, Ruderfer DM, et al. Discovery and statistical genotyping of copy-number variation from whole-exome sequencing depth. *Am J Hum Genet*. 2012; 91: 597–607. <https://doi.org/10.1016/j.ajhg.2012.08.005> PMID: 23040492

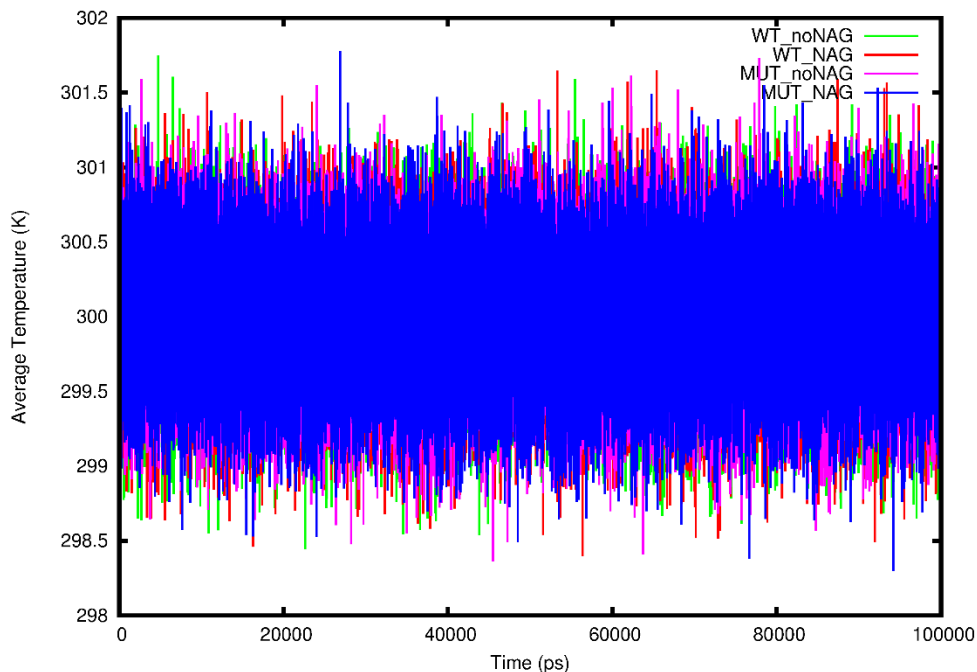
Supplementary Figures



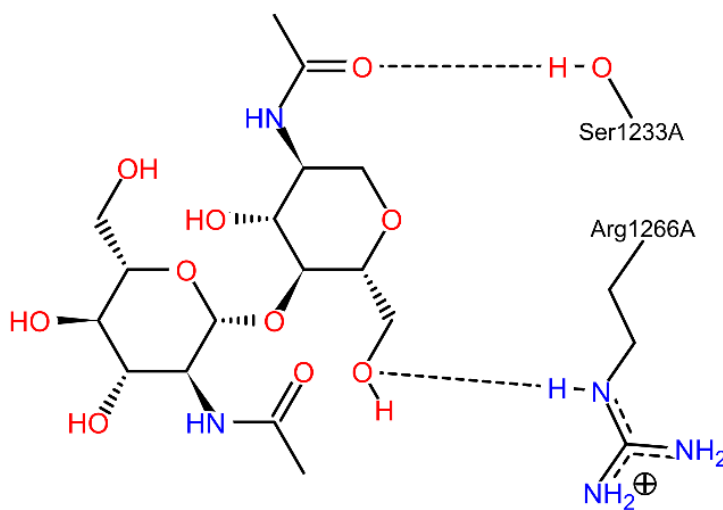
Supplementary Figure S1: Total energy of the four systems of NRXN2 (WT_noNAG, MUT_noNAG, WT_NAG and MUT_NAG) over 100 ns.



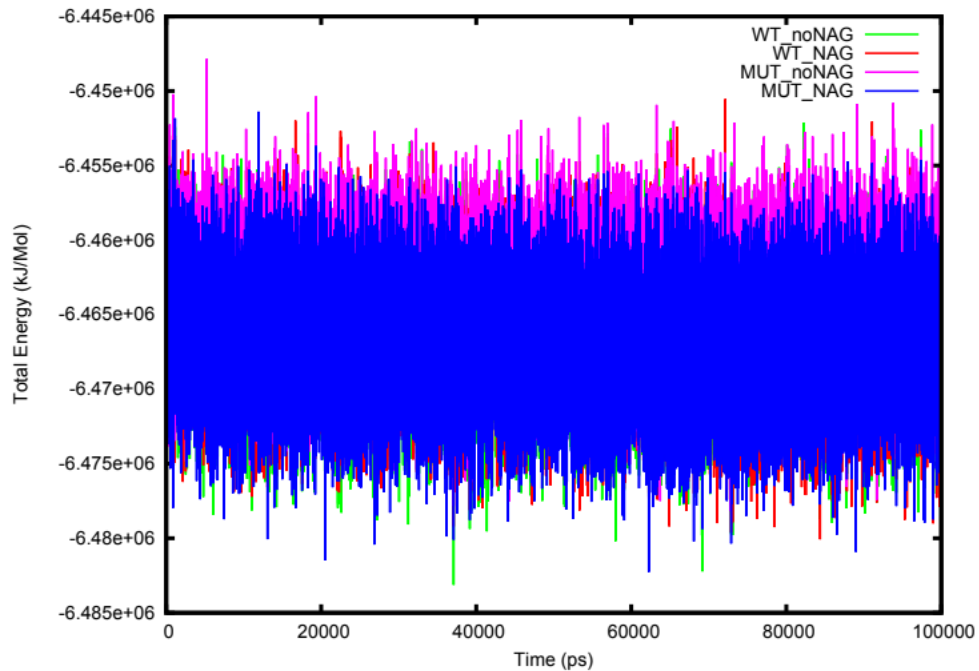
Supplementary Figure S2: Potential energy of the four systems of NRXN2 (WT_noNAG, MUT_noNAG, WT_NAG and MUT_NAG) over 100 ns.



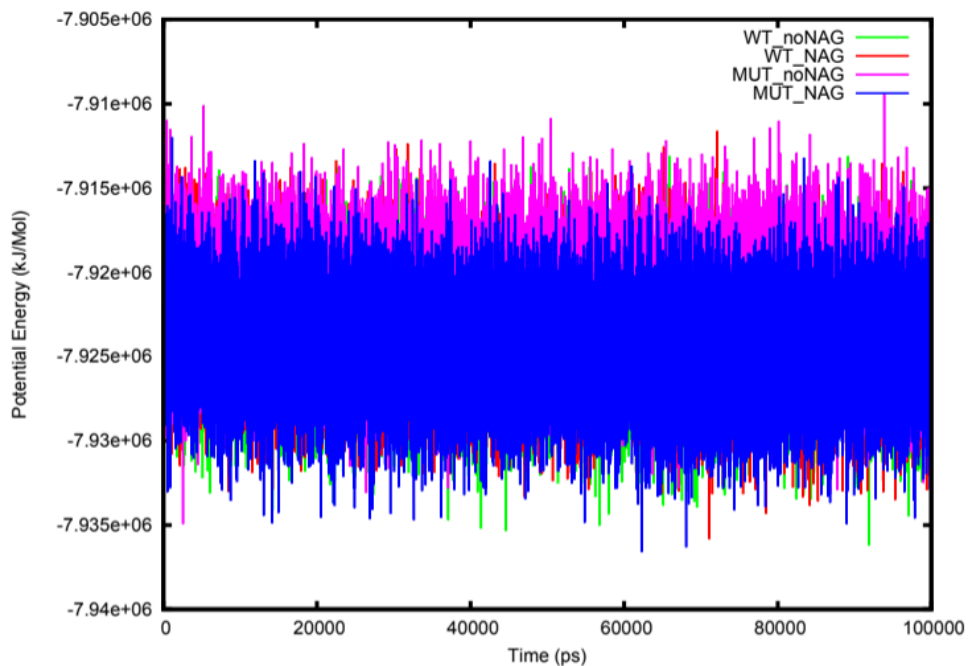
Supplementary Figure S3: The average temperature of the four systems of NRXN2 (WT_noNAG, MUT_noNAG, WT_NAG and MUT_NAG) over 100 ns.



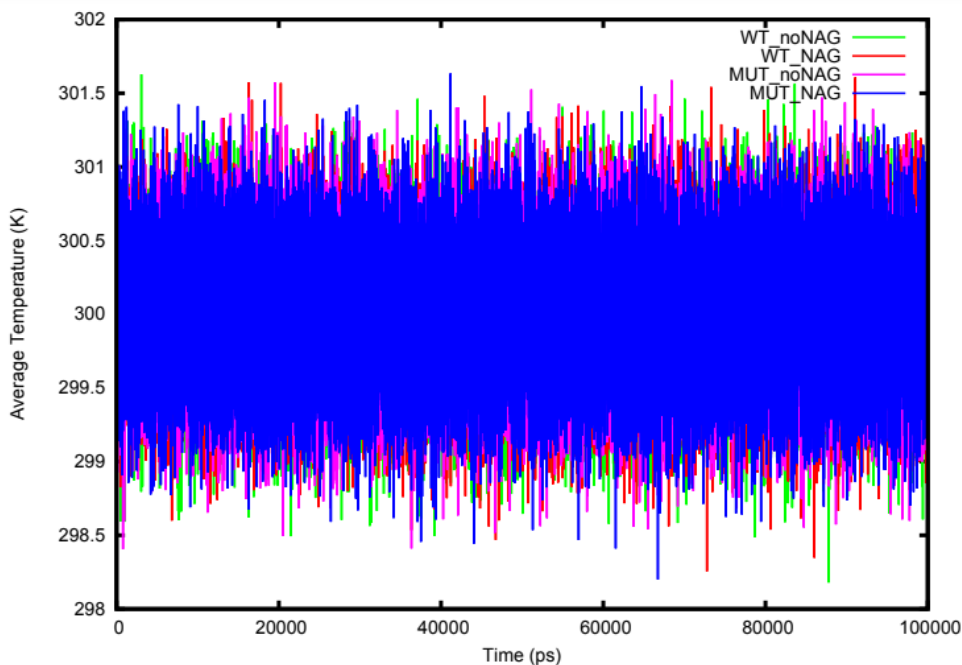
Supplementary Figure S4: 2D interaction diagram showing polar contacts formed between NRXN2 residues and sugar moiety NAG. Figure generated using PoseView. Dashed lines show hydrogen bond contacts formed NAG and NRXN2 residues.



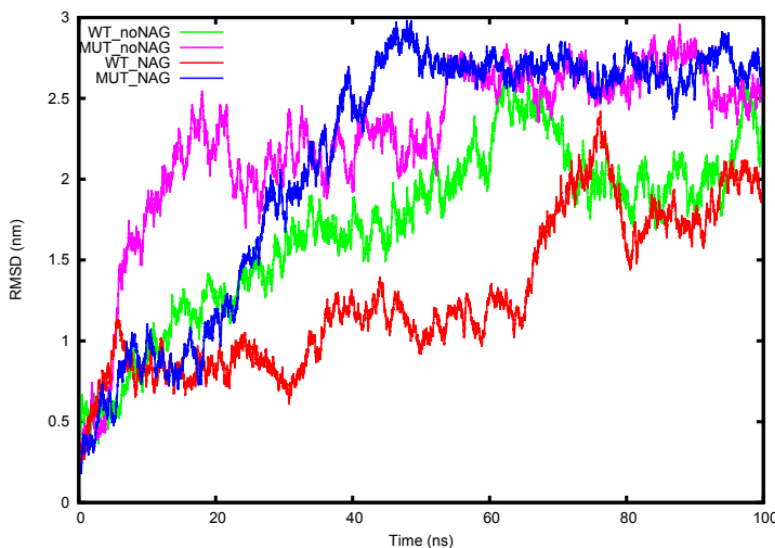
Supplementary Figure S5: Total energy of the four systems of the repeat 1 of NRXN2 (WT_noNAG, MUT_noNAG, WT_NAG and MUT_NAG) over 100 ns.



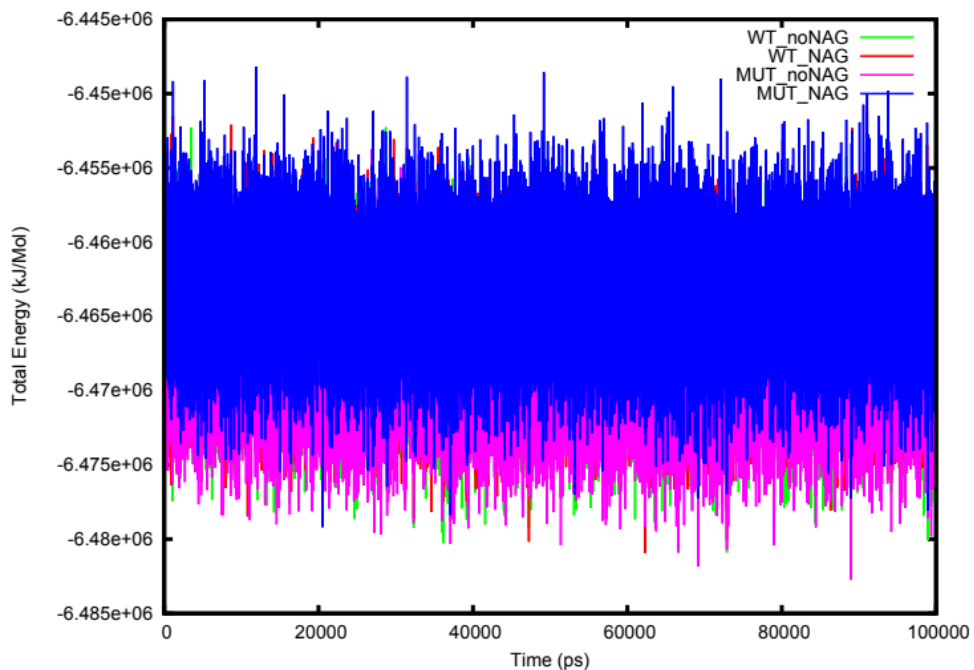
Supplementary Figure S6: Potential energy of the four systems of repeat 1 of NRXN2 (WT_noNAG, MUT_noNAG, WT_NAG and MUT_NAG) over 100 ns.



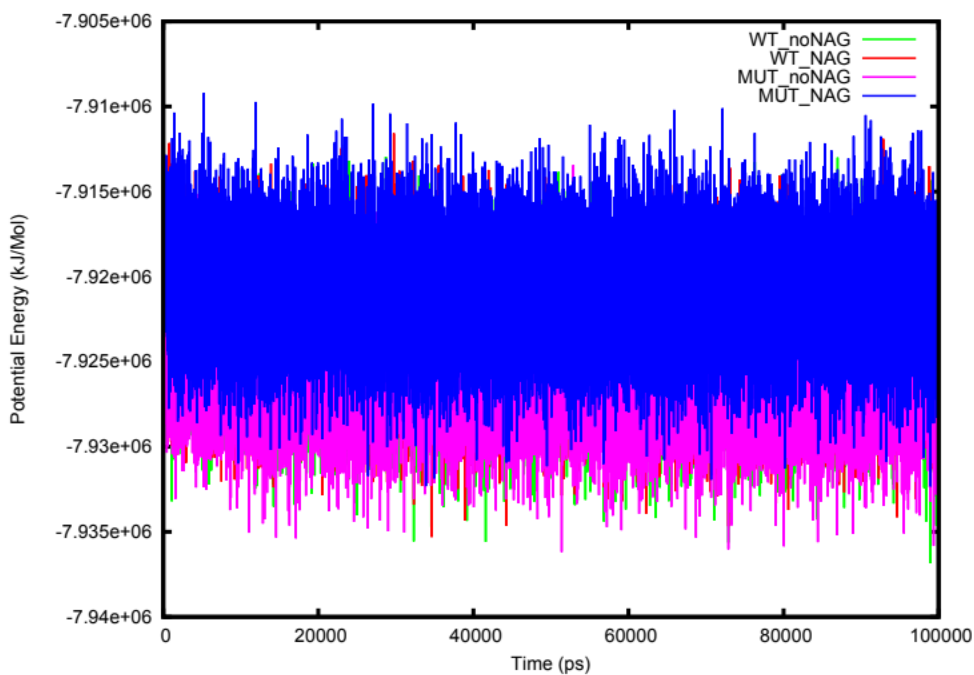
Supplementary Figure S7: The average temperature of the four systems of repeat 1 NRXN2 (WT_noNAG, MUT_noNAG, WT_NAG and MUT_NAG) over 100 ns.



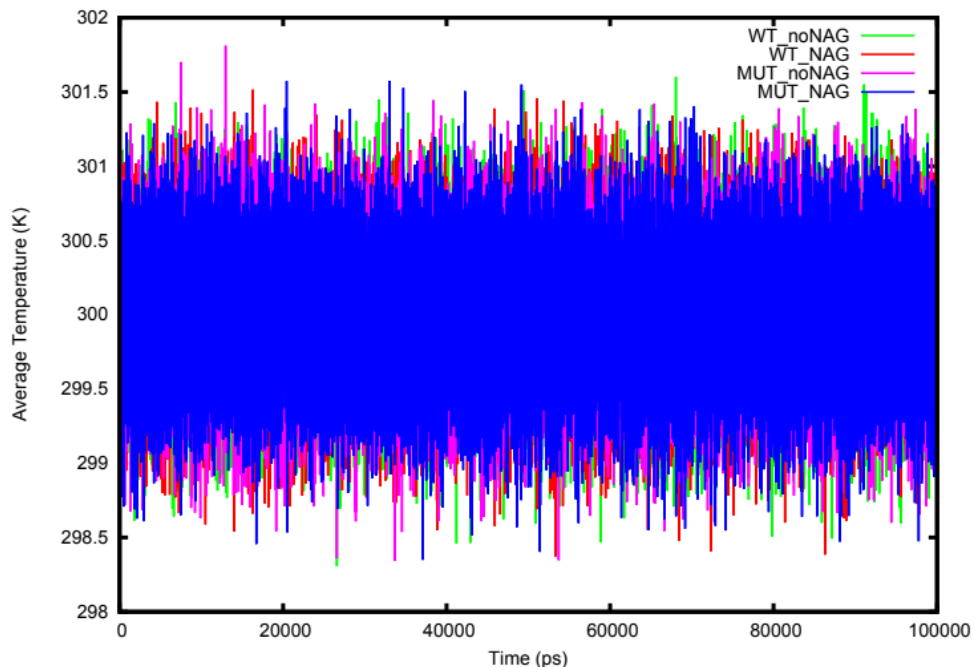
Supplementary Figure S8: RMSD deviation of the backbone atoms for the four systems of repeat 1 NRXN2. MEAN + STDEV ($1.71\text{nm} \pm 0.52$, $2.26\text{nm} \pm 0.52$, $1.27\text{nm} \pm 0.46$ and $2.14\text{nm} \pm 0.79$). Line colours: WT_noNAG = green, MUT_noNAG = light magenta, WT_NAG = red and MUT_NAG = blue.



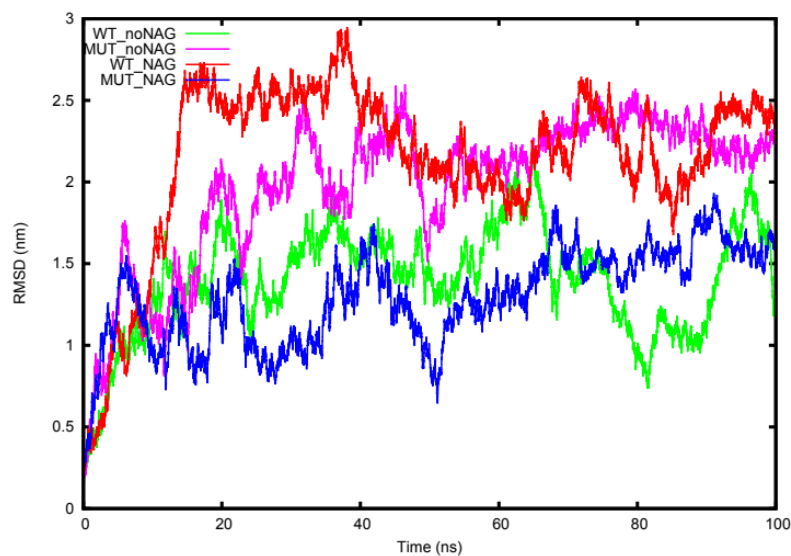
Supplementary Figure S9: Total energy of the four systems of the repeat 2 of NRNX2 (WT_noNAG, MUT_noNAG, WT_NAG and MUT_NAG) over 100 ns.



Supplementary Figure S10: Potential energy of the four systems of repeat 2 of NRNX2 (WT_noNAG, MUT_noNAG, WT_NAG and MUT_NAG) over 100 ns.



Supplementary Figure S11: The average temperature of the four systems of repeat 2 NRNX2 (WT_noNAG, MUT_noNAG, WT_NAG and MUT_NAG) over 100 ns.



Supplementary Figure S12: RMSD deviation of the backbone atoms for the four systems of repeat 2 NRXN2, ($1.40\text{nm} \pm 0.33$, $1.98\text{nm} \pm 0.45$, $2.15\text{nm} \pm 0.51$ and $1.29\text{nm} \pm 0.29$). Line colours: WT_noNAG = green, MUT_noNAG = light magenta, WT_NAG = red and MUT_NAG = blue

Supplementary Tables

Supplementary Table S1: Clinical and demographic information on members of a South African family with Parkinson's disease

	Affected					Unaffected			
Individual lab ID	III-8	III-7	IV-2	III-6	III-2	III-4	IV-1	III-1	III-5
Gender	Male	Male	Male	Female	Female	Male	Male	Female	Male
Age in 2021 (years)	66	72	47	75	83	72	46	74	76
Age at evaluation	55	60	44	72	77	62	35	68	67
Age at onset (years)	48	42	37	70	75	N/A	N/A	N/A	N/A
Childhood symptoms	Reported to have walked	None	None	None	None	N/A	N/A	N/A	N/A

	on toes since childhood								
Initial symptoms	Muscle spasm in left arm, poor balance, walking on toes	Impaired concentration Weakness of legs, and difficulty walking	Difficulty with walking and balance	Cramping lower legs	Difficulty with fine motor ADL; left hand tremor	N/A	N/A	N/A	N/A
Olfaction	Impaired	Normal	Always poor	Normal	Impaired	N/A	N/A	N/A	N/A
Excessive sweating	No	Yes	No	No	No	N/A	N/A	N/A	N/A
RBD	No	No	No	No	Yes	N/A	N/A	N/A	N/A
Orthostatic hypotension	Yes	Onset age 45	No	No	No	N/A	N/A	N/A	N/A
Bladder function	Mild difficulty	Normal	Normal	Normal	Normal	N/A	N/A	N/A	N/A
Constipation	Yes	none	No	No	Yes	N/A	N/A	N/A	N/A
Sleep impairment	No	Yes	No	No	Yes	N/A	N/A	N/A	N/A
Dystonia	Initially walked on toes.	Dystonic flexion of left arm when walking	Facial	No	No	N/A	N/A	N/A	N/A

	Dystonia of left leg after medication								
Tremor	Developed later, predominantly action tremor, with intention component	Action/intention	No	No	Initial complaint	N/A	N/A	N/A	N/A
Bradykinesia	Marked, asymmetrical, predominantly upper limbs	Markedly asymmetrical in upper and lower limbs	Mild bilateral	Mild bilateral	mild bilateral	N/A	N/A	N/A	N/A
Rigidity	Bilateral cogwheel	Marked asymmetry	Mild bilateral, asymmetrical	Normal tone	unilateral	N/A	N/A	N/A	N/A
Gait	Shuffling gait, with absent arm swing	Broad-based, diminished arm swing	Mild slowing	Normal	Slowed	N/A	N/A	N/A	N/A
Additional findings	Diminished vibration sense in toes	Diminished vibration and loss of joint position sense in toes. No evident	Micrographia	None	None	N/A	N/A	N/A	N/A

		axonal or demyelinating changes in tibial, peroneal or sural conductions.							
Total daily dose levodopa (mg)	1000	600	0	0	0	N/A	N/A	N/A	N/A
Levodopa responsive	Yes	Yes	N/A	N/A	Not known	N/A	N/A	N/A	N/A
Blood pressure	No orthostatic drop	No orthostatic drop	No orthostatic drop	No orthostatic drop	No orthostatic drop	N/A	N/A	N/A	N/A
Reflexes	Hyperreflexia present	Hyperreflexia in lower limbs	Hyperreflexia in lower limbs, right > left	Normal	Normal	N/A	N/A	N/A	N/A
Brain CT scan	No abnormality except for internal capsule lacune	Not done	Not done	Not done	Not done	N/A	N/A	N/A	N/A

UPDRS	41	37	16	11	15	N/A	N/A	N/A	N/A
MOCA	26	27	30	28	Not done	N/A	N/A	N/A	N/A

ADL, Activities of Daily Living; RBD, REM sleep behavior disorder; MOCA, Montreal Cognitive Assessment; N/A, not applicable; UPDRS, Unified Parkinson Disease Rating Scale

Supplementary Table S2: Summary of whole exome sequencing (WES) metrics in the three affected individuals

	Individual III-7	III-8	IV-2
Total number of reads	136,048,746	127,298,302	114,750,902
Non-duplicated reads	90,255,052	97,195,484	85,612,771
Reads aligned to target	82,045,320 (90,9%)	83,570,035 (86%)	74,665,623 (87,2%)
Mean target coverage (%)	88.12	79.88	71.04
Total number of variants	22,318	22,566	22,531

CHAPTER 4

Review of Neurexins in Neurodegenerative and Neuropsychiatric Disorders

This chapter consists of a peer-reviewed, published review article that addressed **Objective 2** of this study. Since we prioritised the p.G849D variant in *NRXN2*, we wanted to investigate the potential role of neurexins in human disease. As part of this, we examined the interacting partners of neurexins and their biological pathways using *in silico* tools. Thereafter, we performed a literature search, focusing on neurexins in neurodegenerative disorders as well as neuropsychiatric disorders.

Published Article: Emerging evidence implicating a role for neurexins in neurodegenerative and neuropsychiatric disorders

Authors: Cuttler, K., Hassan, M., Carr, J., Cloete, R., Bardien, S.

Journal: Open Biology (Impact Factor: 5.934)

DOI: <https://doi.org/10.1098/rsob.210091>

Supplementary material: This can be found in the [online version](#) of the article.

Declarations

Declaration by the candidate

With regard to the published review article (DOI: <https://doi.org/10.1098/rsob.210091>) constituting Chapter 4 of the dissertation, the nature and scope of my contribution were as follows:

Comprehensively searched for and collated the appropriate literature for the review article, created all tables and figures, wrote the first manuscript draft, prepared all supplementary material of the article, revised, reviewed, and edited the manuscript (extent of contribution = 80%).

Disclaimer: This article was published under an Open Access CC-BY license. Therefore, this article is permitted to be included in full or in part in a thesis or dissertation for non-commercial purposes without the need to request permission from the publisher (Royal Society of Biology).

The following co-authors have contributed to Chapter 4:

Name	E-mail Address	Nature of Contribution	Extent of Contribution (%)
Maryam Hassan	Hassanmaryam8231@gmail.com	<ul style="list-style-type: none"> Assisted with analyses 	2.5
Jonathan Carr	jcarr@sun.ac.za	<ul style="list-style-type: none"> Clinical expertise Manuscript review and editing. 	2.5
Ruben Cloete	ruben@sanbi.ac.za	<ul style="list-style-type: none"> Assisted with analyses Manuscript review and editing. Supervision 	5
Soraya Bardien	sbardien@sun.ac.za	<ul style="list-style-type: none"> Research project conception and organization. Manuscript review and editing. Supervision 	10

Signature of candidate:

Date: 10/03/2022

Declaration by co-authors

The undersigned hereby confirm that

1. the declaration above accurately reflects the nature and extent of the contributions of the candidate and the co-authors to Chapter 4,
2. no other authors contributed to Chapter 4, besides those specified above, and
3. potential conflicts of interest have been revealed to all interested parties and that the necessary arrangements have been made to use the material in Chapter 4 of this dissertation.

Name	Signature	Affiliation	Date
Maryam Hassan		South African National Bioinformatics Institute (SANBI), University of the Western Cape, Cape Town, South Africa	23/02/2022
Jonathan Carr		Stellenbosch University, Cape Town, South Africa	22/02/2022
Ruben Cloete		South African National Bioinformatics Institute (SANBI), University of the Western Cape, Cape Town, South Africa	24/02/2022
Soraya Bardien		Stellenbosch University, Cape Town, South Africa	10/03/2022

Review



Cite this article: Cuttler K, Hassan M, Carr J, Cloete R, Bardien S. 2021 Emerging evidence implicating a role for neurexins in neurodegenerative and neuropsychiatric disorders. *Open Biol.* **11**: 210091. <https://doi.org/10.1098/rsob.210091>

Received: 13 April 2021

Accepted: 25 August 2021

Subject Area:

genetics/cellular biology/molecular biology

Keywords:

neurexin, neuroligin, synapse, neurodegenerative disorders, neuropsychiatric disorders, protein interactions

Author for correspondence:

Katelyn Cuttler

e-mail: kcuttler@sun.ac.za

Electronic supplementary material is available online at <https://doi.org/10.6084/m9.figshare.c.5628933>.

Emerging evidence implicating a role for neurexins in neurodegenerative and neuropsychiatric disorders

Katelyn Cuttler¹, Maryam Hassan³, Jonathan Carr^{2,4}, Ruben Cloete³ and Soraya Bardien^{1,4}

¹Division of Molecular Biology and Human Genetics, Department of Biomedical Sciences, and ²Division of Neurology, Department of Medicine, Faculty of Medicine and Health Sciences, Stellenbosch University, Cape Town, South Africa

³South African Medical Research Council Bioinformatics Unit, South African National Bioinformatics Institute, University of the Western Cape, Cape Town, South Africa

⁴South African Medical Research Council/Stellenbosch University Genomics of Brain Disorders Research Unit, Cape Town, South Africa

KC, 0000-0003-1833-5426

Synaptopathies are brain disorders characterized by dysfunctional synapses, which are specialized junctions between neurons that are essential for the transmission of information. Synaptic dysfunction can occur due to mutations that alter the structure and function of synaptic components or abnormal expression levels of a synaptic protein. One class of synaptic proteins that are essential to their biology are cell adhesion proteins that connect the pre- and post-synaptic compartments. Neurexins are one type of synaptic cell adhesion molecule that have, recently, gained more pathological interest. Variants in both neurexins and their common binding partners, neuroligins, have been associated with several neuropsychiatric disorders. In this review, we summarize some of the key physiological functions of the neurexin protein family and the protein networks they are involved in. Furthermore, examination of published literature has implicated neurexins in both neuropsychiatric and neurodegenerative disorders. There is a clear link between neurexins and neuropsychiatric disorders, such as autism spectrum disorder and schizophrenia. However, multiple expression studies have also shown changes in neurexin expression in several neurodegenerative disorders, including Alzheimer's disease and Parkinson's disease. Therefore, this review highlights the potential importance of neurexins in brain disorders and the importance of doing more targeted studies on these genes and proteins.

1. Introduction

There is accumulating evidence to suggest that synaptic dysfunction is present in both neuropsychiatric disorders, such as autism spectrum disorders (ASDs), schizophrenia and bipolar disorder (BD), and neurodegenerative disorders, such as Parkinson's disease (PD), Alzheimer's disease (AD) and Huntington's disease (HD) [1]. In fact, involvement of the synapse is such a prominent feature of the pathogenesis of various brain disorders that it has led to the coining of a specific term, 'synaptopathies'. Indeed, in the case of PD, the involvement of synaptopathy as an initial and central event in the disease pathogenesis, which precedes neuronal damage, has been postulated [2]. Synaptic dysfunction can occur due to mutations that alter the structure and function of synaptic components or abnormal expression levels of a synaptic protein.

Synapses are specialized junctions between neurons that transmit information and they connect neurons into millions of 'neural circuits' that underlie all brain functions [3]. The information transmitted allows the nervous system to respond

to external stimuli and controls bodily functions, behaviour, emotions and memories [4]. This system is tightly controlled and regulated, and even slight perturbations can lead to synaptic dysfunction. An important aspect of synapse biology is the cell adhesion molecules that connect pre- and post-synaptic compartments [5]. These interactions in the synaptic cleft help to maintain synapse structure by delineating mutual boundaries [6]. These proteins are also important in synapse plasticity as synaptic cell adhesion is able to regulate the remodelling of synapses [7]. Interestingly, they are also involved in trans-synaptic signalling [5]. Thus, these proteins are highly important in the organization of synaptic junctions and overall brain function.

Neurexins are one type of synaptic cell adhesion molecule. They are pre-synaptically localized and bind to neuroligins and other proteins in the post-synapse (figure 1). Neurexins and their common binding partners, neuroligins, have recently gained more pathological interest as variants in both have been associated with several neuropsychiatric disorders, including autism and schizophrenia [8]. This further suggests that synaptic dysfunction plays a role in the development of these disorders. Synaptic dysfunction is also known to occur in neurodegenerative disorders [9]; however, it was considered an endpoint of these disorders, due to the considerably later onset of clinical symptoms and progressive appearance of cognitive deficits. This dichotomy has, recently, been challenged by the creation of 'disease-in-a-dish' models for multiple central nervous system (CNS) pathologies [9]. This research has identified commonalities between developmental and degenerative disorders, at both the cellular and molecular level, with most of these common mechanisms meeting at the synapse level [9]. Indeed, our laboratory has, recently, found a novel variant (p.G849D) in the *NRXN2* gene which may be implicated in PD [10]. Therefore, we believe it is important to investigate the potential role of neurexins in various neuropsychiatric and neurodegenerative disorders.

In this review, we summarize some of the key physiological functions of the neurexin protein family and the protein networks they are involved in. We also examine the available published literature to determine what research has been done on neurexins in neuropsychiatric and neurodegenerative disorders. This analysis provides an overview on what progress has been made in understanding the roles of synaptic functioning in these disorders and reveals the gaps in knowledge in this field.

2. Structure and biological functions of neurexins

Neurexins were first identified using affinity chromatography when neurexin 1 α was found in rat brain extract on a column of α -latrotoxin [11]. α -latrotoxin is a potent neurotoxin from black widow spider venom that stimulates synaptic vesicle exocytosis and induces massive neurotransmitter release [12]. This work has been continued by Südhof and co-workers [13] who have characterized the neurexin proteins and their binding partners, the neuroligins [14].

In mammals, the neurexins are encoded by three *NRXN* genes (*NRXN1-3*), each of which has both an upstream promoter that is used to generate the α -neurexins, and a downstream promoter that is used to generate the shorter β -neurexins [13,15]. Neurexins also undergo extensive alternate splicing

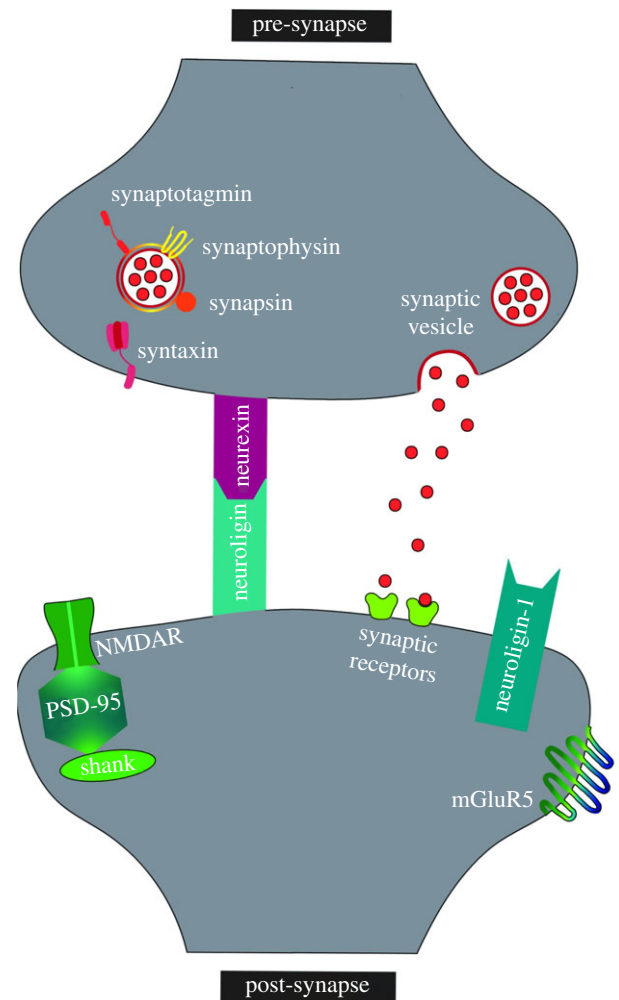


Figure 1. Location of neurexins and their binding partners, neuroligins, in the synapse. Several neurexin–neuroligin pathway proteins are shown as well as synaptic vesicle-binding proteins. NMDAR, *N*-methyl-D-aspartate receptor; mGluR5, metabolic glutamate receptor 5; PSD-95, post-synaptic density protein 95; Shank, SH3 and multiple ankyrin repeat domains protein.

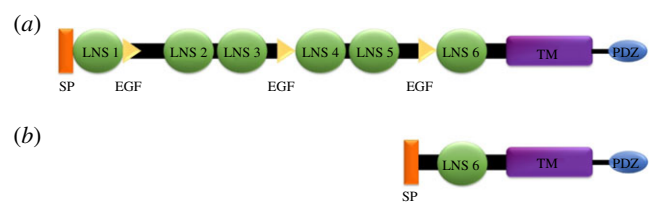


Figure 2. Structural domain organization of the α and β forms of neurexin. (a) α -neurexin. (b) β -neurexin. EGF, epidermal growth factor-like region; LNS, laminin/neurexin/sex hormone-binding domain; PDZ, PSD-95, DLG1, ZO-1 domain; SP, signal peptide; TM, transmembrane domain.

at five splice sites, generating significant diversity of more than 2000 potential variants [13,16]. The fact that neurexin splice insert sequences and their positions are well conserved among neurexin genes and between species supports the idea that alternative splicing has important functional roles.

The neurexins are transmembrane proteins that consist of an extracellular region responsible for trans-synaptic interactions, a transmembrane domain and a smaller cytoplasmic domain named PSD-95, DLG1, ZO-1 binding domain (PDZ) that is involved in intracellular protein interactions and signalling (figure 2) [13]. α -neurexins are composed of six large extracellular laminin/neurexin/sex

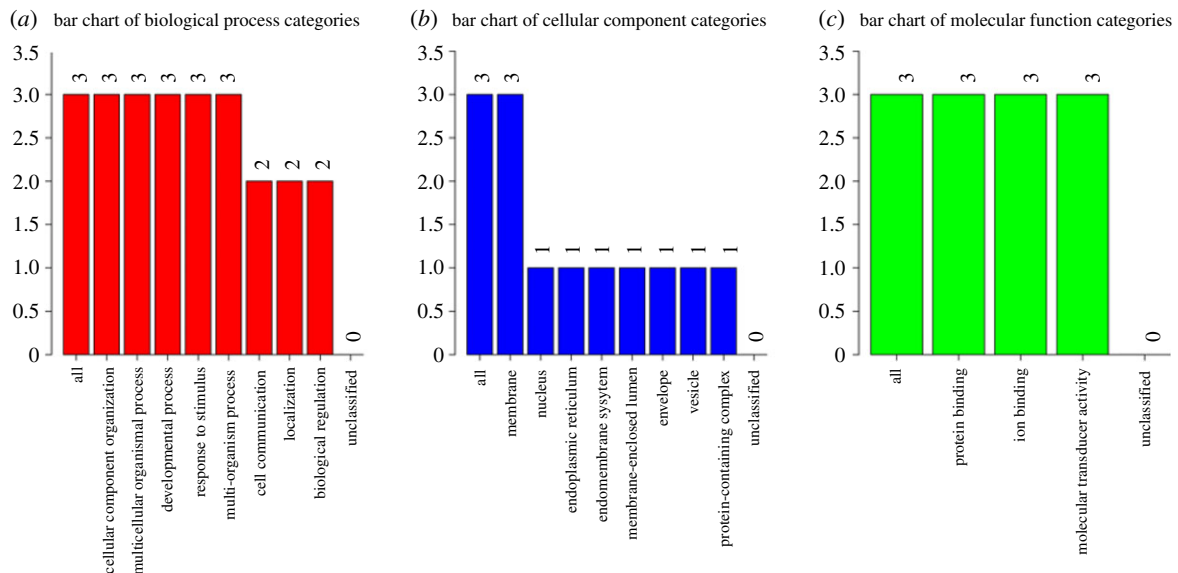


Figure 3. A summary of GO terms associated with neurexins 1–3. (a) Biological processes. (b) Cellular components. (c) Molecular functions. All: total number of proteins analysed. The number above each bar indicates the number of proteins assigned to that category. Figure generated by WebGestalt (<http://www.webgestalt.org>) [18].

hormone-binding (LNS) globulin domains with three interspersed epidermal growth factor (EGF)-like regions (figure 2). β -neurexins are shorter and only have the sixth extracellular LNS domain and no EGF-like regions (figure 2). Only neurexin 1 protein structures (both α and β forms) have been solved experimentally in *Mus musculus*, *Rattus norvegicus* and *Bos taurus*. However, these structures have not yet been solved in humans.

Neurexins are localized pre-synaptically and are distributed to both excitatory and inhibitory synapses [8]. Their functions are mediated by their binding to neuroligins (figure 1). Neuroligins have five known isoforms and are expressed post-synaptically [17]. Consequently, neurexins and neuroligins form synaptic complexes in the synaptic cleft and have been found to control synapse formation, maturation, validation and function [17]. Various combinations of the different neurexins and neuroligin binding partners at synapses may also help determine synapse specificity through differential interactions between multiple splice variants and isoforms of these proteins [8].

Primarily, neurexins function to maintain synaptic organization. Gene ontology (GO) analysis by WebGestalt (<http://www.webgestalt.org>) [18] of the three neurexins indicates that they all function in protein binding, ion binding and possess molecular transducer activity (figure 3). They are also involved in cellular component organization, developmental processes, response to stimuli, cell communication and biological regulation. These processes thus demonstrate how neurexins are able to maintain synaptic organization but also show their multi-functional nature. As such, it is conceivable that disruptions in neurexins could be detrimental to their various functions and affect overall neuronal function and integrity.

3. Biological pathways and interacting partners of neurexins

To understand the broader biological pathways that the neurexins are involved in, protein–protein interaction network

analysis and co-expression analysis was performed using the tools, STRING (<https://string-db.org>) [19] and GeneMania (<https://genemania.org>) [20]. STRING finds related genes by accessing the STRING database which contains experimental data and computational predictions. Data in STRING are weighted and integrated and a confidence score of 0–1 is calculated for all interacting protein partners. GeneMANIA finds proteins related to neurexins by leveraging functional association data, such as interactions, pathways, co-expression, co-localization and protein domain similarity. All functional data for the proteins observed in these networks were obtained from UniProt (<https://www.uniprot.org>) [21], unless otherwise stated, while pathway data were obtained from KEGG (<https://www.kegg.jp>) [22].

3.1. String analysis

Weighted string analysis was conducted on neurexin 1, 2 and 3 individually to determine their binding partners (figure 4a–c). Based on this analysis, there is strong evidence that neurexin 1 interacts with 10 proteins including calcium/calmodulin-dependent serine protein kinase (CASK), leucine-rich repeat transmembrane neuronal protein 1 (LRRTM1), LRRTM2, LRRTM3, neuroligin 1, neuroligin 2, neuroligin 3, neuroligin 4X, SH3 and multiple ankyrin repeat domains protein 2 (SHANK2) and synaptotagmin-1 with scores of 0.987, 0.983, 0.985, 0.975, 0.998, 0.997, 0.998, 0.997, 0.975, 0.974, respectively. Similarly, neurexins 2 and 3 also have 10 interactors each. There is strong evidence that neurexin 2 interacts with CASK, discs large homologue 4 (DLG4), LRRTM1, LRRTM2, LRRTM3, neuroligin 1, neuroligin 2, neuroligin 3, neuroligin 4X and SHANK2 with scores of 0.979, 0.977, 0.984, 0.983, 0.972, 0.998, 0.998, 0.998, 0.997 and 0.969, respectively. There is strong evidence that neurexin 3 interacts with CASK, DLG4, LRRTM1, LRRTM2, LRRTM3, neuroligin 1, neuroligin 2, neuroligin 3, neuroligin 4X and SHANK2 with scores of 0.978, 0.971, 0.979, 0.983, 0.971, 0.998, 0.997, 0.997, 0.997 and 0.969, respectively. The STRING analyses performed on the three neurexins identified

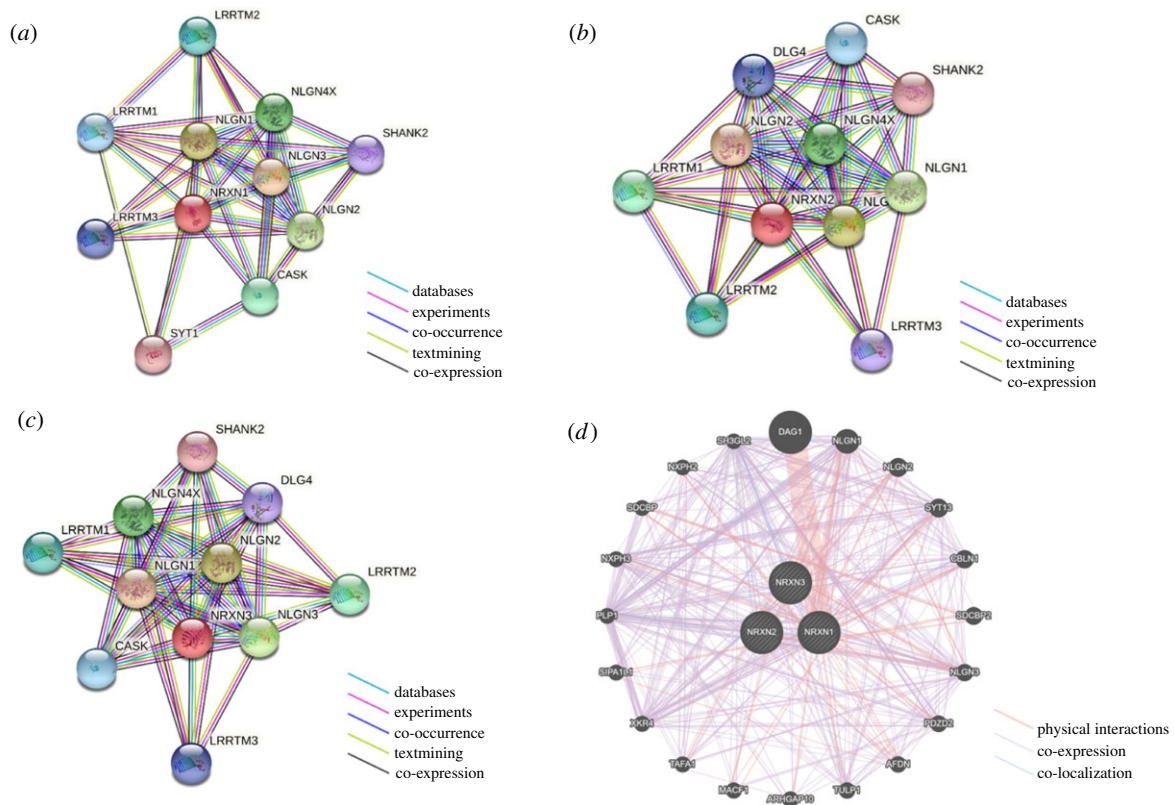


Figure 4. Protein interacting partners of neurexins 1–3. (a–c) STRING network of neurexins 1–3. Nodes represent gene-encoded proteins. Edges represent protein–protein associations. Connections between nodes represent the relationship between proteins. A bold line implies a higher confidence level. (d) GeneMANIA network of all three neurexins. Nodes represent gene-encoded proteins. Larger nodes indicate higher protein scores. Edges represent protein–protein associations. Connections between nodes represent the relationship between proteins. A bold line implies a higher confidence level.

interacting proteins with very high confidence scores since the lowest score across the analyses was 0.969. This means that there is strong experimental evidence that these proteins interact with one or more of the neurexins.

Analysis of the identified neurexin binding partners revealed many proteins important in the maintenance and functioning of synapses. Notably, variants in several of these proteins are implicated in neuropsychiatric and developmental disorders. Variants in neuroligin 1 and SHANK2 have been implicated in susceptibility to autism [23,24], while variants in neuroligin 3 have been implicated in Asperger syndrome and autism [25]. Variants in neuroligin 4X have been implicated in X-linked forms of Asperger syndrome, autism susceptibility and mental retardation [25–27]. Variants in CASK have been implicated in FG syndrome 4, an X-linked genetic disorder and mental retardation [28–32], variants in DLG4 have been implicated in intellectual developmental disorder 62 [33,34] and variants in synaptotagmin-1 have been implicated in Baker–Gordon syndrome [35].

Furthermore, binding partners of these proteins as well as the pathways they occur in could also give insight into the development of disease. CASK binds to amyloid precursor protein and neuroligin 1 binds to amyloid- β , both of which are important in AD. LRRTM3 is also a known positive regulator of amyloid- β formation. Notably, LRRTM3 may be considered a candidate gene for late-onset AD as it promotes the processing of amyloid precursor protein which leads to toxic amyloid- β accumulation [36]. DLG4 is involved in dopamine receptor binding and synaptotagmin-1 regulates dopamine secretion. The loss of dopamine functioning is crucial in PD. Indeed, DLG4 is involved in several pathways of

neurodegeneration (in multiple diseases), the HD pathway as well as cocaine addiction.

3.2. GeneMANIA

GeneMANIA analysis was performed on the neurexins to reveal further potential protein–protein interactions (figure 4d; electronic supplementary material, table S1). We performed the analysis by selecting only proteins with stronger evidence of neurexin interactions, such as interactions with physical evidence, and evidence from co-expression and co-localization studies.

All of the binding partners observed by STRING analysis were still present; however, more interacting proteins were also identified. These proteins have more diverse functions but still function in overall synapse maintenance.

This analysis further identified afadin (AFDN), Rho GTPase activating protein 10 (ARHGAP10), cerebellin 1 (CBLN1), dystroglycan (DAG1), microtubule actin cross-linking factor 1 (MACF1), neurexophilin-2, neurexophilin-3, PDZ domain-containing protein 2 (PDZD2), proteolipid protein 1 (PLP1), syndecan binding protein 1 (SDCBP), SDCBP2, SH3 domain-containing GRB2-like protein 2 (SH3GL2), signal-induced proliferation-associated 1-like protein 1 (SIPA1L1), synaptotagmin-13 (SYT13) Tafa chemokine-like family member 1 (Tafa1), Tubb-like protein 1 (TULP1) and Xk-related protein 4 (XKR4) as interactors of one or more neurexin proteins. AFDN, ARHGAP10, MACF1 and SIPA1L1 are all involved in actin filament binding/organization, while PDZD2, SDCBP and SDCBP2 are involved in cell binding and cytoskeletal organization.

Dysregulation of any of these proteins could thus affect cell adhesion and binding at the synapse. In addition, variants in *MACF1* have been implicated in lissencephaly 9 with complex brainstem malformation [37]. *CBLN1* is essential for synapse integrity and plasticity and its disruption could lead to synapse dysfunction. *DAG1* has multiple functions, such as laminin and basement membrane assembly, cell survival, peripheral nerve myelination, nodal structure and cell migration. Variants in *DAG1* have been implicated in both type A and type C muscular dystrophy–dystroglycanopathy [38–41]. Muscular dystrophies are genetic disorders characterized by the degeneration of skeletal muscle. Type C muscular dystrophy–dystroglycanopathy affects the limb-girdle area [40], while type C is congenital with brain and eye anomalies [39]. Neurexophilin-2 and neurexophilin-3 are both ligands for α -neurexins and are involved in the neuropeptide signalling pathway. Disruption of these proteins could, therefore, affect neurotransmitter release and the subsequent signalling. *PLP1* is the major myelin protein in the CNS and is important for maintaining the structure of myelin. Disruption of this protein could, therefore, negatively affect the downstream myelination of neurons, as is seen in multiple sclerosis (MS). Interestingly, *PLP1* is also involved in the development of the substantia nigra, the main brain region affected by PD. Therefore, *PLP1* alterations could also lead to disruptions in this brain region. *SH3GL2* has been implicated in synaptic vesicle endocytosis, while synaptotagmin-13 may be involved in transport vesicle docking to the plasma membrane. Dysregulation of these proteins could thus affect neurotransmitter functioning. *TAF1* is involved in the modulation of neural stem cell proliferation and differentiation; therefore, dysregulation of this protein could result in developmental disorders. *TULP1* is required for normal development of photoreceptor synapses. Variants in *TULP1* are associated with Leber congenital amaurosis [42,43] and retinitis pigmentosa [42,44–47]. However, this protein is also involved in actin filament binding, therefore, its dysregulation could also affect cell adhesion and binding at the synapse. Not much is known about *XKR4* except that it is involved in apoptosis during development. Therefore, its dysregulation could also possibly result in developmental disorders.

GO terms and physiological/pathway information on all binding partners identified by STRING and GeneMANIA are available in electronic supplementary material, figure S1 and table S1.

4. Role of neurexins in neuropsychiatric disorders

Literature-based searches using neurexin as a search term identified several studies that reported an association of neurexins in various neuropsychiatric disorders. The main findings of these studies are reported in table 1 and are summarized below.

4.1. Human studies

NRXN1 has been well documented for its association with ASDs [54]. Several genetic analyses of families and populations of people with ASD have shown that copy number variations (CNVs) and de novo mutational events at the *NRXN1* locus are enriched in ASD [48,49,51,52,54]. In one

study, *NRXN1* was sequenced in cases of ASD with mental retardation [50]. Mutations (c.–3G > T in the Kozak region, c.3G > T at the initiation codon (p.M1), p.R375Q and p.G378S) were found in the *NRXN1 β* coding region thereby potentially implicate synapse dysfunction an important determinant in ASD [50].

The first evidence for a potential role of *NRXN2* in ASD was provided by a report of a frameshift mutation within *NRXN2* exon 12 (c.2733delT) in a boy with ASD and his father who had severe language delay [57]. This mutation results in a truncated neurexin 2 α protein that lacks the binding sites for the established post-synaptic binding partners *LRRTM2* and *neuroligin 2* [57]. Subsequently, a 21-year-old man with a clinical phenotype including autistic traits, such as speech and language deficits and pathological insistence on routine, was reported to have a 570 kb de novo deletion of 24 genes at chromosome 11q13.1, including *NRXN2* [58].

Using microarray analyses on RNA extracted from brain tissue, *Mirnic et al.* [69] did not observe a difference in neurexin 1 expression between schizophrenia (SCZ) and control samples. However, since then, a link between neurexin 1 and SCZ has been reported in other studies. One study reported that *NRXN1* deletions are more common in those with SCZ; however, it also found that there was incomplete penetrance of these deletions in families with SCZ [72]. *Kirov et al.* [70] observed a deletion in an SCZ patient at 2p16.3 that disrupts *NRXN1* and predicted that it was highly likely to be pathogenic. Also, *NRXN1* deletions were shown to segregate with several neuropsychiatric disorders in a study of a complex family [78]. The proband had SCZ and other members of his family had mental retardation, schizophreniform disorder and affective disorder [78]. After genotyping the proband and eight family members, they found two rare deletions upstream of the *NRXN1* gene (2p16.3) that co-segregate with these disorders [78]. Notably, this shows that deletions in *NRXN1* may manifest as multiple neuropsychiatric phenotypes.

Angione et al. [64] implicated *NRXN1* in epilepsy. They identified a 2p16.3 deletion in an 8-year-old male patient diagnosed with epilepsy showing symptoms of myoclonic-astonic seizures (EMAS) [64]. This deletion included the first five exons of the *NRXN1* gene [64].

NRXN genes may also be involved in treatment response. In one study, it was found that variants in *NRXN1* may affect the long-term treatment outcome of patients with BD by modulating the effects of antipsychotics [61]. In a study of *Levetiracetam* resistance, an antiepileptic drug, *Grimminger et al.* [63] found that neurexin 1 is differentially expressed in non-responder and responder patients with mesial temporal lobe epilepsy (mTLE), whereby lower levels of neurexin 1 were observed in responder patients.

4.1.1. Association studies

A genome-wide association study (GWAS) by *Liu et al.* [51] specifically examined *NRXN1* in an autism cohort of the Chinese Han population and discovered 22 variants that were associated with ASD. In this cohort, one SNP (rs2303298) was also significantly associated with a risk of developing ASD [51]. Furthermore, a GWAS of SCZ in Spain showed that a *NRXN1* single nucleotide polymorphism (SNP) (rs3850333) was close to the significance threshold [71], while another GWAS in American patients of European or African ancestry showed that *NRXN1* is associated with antipsychotic

Table 1. List of studies that have implicated neurexin genes in neuropsychiatric disorders. AAV, adeno-associated virus; AGRE, Autism Genetic Resource Exchange; Array-CGH, array comparative genomic hybridization; CBDB, Clinical Brain Disorders Branch; CIBERSAM, Centro de Investigación Biomédica en Red de Salud Mental; CNV, copy number variation; EMAS, epilepsy with myoclonic-atonic seizures; GWAS, genome-wide association study; hESC, human embryonic stem cell; iN, induced neuron; iPSC, induced pluripotent stem cell; KO, knockout; LC-MS/MS, liquid chromatography mass spectrometry/mass spectrometry; mESC, mouse embryonic stem cell; mTLE, mesial temporal lobe epilepsy; NGS, next-generation sequencing; NIMH, National Institute of Mental Health; RT-PCR, reverse transcriptase–polymerase chain reaction; SNP, single nucleotide polymorphism; SSC, Simons Simplex Collection; STEP-BD, Systematic Treatment Enhancement Program for Bipolar Disorder; WT, wild-type.

disorder/disease process	neurexin gene	type of study	methods	main finding	reference
autism spectrum disorder (ASD)	NRXN1	genetic analysis	used SSC samples and the SSC database to extract ‘trios’ consisting of a mother, father and an ASD-affected child performed genetic analyses to identify CNVs	a de novo CNV in <i>NRXN1</i> was discovered in a large cohort of families with a single ASD-affected child and at least one unaffected sibling	[48]
ASD	NRXN1	GWAS	1174 families from SSC were genotyped identified CNVs and de novo events	rare de novo events/CNVs at <i>NRXN1</i> are strongly associated with autism	[49]
ASD	NRXN1 β	genetic analysis	86 patients with both ASD and mental retardation The coding sequence of the <i>NRXN1β</i> gene was analysed by PCR	four novel mutations in <i>NRXN1β</i> were identified by sequencing the exon of the gene in cases with autism and mental retardation	[50]
ASD	NRXN1	genetic analysis	313 ASD patients and 500 healthy controls from a Chinese autism cohort were recruited performed genomic DNA sequencing	22 variants in the <i>NRXN1</i> gene were discovered in the Chinese Han population; one SNP (rs2303298) was significantly associated with a risk of autism in this cohort	[51]
ASD	NRXN1	genetic analysis	2478 ASD individuals from SSC and 719 ASD individuals from AGRE 580 controls from ClinSeq and NIMH used a custom microarray to analyse CNVs	recurrent CNVs in <i>NRXN1</i> are enriched in autism.	[52]
ASD	NRXN1, 2 and 3	cell culture	iPSCs were produced from probands and unaffected family members iPSCs underwent neuronal differentiation to organoids RNA sequencing was performed on both iPSCs and differentiated organoids	neurexin 1, 2 and 3 mRNA is overexpressed in patient-derived iPSCs and differentiated organoids	[53]
ASD	NRXN1	genetic analysis	2591 families from SSC were genotyped identified CNVs, de novo deletions and ASD risk genes	<i>NRXN1</i> is an ASD risk gene	[54]
ASD	NRXN1 and 2	animal study	RNA was isolated from the whole brain of age-matched monoamine oxidase A KO mice and wild-type mice Microarrays were used to determine gene expression levels	neurexin 1 and 2 are downregulated in monoamine oxidase A KO mice	[55]
ASD	α -NRXNs	animal and cell culture study	transfected <i>C. elegans</i> strains and HEK-293 cells with plasmids expressing NRXN1 α and different α 2 δ subunits performed co-immunoprecipitation and pull-down assays	changes in α -neurexin binding to α 2 δ -3 subunits of N-type calcium channels could be important in some forms of autism spectrum disorders	[56]
ASD	NRXN2	genetic analysis	142 ASD patients and 94 non-syndromic controls sequenced NRXN 1,2 and 3 genes	observed a frameshift mutation in <i>NRXN2</i> exon 12 in a patient with ASD inherited from a father with severe language delay	[57]

(Continued.)

Table 1. (Continued.)

disorder/disease process	neurexin gene	type of study	methods	main finding	reference
ASD	NRXN2	genetic analysis	recruited a patient with speech problems, autistic traits and pancreatic gastrinoma performed array-CGH	a de novo 0.57 Mb microdeletion was observed in chromosome 11q13.1, including <i>NRXN2</i>	[58]
ASD	NRXN2	animal study	used previously collected human faecal samples from typically developing children and children with ASD C57BL/6 J weanlings were colonized with human faecal samples brain tissue RNA was extracted and sequenced	mice colonized by microbiota from ASD patients showed differential splicing of <i>NRXN2</i>	[59]
bipolar disorder (BD)	NRXN3	GWAS	obtained participants from a family study of mood disorders in Taiwan (2008–2012) performed a multi-stage GWAS	<i>NRXN3</i> shows a significant association with bipolar disorder	[60]
BD	NRXN1	genetic analysis	obtained patient genotyping and clinical data from STEP-BD analysed data to determine the effect of individual markers on phenotypes	<i>NRXN1</i> may affect the long-term treatment outcome of bipolar disorder	[61]
borderline personality disorder (BPD)	NRXN3	association study	1439 heroin-dependent BPD cases and 507 neighbourhood controls genotyped NRXN3 SNPs and performed an association analysis	several <i>NRXN3</i> SNPs were nominally associated with BPD phenotype in heroin-dependent cases	[62]
epilepsy	NRXN1	microarray analysis	obtained 53 biopsy specimens from mTLE patients performed microarray analysis	neurexin 1 is differentially expressed in non-responder and responder mTLE patients to the antiepileptic drug Levetiracetam lower levels of neurexin 1 are observed in responder patients	[63]
epilepsy	NRXN1	genetic testing	77 patients were identified at Children's Hospital Colorado various genetic tests were conducted	a 2p16.3 deletion, which includes the first five exons of the <i>NRXN1</i> gene, was identified in an 8-year-old male EMAS patient	[64]
epilepsy/seizures	NRXN2 α	animal study	treated adult Wistar rats with kainite or pentylentetrazole to induce seizures isolated total RNA from whole-rat brains and hippocampi performed RT-PCR to determine the levels of different NRXNs	following kainate- and pentylentetrazole-induced seizures in rats, neurexin 2 α expression increased in the dentate gyrus of the hippocampus	[65]
fragile X syndrome	NRXN3	animal study	used male and female WT and FMR1 KO mice (4–6 per experiment) analysed brain sections using riboprobes for NRXN1, 2 and 3 and NLGN 1, 2 and 3	there is increased neurexin 3 mRNA in female fragile X mice, but decreased neurexin 3 mRNA in male fragile X mice	[66]
major depressive disorder (MDD)	NRXN1, 2 and 3	animal study	81 healthy Sprague–Dawley rats were subjected to various mild stress factors extracted proteins from hippocampal post-synaptic density fractions analysis by LC-MS/MS	neurexin 1, 2 and 3 were not differentially expressed in a rat chronic mild stress model of depression	[67]

(Continued.)

Table 1. (Continued.)

disorder/disease process	neurexin gene	type of study	methods	main finding	reference
neuropsychiatric disorders	NRXN1	cell culture	cultured cortical neurons from NRXN1 α KO mice introduced conditional NRXN1 mutations into hESCs using AAV recombination, and differentiated them into human iNs analysed neuronal development, synapse formation and neurotransmitter release	heterozygous NRXN1 mutations are able to selectively impair neurotransmitter release and increase the levels of the synaptic scaffolding protein, CASK in human iNs but not in the cortical neurons of NRXN1 α KO mice	[68]
schizophrenia (SCZ)	NRXN1	microarray analysis	obtained brain tissue from 12 SCZ patients and 10 controls extracted total RNA performed a microarray analysis	the expression of neurexin 1 was not significantly different between the schizophrenic and control subjects	[69]
SCZ	NRXN1	genetic analysis	selected 45 male and 48 female proband-parent trios from a sample of 600 Bulgarian SCZ trios performed Array-CGH	observed a 0.25 Mb deletion on 2p16.3 in both the proband and affected sibling which disrupts <i>NRXN1</i>	[70]
SCZ	NRXN1	GWAS	3063 SCZ patients and 2847 controls from CIBERSAM performed a GWAS at 95 SNPs	the rs3850333 SNP in the <i>NRXN1</i> gene was close to the significant threshold in a GWAS of schizophrenia in Spain	[71]
SCZ	NRXN1	genetic analysis	obtained DNA of 635 SCZ patients and 635 controls from the CBDB Sibling Study genotyped samples and analysed them for CNVs and deletions	<i>NRXN1</i> deletions are more frequent in schizophrenia patients	[72]
SCZ	NRXN1	genetic analysis	data from 572 SCZ patients and 551 controls were used to select genes for sequencing 153 SCZ patients and 153 controls were sequenced for 21 chosen genes using NGS	there is incomplete penetrance of <i>NRXN1</i> deletions in families with schizophrenia missense variants at <i>NRXN1</i> may be protective against schizophrenia susceptibility	[73]
SCZ	NRXN1	cell culture	isolated primary rat neurons from hippocampi differentiated human neurons derived from human iPSCs overexpressed Caveolin-1 in both cell types western blotting was used to measure the expression of proteins involved in synaptic plasticity as well as DISC1, an SCZ-associated protein	overexpressing Caveolin-1, a potential therapeutic for schizophrenia, in neurons increased expression of proteins involved in synaptic plasticity (PSD95, synaptobrevin, synaptophysin, neurexin 1 and syntaxin 1) as well as DISC1	[74]

(Continued.)

Table 1. (Continued.)

disorder/disease process	neurexin gene	type of study	methods	main finding	reference
SCZ	NRXN1	animal study	generated iPSCs from 5 childhood-onset SCZ patients and 4 controls differentiated iPSCs into glial cells transplanted glial cells into mice via injection into the corpus callosum performed molecular analyses on both the differentiated glial cells and chimeric mice	neurexin 1 was downregulated in chimeric mice produced from iPSCs derived from patients with childhood-onset schizophrenia	[75]
SCZ	NRXN1	GWAS	obtained genetic data and treatment response data of 302 SCZ patients treated with lurasidone and 117 SCZ patients treated with a placebo from two clinical SCZ trials performed a GWAS	<i>NRXN1</i> is associated with antipsychotic response to lurasidone in schizophrenia patients	[76]
SCZ	NRXN1	cell culture	generated iPSCs from 3 NRXN1 deletion SCZ patients and 3 controls and differentiated them into human iNs generated mESCs from NRXN1 KO mice analysed neuronal development, synapse formation and neurotransmitter release	heterozygous NRXN1 deletions impair neurotransmitter release and synaptic function, and increase the levels of the synaptic scaffolding protein, CASK in human iNs but not mESCs generated from NRXN1 KO mice	[77]
SCZ and other neuropsychiatric disorders	NRXN1	genetic analysis	recruited a family with multiple neuropsychiatric disorders the proband has SCZ, while other family members have mental retardation, schizophreniform disorder and affective disorder genotyped the proband and eight family members	two rare deletions upstream of the <i>NRXN1</i> gene (2p16.3) segregate with schizophrenia, schizophreniform disorder, and affective disorder in a family	[78]

response to lurasidone in SCZ patients [76]. Additionally, an association study on Spanish SCZ patients showed that missense mutations in *NRXN1* may actually protect against susceptibility to SCZ [73].

In a Taiwanese GWAS study, a significant association between *NRXN3* and BD was found [60]. And finally, an association study on Australian borderline personality disorder (BPD) patients showed that several *NRXN3* SNPs were nominally associated with BPD in heroin-dependent cases [62].

4.2. *In vitro* and *in vivo* models of disease

Functional *in vitro* and *in vivo* studies have also found evidence for the roles of neurexins in ASD. Monoamine oxidase A knockout (KO) mice, which are an animal model for autism, exhibited downregulated levels of both neurexin 1 and neurexin 2 [55]. Furthermore, mice colonized with the microbiota of ASD patients showed differential splicing of *NRXN2* [59]. Another animal study showed that changes in the binding of α -neurexins to N-type calcium channels could be important for some forms of ASD as it mediates synaptic inhibition [56]. Finally, a study using ASD patient-derived induced pluripotent stem cells (iPSCs) and differentiated organoids showed that neurexin 1, 2 and 3 mRNA is overexpressed in these samples [53].

One study examined neurexins in Fragile X syndrome, a genetic disorder with features similar to ASD, and characterized by the silencing of the *FMR1* gene [79]. Individuals with Fragile X experience a range of neurodevelopmental problems, such as learning disabilities and cognitive impairment, and males are usually more severely affected. Using *FMR1* KO mice, researchers probed brain sections to determine the levels of neurexin 1, 2 and 3 [66]. Interestingly, they found that neurexin 3 mRNA levels are increased in female mice but decreased in male mice and predicted that this may help explain the sex difference observed in this disorder [66].

In an animal study of SCZ, neurexin 1 was found to be downregulated [75]. This study generated iPSCs from patients with childhood-onset SCZ, differentiated them into glial cells and injected the glial cells into mice to form chimeric mice as a model organism [75]. Interestingly, an *in vitro* study of SCZ showed that overexpressing Calveolin-1, a potential therapeutic for SCZ, actually increased the levels of neurexin 1 as well as other proteins involved in synaptic plasticity [74].

Neurexin 2 α has been implicated in epilepsy and, more specifically, in seizures. Researchers observed an increase in neurexin 2 α expression in the dentate gyrus of the hippocampus in an induced-seizure mouse model [65]. Finally, in one study, a rat chronic mild stress model of depression was used to determine if neurexin expression was altered in major depressive disorder; however, no change in neurexin 1, 2 or 3 levels was observed [67].

So far, there have been two studies validating the effect of NRXNs *in vitro*, both by Pak *et al.* [68,77]. These studies cultured human stem cells as well as mice cells generated from *NRXN1* KO mice. The first study introduced two conditional *NRXN1* mutations previously seen in a range of neuropsychiatric disorders, including ASD and SCZ, into human embryonic stem cells (hESCs) using adeno-associated virus recombination and differentiated them into human-induced neurons (iNs) [68]. These cells were compared to cortical

neurons generated from *NRXN1* α KO mice [68]. The second study generated iPSCs from three *NRXN1* deletion SCZ patients and three controls, and again differentiated them into human iNs [77]. These cells were compared to mouse embryonic stem cells (mESCs) from *NRXN1* KO mice [77]. Both studies showed that heterozygous *NRXN1* deletions were able to impair neurotransmitter release and synaptic function, and increase the levels of the synaptic scaffolding protein, CASK, in human iNs but not in mice cells [68,77]. Therefore, these studies provide evidence that *NRXN1* deletions exhibit a major synaptic transmission phenotype in humans and are thus meaningful at a pathophysiological level.

In summary, these studies demonstrate a link between *NRXNs* and neuropsychiatric disorders such as ASD and SCZ, especially involving full or partial deletions of these genes. *NRXNs* have also been associated with BD and BPD. In addition, protein expression studies have shown changes in neurexin expression in animal models of epilepsy/seizures and Fragile X syndrome.

5. Role of neurexins in neurodegenerative disorders

Additionally, literature-based searches provided proof for the involvement of neurexins in various neurodegenerative disorders, and these studies are listed in table 2 and discussed below.

5.1. Human studies

Studies examining cerebrospinal fluid (CSF) from AD patients have observed lowered expression of neurexin 1 [81], as well as neurexin 2 α and neurexin 3 α [85]. In addition, it was found that these changes precede the neurodegeneration markers as they were observed in the preclinical stage 1 of AD [85]. Moreover, A β ₄₂ fibrils in CSF were found to bind to neurexin 1, 2 and 3 as well as proteoglycans and growth factors [83]. Levels of the synaptic proteins neuronal pentraxin 2 (NPTX2), GluA4-containing glutamate (AMPA4), neuroligin 1 and neurexin 2 α are also declined in plasma neuron-derived exomes and this decline was associated with AD progression [82]. Neurexin 3 protein expression has also been seen to be specifically downregulated in blood samples of AD patients [84].

Another expression analysis on CSF from MS patients identified neurexin 2 α levels as a potential biomarker for the disorder [98], while a genetic analysis found that a mutant miRNA, MIR8485, overexpresses neurexin, which leads to a calcium overload in pre-synapses [99]. It was hypothesized that this could induce neurodegeneration in MS [99].

A study examining gene expression in brain tissue samples of patients with PD found that genes related to nerve function, such as protocadherin-8 (PCDH8) and neurexin 3, were downregulated [109].

Two studies on mild cognitive impairment (MCI) found promising results. MCI is a milder form of dementia that is considered the intermediate state of cognitive decline between normal ageing and dementia [114]. Berchtold *et al.* [95] found that neurexin 1 and neurexin 2 are upregulated in MCI. In addition, neurexin 1 expression was found to be associated with longitudinal phenotypes in MCI, but not in AD [96].

One study examined neurexins in order to identify genes that are differentially regulated by HIV encephalitis [94]. This

Table 2. List of studies that have implicated neurexin genes in neurodegenerative disorders and ageing. 6-OHDA, 6-hydroxydopamine; ACP-RT-PCR, annealing control primer reverse transcriptase–polymerase chain reaction; ADNI, Alzheimer’s disease neuroimaging initiative; AMPA4, GluA4-containing glutamate; CSF, cerebrospinal fluid; EAE, experimental autoimmune encephalomyelitis; ELISA, enzyme-linked immunosorbent assay; FTD-GWAS, frontotemporal dementia genome-wide association study; GEO, gene expression omnibus; GWAS, genome-wide association study; HIV, human immunodeficiency virus; HYPERGENES, European Network for Genetic-Epidemiological Studies; LC-MS/MS, liquid chromatography mass spectrometry/mass spectrometry; LC-SRM, liquid chromatography single reaction monitoring; MAP, Rush Memory and Ageing Project; MR, magnetic resonance; MRI, magnetic resonance imaging; NPTX2, neuronal pentraxin 2; ONIND, other non-inflammatory neurological disease; PCDH8, protocadherin-8; PPMI, Parkinson’s Progression Markers Initiative; qRT-PCR, quantitative real-time PCR; RAP-PCR, reverse arbitrarily primed PCR; rMOG, rat myelin oligodendrocyte glycoprotein; RRMS, relapsing–remitting MS; RT-PCR, reverse transcriptase–PCR; SNP, single nucleotide polymorphism; UV-CLIP, ultraviolet cross-linking and immunoprecipitation; WES, whole-exome sequencing.

disorder/disease	neurexin				
process	gene	type of study	methods	main finding	reference
Alzheimer’s disease (AD)	NRXN3	GWAS of brain structure	obtained neuroimaging and genetic data from 818 subjects as part of ADNI performed a GWAS with 546,314 SNPs using temporal lobe and hippocampal volume as quantitative phenotypes	<i>NRXN3</i> (<i>KIAA0743</i>) is associated with temporal lobe structure in AD patients	[80]
AD	NRXN1	protein expression analysis	collected CSF samples from 10 AD patients and 15 healthy controls analysis using LC-MS/MS	the concentrations of the synaptic proteins neurexin 1 and neuronal PTX1, as well as neurofascin, were significantly lowered in AD CSF	[81]
AD	NRXN2 α	protein expression analysis	collected blood and CSF samples from 28 AD patients and 28 controls extracted plasma neuron-derived exomes CD81, NPTX2, AMPA4, neuroligin 1 and neurexin 2 α proteins were quantified using ELISAs	significantly lower levels of the synaptic proteins NPTX2, AMPA4, neuroligin 1 and neurexin 2 α in the plasma neuron-derived exomes correlate with AD progression	[82]
AD	NRXN1, 2 and 3	protein expression analysis	collected CSF samples from six AD patients and five non-AD patients binding assays were performed to determine which proteins in CSF bind to A β ₄₂ fibrils and/or protofibrils	A β ₄₂ fibrils in AD CSF are involved in binding to proteoglycans, growth factors and neuron-associated proteins, such as neurexin 1, 2 and 3	[83]
AD	NRXN3	transcriptome and RNA expression analysis	selected data from 263 AD patients and 151 non-demented controls sampled from the religious orders study performed RNA expression profiling	neurexin 3 expression is downregulated in AD	[84]
AD	NRXN2 α and NRXN3 α	protein expression analysis	collected CSF samples from AD patients and cognitively normal controls (three stage study with different <i>n</i> for each stage) performed LC-MS/MS and LC-SRM	levels of neurexin 2 α and neurexin 3 α , as well as other synaptic proteins are decreased in preclinical AD CSF	[85]
AD and ageing	NRXN1, 2 and 3	microarray analysis	obtained frozen brain samples from 26 AD cases and 55 non-AD controls from National Institute on Ageing Alzheimer’s disease brain banks used microarrays to evaluate expression profiles of 340 synaptic genes	SYNAPTIC proteins, including neurexin 1, 2 and 3, undergo altered expression in ageing and AD	[86]
AD and ageing	NRXN3	animal study	mice were divided into four groups, with four mice in each group: memory intact AD-transgenic mice, memory impaired AD-transgenic mice, memory intact aged mice and memory impaired aged mice performed proteomics on the hippocampus of each mouse	neurexin 3 is downregulated in AD-transgenic mice with impaired memory, but not in normal aged mice with impaired memory	[87]

(Continued.)

Table 2. (Continued.)

disorder/disease process	neurexin gene	type of study	methods	main finding	reference
AD and ageing	NRXN1 and 3	microarray analysis	performed a microarray analysis on 47 post-mortem brain samples from cognitively intact aged individuals from the MAP study identified 48 microarrays from the public GEO: 16 young cases, 18 cognitively intact aged cases and 14 AD cases analysed data to identify genes related to physical activity, ageing and AD	neurexin 1 and 3 have decreased expression in ageing and AD but have increased expression in association with late-life physical activity	[88]
ageing	NRXN3	animal study	cerebella were removed from three adult C57BL/6 J mice and three aged C57BL/6Jnia mice RNA was extracted and sequenced	neurexin 3 is downregulated in the cerebellum of aged mice	[89]
ageing	NRXN2	methylation analysis	monocytes were purified from PBMCS analysis of methylation was performed on genomic DNA from monocytes	CpG sites associated with <i>NRP1</i> , <i>NRXN2</i> and miR-29b-2 are hypomethylated in monocytes during ageing	[90]
ageing	NRXN1	animal study	28 Swiss albino mice were divided into four groups by age: young, adult, middle age and old molecular techniques were used to analyse neurexin 1 and neuroligin 3 expression	neurexin 1 and neuroligin 3 are differentially expressed in cerebral cortex and hippocampus during different stages of ageing, which might be responsible for alterations in synaptic plasticity during ageing	[91]
ageing	NRXN2 and 3	transcriptome analysis	collected data of 2202 post-mortem human brain samples of neurologically healthy individuals with different ages Calculated signal expression of genes	neurexin 2 and 3 are downregulated in ageing	[92]
amyotrophic lateral sclerosis (ALS)	NRXN1	cell culture and expression analysis	performed UV-CLIP experiments on SH-SY5Y cells to find TDP-43 targets validated these results on lumbar spinal cords from 4 ALS patients and 4 controls using RT-PCR	neurexin 1 and other TDP-43 targets are dysregulated in ALS	[93]
HIV encephalitis	NRXN1	microarray analysis	received cortical brain tissue from 13 HIV patients: eight with HIV encephalitis and five without extracted total RNA performed microarray analysis	neurexin 1 is downregulated in HIV encephalitis	[94]
mild cognitive impairment (MCI)	NRXN1 and 2	microarray analysis	obtained frozen brain samples from 16 MCI cases, 25 AD cases and 24 aged controls from National Institute on Aging Alzheimer's Disease brain banks extracted total RNA performed a microarray analysis	neurexin 1 and 2 are upregulated in MCI	[95]

(Continued.)

Table 2. (Continued.)

disorder/disease process	neurexin gene	type of study	methods	main finding	reference
MCI and AD	NRXN1	association study	obtained brain MR images of 400 MCI subjects, 400 AD subjects and 200 aged controls from the ADNI database obtained genotype data for 510 of these subjects from the ADNI database performed an association study	neurexin 1 expression is associated with longitudinal phenotypes in MCI, but not in AD	[96]
multiple sclerosis (MS)	NRXN3	animal study	induced EAE in 17 rats by injecting rMOG six control rats were treated with saline extracted total RNA used a cDNA expression array	neurexin 3 is downregulated in grey matter of EAE-induced rats	[97]
MS	NRXN2 α	protein expression analysis	collected CSF samples from 37 RRMS patients, 50 patients with ONIND and patients with non-neurological (orthopaedic) diseases analysis using LC-MS/MS	neurexin 2 α in CSF is a potential biomarker for MS	[98]
MS	NRXN1	genetic analysis	collected blood from a female patient with RRMS performed WES and screened for mutations	overexpression of neurexin 1 by mutant MIR8485 leads to calcium overload in pre-synapses. This could induce neurodegeneration in MS	[99]
MS	NRXN1	cell culture	treated THP-1 cells with ceramides to induce hypermethylation of DNA isolated genomic DNA measured levels of neurexin 1, FZD7 and TP63 using qRT-PCR	ceramide-induced hypermethylation of DNA was associated with decreased transcript levels of neurexin 1 in cultured human monocytes	[100]
neurodegeneration	NRXN3	animal study	45 DA(RT1 ^{av1}) and 45 PVG(RT1 ^s) adult rats subjected rats to ventral root avulsion extracted total RNA used a cDNA expression assay and performed RT-PCR	neurexin 3 is downregulated in rats with axonal damage caused by ventral root avulsion	[101]
neurodegeneration	NRXN3	animal study	three experimental groups with five ICR mice each injected kainic acid into ICR mice extracted total RNA from the hippocampus performed ACP-RT-PCR and sequenced the PCR products	neurexin 3 is downregulated in the hippocampus of mice treated with kainic acid, an inducer of neurodegeneration	[102]
neurodegeneration	NRXN1	bioinformatics and cell culture	analysed cross-linking, immunoprecipitation and sequencing data from the ArrayExpress archive to identify RNAs bound to TDP-43 in human and mouse brains quantitative RT-PCR was used to measure mRNA expression	a novel TDP-43 binding miRNA, miR-NID1 (miR-8485), represses neurexin 1 expression and may play a role in neurodegeneration	[103]

(Continued.)

Table 2. (Continued.)

disorder/disease process	neurexin gene	type of study	methods	main finding	reference
neurodegeneration	NRXN1 β	cell culture	transfected rat hippocampal neurons to overexpress acetylcholinesterase performed a co-immunoprecipitation assay with neurexin 1 and acetylcholinesterase co-transfected HEK-293 cells to express neurexin 1 β and neuroligin 1 and cultured these cells in acetylcholinesterase conditioned media performed a co-immunoprecipitation assay with neurexin 1 β and neuroligin 1	excessive glycosylated acetylcholinesterase could competitively disrupt neurexin 1 β -neuroligin junctions and impair the integrity of glutamatergic synapses	[104]
neurotoxicity	NRXN3 β	animal study	groups of 3 Sprague–Dawley rats were treated with sarin via intramuscular injection rats were sacrificed 15 min or 3 months after sarin exposure dissected brains and extracted total RNA performed a microarray analysis	sarin exposure causes a persistent downregulation of neurexin 1 β and breakdown of the blood–brain barrier	[105]
neurotoxicity	NRXN2 α	animal study	wild-type zebrafish were repeatedly exposed to domoic acid via intracoelomic injection dissected brains and extracted total RNA performed a microarray analysis	neurexin 2 α was upregulated in zebrafish two weeks after exposure to domoic acid, a neurotoxin	[106]
Parkinson's disease (PD)	NRXN1	cell culture	cultured SH-SY5Y cells and primary mouse mesencephalic cells treated cells with 6-OHDA performed RAP-PCR and analysed the PCR products using RT–PCR and qRT–PCR	downregulation of neurexin 1 mRNA and protein was observed in the 6-OHDA-induced cell culture models of PD	[107]
PD	NRXN2	animal study	transgenic mice were assigned to 4 treatment groups with 20 mice per group cholesterol oximes were administered in food pellets TH+ neurons were isolated from the substantia nigra and subjected to a transcriptome analysis	transgenic mice overexpressing α -synuclein have increased levels of neurexin 2 chronic administration of cholesterol oximes to these mice decreased neurexin 2 levels	[108]
PD	NRXN3	genetics analysis	obtained genomic data of 29 PD samples and 18 controls from the GEO database analysed the data to identify disease-related genes and differential gene expression	genes related to nerve function, such as PCDH8 and neurexin 3, are downregulated in PD brain tissue samples	[109]

(Continued.)

Table 2. (Continued.)

disorder/disease process	neurexin gene	type of study	methods	main finding	reference
PD	NRXN1	animal study	adult Wistar rats were divided into five treatment groups, with 6–8 rats in each group experimental groups had 6-OHDA brain injections with or without different concentrations of allopregnanolone western blots were performed to evaluate the levels of the synaptic proteins PSD95 and neurexin 1 in the striatum	neurexin 1 is significantly decreased in the striatum of 6-OHDA-induced rats treatment with allopregnanolone attenuates this and other molecular changes	[110]
PD	NRXN1	RNA expression analysis	MRI data from 149 PD patients and 64 healthy controls were obtained from the PPMI database 17 genes of interest implicated in PD were selected for whole-brain expression analysis	neurexin 1 does not have an expression pattern that predicts regional atrophy in PD	[111]
PD	NRXN1	animal study	adult Wistar rats were divided into seven treatment groups, with seven rats in each group experimental groups had 6-OHDA brain injections with or without different concentrations of apelin-13 western blots were performed to evaluate the levels of the synaptic proteins PSD95, neurexin 1 and neuroligin in the striatum	neurexin 1 expression is decreased in the striatum of 6-OHDA-induced rats 6-OHDA rats treated with apelin-13 showed increased neurexin 1 expression in the striatum	[112]
spinal muscular atrophy (SMA)	NRXN2 α	animal study	used HB9:D3cpv/MN-transgenic zebrafish and <i>Smn</i> ^{-/-} / <i>SMN2</i> mice isolated total RNA from both models performed a microarray analyses and qRT-PCR	<i>SMN</i> -deficiency downregulates neurexin 2 α expression and alters its splicing in zebrafish and mouse models of SMA	[113]

microarray study showed that neurexin 1 is downregulated in HIV encephalitis.

Finally, González-Velasco *et al.* [92] showed that neurexin 2 and neurexin 3 mRNA levels are downregulated in ageing. Another study found that neurexin 1, 2 and 3 underwent altered expression in both AD and ageing [86]. A more recent study from the same group confirmed decreased expression of both neurexin 1 and neurexin 3 in AD and ageing [88]. Interestingly, they also found that late-life physical activity is associated with increased expression of these proteins [88].

5.1.1. Association study

A GWAS performed by Stein *et al.* [80] showed that the SNP rs7155434 within *NRXN3* is associated with temporal lobe structure in AD patients. Temporal lobe volume deficits are a known risk factor for AD; therefore, this study potentially implicates *NRXN3* with AD risk [80].

5.2. *In vitro* and *in vivo* models of disease

Several studies involving cell culture and/or rodent disease models have also shown differences in the expression of neurexin proteins. Three studies showed that neurexin 1 is downregulated in PD. One of these measured neurexin 1 mRNA in two 6-OHDA (6-hydroxydopamine)-induced cell culture models; one using human neuroblastoma (SH-SY5Y) cells and the other using primary mouse mesencephalic cells [107]. The other studies used a 6-OHDA-induced rat model of PD and both saw a decrease in neurexin 1 in the striatum [110,112]. In addition, these studies showed that treatment with apelin-13 [112] or allopregnanolone [110] is able to attenuate this change. Apelin-13 is an endogenous ligand for APJ [115] that has been investigated as a potential protective neuropeptide due to the role of the apelin-APJ system in neuronal survival [116], while allopregnanolone is a reduced metabolite of progesterone [117] and has reduced CSF levels in PD patients [118]. Freeze *et al.* [111], however, noted that the expression pattern of neurexin 1 does not predict regional atrophy in PD. This suggests that neurexin 1 is not a marker for PD; however, it does not exclude it as an important protein in PD pathogenesis. Another study in PD-transgenic mice overexpressing α -synuclein found that neurexin 2 expression was also upregulated [108]. In addition, chronic administration of cholesterol oximes was able to increase the transcription of cytoprotective genes and undo transcriptome alterations, including the alteration of neurexin 2 expression [108].

Two studies using induced models of MS implicated neu-rexins in this disorder. One study induced experimental autoimmune encephalomyelitis (EAE) in rats and observed downregulation of neurexin 3 [97]. This is a commonly used model that mimics certain aspects of MS. The other study used an *in vitro* model of MS, cultured human monocytes, and observed an association between ceramide-induced hypermethylation of DNA and neurexin 1 mRNA [100].

An animal study performed by Neuner *et al.* [87] showed that neurexin 3 is downregulated in AD-transgenic mice, but not in normal aged mice with impaired memory. However, Popesco *et al.* [89] found that neurexin 3 is downregulated in the cerebellum of aged mice. Another study found that levels of both neurexin 1 and neuroligin 3 are differentially expressed in cerebral cortex and hippocampus of mice and

that these expression levels change during different stages of ageing [91]. They predicted that this may be responsible for the changes in synaptic plasticity observed with age [91]. Finally, a DNA methylation study by Tserel *et al.* [90] showed that CpG sites associated with *NRP1*, *NRXN2* and miR-29b-2 are hypomethylated in monocytes during ageing.

To date, only one study has examined neu-rexins in amyotrophic lateral sclerosis (ALS) and spinal muscular atrophy (SMA). In a cell culture model of ALS, neurexin 1 and other RNA targets of TDP-43 were dysregulated [93]. TDP-43 is a component of the cytoplasmic inclusion bodies present in ALS patients [93]. Fragments of TDP-43 are ubiquitinated, hyperphosphorylated and then accumulate in neurons and glia [119]. In zebrafish and mouse KO models of SMA, the *SMN*-deficiency downregulated neurexin 2 α expression and altered its splicing [113]. SMA is associated with mutation or deletions in the *SMN* gene [120] and lack of the *SMN* protein causes degeneration and results in anterior horn cell dysfunction.

5.3. Models of induced neurodegeneration and toxicity

Several studies investigated neu-rexins in models of neurodegeneration or toxicity instead of studying a specific neurodegenerative disease.

Four studies examined the role of neu-rexins in models of induced neurodegeneration. Two of these studies hypothesized that neurexin 1 could play a role in neurodegeneration. The first study showed that a novel TDP-43 binding miRNA, miR-NID1 (miR-8485) is able to repress neurexin 1 and predicted that this could play a role in neurodegeneration [103]. Xiang *et al.* [104] found *in vitro* that excessive glycosylated acetylcholinesterase could competitively disrupt the neurexin 1 β -neuroligin junctions and impair the integrity of glutamatergic synapses, which could lead to neurodegeneration. The other two studies showed that neurexin 3 is downregulated in animal models of neurodegeneration [101,102]. Suh *et al.* [102] saw that neurexin 3 was downregulated in the hippocampus of mice treated with kainic acid, an inducer of neurodegeneration, while Swanberg *et al.* [101] found that neurexin 3 is downregulated in rats with axonal damage caused by ventral root avulsion.

Two studies were conducted in animal models of neurotoxicity. One study exposed zebrafish to chronic, low levels of the neurotoxin domoic acid and saw an upregulation of neurexin 2 α after two weeks [106]. The other study exposed rats to acute doses of sarin, which caused a persistent down-regulation of neurexin 1 β and breakdown of the blood-brain barrier [105].

In summary, multiple studies have shown changes in neu-rexin expression in AD, ALS, MS, PD and SMA. Many of these studies have observed downregulation of protein expression for neurexin 1, 2 and 3 in these disorders. Similarly, downregulation of neurexin 1, 2 and 3 were observed in disorders such as HIV encephalitis and MCI and in studies on ageing, in models of neuronal toxicity, and animal models of MS and ALS.

6. Concluding remarks

A clear link between synaptic dysfunction and neurodegenerative as well as neuropsychiatric disorders has been established in recent years. Our literature-based searches revealed several

studies that have linked CNVs, deletions or expression changes in neurexins to different disorders. The evidence is most compelling for a role of neurexins in neuropsychiatric disorders, particularly in regard to the involvement of neurexin 1 in ASD and SCZ. Currently, there is comparatively less evidence for the involvement of neurexins in neurodegenerative disorders. Although there have been some studies that have suggested that neurexins may be important in these disorders, at this stage more experimental data are still needed to draw concrete conclusions. Therefore, it is apparent that more targeted studies in various disorders involving these genes as well as the proteins they encode are warranted. In terms of their broader biological and physiological functions, the neurexins function as molecular inducers, are involved in iron and protein binding, and play a role in cell-to-cell communication and response to stimuli, consequently making them critical for normal cell functioning. Furthermore, these proteins interact with various other proteins such as the neuroligins and the LRRTM proteins identified via protein interaction networks. This implicates the neurexins' involvement in synaptic integrity and functioning making them promising candidates as disease genes for a wide range of brain pathologies.

In summary, this review serves to highlight the potential importance of the neurexin genes and proteins in human disease and recommends that more targeted studies on these genes and proteins are warranted. Furthermore, with the wealth of exomic and genomic sequences and genome-wide transcriptomic datasets now available, it has become plausible

to interrogate them for their involvement in various human disorders, on a scale not previously possible. In addition, the human neurexin protein structures urgently need to be solved to understand the function and infer accurate protein–protein interactions as well as to understand the effect of mutations on the protein structure. Ultimately, improved knowledge on synapses and their individual components are necessary to develop novel therapeutic approaches for the emerging and exciting field of synaptopathies.

Data accessibility. This article has no additional data.

Authors' contributions. K.C. performed the research and wrote the first draft of the manuscript. M.H. and R.C. assisted with some of the analysis. K.C. and S.B. conceptualized the study. All authors critically reviewed and edited the manuscript.

Competing interests. The authors declare that there are no competing interests.

Funding. This work is based on the research supported wholly/in part by the National Research Foundation of South Africa (NRF) (grant nos. 106052, 129249); the South African Medical Research Council (SAMRC) (self-initiated research grant); the Harry Crossley Foundation and Stellenbosch University, South Africa. SAMRC and The Higher Education Department, Next Generation of Academic Programme (nGAP), provided support for R.C. in the form of a full-time academic position and salary.

Acknowledgements. We acknowledge Minke Bekker for the drawing of figure 1. We also acknowledge the support of the NRF-DST Centre of Excellence for Biomedical Tuberculosis Research; South African Medical Research Council Centre for Tuberculosis Research; Division of Molecular Biology and Human Genetics, Faculty of Medicine and Health Sciences, Stellenbosch University, Cape Town.

References

- Torres VI, Vallejo D, Inestrosa NC. 2017 Emerging synaptic molecules as candidates in the etiology of neurological disorders. *Neural Plast.* **2017**, 8081758. (doi:10.1155/2017/8081758)
- Imbriani P, Schirizzi T, Meringolo M, Mercuri NB, Pisani A. 2018 Centrality of early synaptopathy in Parkinson's disease. *Front. Neurol.* **9**, 103. (doi:10.3389/fneur.2018.00103)
- Südhof TC. 2017 Synaptic neurexin complexes: a molecular code for the logic of neural circuits. *Cell* **171**, 745–769. (doi:10.1016/j.cell.2017.10.024)
- Lepeta K *et al.* 2016 Synaptopathies: synaptic dysfunction in neurological disorders—a review from students to students. *J. Neurochem.* **138**, 785–805. (doi:10.1111/jnc.13713)
- Missler M, Südhof TC, Biederer T. 2012 Synaptic cell adhesion. *Cold Spring Harb. Perspect. Biol.* **4**, a005694. (doi:10.1101/cshperspect.a005694)
- Schikorski T, Stevens CF. 1997 Quantitative ultrastructural analysis of hippocampal excitatory synapses. *J. Neurosci.* **17**, 5858–5867. (doi:10.1523/jneurosci.17-15-05858.1997)
- Toni N, Buchs PA, Nikonenko I, Bron CR, Müller D. 1999 LTP promotes formation of multiple spine synapses between a single axon terminal and a dendrite. *Nature* **402**, 421–425. (doi:10.1038/46574)
- Krueger DD, Tuffy LP, Papadopoulos T, Brose N. 2012 The role of neurexins and neuroligins in the formation, maturation, and function of vertebrate synapses. *Curr. Opin. Neurobiol.* **22**, 412–422. (doi:10.1016/j.conb.2012.02.012)
- Taoufik E, Kouroupi G, Zygoianni O, Matsas R. 2018 Synaptic dysfunction in neurodegenerative and neurodevelopmental diseases: an overview of induced pluripotent stem-cell-based disease models. *Open Biol.* **8**, 180138. (doi:10.1098/rsob.180138)
- Sebate B, Cuttler K, Cloete R, Britz M, Christoffels A, Williams M, Carr J, Bardien S. 2021 Prioritization of candidate genes for a South African family with Parkinson's disease using in-silico tools. *PLoS ONE* **16**, e0249324. (doi:10.1371/journal.pone.0249324)
- Ushkaryov YA, Petrenko AG, Geppert M, Südhof TC. 1992 Neurexins: synaptic cell surface proteins related to the α -latrotoxin receptor and laminin. *Science* **257**, 50–56. (doi:10.1126/science.1621094)
- Rosenthal L, Meldolesi J. 1989 α -Latrotoxin and related toxins. *Pharmacol. Ther.* **42**, 115–134. (doi:10.1016/0163-7258(89)90024-7)
- Missler M, Südhof TC. 1998 Neurexins: three genes and 1001 products. *Trends Genet.* **14**, 20–26. (doi:10.1016/S0168-9525(97)01324-3)
- Ichtchenko K, Nguyen T, Südhof TC. 1996 Structures, alternative splicing, and neurexin binding of multiple neuroligins. *J. Biol. Chem.* **271**, 2676–2682. (doi:10.1074/jbc.271.5.2676)
- Rudenko G, Nguyen T, Chelliah Y, Su TC, Deisenhofer J, Hughes H. 1999 The structure of the ligand-binding domain of neurexin I β : regulation of LNS domain function. *Cell* **99**, 93–101. (doi:10.1016/S0092-8674(00)80065-3)
- Tabuchi K, Südhof TC. 2002 Structure and evolution of neurexin genes: insight into the mechanism of alternative splicing. *Genomics* **79**, 849–859. (doi:10.1006/geno.2002.6780)
- Craig AM, Kang Y. 2007 Neurexin-neuroligin signaling in synapse development. *Curr. Opin. Neurobiol.* **17**, 43–52. (doi:10.1016/j.conb.2007.01.011)
- Liao Y, Wang J, Jaehnig EJ, Shi Z, Zhang B. 2019 WebGestalt 2019: gene set analysis toolkit with revamped UIs and APIs. *Nucleic Acids Res.* **47**, W199–W205. (doi:10.1093/nar/gkz401)
- Szklarczyk D *et al.* 2019 STRING v11: protein-protein association networks with increased coverage, supporting functional discovery in genome-wide experimental datasets. *Nucleic Acids Res.* **47**, D607–D613. (doi:10.1093/nar/gky1131)
- Warde-Farley D *et al.* 2010 The GeneMANIA prediction server: biological network integration for gene prioritization and predicting gene function. *Nucleic Acids Res.* **38**, W214–W220. (doi:10.1093/nar/gkq537)
- The UniProt Consortium. 2021 UniProt: the universal protein knowledgebase in 2021. *Nucleic Acids Res.* **49**, D480–D489. (doi:10.1093/nar/gkaa1100)
- Kanehisa M, Furumichi M, Sato Y, Ishiguro-Watanabe M, Tanabe M. 2021 KEGG: integrating viruses and cellular organisms. *Nucleic Acids Res.* **49**, D545–D551. (doi:10.1093/nar/gkaa970)

23. Nakanishi M, Nomura J, Ji X, Tamada K, Arai T, Takahashi E, Bucan M, Takumi T. 2017 Functional significance of rare neuroligin 1 variants found in autism. *PLoS Genet.* **13**, e1006940. (doi:10.1371/journal.pgen.1006940)
24. Berkel S *et al.* 2010 Mutations in the SHANK2 synaptic scaffolding gene in autism spectrum disorder and mental retardation. *Nat. Genet.* **42**, 489–491. (doi:10.1038/ng.589)
25. Jamain S *et al.* 2003 Mutations of the X-linked genes encoding neuroligins NLGN3 and NLGN4 are associated with autism. *Nat. Genet.* **34**, 27–29. (doi:10.1038/ng1136)
26. Laumonnier F *et al.* 2004 X-linked mental retardation and autism are associated with a mutation in the NLGN4 gene, a member of the neuroligin family. *Am. J. Hum. Genet.* **74**, 552–557. (doi:10.1086/382137)
27. Lawson-Yuen A, Saldivar JS, Sommer S, Picker J. 2008 Familial deletion within NLGN4 associated with autism and Tourette syndrome. *Eur. J. Hum. Genet.* **16**, 614–618. (doi:10.1038/sj.ejhg.5202006)
28. Najm J *et al.* 2008 Mutations of CASK cause an X-linked brain malformation phenotype with microcephaly and hypoplasia of the brainstem and cerebellum. *Nat. Genet.* **40**, 1065–1067. (doi:10.1038/ng.194)
29. Piluso G *et al.* 2008 A missense mutation in CASK causes FG syndrome in an Italian family. *Am. J. Hum. Genet.* **84**, 162–177. (doi:10.1016/j.ajhg.2008.12.018)
30. Tarpey PS *et al.* 2009 A systematic, large-scale resequencing screen of X-chromosome coding exons in mental retardation. *Nat. Genet.* **41**, 535–543. (doi:10.1038/ng.367)
31. Hackett A *et al.* 2010 CASK mutations are frequent in males and cause X-linked nystagmus and variable XLMR phenotypes. *Eur. J. Hum. Genet.* **18**, 544–552. (doi:10.1038/ejhg.2009.220)
32. Moog U *et al.* 2011 Phenotypic spectrum associated with CASK loss-of-function mutations. *J. Med. Genet.* **48**, 741–751. (doi:10.1136/jmedgenet-2011-100218)
33. Lelieveld SH *et al.* 2016 Meta-analysis of 2,104 trios provides support for 10 new genes for intellectual disability. *Nat. Neurosci.* **19**, 1194–1196. (doi:10.1038/nn.4352)
34. Moutton S *et al.* 2018 Truncating variants of the DLG4 gene are responsible for intellectual disability with marfanoid features. *Clin. Genet.* **93**, 1172–1178. (doi:10.1111/cge.13243)
35. Baker K *et al.* 2018 SYT1-associated neurodevelopmental disorder: a case series. *Brain* **141**, 2576–2591. (doi:10.1093/brain/awy209)
36. Majercak J *et al.* 2006 LRRTM3 promotes processing of amyloid-precursor protein by BACE1 and is a positional candidate gene for late-onset Alzheimer's disease. *Proc. Natl Acad. Sci. USA* **103**, 17 967–17 972. (doi:10.1073/pnas.0605461103)
37. Dobyns WB *et al.* 2018 MACF1 mutations encoding highly conserved zinc-binding residues of the GAR domain cause defects in neuronal migration and axon guidance. *Am. J. Hum. Genet.* **103**, 1009–1021. (doi:10.1016/j.ajhg.2018.10.019)
38. Dong M, Noguchi S, Endo Y, Hayashi YK, Yoshida S, Nonaka I, Nishino I. 2015 DAG1 mutations associated with asymptomatic hyperCKemia and hypoglycosylation of α -dystroglycan. *Neurology* **84**, 273–279. (doi:10.1212/WNL.0000000000001162)
39. Geis T, Marquard K, Rödl T, Reihle C, Schirmer S, Von Kalle T, Bornemann A, Hehr U, Blankenburg M. 2013 Homozygous dystroglycan mutation associated with a novel muscle-eye-brain disease-like phenotype with multicystic leucodystrophy. *Neurogenetics* **14**, 205–213. (doi:10.1007/s10048-013-0374-9)
40. Hara Y *et al.* 2011 A dystroglycan mutation associated with limb-girdle muscular dystrophy. *N. Engl. J. Med.* **364**, 939–946. (doi:10.1056/nejmoa1006939)
41. Riemersma M *et al.* 2015 Absence of α - and β -dystroglycan is associated with Walker-Warburg syndrome. *Neurology* **84**, 2177–2182. (doi:10.1212/WNL.0000000000001615)
42. Hanein S *et al.* 2004 Leber congenital amaurosis: comprehensive survey of the genetic heterogeneity, refinement of the clinical definition, and genotype-phenotype correlations as a strategy for molecular diagnosis. *Hum. Mutat.* **23**, 306–317. (doi:10.1002/humu.20010)
43. Mataftsi A, Schorderet DF, Chachoua L, Boussalah M, Nouri MT, Barthelmes D, Borrut FX, Munier FL. 2007 Novel TULP1 mutation causing leber congenital amaurosis or early onset retinal degeneration. *Investig. Ophthalmol. Vis. Sci.* **48**, 5160–5167. (doi:10.1167/iovs.06-1013)
44. Banerjee P *et al.* 1998 TULP1 mutation in two extended Dominican kindreds with autosomal recessive Retinitis pigmentosa. *Nat. Genet.* **18**, 177–179. (doi:10.1038/ng0298-177)
45. Den Hollander AI, Van Lith-Verhoeven JJC, Arends ML, Strom TM, Cremers FPM, Hoyng CB. 2007 Novel compound heterozygous TULP1 mutations in a family with severe early-onset retinitis pigmentosa. *Arch. Ophthalmol.* **125**, 932–935. (doi:10.1001/archoph.125.7.932)
46. Hagstrom SA, North MA, Nishina PM, Berson EL, Dryja TP. 1998 Recessive mutations in the gene encoding the tubby-like protein TULP1 in patients with Retinitis pigmentosa. *Nat. Genet.* **18**, 174–176. (doi:10.1038/ng0298-174)
47. Kondo H, Qin M, Mizota A, Kondo M, Hayashi H, Hayashi K, Oshima K, Tahira T, Hayashi K. 2004 A homozygosity-based search for mutations in patients with autosomal recessive retinitis pigmentosa, using microsatellite markers. *Investig. Ophthalmol. Vis. Sci.* **45**, 4433–4439. (doi:10.1167/iovs.04-0544)
48. Levy D *et al.* 2011 Rare de novo and transmitted copy-number variation in autistic spectrum disorders. *Neuron* **70**, 886–897. (doi:10.1016/j.neuron.2011.05.015)
49. Sanders SJ *et al.* 2011 Multiple recurrent de novo CNVs, including duplications of the 7q11.23 Williams Syndrome region, are strongly associated with autism. *Neuron* **70**, 863–885. (doi:10.1016/j.neuron.2011.05.002)
50. Camacho-Garcia RJ, Planelles MI, Margalef M, Pecero ML, Martínez-Leal R, Aguilera F, Vilella E, Martínez-Mir A, Scholl FG. 2012 Mutations affecting synaptic levels of neurexin-1 β in autism and mental retardation. *Neurobiol. Dis.* **47**, 135–143. (doi:10.1016/j.nbd.2012.03.031)
51. Liu Y *et al.* 2012 Mutation analysis of the NRXN1 gene in a Chinese autism cohort. *J. Psychiatr. Res.* **46**, 630–634. (doi:10.1016/j.jpsychires.2011.10.015)
52. Girirajan S *et al.* 2013 Refinement and discovery of new hotspots of copy-number variation associated with autism spectrum disorder. *Am. J. Hum. Genet.* **92**, 221–237. (doi:10.1016/j.ajhg.2012.12.016)
53. Mariani J *et al.* 2015 FOXG1-dependent dysregulation of GABA/glutamate neuron differentiation in autism spectrum disorders. *Cell* **162**, 375–390. (doi:10.1016/j.cell.2015.06.034)
54. Sanders SJ *et al.* 2015 Insights into autism spectrum disorder genomic architecture and biology from 71 risk loci. *Neuron* **87**, 1215–1233. (doi:10.1016/j.neuron.2015.09.016)
55. Chen K, Kardys A, Chen Y, Flink S, Tabakoff B, Shih JC. 2017 Altered gene expression in early postnatal monoamine oxidase A knockout mice. *Brain Res.* **1669**, 18–26. (doi:10.1016/j.brainres.2017.05.017)
56. Tong XJ, López-Soto EJ, Li L, Liu H, Nedelcu D, Lipscombe D, Hu Z, Kaplan JM. 2017 Retrograde synaptic inhibition is mediated by α -neuroligin binding to the α 2 δ subunits of N-type calcium channels. *Neuron* **95**, 326–340. (doi:10.1016/j.neuron.2017.06.018)
57. Gauthier J *et al.* 2011 Truncating mutations in NRXN2 and NRXN1 in autism spectrum disorders and schizophrenia. *Hum. Genet.* **130**, 563–573. (doi:10.1007/s00439-011-0975-z)
58. Mohrmann I, Gillissen-Kaesbach G, Siebert R, Caliebe A, Hellenbroich Y. 2011 A de novo 0.57 Mb microdeletion in chromosome 11q13.1 in a patient with speech problems, autistic traits, dysmorphic features and multiple endocrine neoplasia type 1. *Eur. J. Med. Genet.* **54**, 6. (doi:10.1016/j.ejmg.2011.04.006)
59. Sharon G *et al.* 2019 Human gut microbiota from autism spectrum disorder promote behavioral symptoms in mice. *Cell* **177**, 1600–1618. (doi:10.1016/j.cell.2019.05.004)
60. Kuo PH *et al.* 2014 Identification of novel loci for bipolar I disorder in a multi-stage genome-wide association study. *Prog. Neuro-Psychopharmacol. Biol. Psychiatry* **51**, 58–64. (doi:10.1016/j.pnpb.2014.01.003)
61. Fabbri C, Serretti A. 2016 Genetics of long-term treatment outcome in bipolar disorder. *Prog. Neuro-Psychopharmacol. Biol. Psychiatry* **65**, 17–24. (doi:10.1016/j.pnpb.2015.08.008)
62. Panagopoulos VN *et al.* 2013 Examining the association of NRXN3 SNPs with borderline personality disorder phenotypes in heroin dependent cases and socio-economically disadvantaged controls. *Drug Alcohol Depend.* **128**, 187–193. (doi:10.1016/j.drugalcdep.2012.11.011)

63. Grimminger T *et al.* 2013 Levetiracetam resistance: synaptic signatures & corresponding promoter SNPs in epileptic hippocampi. *Neurobiol. Dis.* **60**, 115–125. (doi:10.1016/j.nbd.2013.08.015)
64. Angione K, Eschbach K, Smith G, Joshi C, Demarest S. 2019 Genetic testing in a cohort of patients with potential epilepsy with myoclonic-atonic seizures. *Epilepsy Res.* **150**, 70–77. (doi:10.1016/j.eplepsyres.2019.01.008)
65. Górecki DC, Szklarczyk A, Lukasiuk K, Kaczmarek L, Simons JP. 1999 Differential seizure-induced and developmental changes of neuexin expression. *Mol. Cell. Neurosci.* **13**, 218–227. (doi:10.1006/mcne.1999.0740)
66. Lai JKY, Doering LC, Foster JA. 2016 Developmental expression of the neuroligins and neuexins in fragile X mice. *J. Comp. Neurol.* **524**, 807–828. (doi:10.1002/cne.23868)
67. Han X, Shao W, Liu Z, Fan S, Yu J, Chen J, Qiao R, Zhou J, Xie P. 2015 ITRAQ-based quantitative analysis of hippocampal postsynaptic density-associated proteins in a rat chronic mild stress model of depression. *Neuroscience* **298**, 220–292. (doi:10.1016/j.neuroscience.2015.04.006)
68. Pak CH, Danko T, Zhang Y, Aoto J, Anderson G, Maxeiner S, Yi F, Wernig M, Südhof TC. 2015 Human neuropsychiatric disease modeling using conditional deletion reveals synaptic transmission defects caused by heterozygous mutations in NRXN1. *Cell Stem Cell* **17**, 316–328. (doi:10.1016/j.stem.2015.07.017)
69. Mirnics K, Middleton FA, Marquez A, Lewis DA, Levitt P. 2000 Molecular characterization of schizophrenia viewed by microarray analysis of gene expression in prefrontal cortex. *Neuron* **28**, 53–67. (doi:10.1016/S0896-6273(00)00085-4)
70. Kirov G *et al.* 2008 Comparative genome hybridization suggests a role for NRXN1 and APBA2 in schizophrenia. *Hum. Mol. Genet.* **17**, 458–465. (doi:10.1093/hmg/ddm323)
71. Ivorra JL *et al.* 2014 Replication of previous genome-wide association studies of psychiatric diseases in a large schizophrenia case-control sample from Spain. *Schizophr. Res.* **159**, 107–113. (doi:10.1016/j.schres.2014.07.004)
72. Todarello G, Feng N, Kolachana BS, Li C, Vakkalanka R, Bertolino A, Weinberger DR, Straub RE. 2014 Incomplete penetrance of NRXN1 deletions in families with schizophrenia. *Schizophr. Res.* **155**, 1–7. (doi:10.1016/j.schres.2014.02.023)
73. Suárez-Rama JJ *et al.* 2015 Resequencing and association analysis of coding regions at twenty candidate genes suggest a role for rare risk variation at AKAP9 and protective variation at NRXN1 in schizophrenia susceptibility. *J. Psychiatr. Res.* **66–67**, 38–44. (doi:10.1016/j.jpsychires.2015.04.013)
74. Kassan A *et al.* 2017 Caveolin-1 regulation of disrupted-in-schizophrenia-1 as a potential therapeutic target for schizophrenia. *J. Neurophysiol.* **117**, 436–444. (doi:10.1152/jn.00481.2016)
75. Windrem MS *et al.* 2017 Human iPSC glial mouse chimeras reveal glial contributions to schizophrenia. *Cell Stem Cell* **21**, 195–208. (doi:10.1016/j.stem.2017.06.012)
76. Li J, Yoshikawa A, Brennan MD, Ramsey TL, Meltzer HY. 2018 Genetic predictors of antipsychotic response to lurasidone identified in a genome wide association study and by schizophrenia risk genes. *Schizophr. Res.* **192**, 194–204. (doi:10.1016/j.schres.2017.04.009)
77. Pak CH *et al.* 2021 Cross-platform validation of neurotransmitter release impairments in schizophrenia patient-derived NRXN1-mutant neurons. *Proc. Natl Acad. Sci. USA* **118**, 2021. (doi:10.1073/pnas.2025598118)
78. Duong LTT, Hoeffding LK, Petersen KB, Knudsen CD, Thygesen JH, Klitten LL, Tommerup N, Ingason A, Werge T. 2015 Two rare deletions upstream of the NRXN1 gene (2p16.3) affecting the non-coding mRNA AK127244 segregate with diverse psychopathological phenotypes in a family. *Eur. J. Med. Genet.* **58**, 650–653. (doi:10.1016/j.ejmg.2015.11.004)
79. Verkerk AJMH *et al.* 1991 Identification of a gene (FMR-1) containing a CGG repeat coincident with a breakpoint cluster region exhibiting length variation in fragile X syndrome. *Cell* **65**, 905–914. (doi:10.1016/0092-8674(91)90397-H)
80. Stein JL *et al.* 2010 Genome-wide analysis reveals novel genes influencing temporal lobe structure with relevance to neurodegeneration in Alzheimer's disease. *Neuroimage* **51**, 542–554. (doi:10.1016/j.neuroimage.2010.02.068)
81. Brinkmalm G, Sjödin S, Simonsen AH, Hasselbalch SG, Zetterberg H, Brinkmalm A, Blennow K. 2018 A parallel reaction monitoring mass spectrometric method for analysis of potential CSF biomarkers for Alzheimer's disease. *Proteom. Clin. Appl.* **12**, 1700131. (doi:10.1002/prca.201700131)
82. Goetzl EJ, Abner EL, Jicha GA, Kapogiannis D, Schwartz JB. 2018 Declining levels of functionally specialized synaptic proteins in plasma neuronal exosomes with progression of Alzheimer's disease. *FASEB J.* **32**, 888–893. (doi:10.1096/fj.201700731R)
83. Rahman MM, Westermark GT, Zetterberg H, Härd T, Sandgren M. 2018 Protofibrillar and fibrillar amyloid- β binding proteins in cerebrospinal fluid. *J. Alzheimer's Dis.* **66**, 1053–1064. (doi:10.3233/JAD-180596)
84. Canchi S, Raaouf B, Masliah D, Rosenthal SB, Sasik R, Fisch KM, De Jager PL, Bennett DA, Rissman RA. 2019 Integrating gene and protein expression reveals perturbed functional networks in Alzheimer's disease. *Cell Rep.* **28**, 1103–1116. (doi:10.1016/j.celrep.2019.06.073)
85. Lleó A *et al.* 2019 Changes in synaptic proteins precede neurodegeneration markers in preclinical Alzheimer's disease cerebrospinal fluid. *Mol. Cell. Proteom.* **18**, 546–560. (doi:10.1074/mcp.RA118.001290)
86. Berchtold NC, Coleman PD, Cribbs DH, Rogers J, Gillen DL, Cotman CW. 2013 Synaptic genes are extensively downregulated across multiple brain regions in normal human aging and Alzheimer's disease. *Neurobiol. Aging* **34**, 1653–1661. (doi:10.1016/j.neurobiolaging.2012.11.024)
87. Neuner SM, Wilmott LA, Hoffmann BR, Mozhui K, Kaczorowski CC. 2017 Hippocampal proteomics defines pathways associated with memory decline and resilience in normal aging and Alzheimer's disease mouse models. *Behav. Brain Res.* **322**, 288–298. (doi:10.1016/j.bbr.2016.06.002)
88. Berchtold NC, Prieto GA, Phelan M, Gillen DL, Baldi P, Bennett DA, Buchman AS, Cotman CW. 2019 Hippocampal gene expression patterns linked to late-life physical activity oppose age and AD-related transcriptional decline. *Neurobiol. Aging* **78**, 142–154. (doi:10.1016/j.neurobiolaging.2019.02.012)
89. Popesco MC, Lin S, Wang Z, Ma ZJ, Friedman L, Frostholm A, Rotter A. 2008 Serial analysis of gene expression profiles of adult and aged mouse cerebellum. *Neurobiol. Aging* **29**, 774–788. (doi:10.1016/j.neurobiolaging.2006.12.006)
90. Tserel L, Limbach M, Saare M, Kisand K, Metspalu A, Milani L, Peterson P. 2014 CpG sites associated with NRP1, NRXN2 and miR-29b-2 are hypomethylated in monocytes during ageing. *Immun. Ageing* **11**, 1. (doi:10.1186/1742-4933-11-1)
91. Kumar D, Thakur MK. 2015 Age-related expression of neuexin1 and neuroligin3 is correlated with presynaptic density in the cerebral cortex and hippocampus of male mice. *Age (Omaha)* **37**, 17. (doi:10.1007/s11357-015-9752-6)
92. González-Velasco O, Papy-García D, Le Douaron G, Sánchez-Santos JM, De Las Rivas J. 2020 Transcriptomic landscape, gene signatures and regulatory profile of aging in the human brain. *Biochim. Biophys. Acta - Gene Regul. Mech.* **1863**, 194491. (doi:10.1016/j.bbagr.2020.194491)
93. Xiao S *et al.* 2011 RNA targets of TDP-43 identified by UV-CLIP are deregulated in ALS. *Mol. Cell. Neurosci.* **47**, 167–180. (doi:10.1016/j.mcn.2011.02.013)
94. Everall I, Salaria S, Roberts E, Corbeil J, Sasik R, Fox H, Grant I, Masliah E. 2005 Methamphetamine stimulates interferon inducible genes in HIV infected brain. *J. Neuroimmunol.* **170**, 158–171. (doi:10.1016/j.jneuroim.2005.09.009)
95. Berchtold NC, Sabbagh MN, Beach TG, Kim RC, Cribbs DH, Cotman CW. 2014 Brain gene expression patterns differentiate mild cognitive impairment from normal aged and Alzheimer's disease. *Neurobiol. Aging* **35**, 1961–1972. (doi:10.1016/j.neurobiolaging.2014.03.031)
96. Vounou M, Janousova E, Wolz R, Stein JL, Thompson PM, Rueckert D, Montana G. 2012 Sparse reduced-rank regression detects genetic associations with voxel-wise longitudinal phenotypes in Alzheimer's disease. *Neuroimage* **60**, 700–716. (doi:10.1016/j.neuroimage.2011.12.029)
97. Zeis T, Kinter J, Herrero-Herranz E, Weissert R, Schaeren-Wiemers N. 2008 Gene expression analysis of normal appearing brain tissue in an animal model for multiple sclerosis revealed grey matter alterations, but only minor white matter changes.

- J. Neuroimmunol.* **205**, 10–19. (doi:10.1016/j.jneuroim.2008.09.009)
98. Opsahl JA *et al.* 2016 Label-free analysis of human cerebrospinal fluid addressing various normalization strategies and revealing protein groups affected by multiple sclerosis. *Proteomics* **16**, 1154–1165. (doi:10.1002/pmic.201500284)
99. Kattimani Y, Veerappa AM. 2018 Dysregulation of NRXN1 by mutant MIR8485 leads to calcium overload in pre-synapses inducing neurodegeneration in Multiple sclerosis. *Mult. Scler. Relat. Disord.* **22**, 153–156. (doi:10.1016/j.msard.2018.04.005)
100. Castro K *et al.* 2019 Body mass index in multiple sclerosis modulates ceramide-induced DNA methylation and disease course. *EBioMedicine* **43**, 392–410. (doi:10.1016/j.ebiom.2019.03.087)
101. Swanberg M, Duvefelt K, Diez M, Hillert J, Olsson T, Piehl F, Lidman O. 2006 Genetically determined susceptibility to neurodegeneration is associated with expression of inflammatory genes. *Neurobiol. Dis.* **24**, 67–88. (doi:10.1016/j.nbd.2006.05.016)
102. Suh YA, Kwon OM, Yim SY, Lee HJ, Kim SS. 2007 Identification of differentially expressed genes in murine hippocampus by modulation of nitric oxide in kainic acid-induced neurotoxic animal model. *Korean J. Physiol. Pharmacol.* **11**, 149–154.
103. Fan Z, Chen X, Chen R. 2014 Transcriptome-wide analysis of TDP-43 binding small RNAs identifies miR-NID1 (miR-8485), a novel miRNA that represses NRXN1 expression. *Genomics* **103**, 76–82. (doi:10.1016/j.ygeno.2013.06.006)
104. Xiang YY, Dong H, Yang BB, Macdonald JF, Lu WY. 2014 Interaction of acetylcholinesterase with neurexin-1 β regulates glutamatergic synaptic stability in hippocampal neurons. *Mol. Brain* **7**, 1–7. (doi:10.1186/1756-6606-7-15)
105. Damodaran TV, Patel AG, Greenfield ST, Dressman HK, Lin SM, Abou-Donia MB. 2006 Gene expression profiles of the rat brain both immediately and 3 months following acute sarin exposure. *Biochem. Pharmacol.* **71**, 497–520. (doi:10.1016/j.bcp.2005.10.051)
106. Hiolski EM *et al.* 2014 Chronic low-level domoic acid exposure alters gene transcription and impairs mitochondrial function in the CNS. *Aquat. Toxicol.* **155**, 151–159. (doi:10.1016/j.aquatox.2014.06.006)
107. Noelker C *et al.* 2012 Differentially expressed gene profile in the 6-hydroxy-dopamine-induced cell culture model of Parkinson's disease. *Neurosci. Lett.* **507**, 10–15. (doi:10.1016/j.neulet.2011.11.035)
108. Richter F *et al.* 2014 Chronic administration of cholesterol oximes in mice increases transcription of cytoprotective genes and improves transcriptome alterations induced by alpha-synuclein overexpression in nigrostriatal dopaminergic neurons. *Neurobiol. Dis.* **69**, 263–275. (doi:10.1016/j.nbd.2014.05.012)
109. Fu LM, Fu KA. 2015 Analysis of Parkinson's disease pathophysiology using an integrated genomics-bioinformatics approach. *Pathophysiology* **22**, 15–29. (doi:10.1016/j.pathophys.2014.10.002)
110. Nezhadi A, Esmaeili-Mahani S, Sheibani V, Shabani M, Darvishzadeh F. 2017 Neurosteroid allopregnanolone attenuates motor disability and prevents the changes of neurexin 1 and postsynaptic density protein 95 expression in the striatum of 6-OHDA-induced rats' model of Parkinson's disease. *Biomed. Pharmacother.* **88**, 1188–1197. (doi:10.1016/j.biopha.2017.01.159)
111. Freeze B, Acosta D, Pandya S, Zhao Y, Raj A. 2018 Regional expression of genes mediating trans-synaptic alpha-synuclein transfer predicts regional atrophy in Parkinson disease. *NeuroImage Clin.* **18**, 456–466. (doi:10.1016/j.nicl.2018.01.009)
112. Haghparast E, Sheibani V, Abbasnejad M, Esmaeili-Mahani S. 2019 Apelin-13 attenuates motor impairments and prevents the changes in synaptic plasticity-related molecules in the striatum of Parkinsonism rats. *Peptides* **117**, 170091. (doi:10.1016/j.peptides.2019.05.003)
113. See K *et al.* 2014 SMN deficiency alters Nrnx2 expression and splicing in zebrafish and mouse models of spinal muscular atrophy. *Hum. Mol. Genet.* **23**, 1754–1770. (doi:10.1093/hmg/ddt567)
114. Petersen RC. 2011 Mild cognitive impairment. *N. Engl. J. Med.* **364**, 2227–2234. (doi:10.1056/NEJMc0910237)
115. Tatemoto K *et al.* 1998 Isolation and characterization of a novel endogenous peptide ligand for the human APJ receptor. *Biochem. Biophys. Res. Commun.* **251**, 471–476. (doi:10.1006/bbrc.1998.9489)
116. Zhang X *et al.* 2011 Up-regulation of apelin in brain tissue of patients with epilepsy and an epileptic rat model. *Peptides* **32**, 1793–1799. (doi:10.1016/j.peptides.2011.08.006)
117. Baulieu EE, Robel P, Schumacher M. 2001 Neurosteroids: beginning of the story. *Int. Rev. Neurobiol.* **46**, 1–32. (doi:10.1016/S0074-7742(01)46057-0)
118. di Michele F, Longone P, Romeo E, Lucchetti S, Brusa L, Pierantozzi M, Bassi A, Bernardi G, Stanzione P. 2003 Decreased plasma and cerebrospinal fluid content of neuroactive steroids in Parkinson's disease. *Neurol. Sci.* **24**, 172–173. (doi:10.1007/s10072-003-0115-1)
119. Mackenzie IRA, Rademakers R. 2008 The role of transactive response DNA-binding protein-43 in amyotrophic lateral sclerosis and frontotemporal dementia. *Curr. Opin. Neurol.* **21**, 693–700. (doi:10.1097/WCO.0b013e3283168d1d)
120. Lefebvre S *et al.* 1995 Identification and characterization of a spinal muscular atrophy-determining gene. *Cell* **80**, 155–165. (doi:10.1016/0092-8674(95)90460-3)

CHAPTER 5

Functional Analysis of the *NRXN2* p.G849D Variant

This chapter consists of a submitted manuscript that addressed **Objectives 3-5** of this study. In this chapter we performed functional studies on the identified *NRXN2* p.G849D variant to better understand its potential role in PD. We first obtained the *NRXN2* α -ECFP-N1 plasmid from Prof. Ann Marie Craig (University of British Columbia, Canada), which expresses mouse *NRXN2* α . We used site-directed mutagenesis to generate the mutant plasmid (p.G882D in our mouse model). The plasmids were transfected into SH-SY5Y neuroblastoma cells and functional assays were performed to evaluate the effect of the mutant on cellular health, mitochondrial health, and oxidative stress.

Submitted Article: Neurexin 2 p.G849D variant, implicated in Parkinson's disease, increases reactive oxygen species, and reduces cell viability and mitochondrial membrane potential in SH-SY5Y cells

Authors: Cuttler, K., de Swart, D., Engelbrecht, L., Kriel, J., Cloete, R., Bardien, S.

Target Journal: Journal of Neural Transmission (Impact Factor: 3.575). Currently under review.

Supplementary material: This follows directly after the article, in text.

Declarations

Declaration by the candidate

With regard to the submitted research article constituting Chapter 5 of the dissertation, the nature and scope of my contribution were as follows:

Planned and conducted all experiments, analyzed the experimental data, created all tables, and figures, wrote the first manuscript draft, prepared supplementary material of the article, revised, reviewed and edited the manuscript (extent of contribution = 70%).

The following co-authors have contributed to Chapter 5:

Name	E-mail Address	Nature of Contribution	Extent of Contribution (%)
Dalene de Swardt	ddeswardt@sun.ac.za	<ul style="list-style-type: none"> Assisted with flow cytometry analysis Manuscript review and editing 	4
Lize Engelbrecht	lizeb@sun.ac.za	<ul style="list-style-type: none"> Assisted with microscopy analysis Manuscript review and editing. 	4
Jurgen Kriel	jkriel@sun.ac.za	<ul style="list-style-type: none"> Assisted with microscopy analysis Manuscript review and editing 	4
Ruben Cloete	ruben@sanbi.ac.za	<ul style="list-style-type: none"> Manuscript review and editing. Supervision 	8
Soraya Bardien	sbardien@sun.ac.za	<ul style="list-style-type: none"> Research project conception and organization. Manuscript review and editing. Supervision 	10

Signature of candidate:

Date: 07/07/2022

Declaration by co-authors

The undersigned hereby confirm that

1. the declaration above accurately reflects the nature and extent of the contributions of the candidate and the co-authors to Chapter 5,
2. no other authors contributed to Chapter 5, besides those specified above, and
3. potential conflicts of interest have been revealed to all interested parties and that the necessary arrangements have been made to use the material in Chapter 5 of this dissertation.

Name	Signature	Affiliation	Date
Dalene de Swardt		Stellenbosch University, Cape Town, South Africa	07/07/2022
Lize Engelbrecht		Stellenbosch University, Cape Town, South Africa	07/07/2022
Jurgen Kriel		Stellenbosch University, Cape Town, South Africa	05/07/2022
Ruben Cloete		South African National Bioinformatics Institute (SANBI), University of the Western Cape, Cape Town, South Africa	07/07/2022
Soraya Bardien		Stellenbosch University, Cape Town, South Africa	06/07/2022

Neurexin 2 p.G849D variant, implicated in Parkinson's disease, increases reactive oxygen species, and reduces cell viability and mitochondrial membrane potential in SH-SY5Y cells

Katelyn Cuttler¹, Dalene de Swardt², Lize Engelbrecht², Jurgen Kriel², Ruben Cloete³, Soraya Bardien^{1, 4*}

¹ Division of Molecular Biology and Human Genetics, Faculty of Medicine and Health Sciences, Stellenbosch University, Cape Town, South Africa

² Central Analytical Facilities, Stellenbosch University, Cape Town, South Africa

³ South African Medical Research Council Bioinformatics Unit, South African National Bioinformatics Institute, University of the Western Cape, Cape Town, South Africa

⁴ South African Medical Research Council/Stellenbosch University Genomics of Brain Disorders Research Unit, Cape Town, South Africa

*Soraya Bardien sbardien@sun.ac.za

Target Journal: Journal of Neural Transmission

ABSTRACT

Background: Parkinson's disease (PD) is a neurodegenerative movement disorder, affecting 1-2% of the human population over 65. A previous study by our group identified a p.G849D variant in neurexin 2 α (*NRXN2*) co-segregating with PD, prompting validation of its role using experimental methods. This novel variant had been found in a South African family with autosomal dominant PD. *NRXN2 α* is an essential synaptic maintenance protein with multiple functional roles at the synaptic cleft.

Objective: The aim of the present study was to investigate the potential role of the translated protein *NRXN2 α* and the observed mutant in PD by performing functional studies in an *in vitro* model.

Methods: Wild-type and mutant *NRXN2 α* plasmids were transfected into SH-SY5Y cells to assess the effect of the mutant on cell viability and apoptosis [(3-(4,5-dimethylthiazol-2-yl)-2,5-diphenyltetrazolium bromide (MTT) Assay; ApoTox-Glo™ Triplex Assay)], mitochondrial membrane potential (MMP; MitoProbe™ JC-1 Assay), mitochondrial network analysis (MitoTracker®) and reactive oxygen species (ROS; ROS-Glo™ H₂O₂ Assay).

Results: Cells transfected with the mutant *NRXN2 α* plasmid showed decreased cell viability and MMP. They also exhibited increased ROS production. However, these cells showed no changes in mitochondrial fragmentation.

Conclusion: Our findings led us to speculate that the p.G849D variant may be involved in a toxic feedback loop leading to neuronal death in PD. Mitochondrial dysfunction and synaptic dysfunction have been linked to PD. Therefore, findings from this exploratory study are in line with previous studies connecting these two processes and warrants further investigation into the role of this variant in other cellular and animal models.

Keywords Parkinson's disease; neurexin 2 α (*NRXN2*), p.G849D variant; cell viability; mitochondrial membrane potential; oxidative stress

Introduction

Parkinson's disease (PD) is the fastest growing neurological disorder globally in terms of prevalence (Feigin et al. 2017). It is a neurodegenerative disorder of movement, affecting 1-2% of the population over the age of 65 (de Rijk et al. 2000). The cardinal symptoms include resting tremor, bradykinesia, and postural instability (Jankovic 2008). In addition, the non-motor symptoms of PD usually develop before the motor symptoms and include constipation, depression, dementia, and sleep disturbances (Tyson et al. 2016). PD is pathologically defined by the loss of dopaminergic neurons in the *substantia nigra* and the presence of intraneuronal cytoplasmic inclusions, called Lewy bodies (Dauer and Przedborski 2003). The *substantia nigra pars compacta* (*SNpc*) is responsible for dopaminergic innervation to the striatum, to integrate cortical and thalamic innervation, and to control movement initiation (Lima et al. 2009). Therefore, the loss of dopamine neurons negatively impacts the communication of the *substantia nigra* with the neurons of the dorsal striatum, resulting in the motor symptoms observed in PD (MacDonald et al. 2013).

PD can present as either sporadic or familial forms, with sporadic forms comprising approximately 90% of the cases (Yasuda and Mochizuki 2010). In sporadic PD, ~90 associated loci have been implicated through genome-wide association studies (GWAS), that harbor ~187 genes (Blauwendraat et al. 2019). These polymorphisms contribute only marginally to disease susceptibility (ORs <1.5, with the majority <1.1). The factors implicated in familial PD are better understood and provides clues as to the molecular pathogenesis of the disorder (Klein and Westenberger 2012). Mutations consistent with a Mendelian pattern of inheritance are rare and globally account for <1% PD. In total, there are ~30-40 genes "linked" to disease (in genes such as *LRRK2* and *SNCA*), with mutant alleles of major effect (ORs >10) (Lill 2016; Puschmann 2017).

In contrast to the global advances in the understanding of PD genetics, studies on sub-Saharan African (SSA) populations are scarce. In addition, many studies have shown that the known PD mutations are only minor contributors to the etiology of PD in SSA populations (Okubadejo et al. 2008; Barden et al. 2009, 2010; Keyser et al. 2009, 2010; Cilia et al. 2012; Yonova-Doing et al. 2012; Blanckenberg et al. 2013, 2014; van der Merwe et al. 2016).

In order to help bridge this knowledge gap, we previously recruited a multiplex South African family for a whole-exome sequencing study to identify a possible novel PD-causing gene (Sebate et al. 2021). After the sequencing, *in silico* pathogenicity analysis, allele frequency analysis and pathway and expression analysis was performed, a novel variant, p.G849D, in neurexin 2 α (*NRXN2 α*) was prioritized as a potential candidate for PD (dbSNP: ss2137544362; genomic position: 64651507_chr11 (GRCh38), transcript ENST00000377559.7) (Sebate et al. 2021). This variant is heterozygous and has an autosomal dominant mode of inheritance within the family (Sebate et al. 2021). Neurexin proteins are embedded in the presynaptic membrane and interact with key postsynaptic surface proteins to regulate synapse maintenance and function (Craig and Kang 2007). In addition, neurexins and their common binding partners, neuroligins, have been associated with multiple developmental disorders and there is increasing evidence that they are

associated with several neurodegenerative disorders (For Review: Cuttler et al., 2021). There is a clear link between neurexins and neuropsychiatric disorders, such as autism spectrum disorder and schizophrenia. However, multiple expression studies have also shown changes in neurexin expression in several neurodegenerative disorders, including Alzheimer's disease (Goetzl et al. 2018; Lleó et al. 2019) and PD (Fu and Fu 2015) (For Review: Cuttler et al., 2021).

Notably, a study using synaptosomes (representing synapses detached from neuronal cell bodies), which were isolated from the *SNpc*, showed altered mitochondrial translation in people with PD compared to healthy controls (Plum et al. 2020). These findings imply that there is mitochondrial dysfunction in synapses in individuals with PD and we hypothesize that this is due to synaptic dysfunction. Therefore, the aim of the present study was to investigate the potential role of wild-type and p.G849D NRXN2 α on mitochondrial function. This work could form the foundation necessary for the design of future studies on this variant in PD animal models.

Methods

Ethical Considerations

Ethical approval was obtained from the Health Research Ethics Committee (Protocol numbers 2002/C059 and S20/01/005 PhD) and the Research Ethics Committee: Biological and Environmental Safety (Protocol number BEE-2021-13149). Both committees are based at Stellenbosch University, Cape Town, South Africa.

Cell Culture

SH-SY5Y cells were cultured in DMEM with high glucose (4.5 g/l) and 4 mM L-Glutamine (Lonza). In addition, the media was supplemented with 15% FBS (Gibco) and 1% penicillin/streptomycin (Sigma Aldrich). Cells were maintained at 37 °C and 5% CO₂ in a humidified incubator (ESCO Technologies).

Plasmids

NRXN2 α Wild-type

Since human NRXN2 α cDNA was not available at the time this study was started, we used wild type mouse NRXN2 α cDNA (ENSMUST00000236635.2) instead, after checking its alignment against the human NRXN2 α transcript ENST00000377559.7 (71% identity). The NRXN2 α -ECFP-N1 plasmid was provided by Prof. Ann Marie Craig (University of British Columbia, Canada) and was generated as per Kang et al., (2008), using *mus musculus* transcribed RNA AK129239 (NCBI). The pECFP-N1 plasmid without an insert (empty vector) was obtained from Prof. Harald Sitte (Medical University of Vienna, Austria).

Site-directed Mutagenesis

In order to generate the p.G849D mutant plasmid (p.G882D in our mouse model (mouse genomic position: 540693_chr19 (GRCm39)), site-directed mutagenesis was performed on the wild-type NRXN2 α -ECFP-N1 plasmid using the Q5 Site-Directed Mutagenesis kit (New England Biolabs) as per the manufacturer's instructions. Briefly, the wild-type plasmid was used as template DNA in a PCR reaction with a mutagenic forward primer, containing the single base pair change that leads to the generation of the G to D substitution, and back-to-back reverse primer. The primer sequences are shown in **Table 1**. The PCR reaction consisted of an initial denaturation at 98 °C for 30 seconds, followed by 25 cycles of 98 °C for 10 seconds, 69 °C for 30 seconds and 72 °C for 5 minutes, and a final extension at 72 °C for 2 minutes. Following the PCR reaction, the kinase, ligase and DpnI enzyme mixture was added to the PCR product and incubated at room temperature for five minutes. This mixture is used to efficiently phosphorylate, ligate, and circularize the new construct and remove the template construct. After the incubation period, 5 μ l of the reaction mixture was used for bacterial transformation of the NEB 5-alpha competent *E. coli* cells. Confirmation of mutagenesis was performed using Sanger sequencing of plasmid DNA at Stellenbosch University's Central Analytical Facilities (CAF).

Table 1 Primer sequences used to generate the novel NRXN2 p.D889 construct.

Primer	Sequence (5'-3')	Tm (°C)	Ta (°C)
Q5 G882D Forward	5'-GTG TTC AAT GAT CAA CCC TAC ATG GAC C-3'	68	69
Q5 G882D Reverse	5'-CAG CCC ACT CAG GTG CCC-3'	72	

Transfection

SH-SY5Y cells were seeded at optimized densities in specific sterile cell culture plates and transfected using Lipofectamine3000 (Invitrogen). In brief, depending on the volume of the culture plate, optimized concentrations of plasmid DNA and volumes of Lipofectamine3000 and P3000 were separately prepared with a pre-determined volume of serum free media. Optimized conditions are shown in **Table 2**. Thereafter, the two volumes were combined, gently mixed, and incubated for 10-20 minutes at room temperature. DMEM supplemented with 15% FBS without penicillin/streptomycin was then added to each well. The combined transfection reagents were then added dropwise to each well and plates incubated at 37°C, 5% CO₂. After 24 hours the media was removed and replaced with pre-warmed complete media. The transfection efficiency was

determined by examining the cells under an Oxion Inverso Fluo E4 fluorescent microscope (Euromex) at 100x magnification for the presence of cyan fluorescent protein (CFP).

Table 2 Transfection of SH-SY5Y cells with Lipofectamine3000 transfection reagent.

Plate Type	Total SFM	Lipofectamine3000	P3000	Plasmid DNA
25 cm ³	500 µl	7.5 µl	10 µl	5 µg
6-well	250 µl	3.75 µl	5 µl	2.5 µg
96-well	10 µl	0.15 µl	0.2 µl	0.1 µg

SFM: serum-free media

NRXN2 α Levels

In order to confirm that transfection of the cells with the plasmids resulted in expression of NRXN2 α protein, we used immunofluorescent flow cytometry and an anti-NRXN2 antibody. Cells were seeded at a density of 500 000 cells per well in a 6-well plate and transfected with the wild-type, mutant, or empty vector plasmids. After 24 hours the media was removed, and cells were trypsinized and transferred to 1.5 ml Eppendorf tubes. Cell pellets were harvested by centrifugation at 438 x g for 10 minutes. The cells were fixed using 3% formaldehyde in PBS for 15 minutes and permeabilized using 0.25% Triton X-100 in PBS for 15 minutes. Cells were then blocked with 0.5% BSA in PBS for 10 minutes and resuspended in 1:100 rabbit anti-NRXN2 primary antibody (Abcam: ab34245) in PBS. These suspensions were incubated overnight at 4 °C. The following morning, the cells were washed in PBS by centrifuging at 2739 x g for 5 minutes and resuspended in 1:100 anti-rabbit Cy3 secondary antibody (Jackson ImmunoResearch Laboratories: 111-165-003) in PBS. These suspensions were incubated in the dark at room temperature for 2 hours. Cells were washed twice in PBS by centrifuging at 2739 x g for 5 minutes and resuspended in deionized water for analysis with the Guava® Muse® Cell Analyzer (Luminex). Unstained, non-transfected cells and stained, non-transfected cells were used to set the gating parameters. Readings were obtained using the Open Module Red option with 5000 events recorded for each sample. Median fluorescence values were used for analysis of NRXN2 α levels.

Cellular Health Assays

3-(4,5-dimethylthiazol-2-yl)-2,5-diphenyltetrazolium bromide (MTT) Assay

SH-SY5Y cells were seeded at a density of 10 000 cells per well in a 96-well plate and transfected with the three plasmids. After 24 hours, 10 µl of 10 mg/ml MTT in DMSO was added to the wells. The plate was incubated in the dark for 4 hours at 37 °C. Thereafter, the solution was aspirated, and the Formazan aggregates were dissolved in 50 µl DMSO. The absorbance was measured at 570 nm using the Synergy HTX microplate reader (BioTek). Analysis was performed using Gen5

3.10 software (BioTek). In addition to the test samples, positive control cells treated with 10% DMSO were analyzed.

CyQUANT® NF Cell Proliferation Assay

To quantify the number of SH-SY5Y cells plated per sample the CyQUANT® NF Cell Proliferation Assay (Thermo Fisher Scientific) was used as per the manufacturer's instructions. Briefly, cells were seeded at a density of 10 000 cells per well in a 96-well plate at the same time as those seeded for the MTT assay. The cells were transfected with the plasmids and incubated for 24 hours. The media was removed and 100 µl of dye binding solution was added to all wells. The dye binding solution was prepared by adding CyQUANT® NF dye reagent to HBSS at a dilution factor of 0.02. The plate was incubated in the dark for 1 hour at 37 °C and fluorescence was measured at 485/20_{Ex}, 528/20_{Em} using the Synergy HTX microplate reader (BioTek). Analysis was performed using Gen5 3.10 software (BioTek). The resulting values were subtracted from the values obtained from the MTT assay in order to normalize the results.

ApoTox-Glo™ Triplex Assay

The ApoTox-Glo™ Triplex Assay (Promega) was used to measure cell viability, cytotoxicity, and apoptosis in the same well, as per the manufacturer's instructions. The first part of the assay measures cell viability and cytotoxicity simultaneously by looking at the activities of live-cell and dead-cell proteases. Briefly, 10 000 cells were seeded per well in a 96-well plate. After a 24-hour transfection period, 20 µl of the viability/cytotoxicity reagent was added directly to the cells. Cells were then incubated in the dark at 37°C for 90 minutes. Viability was measured at 360/40_{Ex}, 528/20_{Em}, while cytotoxicity was measured at 485/20_{Ex}, 528/20_{Em} using the Synergy HTX microplate reader (BioTek). Afterwards, 100 µl of the Caspase-Glo 3/7 reagent was added to the cells and cells were incubated in the dark for 30 minutes at 37 °C. Total luminescence was then measured using the Synergy HTX microplate reader to determine caspase-3/7 activity. Analysis was performed using Gen5 3.10 software (BioTek). In addition to the test samples, positive control cells treated with 10% DMSO were analyzed.

Mitochondrial Health Assays

Mitochondrial Membrane Potential

The MitoProbe™ JC-1 Assay Kit (Life Technologies) was used as per the manufacturer's instructions to determine mitochondrial membrane potential (MMP; $\Delta\Psi_M$). Briefly, SH-SY5Y cells were seeded at a density of 500 000 cells per well in a 6-well plate. Following transfection, the media was removed, and PBS was added to the cells. Thereafter, 10 µl of 200 µM JC-1 dye was added to the samples. The cells were incubated in the dark at 37 °C for 30 minutes. Cells were then trypsinized and pelleted by centrifugation at 1902 x g for 5 minutes. The pellet was resuspended in PBS for analysis with the DxFLEX Flow Cytometer (Beckman Coulter) with 488nm excitation and using the FITC and PE emission filters. Three biological repeats were

performed, and 10 000 cells were analyzed per sample. Cells treated with CCCP, a potent mitochondrial uncoupler, were used as a positive control in order to perform compensation. Unstained, non-transfected cells and stained, non-transfected cells were used to set the gating parameters. Analysis was performed by CAF using FlowJo™ 10.8 software. The ratio between the median PE fluorescence values and median FITC fluorescence values was then calculated and represents the mitochondrial membrane potential ($\Delta\Psi_M$).

Mitochondrial Network Analysis

In order to examine the mitochondrial network, cells were stained with MitoTracker® Red-CMXRos (Invitrogen). Briefly, 10 000 cells were seeded per well in an 8-well chambered slide and transfected. MitoTracker® Red-CMXRos was added to the cells at a final concentration of 75 nM. Confocal images were acquired by CAF using the Zeiss LSM780 confocal microscope with ZEN 2012 software. The microscope is equipped with an INU incubation system (Tokai HIT) to control the temperature at 37°C and supply of 5% CO₂. MitoTracker® Red-CMXRos was excited with a 561 nm laser and emission detected with a GaAsP detector in the range 570-695 nm. Image stacks were acquired using a Plan Apochromat 63x/1.4 oil objective at a step width of 640 nm. Three image stacks were acquired from each well.

For the 2D analysis, the image stacks were processed using ImageJ software with the FIJI plugin. Morphometric measurements were calculated as described by Merrill et al., (2017). The FIJI plugin, *Mitochondria Analyzer* (<https://github.com/AhsenChaudhry/Mitochondria-Analyzer>), was used for quantification of mitochondrial networks in a 3-dimensional space. Parameters of interest were chosen on both a per cell and per mitochondria basis to quantify network parameters such as number of branches, branch end points and branch junctions.

ROS-Glo™ H₂O₂ Assay

The ROS-Glo™ H₂O₂ Assay (Promega) was used to measure H₂O₂ levels as an indicator of oxidative stress, as per the manufacturer's instructions. Briefly, 10 000 cells were seeded per well in a 96-well plate and transfected with the plasmids. After 18 hours of the transfection period, 20 µl of the H₂O₂ substrate was added directly to the cells. Cells were then incubated in the dark in a humidified incubator for the remainder of the 24-hour transfection period. Thereafter, 100 µl of the ROS-Glo detection reagent was added to the cells and cells were incubated in the dark for 20 minutes at room temperature. Total luminescence was then measured using the Synergy HTX microplate reader (BioTek). Analysis was performed using Gen5 3.10 software (BioTek). In addition to the test samples, positive control cells treated with 50 µM menadione, a H₂O₂ inducer, were analyzed. Since cell culture media can affect H₂O₂ production independently of cells, all treatments were repeated in media only controls without the addition of cells.

Statistical Analysis

A one-way ANOVA followed by a two-tailed student's *t*-test with a confidence interval of 95% was used as a means of analyzing the data, with *p*-values of less than 0.05 considered to be significant. All statistical analysis was performed using GraphPad Prism® 5.02.

Results

Confirmation of NRXN2 α overexpression

After site-directed mutagenesis, Sanger sequencing confirmed successful mutagenesis of the mutant plasmid DNA (**Supplementary Figure S1**). The wild-type and mutant plasmids, along with the empty vector plasmid (pECFP-N1), were then transfected into SH-SY5Y cells. Transfection efficiency, determined by microscopically examining the cells for the presence of CFP-positive cells, was 68% for the wild-type construct, 65% for the mutant construct and 67% for the empty vector construct (**Supplementary Figure S2**). Thereafter, overexpression of NRXN2 α was confirmed using the Guava® Muse® Cell Analyzer (Luminex). **Figure 1** shows a 26% and 21% increase in NRXN2 α levels in the wild-type ($p = 0.03$) and mutant ($p = 0.02$) samples, respectively, with no change in the empty vector ($p = 0.70$) sample compared to non-transfected cells.

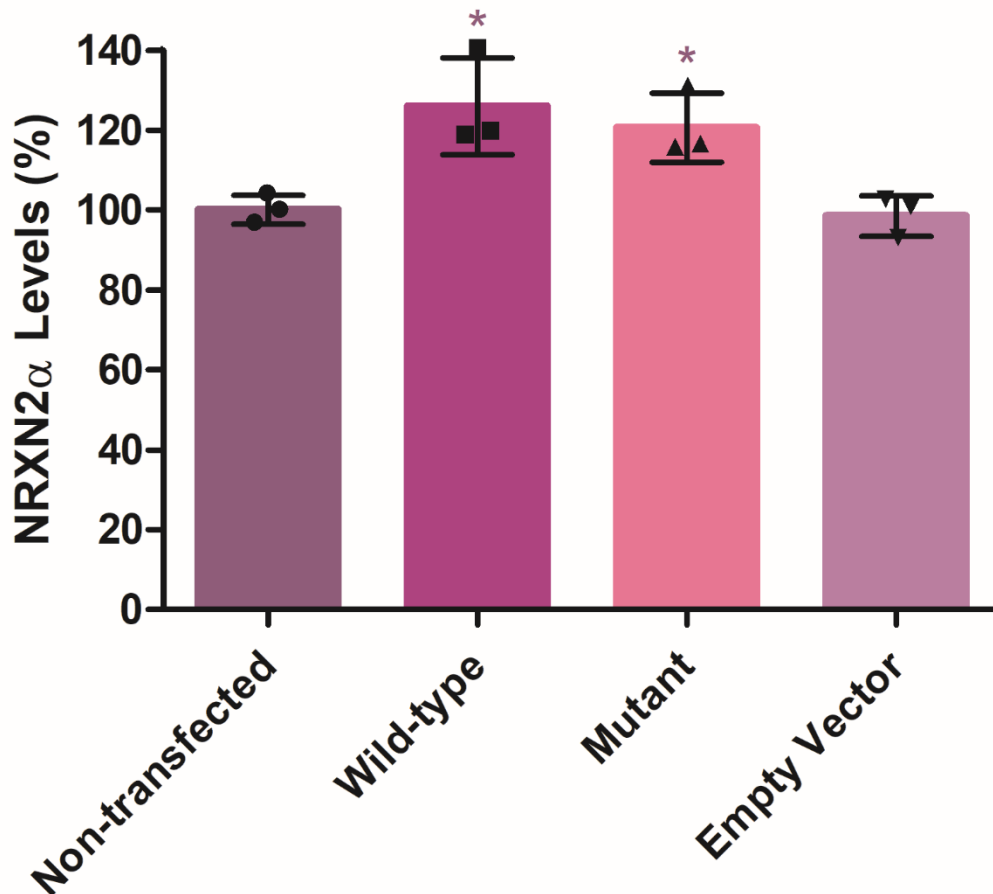


Fig. 1 Overexpression of wild-type and mutant NRXN2 α in SH-SY5Y cells increases NRXN2 α protein levels. Flow cytometric analysis of NRXN2 α levels shows an increase in NRXN2 α levels in both the wild-type ($p = 0.03$) and mutant ($p = 0.02$) transfected cells when compared to the non-transfected cells. There is no significant change in the empty vector ($p = 0.70$) transfected cells compared to non-transfected cells. $n = 3$; one-way ANOVA and student's t -test.

Mutant NRXN2 α overexpression decreases cell viability but has no effect on cytotoxicity or apoptosis

After confirming that NRXN2 α levels were increased in the wild-type and mutant samples, we examined the effect of the variant on cellular health. We used an MTT assay with CyQUANT® correction to determine the effect of the plasmids on the metabolic activity of the cells. This method is dependent on the mitochondrial activity of nicotinamide adenine dinucleotide phosphate (NADPH)-dependent cellular oxidoreductase enzymes that function in reducing the MTT dye.

Figure 2A shows that there is an approximate 23% and 38% reduction in the metabolic activity of the wild-type ($p = 0.04$) and mutant ($p = 0.01$) NRXN2 α transfected cells, respectively. There is also a significant 15% decrease in the mutant cells compared to the wild-type cells ($p = 0.01$).

This finding was confirmed by the ApoTox-Glo™ Triplex Assay (Promega). This kit measures three parameters (cell viability, cytotoxicity, and apoptosis) in the same well. **Figure 2B** shows that there is a 15% and 28% reduction in the viability of the wild-type ($p < 0.01$) and mutant ($p < 0.01$) transfected cells, respectively. There is also a significant 13% decrease in the mutant cells compared to the wild-type cells ($p = 0.03$).

Our study found no difference in terms of the cytotoxicity of the samples (**Figure 2C**; $p = 0.98$) or apoptosis (specifically caspase 3/7 levels; **Figure 2D**; $p = 0.82$). The measurement of cytotoxicity using this assay is dependent on changes in the membrane integrity of the cell and this does not appear to be affected in our study. The similar caspase 3/7 levels across the samples suggests that NRXN2 α overexpression does not induce apoptosis, as caspases 3 and 7 are the executor caspases in the apoptosis pathway and are responsible for executing the hallmarks of apoptosis, such as DNA fragmentation and nuclear morphological changes (Shi 2002).

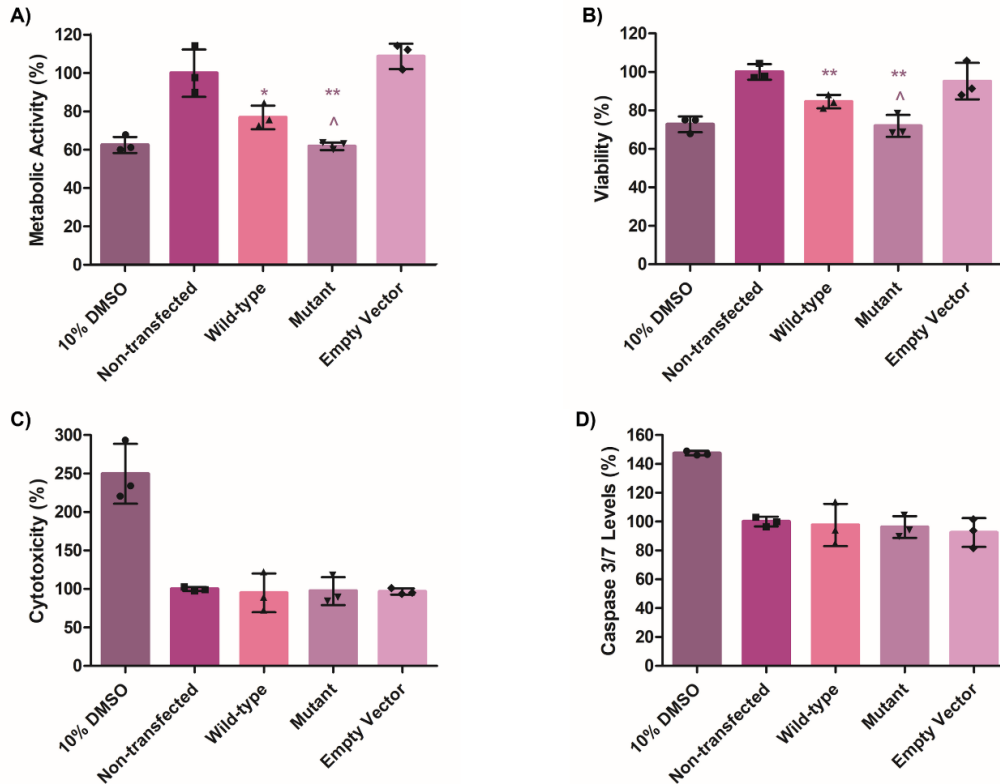


Fig. 2 Overexpression of wild-type and mutant NRXN2 α in SH-SY5Y cells decreases metabolic activity and cell viability. A) MTT analysis shows a significant reduction of metabolic activity in wild-type ($p = 0.04$) and mutant ($p < 0.01$ transfected cells compared to non-transfected cells). There is also a significant metabolic activity reduction in the mutant cells compared to the wild-type cells ($p = 0.01$). B) Decreased cell viability observed in wild-type ($p < 0.01$) and mutant ($p < 0.01$) transfected cells compared to non-transfected cells. There is also a significant decrease in the mutant cells compared to the wild-type cells ($p = 0.03$). No significant changes were seen in the empty vector transfected cells compared to the non-transfected cells in either assay ($p = 0.34$; $p = 0.47$, respectively) C) No difference in cytotoxicity is observed across the treatment groups ($p = 0.98$). D) No difference in caspase 3/7 levels are observed across the treatment groups ($p = 0.82$). In all analyses, the positive control, 10% DMSO, had a detrimental effect on the cells, as expected. $n = 3$; one-way ANOVA and student's t -test.

In order to confirm the apoptosis results seen with the ApoTox-Glo™ Triplex Assay, we performed western blotting to examine the expression of caspases 8 and 9 (**Supplementary Figure S3**). Caspase 8 is an initiator caspase involved in death receptor-mediated (extrinsic) apoptosis, while caspase 9 is an initiator caspase involved in mitochondrial-mediated (intrinsic) apoptosis (Cotter and Al-Rubeai 1995). Densitometric analysis of these blots shows no changes in the caspase 8 and caspase 9 levels across the samples.

Mutant NRXN2 α overexpression decreases mitochondrial membrane potential but has no effect on mitochondrial fragmentation

Thereafter, we performed a JC-1 assay to determine the effects of the plasmids on mitochondrial membrane potential (MMP; $\Delta\Psi_M$). During cell death, $\Delta\Psi_M$ decreases as mitochondrial permeability pores open resulting in a loss of electrochemical gradient. Therefore, the $\Delta\Psi_M$ can be used as a measure of mitochondrial health. Initially, we analyzed the basal polarization levels of cells transfected with the plasmids. **Figure 3A** shows that there is a 32% and 47% decrease in mitochondrial polarization in wild-type ($p < 0.0001$) and mutant ($p < 0.0001$) transfected cells, respectively. There is also a significant 15% decrease in the mutant cells compared to the wild-type cells ($p < 0.0001$).

Thereafter, we looked at $\Delta\Psi_M$ in a stressed environment by treating all of the cells with 10 μM CCCP, a potent mitochondrial uncoupler (**Figure 3B**). Treatment with CCCP decreases the mitochondrial polarization. However, there is no change between the wild-type and mutant samples treated with CCCP compared to the non-transfected sample treated with CCCP ($p = 0.29$).

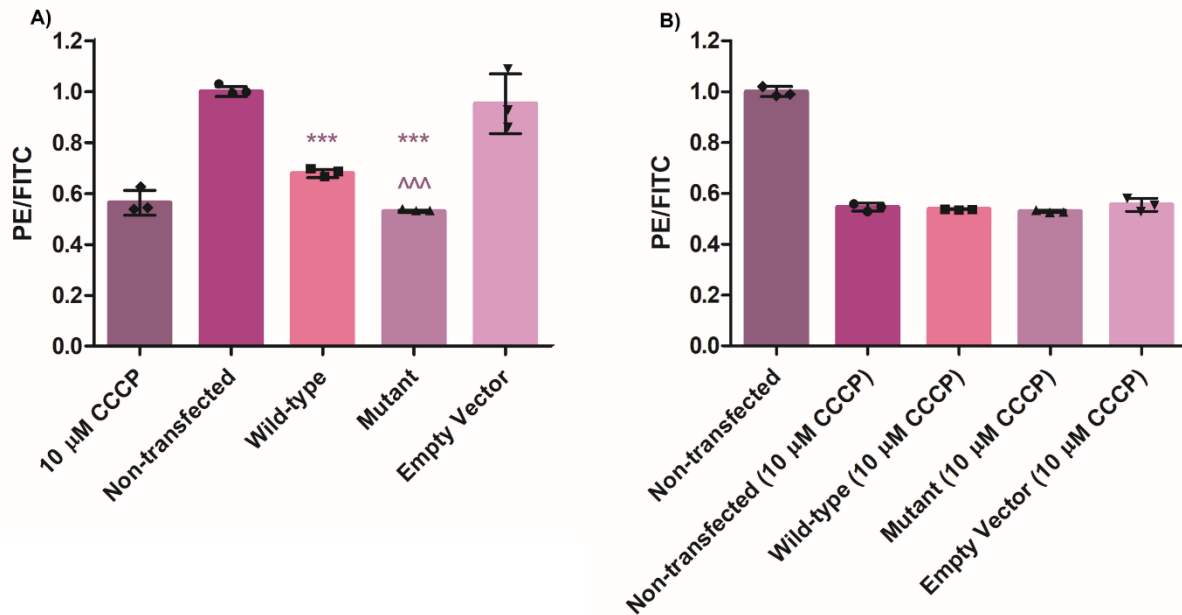


Fig. 3 Overexpression of wild-type and mutant NRXN2 α in SH-SY5Y cells decreases mitochondrial membrane potential (MMP). A) Decreased PE/FITC ratios in wild-type ($p < 0.0001$) and mutant ($p < 0.0001$) transfected cells compared to non-transfected cells are indicative of a decrease in MMP. There is also a significant PE/FITC decrease in the mutant cells compared to the wild-type cells ($p < 0.0001$). No significant changes were seen in the empty vector transfected cells compared to the non-transfected cells ($p = 0.52$). 10 μ M CCCP is used as a positive control. B) No change in the PE/FITC ratio is observed between the wild-type and mutant samples treated with CCCP compared to the non-transfected sample treated with CCCP ($p = 0.29$). $n = 3$; one-way ANOVA and student's t -test.

Since NRXN2 α overexpression had a negative effect on MMP, we also wanted to investigate if it had an effect on the mitochondrial network. Cells were stained with MitoTracker® Red-CMXRos to visualize the mitochondria. Two types of analyses were then performed to investigate the mitochondrial network. A 2D analysis was conducted using ImageJ to calculate the aspect ratio and form factor of individual mitochondria. Form factor is representative of the degree of mitochondrial branching while aspect ratio provides information on mitochondrial elongation. The analyses show no significant differences in the fragmentation of the mitochondrial network (**Supplementary Figure S4 A-B**). 3D Morphometric analysis was further conducted to determine the level of mitochondrial network connectivity in terms of branching and interacting nodes, to account for possible limitations of 2D form factor analysis. However, no significant differences were seen using this analysis either (**Supplementary Figure S4 C-E**).

Mutant NRXN2 α overexpression induces oxidative stress

Finally, we investigated if overexpression of NRXN2 α could also affect ROS production and oxidative stress. Oxidative stress and mitochondrial dysfunction are intrinsically linked, so changes in ROS may help to understand the mechanisms by which a synaptic protein can induce cell death. The ROS-Glo™ H₂O₂ Assay (Promega) was used to measure H₂O₂ levels as an indicator of oxidative stress. Notably, an 84% and 235% increase in H₂O₂ levels in wild-type ($p = 0.03$) and mutant ($p < 0.0001$) transfected cells, respectively was observed (**Figure 4A**). There is also a significant 151% increase in mutant cells compared to the wild-type cells ($p = 0.01$).

Since cell culture media can affect H₂O₂ production independently of cells, all treatments were repeated in media only controls (i.e., no cells present). **Figure 4B** shows a similar trend whereby there is a 35% and 86% increase in H₂O₂ levels in wild-type ($p = 0.04$) and mutant ($p < 0.001$) transfected media, respectively. There is also a significant 51% increase in mutant transfected media compared to the wild-type transfected media ($p = 0.02$). When directly comparing the cells to the media only controls however, there is a significant increase in H₂O₂ levels in cells across the treatment groups (non-transfected: $p < 0.0001$; wild-type: $p = 0.01$; mutant: $p < 0.0001$; empty Vector: $p = 0.03$) (**Figure 4C**). This shows that, although there is abiotic ROS production in the media (likely due to oxidation of certain components in the media), the addition of cells significantly increases H₂O₂ levels. Furthermore, both the wild-type and mutant NRXN2 α are also significantly increasing H₂O₂ levels thereby possibly inducing oxidative stress in the cells.

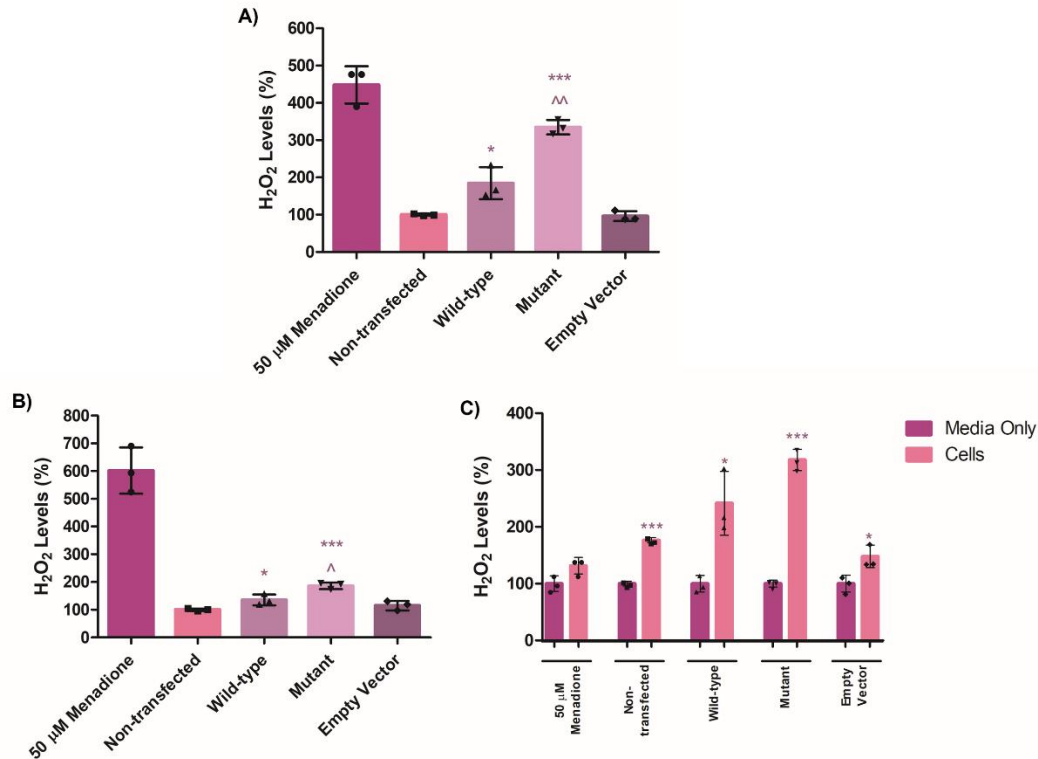


Fig. 4 Overexpression of wild-type and mutant NRXN2 α in SH-SY5Y cells induces ROS. A) There is a significant increase in H₂O₂ levels in wild-type ($p = 0.03$) and mutant ($p < 0.0001$) transfected cells when compared to non-transfected cells. There is also a significant increase in mutant cells transfected cells compared to the wild-type transfected cells ($p < 0.01$). B) There is a significant increase in H₂O₂ levels in wild-type ($p = 0.04$) and mutant ($p < 0.001$) transfected media compared to non-transfected media. There is also a significant increase in mutant transfected media compared to the wild-type transfected media ($p = 0.02$). No significant changes were seen in the empty vector transfected cells compared to the non-transfected cells ($p = 0.49$), or in the empty vector transfected media compared to non-transfected media ($p = 0.21$). C) Direct comparison between the H₂O₂ levels in media only controls versus cells shows a significant increase in H₂O₂ levels in cells across the treatment groups (non-transfected: $p < 0.0001$; wild-type: $p = 0.01$; mutant: $p < 0.0001$; empty vector: $p = 0.03$). In all analyses, the positive control, 50 μ M menadione, induced ROS production, as expected. $n = 3$; one-way ANOVA and student's t -test.

Discussion

The aim of the present study was to investigate the potential role of wild-type and p.G849D NRXN2 α on mitochondrial function. To this end, we transfected SH-SY5Y cells with wild-type and mutant plasmids and examined their effect on overall cell health, mitochondrial health, and ROS generation in order to link a synaptic protein to dysfunctional mitochondria.

Using both an MTT assay as well as the ApoTox-Glo™ Triplex assay, we observed a decrease in cellular metabolic activity and cellular viability, respectively (**Figure 2A-B**). In both cases, while overexpression of wild-type NRXN2 α has a negative effect on cell health, overexpression of the mutant NRXN2 α worsens this effect. Thus, it can be postulated that since NRXN2 α is highly expressed in the *SNpc* (Sunkin et al. 2012), the mutant could possibly result in dopaminergic cell death. The ApoTox-Glo™ Triplex assay also looks at cytotoxicity and apoptosis. The measurement of cytotoxicity using this assay is dependent on changes in the membrane integrity of the cell and this does not appear to be affected in our study (**Figure 2C**). The similar caspase 3/7 levels across the samples also suggests that NRXN2 α overexpression does not induce apoptosis (**Figure 2D**). We thereafter used western blotting to confirm the apoptosis results by measuring the levels of caspases 8 and 9 (**Supplementary Figure S3**). This further suggests that neither the overexpressed wild-type nor the overexpressed mutant NRXN2 α are inducing apoptosis in SH-SY5Y cells. However, apoptosis is a dynamic process that is highly dependent on the type of cell stressor (Cotter and Al-Rubeai 1995), so it is possible that measurements at different post-transfection time points or using different assays may show different results.

$\Delta\Psi_M$ can be used as a measure of mitochondrial health as, during cell death, $\Delta\Psi_M$ decreases as mitochondrial permeability pores open resulting in a loss of electrochemical gradient. Therefore, we performed a JC-1 assay to determine the effects of the plasmids on $\Delta\Psi_M$. We observed a decrease in mitochondrial polarization using this assay which is indicative of a decreased $\Delta\Psi_M$ (**Figure 3A**). It is essential for cells to maintain a high $\Delta\Psi_M$ as the import of mitochondrial proteins and ATP-generating oxidative phosphorylation is reliant on a high $\Delta\Psi_M$ (Zorova et al., 2018). This is especially important in highly energy-dependent neurons. In neurons, mitochondria are distributed to areas of the axon where metabolic demand is high, such as the active growth cones or branches (Morris and Hollenbeck 1993; Ruthel and Hollenbeck 2003), and synapses (Treck and Pirsig 1979; Gotow et al. 1991). It could be speculated that, since NRXN2 α is present at the synapse (Krueger et al. 2012), mutant NRXN2 α could result in synaptic dysfunction as a result of mitochondrial dysfunction. The lowered MMP observed across the mitochondria would reduce ATP generation, leading to an energy depletion in the synapses and thereby affecting their normal functioning (Mattson and Liu 2002). Indeed, the *SNpc* neurons are likely the most dependent on mitochondrial function due to their roles in sensorimotor networks that are necessary for rapid and effective actions (Surmeier et al., 2017), and therefore they are particularly vulnerable to mitochondrial dysfunction. It is important to note that, while we did observe a decrease in $\Delta\Psi_M$ in cells transfected with the plasmids, we did not see any difference when cells were also treated with

CCCP, a potent mitochondrial uncoupler (**Figure 3B**). This suggests that although overexpression of both wild-type and mutant NRXN2 α can decrease $\Delta\Psi_M$, cells with these proteins are not more vulnerable to extracellular stressors.

Since NRXN2 α overexpression had a negative effect on MMP, we also wanted to investigate if it had an effect on the mitochondrial network. Cells were stained with MitoTracker® Red-CMXRos to visualize the mitochondria. However, we saw no differences in both the 2D and 3D analyses of mitochondrial network (**Supplementary Figure S4**) Mitochondria naturally undergo frequent morphological changes in response to the energy demands of the cell (Huang et al. 2011). Thus, it is possible that measurements at different post-transfection time points may show different results. However, it is understandable that overexpressing NRXN2 α , a synaptic protein, would not immediately cause mitochondrial fragmentation. We speculate that, given the changes in MMP seen in Figure 3A, it would most likely be an ongoing process whereby over time the decreased polarization could ultimately result in mitochondrial fragmentation and death. It is also possible that, even though no fragmentation was observed, the rate at which fission and fusion occur has been impacted, which could also negatively impact mitochondrial function.

Since oxidative stress and mitochondrial dysfunction are intrinsically linked, we also wanted to investigate ROS generation to help understand the mechanisms by which NRXN2 α can induce cell death. The ROS-Glo™ H₂O₂ Assay (Promega) was used to measure H₂O₂ levels as an indicator of oxidative stress. We observed an increase in H₂O₂ levels, independent of the cell culture media used (**Figure 4**). ROS is normally produced in mitochondria during electron transport chain and redox reactions and is necessary for cellular homeostasis. In PD, ROS is dysregulated (Bosco et al. 2006; Nakabeppu et al. 2007) resulting in oxidative stress and even cell death (Rego and Oliveira 2003). Indeed, the neurons of the *SNpc* naturally have higher concentrations of oxidative proteins when compared to other areas of the brain, such as the basal ganglia (Floor and Wetzel 1998) and are therefore more vulnerable to ROS dysregulation and oxidative stress.

Since mutant NRXN2 α is able to both decrease mitochondrial polarization and increase H₂O₂ levels, we speculate this could initiate a toxic feedback loop whereby either mitochondrial dysfunction or ROS dysregulation results in increased resultant oxidative stress which negatively affects mitochondrial function. Indeed, studies on the known PD genes; *PINK1*, *PRKN* and *LRRK2*, have shown that a single mutation in these genes can disrupt cellular homeostasis, resulting in abnormal mitochondria and increased sensitivity to oxidative stress inducing agents (Nguyen et al. 2011; Chung et al. 2016). We speculate that the mutant NRXN2 α may play a similar role and that the p.G849D variant could disrupt cellular homeostasis, leading to a multitude of interactions that stress the neurons ultimately leading to neurodegeneration.

In our previous study, it was shown that the p.G849D variant has a destabilizing effect on the NRXN2 α protein structure (Sebate et al. 2021). *In vitro* elucidation of this effect was beyond the scope of this study; however, it would be important to examine this further to determine the effect of the variant on protein's structure, stability, and degradation.

Study Limitations

We acknowledge several limitations to this study. A major limitation is that the p.G849D variant in NRXN2 α is heterozygous in the family, therefore overexpression of mutant NRXN2 α cDNA in a plasmid is only a model in an attempt to understand the possible functional impact of the variant. We also acknowledge the limitations of overexpressing a murine gene in a human cell line to study a human disorder. It would, thus, also be important to repeat these experiments using human NRXN2 α cDNA, which is now commercially available. It should be noted that many alternative transcripts are generated from the *NRXN2* gene, each with their own expression profile (Missler and Südhof 1998) and cell specific expression of these transcripts differs between the mouse brain and human brain. The human NRXN2 α transcript in which the variant was found, ENST00000377559.7, is expressed in the brain and is present in all of the alternative transcripts produced for this gene. In this study, we utilized an *in vitro* model to study the potential effects of the identified mutation, however, it must be stressed that these results would need to be validated using a mouse model, where one would be able to examine all NRXN2 α transcripts that are being expressed. Furthermore, transfection of cells is time dependent. While this study was explorative, it may also be worthwhile to test different transfection time points in future. The study findings could be partly explained by the toxicity of transfection reagents. Although transfection reagents have greatly improved over the years, the process is still stressful to the cells (Wang et al. 2018). Here, a 24-hour transfection period was chosen to maximize transfection efficiency and avoid the toxicity observed at 48-hours. Notably, transfection with the empty vector plasmid did not significantly alter any of the cellular responses examined, however, the addition of a large sequence into the vector may have an effect.

Conclusion

In summary, mutant NRXN2 α was found to have a negative effect on cellular health (reduced cell viability) and mitochondrial health (reduced mitochondrial membrane potential and increased oxidative stress). Although the wild-type protein was observed to have a negative effect, the mutant NRXN2 α has an even worse effect on the SH-SY5Y cells. While there have been very few studies on the overexpression of NRXNs to compare to, Kattimani and Veerappa (2018) observed that the overexpression of NRXN1 in multiple sclerosis patients caused by mutant MIR8485 induced neurodegeneration via calcium overload in pre-synapses. This suggests that increased expression of wild-type NRXNs could also be toxic. However, further work would be required to confirm this.

Findings from our study implicate a synaptic protein in mitochondrial dysfunction. Both mitochondrial dysfunction (Rego and Oliveira 2003; Winklhofer and Haass 2010) and synaptic dysfunction (Belluzzi et al. 2012; Picconi et al. 2012; Lepeta et al. 2016; Taoufik et al. 2018) have been linked separately and together (Nguyen et al. 2019; Plum et al. 2020) to the etiology of PD.

However, to the best of our knowledge, this is the first time a variant in a pre-synaptic cellular adhesion protein has been linked to PD. This work further connects these two etiologies but future studies in PD cellular models or animal models are necessary to validate these findings. Notwithstanding the various limitations, the present study's findings may lead us one step closer to trying to understand the complex pathobiology underlying this disorder.

Acknowledgments

We thank the study participants for their participation in and contribution to this study. We also thank Dr. Annika Neethling for her assistance with the site-directed mutagenesis experiments. We would like to thank Prof. Matthew Farrer for his review of the manuscript. The authors would also like to thank Prof. Ann Marie Craig (University of British Columbia, Canada) and Prof. Harald Sitte (Medical University of Vienna, Austria) for the NRXN2 α -ECFP-N1 plasmid and pECFP-N1 plasmid, respectively. We additionally acknowledge the support of the DSI-NRF Centre of Excellence for Biomedical Tuberculosis Research, South African Medical Research Council Centre for Tuberculosis Research, Division of Molecular Biology and Human Genetics, Faculty of Medicine and Health Sciences, Stellenbosch University, Cape Town, South Africa.

Author Contributions

K.C conducted all the experiments, performed all the statistical analyses, and wrote the first draft of the manuscript. D.d.S and L.E assisted with the analysis of flow cytometry and confocal microscopy samples, respectively. J.K assisted with the 3D analysis of the mitochondrial network. R.C acquired funding for the study. K.C and S.B conceptualized the study and acquired funding for the study. All authors critically reviewed and edited the manuscript.

Funding

This work is based on the research supported in part by the National Research Foundation of South Africa (NRF) (Grant Number: 129249); the South African Medical Research Council (SAMRC) (self-initiated research grant); the Harry Crossley Foundation and Stellenbosch University, South Africa. SAMRC and The Higher Education Department, Next Generation of Academic Programme (nGAP), provided support for R.C. in the form of a fulltime academic position and salary.

Availability of data and material

The datasets generated during and/or analyzed during the current study are available from the corresponding author on reasonable request.

Declarations

Conflict of interest: The authors have no conflict of interest to declare.

Ethical approval: The Health Research Ethics Committee and the Research Ethics Committee: Biological and Environmental Safety of Stellenbosch University approved this study.

References

- Bardien S, Keyser R, Yako Y, et al (2009) Molecular analysis of the parkin gene in South African patients diagnosed with Parkinson's disease. *Park Relat Disord* 15:116–121. <https://doi.org/10.1016/j.parkreldis.2008.04.005>
- Bardien S, Marsberg A, Keyser R, et al (2010) LRRK2 G2019S mutation: Frequency and haplotype data in South African Parkinson's disease patients. *J Neural Transm* 117:847–853. <https://doi.org/10.1007/s00702-010-0423-6>
- Belluzzi E, Greggio E, Piccoli G (2012) Presynaptic dysfunction in Parkinson's disease: a focus on LRRK2. *Biochem Soc Trans* 40:1111–1116. <https://doi.org/10.1042/bst20120124>
- Blanckenberg J, Bardien S, Glanzmann B, et al (2013) The prevalence and genetics of Parkinson's disease in sub-Saharan Africans. *J Neurol Sci* 335:22–25. <https://doi.org/10.1016/j.jns.2013.09.010>
- Blanckenberg J, Ntsapi C, Carr JA, Bardien S (2014) EIF4G1 R1205H and VPS35 D620N mutations are rare in Parkinson's disease from South Africa. *Neurobiol Aging* 35:445.e1-445.e3. <https://doi.org/10.1016/j.neurobiolaging.2013.08.023>
- Blauwendraat C, Heilbron K, Vallerga CL, et al (2019) Parkinson's disease age at onset genome-wide association study: Defining heritability, genetic loci, and α -synuclein mechanisms. *Mov Disord* 34:866–875. <https://doi.org/10.1002/mds.27659>
- Bosco DA, Fowler DM, Zhang Q, et al (2006) Elevated levels of oxidized cholesterol metabolites in Lewy body disease brains accelerate α -synuclein fibrilization. *Nat Chem Biol* 2:249–253. <https://doi.org/10.1038/nchembio782>
- Chung SY, Kishinevsky S, Mazzulli JR, et al (2016) Parkin and PINK1 Patient iPSC-Derived

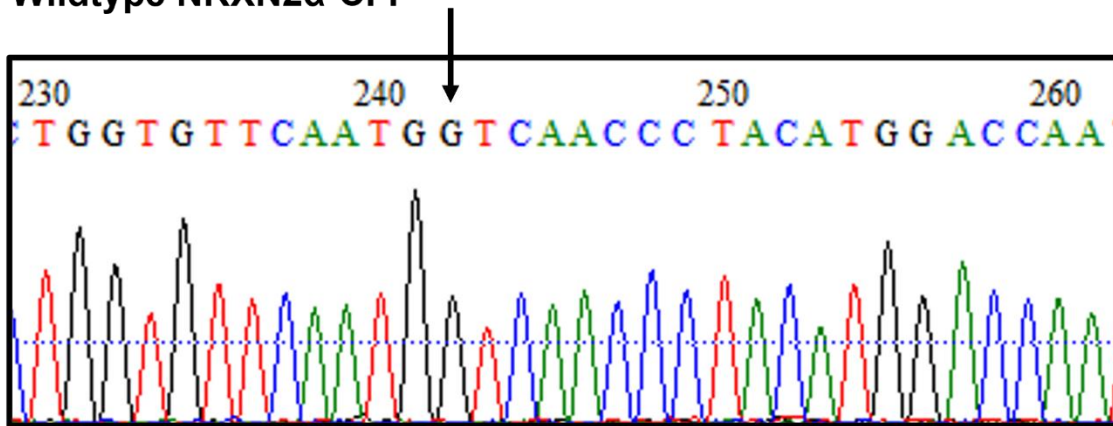
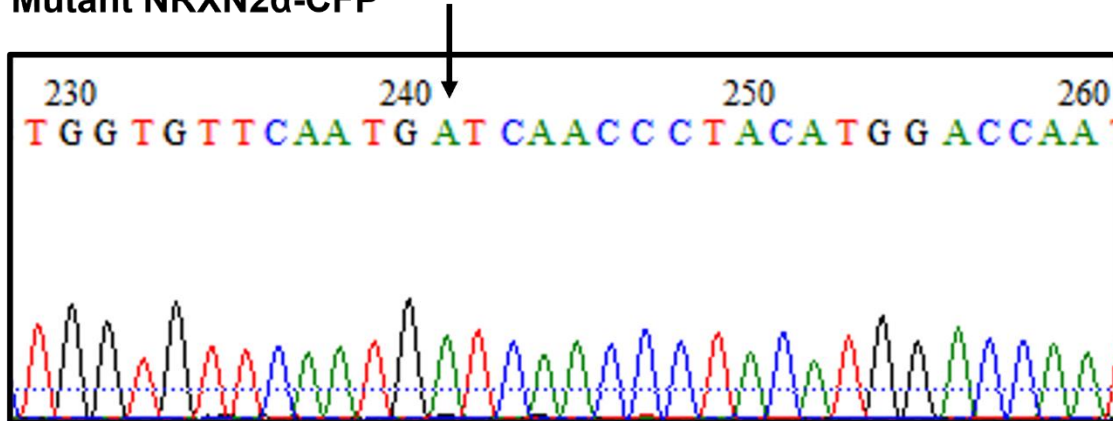
- Midbrain Dopamine Neurons Exhibit Mitochondrial Dysfunction and α -Synuclein Accumulation. *Stem Cell Reports* 7:664–677. <https://doi.org/10.1016/j.stemcr.2016.08.012>
- Cilia R, Sironi F, Akpalu A, et al (2012) Screening LRRK2 gene mutations in patients with Parkinson's disease in Ghana. *J Neurol* 259:569–570. <https://doi.org/10.1007/s00415-011-6210-y>
- Cotter TG, Al-Rubeai M (1995) Cell death (apoptosis) in cell culture systems. *Trends Biotechnol* 13:150–155. [https://doi.org/10.1016/S0167-7799\(00\)88926-X](https://doi.org/10.1016/S0167-7799(00)88926-X)
- Craig AM, Kang Y (2007) Neurexin-neurologin signaling in synapse development. *Curr Opin Neurobiol* 17:43–52. <https://doi.org/10.1016/j.conb.2007.01.011>
- Cuttler K, Hassan M, Carr J, et al (2021) Emerging evidence implicating a role for neurexins in neurodegenerative and neuropsychiatric disorders. *Open Biol* 11:. <https://doi.org/10.1098/RSOB.210091>
- Dauer W, Przedborski S (2003) Parkinson's disease: mechanisms and models. *Neuron* 39:889–909. [https://doi.org/10.1016/S0896-6273\(03\)00568-3](https://doi.org/10.1016/S0896-6273(03)00568-3)
- de Rijk MC, Launer LJ, Berger K, et al (2000) Prevalence of Parkinson's disease in Europe: A collaborative study of population-based cohorts. Neurologic Diseases in the Elderly Research Group. *Neurology* 54:S21-3
- Feigin VL, Krishnamurthi R V., Theadom AM, et al (2017) Global, regional, and national burden of neurological disorders during 1990–2015: a systematic analysis for the Global Burden of Disease Study 2015. *Lancet Neurol* 16:877–897. [https://doi.org/10.1016/S1474-4422\(17\)30299-5](https://doi.org/10.1016/S1474-4422(17)30299-5)
- Floor E, Wetzel MG (1998) Increased protein oxidation in human substantia nigra pars compacta in comparison with basal ganglia and prefrontal cortex measured with an improved dinitrophenylhydrazine assay. *J Neurochem* 70:268–275. <https://doi.org/10.1046/j.1471-4159.1998.70010268.x>
- Fu LM, Fu KA (2015) Analysis of Parkinson's disease pathophysiology using an integrated genomics-bioinformatics approach. *Pathophysiology* 22:15–29. <https://doi.org/10.1016/j.pathophys.2014.10.002>
- Goetzl EJ, Abner EL, Jicha GA, et al (2018) Declining levels of functionally specialized synaptic proteins in plasma neuronal exosomes with progression of Alzheimer's disease. *FASEB J* 32:888–893. <https://doi.org/10.1096/fj.201700731R>
- Gotow T, Miyaguchi K, Hashimoto PH (1991) Cytoplasmic architecture of the axon terminal: Filamentous strands specifically associated with synaptic vesicles. *Neuroscience* 40:587–598. [https://doi.org/10.1016/0306-4522\(91\)90143-C](https://doi.org/10.1016/0306-4522(91)90143-C)

- Huang P, Galloway CA, Yoon Y (2011) Control of mitochondrial morphology through differential interactions of mitochondrial fusion and fission proteins. *PLoS One* 6:e20655. <https://doi.org/10.1371/journal.pone.0020655>
- Jankovic J (2008) Parkinson's disease: clinical features and diagnosis. *J Neurol Neurosurg Psychiatry* 79:368–375. <https://doi.org/10.1136/jnnp.2007.131045>
- Kang Y, Zhang X, Dobie F, et al (2008) Induction of GABAergic postsynaptic differentiation by α -neurexins. *J Biol Chem* 283:2323–2334. <https://doi.org/10.1074/jbc.M703957200>
- Kattimani Y, Veerappa AM (2018) Dysregulation of NRXN1 by mutant MIR8485 leads to calcium overload in pre-synapses inducing neurodegeneration in Multiple sclerosis. *Mult Scler Relat Disord* 22:153–156. <https://doi.org/10.1016/j.msard.2018.04.005>
- Keyser RJ, Lesage S, Brice A, et al (2010) Assessing the prevalence of PINK1 genetic variants in South African patients diagnosed with early- and late-onset Parkinson's disease. *Biochem Biophys Res Commun* 398:125–129. <https://doi.org/10.1016/j.bbrc.2010.06.049>
- Keyser RJ, van der Merwe L, Venter M, et al (2009) Identification of a novel functional deletion variant in the 5'-UTR of the DJ-1 gene. *BMC Med Genet* 10:105. <https://doi.org/10.1186/1471-2350-10-105>
- Klein C, Westenberger A (2012) Genetics of Parkinson's Disease. *Cold Spring Harb Perspect Med* 2:. <https://doi.org/10.1101/cshperspect.a008888>
- Krueger DD, Tuffey LP, Papadopoulos T, Brose N (2012) The role of neurexins and neuroligins in the formation, maturation, and function of vertebrate synapses. *Curr Opin Neurobiol* 22:412–422. <https://doi.org/10.1016/j.conb.2012.02.012>
- Lepeta K, Lourenco M V., Schweitzer BC, et al (2016) Synaptopathies: synaptic dysfunction in neurological disorders – A review from students to students. *J Neurochem* 138:785–805. <https://doi.org/10.1111/jnc.13713>
- Lill CM (2016) Genetics of Parkinson's disease. *Mol Cell Probes* 3:386–396. <https://doi.org/https://doi.org/10.1016/j.mcp.2016.11.001>
- Lima MMS, Reksidler ABB, Vital MABF (2009) The neurobiology of the substantia nigra pars compacta: From motor to sleep regulation. In: Giovanni G, Di Matteo V, Esposito E (eds) *Journal of Neural Transmission. Supplementa: Birth, Life and Death of Dopaminergic Neurons in the Substantia Nigra*. Springer Vienna, Vienna, pp 135–145
- Lleó A, Núñez-Llaves R, Alcolea D, et al (2019) Changes in synaptic proteins precede neurodegeneration markers in preclinical Alzheimer's disease cerebrospinal fluid. *Mol Cell Proteomics* 18:546–560. <https://doi.org/10.1074/mcp.RA118.001290>

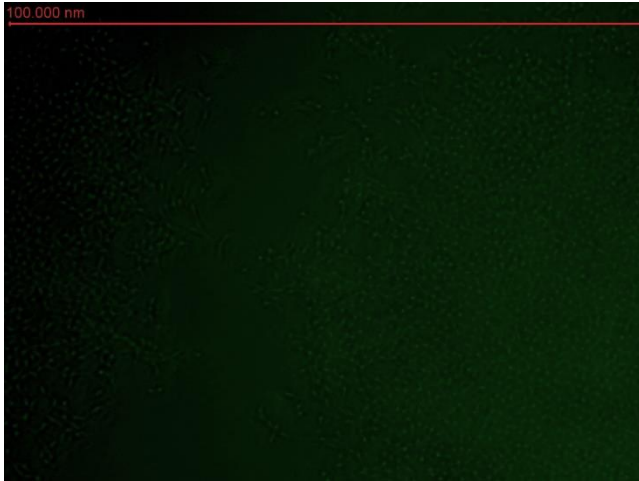
- MacDonald AA, Seergobin KN, Owen AM, et al (2013) Differential Effects of Parkinson's Disease and Dopamine Replacement on Memory Encoding and Retrieval. *PLoS One* 8:. <https://doi.org/10.1371/journal.pone.0074044>
- Mattson MP, Liu D (2002) Energetics and Oxidative Stress in Synaptic Plasticity and Neurodegenerative Disorders. *NeuroMolecular Med* 2:215–232. <https://doi.org/10.1385/NMM:2:2:215>
- Merrill RA, Flippo KH, Strack S (2017) Measuring mitochondrial shape with imageJ. In: *Neuromethods*. Humana Press Inc., pp 31–48
- Missler M, Südhof TC (1998) Neurexins: Three genes and 1001 products. *Trends Genet* 14:20–26. [https://doi.org/10.1016/S0168-9525\(97\)01324-3](https://doi.org/10.1016/S0168-9525(97)01324-3)
- Morris RL, Hollenbeck PJ (1993) The regulation of bidirectional mitochondrial transport is coordinated with axonal outgrowth. *J Cell Sci* 104:917–27. <https://doi.org/10.1242/jcs.104.3.917>
- Nakabeppu Y, Tsuchimoto D, Yamaguchi H, Sakumi K (2007) Oxidative damage in nucleic acids and Parkinson's disease. *J Neurosci Res* 85:919–934. <https://doi.org/10.1002/jnr.21191>
- Nguyen HN, Byers B, Cord B, et al (2011) LRRK2 mutant iPSC-derived da neurons demonstrate increased susceptibility to oxidative stress. *Cell Stem Cell* 8:267–280. <https://doi.org/10.1016/j.stem.2011.01.013>
- Nguyen M, Wong YC, Ysselstein D, et al (2019) Synaptic, Mitochondrial, and Lysosomal Dysfunction in Parkinson's Disease. *Trends Neurosci* 42:140–149. <https://doi.org/10.1016/j.tins.2018.11.001>
- Okubadejo N, Britton A, Crews C, et al (2008) Analysis of Nigerians with apparently sporadic Parkinson disease for mutations in LRRK2, PRKN and ATXN3. *PLoS One* 3:. <https://doi.org/10.1371/journal.pone.0003421>
- Picconi B, Piccoli G, Calabresi P (2012) Synaptic dysfunction in Parkinson's disease. In: Kreutz M, Sala C (eds) *Advances in Experimental Medicine and Biology: Synaptic Plasticity*. Springer Vienna, Vienna, pp 553–572
- Plum S, Eggers B, Helling S, et al (2020) Proteomic Characterization of Synaptosomes from Human Substantia Nigra Indicates Altered Mitochondrial Translation in Parkinson's Disease. *Cells* 9:2580. <https://doi.org/10.3390/cells9122580>
- Puschmann A (2017) New Genes Causing Hereditary Parkinson's Disease or Parkinsonism. *Curr Neurol Neurosci Rep* 17:66. <https://doi.org/https://doi.org/10.1007/s11910-017-0780-8>
- Rego AC, Oliveira CR (2003) Mitochondrial dysfunction and reactive oxygen species in

- excitotoxicity and apoptosis: Implications for the pathogenesis of neurodegenerative diseases. *Neurochem Res* 28:1563–1574. <https://doi.org/10.1023/A:1025682611389>
- Ruthel G, Hollenbeck PJ (2003) Response of Mitochondrial Traffic to Axon Determination and Differential Branch Growth. *J Neurosci* 23:8618–8624. <https://doi.org/10.1523/JNEUROSCI.23-24-08618.2003>
- Sebate B, Cuttler K, Cloete R, et al (2021) Prioritization of candidate genes for a South African family with Parkinson’s disease using in-silico tools. *PLoS One* 16:e0249324. <https://doi.org/10.1371/journal.pone.0249324>
- Shi Y (2002) Mechanisms of caspase activation and inhibition during apoptosis. *Mol Cell* 9:459–470. [https://doi.org/10.1016/S1097-2765\(02\)00482-3](https://doi.org/10.1016/S1097-2765(02)00482-3)
- Sunkin SM, Ng L, Lau C, et al (2012) Allen Brain Atlas: An integrated spatio-temporal portal for exploring the central nervous system. *Nucleic Acids Res* 41:D996–D1008. <https://doi.org/https://doi.org/10.1093/nar/gks1042>
- Surmeier DJ, Obeso JA, Halliday GM (2017) Selective neuronal vulnerability in Parkinson disease. *Nat Rev Neurosci* 18:101–113. <https://doi.org/10.1038/nrn.2016.178>
- Taoufik E, Kouroupi G, Zygogianni O, Matsas R (2018) Synaptic dysfunction in neurodegenerative and neurodevelopmental diseases: An overview of induced pluripotent stem-cell-based disease models. *Open Biol* 8:. <https://doi.org/10.1098/rsob.180138>
- Treack H-H, Pirsig W (1979) Differentiation of Nerve Endings in the Cochlear Nucleus on Morphological and Experimental Basis. *Acta Otolaryngol* 87:47–60. <https://doi.org/10.3109/00016487909126386>
- Tyson T, Steiner JA, Brundin P (2016) Sorting out release, uptake and processing of alpha-synuclein during prion-like spread of pathology. *J Neurochem* 139:275–289. <https://doi.org/10.1111/jnc.13449>
- van der Merwe C, Carr J, Glanzmann B, Bardien S (2016) Exonic rearrangements in the known Parkinson’s disease-causing genes are a rare cause of the disease in South African patients. *Neurosci Lett* 619:168–171. <https://doi.org/10.1016/j.neulet.2016.03.028>
- Wang T, Larcher LM, Ma L, Veedu RN (2018) Systematic screening of commonly used commercial transfection reagents towards efficient transfection of single-stranded oligonucleotides. *Molecules* 23:. <https://doi.org/10.3390/molecules23102564>
- Winklhofer KF, Haass C (2010) Mitochondrial dysfunction in Parkinson’s disease. *Biochim Biophys Acta - Mol Basis Dis* 1802:29–44. <https://doi.org/https://doi.org/10.1016/j.bbadis.2009.08.013>

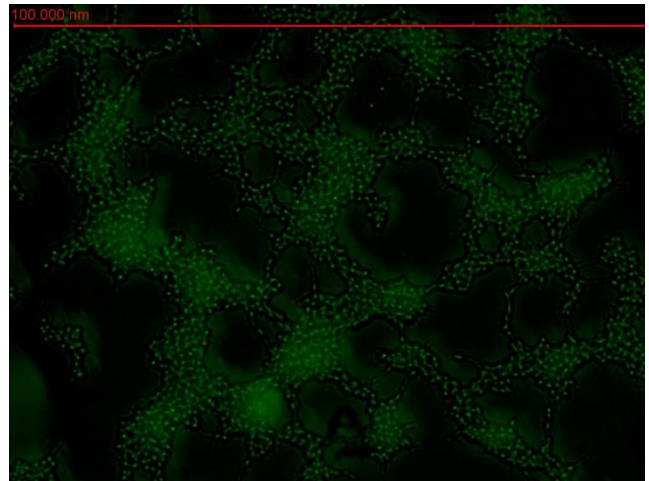
- Yasuda T, Mochizuki H (2010) The regulatory role of α -synuclein and parkin in neuronal cell apoptosis; Possible implications for the pathogenesis of Parkinson's disease. *Apoptosis* 15:1312–1321. <https://doi.org/10.1007/s10495-010-0486-8>
- Yonova-Doing E, Atadzhanov M, Quadri M, et al (2012) Analysis of LRRK2, SNCA, Parkin, PINK1, and DJ-1 in Zambian patients with Parkinson's disease. *Park Relat Disord* 18:567–571. <https://doi.org/10.1016/j.parkreldis.2012.02.018>
- Zorova LD, Popkov VA, Plotnikov EY, et al (2018) Mitochondrial membrane potential. *Anal Biochem* 552:50–59. <https://doi.org/10.1016/j.ab.2017.07.009>

Supplementary Figures**Wildtype NRXN2 α -CFP****Mutant NRXN2 α -CFP**

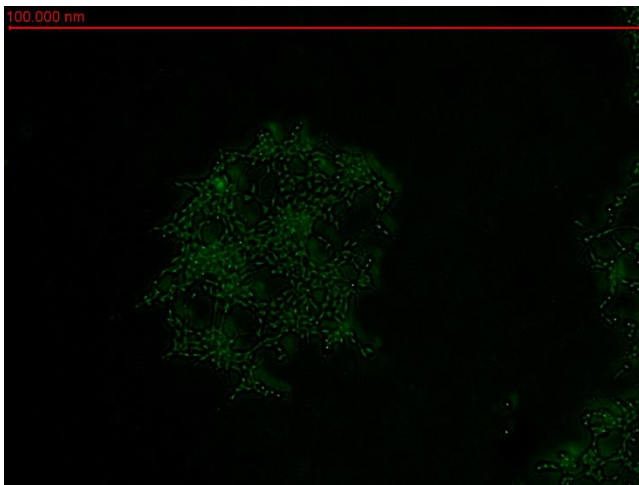
Supplementary Figure S1: Generation of the p.D882 mutant construct. Sequence chromatographs showing successful generation of the p.D882 construct (GAT) compared to the wild-type p.G882 construct (GGT).



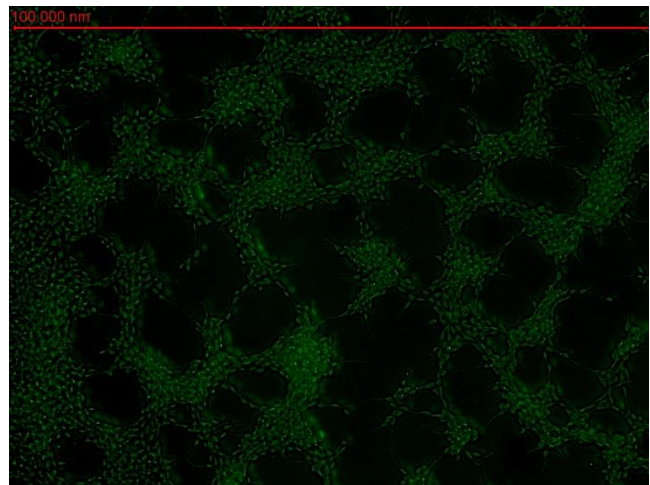
Non-transfected SH-SY5Y cells



Wild-type transfected SH-SY5Y cells

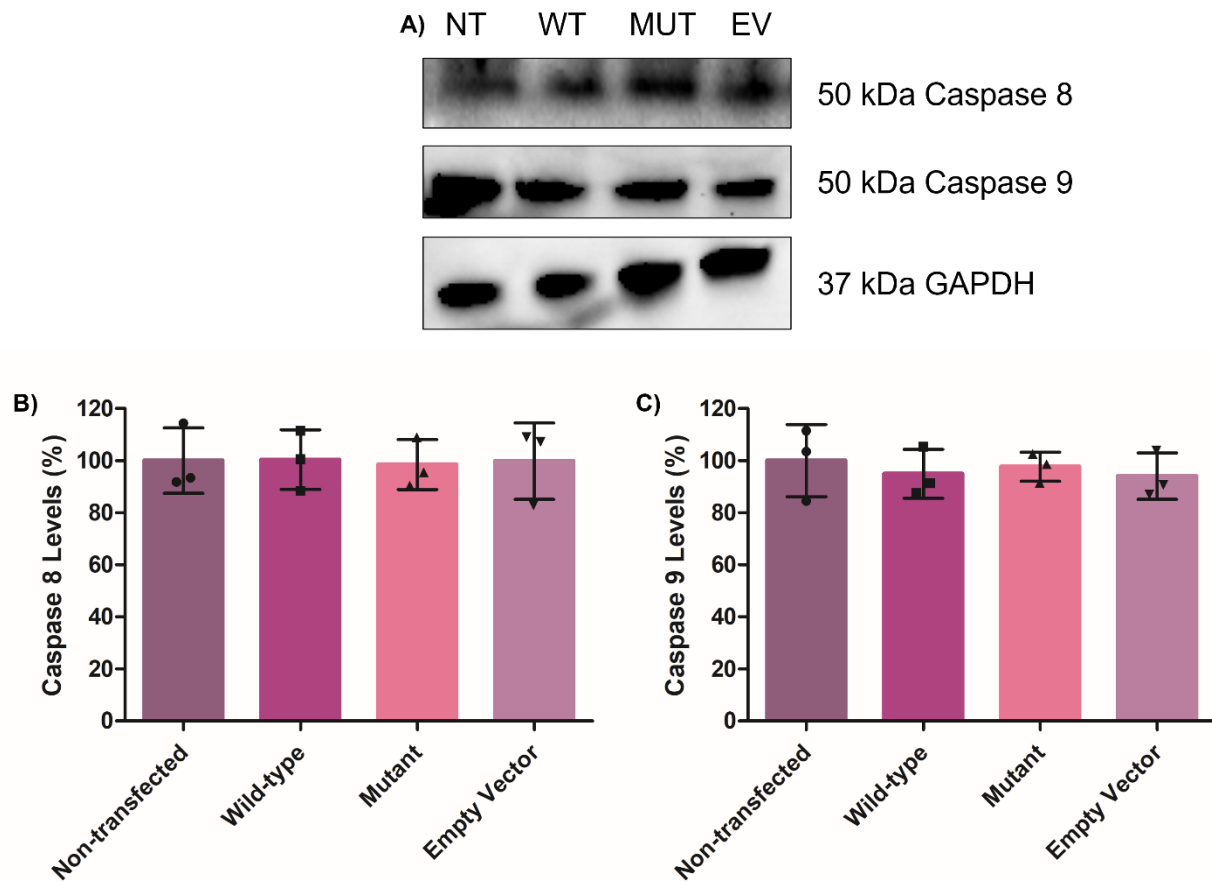


Mutant transfected SH-SY5Y cells

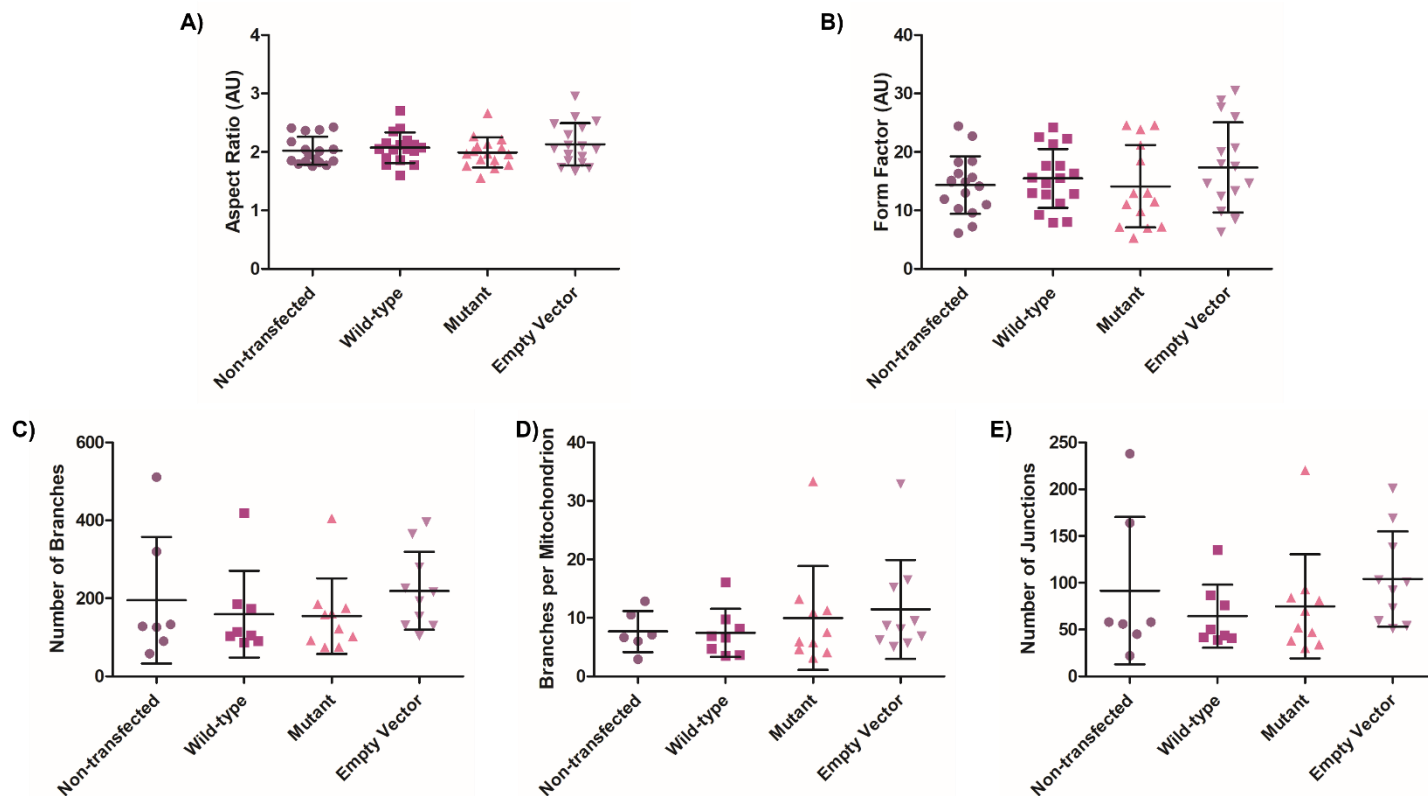


Empty vector transfected SH-SY5Y cells

Supplementary Figure S2: Transfection efficiency examined by CFP fluorescence in SH-SY5Y cells.



Supplementary Figure S3: Caspase 8 and 9 levels in wild-type and mutant NRXN2 α overexpressing SH-SY5Y cells. A) Representative western blots of caspase 8 and 9 levels. GAPDH is used as a loading control. B) Densitometric analysis of caspase 8 levels show no significant differences across treatment groups ($p = 0.99$). C) Densitometric analysis of caspase 9 levels show no significant differences across treatment groups ($p = 0.86$). $n = 3$; one-way ANOVA.



Supplementary Figure S4: Mitochondrial network analysis of wild-type and mutant NRXN2a overexpressing SH-SY5Y cells. A-B) 2D analysis of the mitochondrial network. No significant differences were observed in the aspect ratio ($p = 0.51$) (A) and form factor ($p = 0.46$) (B) of mitochondria across treatment groups. C-E) 3D analysis of the mitochondrial network. No significant differences were observed in the number of branches ($p = 0.59$) (C), branches per mitochondrion ($p = 0.61$) (D) or number of junctions ($p = 0.45$) (E) across treatment groups. $n \geq 9$; one-way ANOVA.

Supplementary Methods

Plasmid DNA Isolation

After successful transformation of competent *E. coli*, colonies were inoculated in a 5 ml starter culture of LB media supplemented with 5 µl kanamycin sulfate (50 mg/ml). The starter culture was incubated at 37 °C for 8 hours in a shaking incubator set at 200 rpm. Thereafter, 100 µl of the starter culture was added to 100 ml of LB media supplemented with 100 µl kanamycin sulfate (50 mg/ml). This culture was incubated at 37 °C for 16 hours in a shaking incubator set at 200 rpm. The culture was then centrifuged at 3 400 x g to pellet the cells. Plasmid DNA was isolated from the bacteria using the ZymoPURE II Plasmid MidiPrep Kit (Zymo Research Corp.) as per the manufacturer's centrifugation protocol. Isolated plasmid DNA was stored at -20 °C until required.

Western Blotting

Western blotting was used to detect total protein levels of caspases 8 and 9 post-transfection. GAPDH was used as the loading control. Briefly, cell lysates were prepared using lysis buffer (33,3 mM Tris, 100 mM NaCl, 2.25% Triton X-100, 1 mM MgCl₂) supplemented with 1% Halt™ Protease and Phosphatase Inhibitor Cocktail (Thermo Fisher Scientific) , and protein levels were quantified using a Bradford assay. Proteins were resolved using 4-20% Mini-PROTEAN TGX gels (Bio-Rad) for approximately 1 hour at 120 V in 1X electrophoresis buffer (25mM Tris, 192 mM glycine and 0.1% SDS). A total of 50 µg protein was resolved. Thereafter, the separated proteins were transferred onto a polyvinylidene fluoride (PVDF) membrane using the Trans-Blot® Turbo™ (Bio-Rad) at 21 V for 1 minute, 23 V for 4 minutes and 25 V for 1 minute, in 1X Trans-

Blot Turbo Transfer Buffer (Bio-Rad) with 20% ethanol. Membranes were blocked in 3% BSA in TBS for 1 hour. The blots were incubated overnight with the appropriate primary antibody, diluted in 3% BSA in TBS, with gentle shaking at 4 °C. Subsequently, the membranes were washed in 0.1% Tween-20 in TBS (TBST). The membranes were then incubated with the appropriate secondary antibody, diluted in 3% BSA in TBS, for 1 hour in the dark and, thereafter, washed with TBST. The primary and secondary antibodies used are listed in **Supplementary Table S1**. Membranes were incubated with Pierce™ ECL Western Blotting Substrate (Thermo Fisher Scientific) and imaged using the ChemiDoc™ MP Imaging System (Bio-Rad). Densitometric analysis was performed using Image Lab 5.1 software (Bio-Rad).

Supplementary Table S1: Antibodies used for this study

Target Protein	Primary Antibody	Species Reactivity	Dilution	Secondary Antibody	Dilution
<i>Flow Cytometry (Guava® Muse® Cell Analyzer)</i>					
NRXN2α	Rabbit anti-NRXN2 (Abcam: ab34245)	Rat, human, mouse	1:100	Anti-rabbit IgG-Cy3 (Jackson ImmunoResearch Laboratories: 111-165-003)	1:100
<i>Western Blotting</i>					
Caspase 8	Mouse anti-Caspase 8	Human	1:500	Anti-mouse IgG-HRP (Santa Cruz)	1:3333

	(Invitrogen: MA1-41260)			Biotechnology: sc-2005)	
Caspase 9	Mouse anti-Caspase 9 (Invitrogen: MA1-12562)	Human	1:500	Anti-mouse IgG-HRP (Santa Cruz Biotechnology: sc-2005)	1:3333
GAPDH	Rabbit anti-GAPDH (Santa Cruz Biotechnology: sc-25778)	Human	1:5000	Anti-rabbit IgG-HRP (Cell Signalling: 7074S)	1:3333

CHAPTER 6

Proteomics Analysis of the *NRXN2* p.G849D Variant

This chapter consists of a submitted brief report that addressed **Objective 6** of this study. In this chapter, we performed proteomics using an LC-MS/MS to obtain a better understanding of the pathways affected by NRXN2 α . We used the wild-type NRXN2 α -ECFP-N1 plasmid and our generated mutant plasmid and transfected them into SH-SY5Y cells. Total protein was then isolated from these cells and prepared for mass spectrometry. Enrichment analysis and pathway analysis was performed on the unique proteins and the significantly differentially abundant proteins identified.

Submitted Article: Proteomics analysis of the p.G849D variant in neurexin 2 alpha may reveal insight into Parkinson's disease pathobiology

Authors: Cuttler, K., Fortuin, S., Müller-Nedebock, A.C., Vlok, M., Cloete, R., Bardien, S.

Target Journal: Frontiers in Aging Neuroscience (Impact Factor: 5.750). Currently under review.

Supplementary material: This follows directly after the article, in text. However, due to the length of the Supplementary Tables S1-S8, these have been included in **Appendix II**.

Declarations

Declaration by the candidate

With regard to the submission-ready article constituting Chapter 6 of the dissertation, the nature and scope of my contribution were as follows:

Planned and conducted all experiments, analyzed the experimental data, created all tables, and figures, wrote the first manuscript draft, prepared supplementary material of the article, revised, reviewed and edited the manuscript (extent of contribution = 70%).

The following co-authors have contributed to Chapter 6:

Name	E-mail Address	Nature of Contribution	Extent of Contribution (%)
Suereta Fortuin	sueretaf@sun.ac.za	<ul style="list-style-type: none"> Assisted with analysis of proteomics data Manuscript review and editing 	7.5
Amica C. Müller-Nedebock	amicamuller@sun.ac.za	<ul style="list-style-type: none"> Assisted with data processing Manuscript review and editing 	2
Maré Vlok	marevlok@sun.ac.za	<ul style="list-style-type: none"> Performed protein extraction and mass spectrometry 	3
Ruben Cloete	ruben@sanbi.ac.za	<ul style="list-style-type: none"> Manuscript review and editing. Supervision 	7.5
Soraya Bardien	sbardien@sun.ac.za	<ul style="list-style-type: none"> Research project conception and organization. Manuscript review and editing. Supervision 	10

Signature of candidate:

Date: 07/07/2022

Declaration by co-authors

The undersigned hereby confirm that

1. the declaration above accurately reflects the nature and extent of the contributions of the candidate and the co-authors to Chapter 6,
2. no other authors contributed to Chapter 6, besides those specified above, and
3. potential conflicts of interest have been revealed to all interested parties and that the necessary arrangements have been made to use the material in Chapter 6 of this dissertation.

Name	Signature	Affiliation	Date
Suereta Fortuin		Stellenbosch University, Cape Town, South Africa	05/07/2022
Amica C. Müller-Nedebock		Stellenbosch University, Cape Town, South Africa	07/07/2022
Maré Vlok		Stellenbosch University, Cape Town, South Africa	05/07/2022
Ruben Cloete		South African National Bioinformatics Institute (SANBI), University of the Western Cape, Cape Town, South Africa	07/07/2022
Soraya Bardien		Stellenbosch University, Cape Town, South Africa	06/07/2022

Proteomics analysis of the p.G849D variant in neurexin 2 alpha may reveal insight into Parkinson's disease pathobiology

1 **Katelyn Cuttler¹, Suereta Fortuin², Amica C. Müller-Nedebock^{1,3}, Maré Vlok⁴, Ruben Cloete⁵,**
2 **Soraya Bardien^{1,3*}**

3 ¹Division of Molecular Biology and Human Genetics, Faculty of Medicine and Health Sciences,
4 Stellenbosch University, Cape Town, South Africa

5 ²African Microbiome Institute, Faculty of Medicine and Health Sciences, Stellenbosch University,
6 Cape Town, South Africa

7 ³South African Medical Research Council/Stellenbosch University Genomics of Brain Disorders
8 Research Unit, Cape Town, South Africa

9 ⁴Central Analytical Facilities, Mass Spectrometry Unit, Stellenbosch University, Cape Town, South
10 Africa

11 ⁵South African Medical Research Council Bioinformatics Unit, South African National Bioinformatics
12 Institute, University of the Western Cape, Cape Town, South Africa

13 * Correspondence:

14 Prof. Soraya Bardien

15 sbardien@sun.ac.za

16 Target Journal: Frontiers in Aging Neuroscience

17 **Keywords: neurexin 2 α (NRXN2), Parkinson's disease, proteomics, mass spectrometry,**
18 **p.G849D, synaptic translation, mitochondrial dysfunction, ribosomal functioning**

19 Abstract

20 Parkinson's disease (PD), the fastest growing neurological disorder globally, has a complex etiology.
21 A previous study by our group identified the p.G849D variant in *neurexin 2* (*NRXN2*), encoding the
22 synaptic protein, NRXN2 α , as a possible causal variant of PD. Therefore, we aimed to perform
23 functional studies using proteomics in an attempt to understand the biological pathways affected by
24 the variant. We hypothesized that this may reveal insight into the pathobiology of PD. Wild-type and
25 mutant NRXN2 α plasmids were transfected into SH-SY5Y cells. Thereafter, total protein was
26 extracted and prepared for mass spectrometry using a Thermo Scientific Fusion mass spectrometer
27 equipped with a Nanospray Flex ionization source. The data was then interrogated against the UniProt
28 *H. sapiens* database and afterwards, pathway and enrichment analyses were performed using *in silico*
29 tools. Overexpression of the wild-type protein led to the enrichment of proteins involved in
30 neurodegenerative diseases, while overexpression of the mutant protein led to the decline of proteins
31 involved in ribosomal functioning. Thus, we concluded that the wild-type NRXN2 α may be involved
32 in pathways related to the development of neurodegenerative disorders, and that biological processes
33 related to the ribosome, transcription and tRNA, specifically at the synapse, could be an important
34 mechanism in PD. Future studies targeting translation at the synapse in PD could therefore provide
35 further information on the pathobiology of the disease.

36 1 Introduction

37 Parkinson's disease (PD) is a neurodegenerative disorder which primarily affects movement. It affects
38 approximately 1-2% of the population over the age of 65 (Antony et al., 2013). Over the past two and
39 a half decades, several genetic causes of PD have been identified, implicating various biological
40 processes including mitochondrial dysfunction, toxic protein accumulation, dysfunctional vesicle
41 recycling, and synaptic dysfunction in PD development (Panicker et al., 2021).

42 Recently, we reported the finding of a p.G849D variant in the neurexin 2 gene (*NRXN2*) in a South
43 African multiplex PD family (Sebate et al., 2021). The translated protein, NRXN2 α , is a synaptic
44 protein involved in calcium channel regulation, synaptic organization, neuronal cell adhesion,
45 transmembrane signaling and neuroligin family protein binding (Craig and Kang, 2007). While studies
46 on NRXN2 α in disease are limited, it has been shown that neurexins and their common binding
47 partners, neuroligins link synaptic dysfunction to cognitive disease (Südhof, 2008). In addition, studies
48 specifically investigating NRXN2 α have implicated the protein in neuronal and synaptic disorders
49 (Missler et al., 2003; Dachtler et al., 2015).

50 Here, we aimed to further investigate the effect of this variant on biological pathways by using a
51 proteomics approach in an SH-SY5Y cellular model of PD, transfected with wild-type and mutant
52 NRXN2 α plasmids. To this end, we examined the total proteome of the different treatment groups in
53 an attempt to understand the changes in biological pathways. We hypothesized that overexpression of
54 the wild-type NRXN2 α would provide an indication of the pathways related to NRXN2 α 's function,
55 while overexpression of the mutant NRXN2 α could give an indication of the method of action by which
56 it potentially leads to neurodegeneration. Together, these findings may provide a better understanding
57 of the function of both the wild-type and mutant NRXN2 α , and its possible involvement in PD.

58

59 2 Materials and Methods

60 2.1 Ethical Considerations

61 Ethical approval was obtained from the Health Research Ethics Committee (Protocol numbers
62 2002/C059 and S20/01/005 PhD) and the Research Ethics Committee: Biological and Environmental
63 Safety (Protocol number BEE-2021-13149). Both committees are located at Stellenbosch University,
64 Cape Town, South Africa.

65 2.2 Cell Culture

66 SH-SY5Y cells were cultured in DMEM with high glucose (4.5 g/l) and 4 mM L-Glutamine (Lonza).
67 In addition, the media was supplemented with 15% FBS (Gibco) and 1% penicillin/streptomycin
68 (Sigma Aldrich). Cells were maintained at 37 °C and 5% CO₂ in a humidified incubator (ESCO
69 Technologies).

70 2.3 Plasmids

71 2.3.1 NRXN2 α Wild-type

72 The NRXN2 α -ECFP-N1 plasmid is a kind gift from Prof. Ann Marie Craig (University of British
73 Columbia, Canada). This plasmid expresses wild type mouse NRXN2 α -CFP and was generated as per

Proteomics analysis of the p.G849D variant in neurexin 2 alpha

74 Kang et al (Kang et al., 2008). The pECFP-N1 plasmid without an insert (empty vector) was a kind
75 gift from Prof. Harald Sitte (Medical University of Vienna, Austria).

76 2.3.2 Site-directed Mutagenesis

77 In order to generate the p.G849D mutant plasmid (p.G882D in our mouse model; mouse genomic
78 position: 540693_chr19 (GRCm39)), site-directed mutagenesis was performed on the wild-type
79 NRXN2 α -ECFP-N1 plasmid using the Q5 Site-Directed Mutagenesis kit (New England Biolabs), as
80 per the manufacturer's instructions. More information on the primers used and PCR conditions can be
81 found in the Supplementary Methods.

82 2.4 Treatment Groups

83 A total of four treatment groups were used for the analysis: (1) non-transfected cells (NT), (2) cells
84 transfected with the wild-type plasmid (WT), (3) cells transfected with the mutant plasmid (MUT) and
85 (4) cells transfected with the empty vector (EV). All treatments were performed in triplicate.

86 2.5 Transfection

87 SH-SY5Y cells were grown in sterile 25 cm³ flasks until 70% confluent and transfected using
88 Lipofectamine3000 (Invitrogen) as per the manufacturer's instructions. The transfection efficiency was
89 determined by examining the cells under an Oxion Inverso Fluo E4 fluorescent microscope (Euromex)
90 at 100x magnification for the presence of cyan fluorescent protein (CFP).

91 2.6 NRXN2 α Levels

92 Prior to proteomics analysis, NRXN2 α protein levels were determined using immunofluorescent flow
93 cytometry and measured with the Guava® Muse® Cell Analyzer (Luminex) to confirm overexpression
94 of NRXN2 α . Please see Supplementary Methods for more details.

95 2.7 Proteomics Analysis

96 2.7.1 Protein Extraction and Clean-up

97 Cells were detached using Trypsin-EDTA and centrifuged at 2739 x g for 5 minutes to collect cell
98 pellets. Cell pellets were stored at -80 °C until required. The pellets were then thawed in 100 mM Tris
99 buffer pH 8 containing 0.5% sodium dodecyl sulfate (SDS, Sigma), 100 mM NaCl (Sigma), 5 mM
100 triscarboxyethyl phosphine (TCEP, Sigma), protease inhibitor cocktail (Thermo Fisher) and 2 mM
101 EDTA (Thermo Fisher). Once thawed, the pellets were submerged in an ice-cold sonic bath for 30
102 seconds prior to vortexing for 30 seconds. This cycle was repeated three times and the pellets were
103 completely dissolved. Extraction reagents were then removed using a chloroform-methanol-water
104 liquid-liquid extraction method. More information on the protein extraction, on-bead digest and liquid
105 chromatography performed in preparation for mass spectrometry, can be found in the Supplementary
106 Methods.

107 2.7.2 Mass Spectrometry

108 Mass spectrometry was performed by Stellenbosch University's Central Analytical Facilities (CAF)
109 using a Thermo Scientific Fusion mass spectrometer equipped with a Nanospray Flex ionization
110 source. The sample was introduced through a stainless-steel emitter. Data was collected in positive
111 mode with spray voltage set to 1.8 kV and ion transfer capillary set to 280 °C. Spectra were internally
112 calibrated using polysiloxane ions at m/z = 445.12003 and 371.10024. MS1 scans were performed

Proteomics analysis of the p.G849D variant in neurexin 2 alpha

113 using the orbitrap detector set at 120 000 resolution over the scan range 350-1650 with automatic gain
114 control (AGC) target at 3 E5 and maximum injection time of 40 milliseconds. Data was acquired in
115 profile mode.

116 MS2 acquisitions were performed using monoisotopic precursor selection for ion with charges +2 - +7
117 with error tolerance set to +/- 10 ppm. Precursor ions were excluded from fragmentation once for a
118 period of 60 seconds. Precursor ions were selected for fragmentation in higher-energy C-trap
119 dissociation (HCD) mode using the quadrupole mass analyzer with HCD energy set to 32.5%.
120 Fragment ions were detected in the orbitrap mass analyzer set to 30 000 resolution. The AGC target
121 was set to 5E4 and the maximum injection time to 80 milliseconds. The data was acquired in centroid
122 mode.

123 2.7.3 Data Analysis

124 The raw files generated by the mass spectrometer were imported into Proteome Discoverer v1.4
125 (Thermo Fisher) and processed using the SequestHT algorithm. Database interrogation was performed
126 against the UniProt *H. Sapiens* database concatenated with the cRAP contaminant protein database
127 (<https://www.thegpm.org/crap>). Semi-tryptic cleavage with 2 missed cleavages was allowed for.
128 Precursor mass tolerance was set to 10 ppm and fragment mass tolerance set to 0.02 Da. Demamidation
129 (NQ) and oxidation (M) was allowed as dynamic modifications and thiomethyl of C as static
130 modification. Peptide validation was performed using the Target-Decoy PSM validator node. The
131 results files were imported into Scaffold 1.4.4 (Searle, 2010) and identified peptides validated with
132 X!Tandem and the Peptide and Protein Prophet algorithms included in Scaffold. Quantitation was
133 performed by Scaffold after a one-way ANOVA and student's *t*-test was performed.

134 2.8 Pathway Analysis and Enrichment Analysis

135 First, the data for the separate treatment groups were combined into a Venn diagram using Venny 2.1
136 (<https://bioinfogp.cnb.csic.es/tools/venny>) (Oliveros, 2015) to identify proteins unique to each
137 treatment group. Thereafter, in order to identify differentially abundant proteins, the data was compared
138 as follows: empty vector transfected cells vs non-transfected cells (EV vs NT); wild-type transfected
139 cells vs non-transfected cells (WT vs NT), mutant transfected cells vs non-transfected cells (MUT vs
140 NT), and mutant transfected cells vs wild-type transfected cells (MUT vs WT). Functional information
141 for unique and differentially abundant proteins was obtained from UniProt (<https://www.uniprot.org>)
142 (The UniProt Consortium, 2021). Pathway analysis was conducted using the KEGG
143 (<https://www.kegg.jp>) (Kanehisa et al., 2021) and STRING (<https://string-db.org>) (Szklarczyk et al.,
144 2019) databases. Each protein set was then uploaded to WebGestalt (<http://www.webgestalt.org>) (Liao
145 et al., 2019) for enrichment analysis as per the default parameters.

146

147 3 Results

148 3.1 Overexpression of NRXN2 α

149 Transfection efficiency, determined by evaluating CFP microscopically, was 68% for the wild-type
150 construct, 65% for the mutant construct, and 67% for the empty vector construct. In addition,
151 overexpression of NRXN2 α was confirmed using the Guava® Muse® Cell Analyzer (Luminex). There
152 was a 26% and 21% increase in NRXN2 α levels in the wild-type and mutant samples, respectively,

153 with no change in the empty vector sample when compared to non-transfected cells (**Supplementary**
154 **Figure S1**).

155 **3.2 Total Proteins Identified**

156 Quantitation and regression analysis performed in Scaffold, showed that most data points clustered
157 within one standard deviation from the mean and that all the sample sets showed the same grouping
158 (**Supplementary Figure S2**), indicating a successful experiment. The total number of proteins detected
159 were 2667, 2630, 2691, and 2646 for the non-transfected cells (NT), wild-type transfected cells (WT),
160 mutant transfected cells (MUT), and empty vector transfected cells (EV), respectively. Since all
161 treatments were performed in triplicate, a protein had to be present in a minimum of 2 replicates in
162 order to be considered an identified protein.

163 **3.3 Unique Proteins in Each Group**

164 The Venn diagram in **Supplementary Figure S3** shows that 1822 proteins were shared by all four
165 treatment groups. NT cells had 31 unique proteins, while WT, MUT and EV cells had 22, 44 and 28
166 unique proteins, respectively. Functional information for all of these proteins can be found in
167 **Supplementary Tables S1-S4**. Each protein set was then uploaded to STRING (<https://string-db.org>)
168 (Szklarczyk et al., 2019) for pathway analysis.

169 Enrichment terms obtained from STRING for the unique proteins in each treatment group are shown
170 in **Table 1**. There were no enriched terms for the EV cells, so they were excluded from the table. The
171 NT cells showed enrichment terms for “compound binding”. “Acetylation” was the only term enriched
172 for in the WT cells. STRING analysis of the proteins involved in acetylation shows that they are not
173 predicted to interact with each other and do not form part of the same networks. Therefore, enrichment
174 of “acetylation” in these cells is likely to be a chance finding showing that the cells are undergoing
175 modification upon transfection with the WT plasmid. However, since acetylation of proteins is also
176 potentially implicated in neurodegenerative disorders, such as PD (Yakhine-Diop et al., 2019), it could
177 also be an important mechanism of action for the WT NRXN2 α . “Metabolic processes” were enriched
178 in the MUT cells, which is also possibly a result of introducing the MUT NRXN2 α into the cells.
179 Interestingly, terms related to RNA processes were also enriched in the MUT cells. These cells contain
180 several unique proteins which are involved in RNA metabolism and processing, thus showing that there
181 may be changes in transcription in these cells. Therefore, it is possible that the MUT protein is
182 somehow disrupting RNA processing.

183

184

185

186

187

188

189

190 **Table 1: Enrichment terms obtained from the STRING online tool for the unique proteins in**
 191 **each treatment group**

NT (no. of proteins)	WT (no. of proteins)	MUT (no. of proteins)
Heterocyclic compound binding (24)	Acetylation (12)	Cellular metabolic process (31)
Organic compound binding (24)		Macromolecule metabolic process (28)
		RNA processing (12)
		Metabolism of RNA (9)

192 STRING: <https://string-db.org> (Szklarczyk et al., 2019). Abbreviations: NT: non-transfected cells;
 193 MUT: mutant transfected cells; WT: wild-type transfected cells

194 3.4 Differentially Abundant Proteins Between Groups

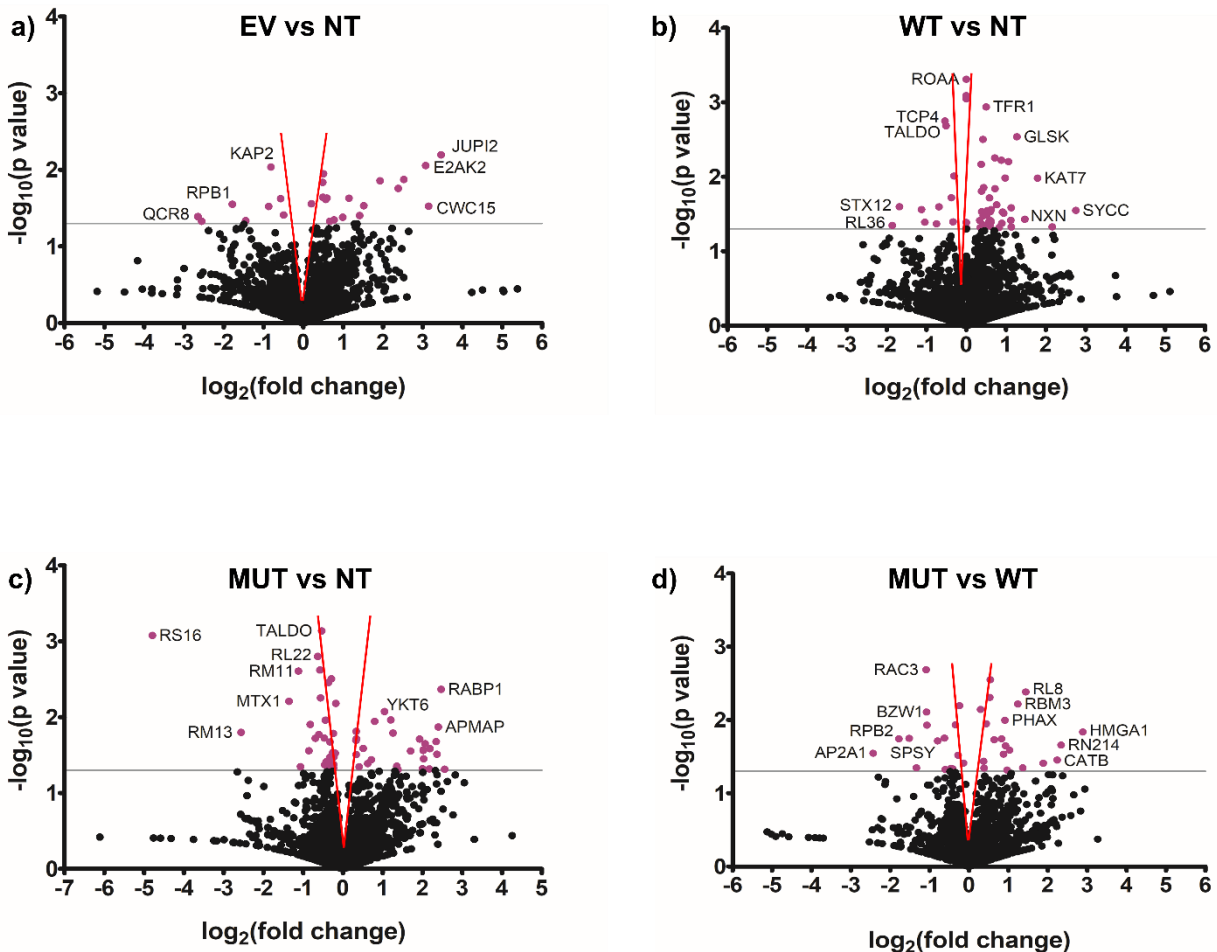
195 For downstream analyses, all proteins identified in the EV cells were then compared to those in the NT
 196 cells as a control since we speculate that the vector backbone should not cause significant changes to
 197 the cellular proteome. The proteins in the WT cells and MUT cells were then each compared to the NT
 198 to better understand their individual contributions to the proteome. Finally, the main analysis involved
 199 comparison of the MUT cells to the WT cells in an attempt to understand the effect of the p.G849D
 200 variant. **Table 2** shows the number of differentially abundant proteins found for each comparison
 201 group, divided into those that are less abundant and those that are more abundant. Volcano plots
 202 representing the differentially abundant proteins in each analysis are shown in **Figure 1**. Functional
 203 information for all of these proteins can be found in **Supplementary Tables S5-S8**.

204 **Table 2: The number of differentially abundant proteins found for each comparison**

Treatment Comparison	Total Differentially Abundant Proteins (No.)	More Abundant Proteins (No.)	Less Abundant Proteins (No.)
EV vs NT	28	8	20
WT vs NT	52	11	41
MUT vs NT	61	31	30
MUT vs WT	37	16	21

205 Abbreviations: EV: empty vector transfected cells; NT: non-transfected cells; MUT: mutant
 206 transfected cells; WT: wild-type transfected cells

Proteomics analysis of the p.G849D variant in neurexin 2 alpha



207

208 **Figure 1: Differentially abundant proteins present when comparing several treatment groups to**
 209 **each other.** Volcano plots showing differentially abundant proteins when comparing EV vs NT (a),
 210 WT vs NT (b), MUT vs NT (c), and MUT vs WT (d). The grey line indicates the significance threshold.
 211 Significant proteins ($p \leq 0.05$, students *t*-test) are colored purple. Where possible, individual proteins
 212 have been labelled. Proteins found within the red funnel may become statistically insignificant with
 213 increased sample sizes. Graphs generated with GraphPad Prism® 5.02. Abbreviations: EV: empty
 214 vector transfected cells; NT: non-transfected cells; MUT: mutant transfected cells; WT: wild-type
 215 transfected cells.

216 Each protein set was uploaded to both KEGG (<https://www.kegg.jp>) (Kanehisa et al., 2021) and
 217 STRING (<https://string-db.org>) (Szklarczyk et al., 2019) for pathway analysis. KEGG examines which
 218 pathways the proteins in each set are involved in, whereas STRING identifies the pathways that both
 219 the proteins and their immediate interactors are involved in.

220 Enrichment terms from each tool were combined and are shown in **Table 3**. “Metabolic pathways” are
 221 enriched across all analyses, suggesting that any treatment could have an effect on the general cellular
 222 metabolic pathways. In the EV vs NT analysis, “Alzheimer disease”, “Huntington disease” and
 223 “Parkinson disease” were enriched. However, the same three proteins (QCR8, ATPD and SNCA) were
 224 present in each group, showing that this may be a chance finding. “Alzheimer disease”, “Amyotrophic
 225 lateral sclerosis”, “Huntington disease”, “prion disease” and “Parkinson disease” were enriched in both
 226 the WT vs NT and MUT vs NT analyses. When examining the MUT vs WT, the only enrichment term
 227 related to neurodegenerative disorders was “Huntington disease”. However, “ribosome”,

Proteomics analysis of the p.G849D variant in neurexin 2 alpha

228 “spliceosome”, “mRNA surveillance pathway” and “nucleocytoplasmic transport” were also enriched
 229 in the MUT vs WT analysis. This may hint towards a mode of action of the mutant protein whereby
 230 protein translation and transport are affected by its overexpression.

231 In the MUT vs WT analysis, the only enrichment term related to neurodegenerative disorders was
 232 “Huntington disease”. The three proteins involved in this pathway were AP2A1, RPB2, and SDHB.
 233 STRING analysis shows that these proteins are not predicted to interact with each other and do not
 234 form part of the same networks. Therefore, this enrichment is more likely to be a random result of
 235 introducing cDNA to the cells. However, “ribosome”, “spliceosome”, “mRNA surveillance pathway”
 236 and “nucleocytoplasmic transport” were also enriched in this analysis. RPL8, RPS6, RPS21 and RPS25
 237 are shown to be part of the “ribosome”. XPO2, PHAX and PNN are involved in “nucleocytoplasmic
 238 transport”. FUS, PNN and PP1B are involved in the “mRNA surveillance pathway”. FUS, RBMX and
 239 PRP4 are involved in the “spliceosome”. RPL8, RPS6, RPS21 and RPS25 are all ribosomal subunits,
 240 involved in ribosomal and mRNA pathways.

241 STRING analysis shows that PHAX, XPO2, FUS, RBMX, and PNN potentially interact in sequence.
 242 PHAX is a phosphoprotein adaptor involved in RNA export and CSE1L plays a role in protein
 243 import/export within the nucleus. FUS and RBMX are both RNA binding proteins. FUS plays a role
 244 in processes such as transcription regulation, RNA splicing, RNA transport, DNA repair and damage
 245 responses, while RBMX plays several roles in the regulation of pre- and post-transcriptional processes.
 246 PNN is a transcriptional activator for the E-cadherin promoter gene, but it is also involved in RNA
 247 binding and mRNA splicing via the spliceosome. PRP4 is a U4/U6 small nuclear ribonucleoprotein
 248 which participates in pre-mRNA splicing. PP1B is a serine/threonine-protein phosphatase. Protein
 249 phosphatases are essential for cell division, and PP1B participates in the regulation of glycogen
 250 metabolism, muscle contractility and protein synthesis. It has also been shown to be involved in the
 251 mRNA surveillance pathway. Taken together, the pathways of these proteins all relate back to the
 252 regulation of transcription, strongly suggesting that this process is being affected in the MUT cells.

253 **Table 3: Enrichment terms obtained from the KEGG and STRING online tools for each**
 254 **protein set**

EV vs NT (no. of proteins)	WT vs NT (no. of proteins)	MUT vs NT (no. of proteins)	MUT vs WT (no. of proteins)
Metabolic pathways (7)	Metabolic pathways (15)	Metabolic pathways (12)	Metabolic pathways (5)
Alzheimer disease (4)	Alzheimer disease (7)	Ribosome (8)	Coronavirus disease – COVID-19 (4)
Pathways of neurodegeneration – multiple diseases (3)	Amyotrophic lateral sclerosis (7)	Amyotrophic lateral sclerosis (5)	Ribosome (4)

Proteomics analysis of the p.G849D variant in neurexin 2 alpha

Huntington disease (3)	Huntington disease (7)	Alzheimer disease (5)	Alcoholism (3)
Oxidative phosphorylation (3)	Parkinson disease (6)	Biosynthesis of amino acids (5)	Diabetic cardiomyopathy (3)
Parkinson disease (3)	Prion disease (6)	Carbon metabolism (5)	Huntington disease (3)
	Alanine, aspartate and glutamate metabolism (4)	Pathways of neurodegeneration – multiple diseases (5)	mRNA Surveillance Pathway (3)
	Aminoacyl-tRNA biosynthesis (3)	Salmonella infection (5)	Nucleocytoplasmic transport (3)
	Cysteine and methionine metabolism (3)	Diabetic cardiomyopathy (4)	Spliceosome (3)
	Carbon metabolism (3)	DNA replication (4)	
		Huntington disease (4)	
		Parkinson disease (4)	
		Prion disease (4)	

255 KEGG: <https://www.kegg.jp> (Kanehisa et al., 2021), STRING: <https://string-db.org> (Szklarczyk et
256 al., 2019). Abbreviations: EV: empty vector transfected cells; NT: non-transfected cells, MUT:
257 mutant transfected cells; WT: wild-type transfected cells

258 3.5 Enrichment Analysis

259 WebGestalt facilitates the uploading of a gene or protein set and the corresponding fold changes and
260 then provides enriched Gene Ontology (GO) terms. The graphical results of this analysis are shown in
261 **Supplementary Figure S4**. “Negative enrichment” scores refer to GO terms that are downregulated
262 or suppressed, while “positive enrichment” scores refer to GO terms that are upregulated or promoted.
263 No specific enrichment was observed for the EV vs NT analysis, suggesting that transfecting the cells
264 with the empty vector had a minimal effect.

265 In the WT vs NT analysis, the highest positive enrichment was for “aminoacyl-tRNA biosynthesis”.
266 Interestingly, “oxidative phosphorylation”, “Alzheimer disease” and “Parkinson disease” also showed

Proteomics analysis of the p.G849D variant in neurexin 2 alpha

267 positive enrichment scores. The mitochondrial proteins QCR1, QCR2 and SDHB were the ones
268 enriched in all these pathways, again showing that the mitochondrial dysfunction may be affected in
269 the WT cells.

270 In the MUT vs NT analysis, “metabolic pathways” was positively enriched with the increased
271 abundance of NADC, a protein involved in the catabolism of quinolinic acid. In the MUT vs WT
272 analysis “Huntington disease” and “metabolic pathways” were negatively enriched and had false
273 discovery rates (FDRs) lower than 0.05. RPB2, SPSY, SDHB, PGM1, PUR9, and ODPB were
274 negatively enriched for “metabolic pathways”. All these proteins, except RPB2, are involved in
275 carboxylic acid metabolism. AP2A1 and RPB2 were negatively enriched in “Huntington disease”.
276 AP2A1 is part of the adaptor protein complex 2 which functions in protein transport via transport
277 vesicles. It is also involved in endolysosomal trafficking and is thus implicated in several
278 neurodegenerative disorders (Müller, 2014; Heaton et al., 2020; Srinivasan et al., 2022). RPB2 is a
279 subunit of DNA-dependent RNA polymerase II, and therefore its main function is in RNA
280 transcription.

281 Findings from our study suggest that transfecting cells with the plasmids is having an effect on
282 ribosomal processes. Therefore, enrichment scores for the GO term “ribosome” across each analysis
283 have been summarized in **Supplementary Figure S5**. In the WT vs NT analysis, only this GO term
284 had an $FDR \leq 0.05$, showing that it highly likely that it has been negatively enriched in this protein set.
285 In the MUT vs NT analysis, “ribosome” was again negatively enriched and had an $FDR \leq 0.05$.
286 However, in the MUT vs WT analysis, “ribosome” was positively enriched, but its FDR was above
287 0.05. Still, dysregulated ribosomal functioning seems to be common amongst the analyses and may be
288 an important biological process related to the NRXN2 α protein.

289

290 **4 Discussion**

291 This exploratory analysis has revealed that wild-type NRXN2 α may play a role in pathways related to
292 neurodegenerative disorders. Since the transfection efficiency and NRXN2 α levels between the WT
293 and MUT were similar, we can be relatively confident that the proteomics analysis showed differences
294 caused by the overexpressed proteins and not by other technical differences between the two groups.
295 In addition, while overexpression of the empty vector plasmid did show similar enrichment terms to
296 the other analyses (**Table 2**), when performing enrichment analysis for the EV transfected cells vs NT
297 cells, it can be seen that none of these terms were significantly enriched (**Supplementary Figure S4A**).
298 Therefore, we postulate that the EV only had a minimal effect on the cells and the majority of changes
299 in the other analyses are in fact due to the NRXN2 α cDNA insert (WT or MUT).

300 Overexpression of the WT protein in SH-SY5Y cells led to the enrichment of proteins involved in
301 neurodegenerative diseases, such as Alzheimer’s disease, Amyotrophic lateral sclerosis, and
302 Parkinson’s disease. In particular, the enriched proteins were involved in mitochondrial and lysosomal
303 functioning, which are known to be dysregulated in PD and other neurodegenerative disorders (Rego
304 and Oliveira, 2003; Wang et al., 2018). Thus, the wild-type protein may be involved in pathways
305 related to the development of neurodegenerative disorders, such as PD. This provides further evidence
306 potentially implicating synaptic proteins in the pathobiology of PD. Overexpression of the MUT
307 NRXN2 α -CFP protein showed similar results. Proteins unique to the MUT cells were enriched for
308 terms related to “ribosome”. In addition, when directly comparing the WT transfected cells with the
309 MUT transfected cells, terms related to “ribosome” were enriched. This may thus hint at a mode of

Proteomics analysis of the p.G849D variant in neurexin 2 alpha

310 action for the p.G849D mutant protein. Since the main function of the ribosome is translation of mRNA
311 into protein, dysregulated translation could be implicated as a biological process involved in
312 neurodegeneration. Furthermore, both cytoplasmic and mitochondrial ribosomal proteins were
313 enriched. Indeed, it has been shown that if synaptic translation is dysregulated, mitochondrial
314 physiology can be altered (Kuzniewska et al., 2020). In addition, EIF4G1, another protein implicated
315 in PD, is known to be involved in protein translation processes (Chartier-Harlin et al., 2011).
316 Furthermore, the DJ-1 and SYNJ1 proteins implicated in PD (Bonifati et al., 2003; Krebs et al., 2013)
317 also have RNA binding functions. DJ-1 acts to protect cells from oxidative stress and cell death by
318 acting as an oxidative stress sensor and redox-sensitive chaperone and protease, while SYNJ1 is a
319 phosphatase involved in synaptic vesicle endocytosis and neurotransmitter transport. A few studies
320 have additionally identified mitochondrial ribosomal proteins in PD. Gaare *et al.*, (2018) identified
321 *MRPL4*, which encodes a component of the large mitochondrial ribosome subunit, in an analysis of
322 two PD cohorts, while Billingsley *et al.*, (2019) identified *MRPL43* and *MRPS34*, encoding
323 components of the large and small mitochondrial ribosome subunits, using data from a PD genome-
324 wide association study (GWAS). Both these studies thus link mtDNA translation to PD risk.
325 Dysregulated mRNA translation can therefore be considered to play a role in PD pathogenesis (Martin,
326 2016). In addition, a recent RNA-sequencing analysis showed that there was differential expression of
327 ribosomal-related pathways in their PD cohort (Hemmings et al., 2022). Therefore, it is plausible that
328 synaptic translation could also be important in PD pathogenesis. Here, changes in translation could
329 affect oxidative stress and the transport of neurotransmitters, thereby causing cells to be more
330 susceptible to cell damage and death. Thus, biological processes related to the ribosome, translation
331 and tRNA, specifically at the synapse, could possibly be an important mechanism in PD pathobiology.

332 The strength of this study is that we examined the effect of overexpression of both the wild-type and
333 mutant protein using a hypothesis-free approach. In this way we were able to show that potential mode
334 of action of the mutant protein but were also able to conclude that the wild-type protein is also involved
335 in pathways related to neurodegeneration. Therefore, it is possible that any dysregulation of NRXN2 α
336 could potentially lead to neurodegeneration.

337 However, we also acknowledge several limitations, including the use of a commercial cell line for this
338 study. While SH-SY5Y cells are a good *in vitro* model for PD as they display a catecholaminergic
339 phenotype, producing both dopamine and noradrenaline (Xicoy et al., 2017), there are always
340 limitations when using cell lines to study a complex human disorder. Unfortunately, we were not able
341 to obtain dermal fibroblast samples from the individuals harbouring the *NRXN2* variant as an *ex-vivo*
342 model for this study. We also acknowledge the limitations of overexpressing a murine gene in a human
343 cell line. Therefore, in future it would be important to repeat these experiments in fibroblasts from the
344 patients or in animal models. Another limitation is the use of shotgun proteomics. Since this study is
345 explorative, we investigated the total proteome to determine which biological pathways were being
346 affected. However, it may be important to do more targeted proteomics work in future, such as looking
347 into post-translational modifications as well as investigating phospho-proteomics to determine
348 signalling changes. Indeed, several kinases and phosphatases were observed in the different analyses,
349 therefore phospho-proteomics would be required to better understand the effect of these protein
350 changes.

351 In conclusion, findings from this exploratory study possibly implicate the NRXN2 α protein in
352 neurodegenerative processes and show that synaptic ribosomal and translation processes may be
353 important in PD and/ or other neurodegenerative disorders. However, further validation of NRXN2 α
354 and the proteins implicated in synaptic ribosomal and translation processes in other models of PD or
355 neurodegenerative disorders would be required to prove or disprove this hypothesis.

356 **5 Conflict of Interest**

357 The authors declare that the research was conducted in the absence of any commercial or financial
358 relationships that could be construed as a potential conflict of interest.

359

360 **6 Author Contributions**

361 K.C. conducted all experiments, performed all analyses, and wrote the first draft of the manuscript.
362 S.F. assisted with analysis of the mass spectrometry data. A.C.M. assisted with data processing. M.V.
363 performed the protein extraction and mass spectrometry. R.C. assisted with writing and editing of the
364 manuscript. K.C. and S.B. conceptualized the study and acquired funding. All authors critically
365 reviewed and edited the manuscript.

366

367 **7 Funding**

368 This work is based on the research supported in part by the National Research Foundation of South
369 Africa (NRF) (Grant Numbers: 129249); the South African Medical Research Council (SAMRC) (self-
370 initiated research grant); the Harry Crossley Foundation and Stellenbosch University, South Africa.
371 SAMRC and The Higher Education Department, Next Generation of Academic Programme (nGAP),
372 provided support for R.C. in the form of a fulltime academic position and salary.

373

374 **8 Acknowledgments**

375 We thank the study participants for their participation in and contribution to this study. The authors
376 would also like to thank Prof. Ann Marie Craig (University of British Columbia, Canada) and Prof.
377 Harald Sitte (Medical University of Vienna, Austria) for the NRXN2 α -ECFP-N1 plasmid and pECFP-
378 N1 plasmid, respectively. We additionally acknowledge the support of the DSI-NRF Centre of
379 Excellence for Biomedical Tuberculosis Research, South African Medical Research Council Centre
380 for Tuberculosis Research, Division of Molecular Biology and Human Genetics, Faculty of Medicine
381 and Health Sciences, Stellenbosch University, Cape Town, South Africa.

382

383 **9 References**

384 Antony, P. M. A., Diederich, N. J., Krüger, R., and Balling, R. (2013). The hallmarks of Parkinson's
385 disease. *FEBS J.* 280, 5981–5993. doi: 10.1111/febs.12335.

386 Billingsley, K. J., Barbosa, I. A., Bandrés-Ciga, S., Quinn, J. P., Bubb, V. J., Deshpande, C., et al.
387 (2019). Mitochondria function associated genes contribute to Parkinson's Disease risk and later
388 age at onset. *npj Park. Dis.* 5, 1–9. doi: 10.1038/s41531-019-0080-x.

389 Bonifati, V., Rizzu, P., Van Baren, M. J., Schaap, O., Breedveld, G. J., Krieger, E., et al. (2003).
390 Mutations in the DJ-1 gene associated with autosomal recessive early-onset parkinsonism.

Proteomics analysis of the p.G849D variant in neurexin 2 alpha

- 391 *Science* (80-.). 299, 256–259. doi: 10.1126/science.1077209.
- 392 Chartier-Harlin, M. C., Daxsel, J. C., Vilariño-Güell, C., Lincoln, S. J., Leprêtre, F., Hulihan, M. M.,
393 et al. (2011). Translation initiator EIF4G1 mutations in familial parkinson disease. *Am. J. Hum.*
394 *Genet.* 89, 398–406. doi: 10.1016/j.ajhg.2011.08.009.
- 395 Craig, A. M., and Kang, Y. (2007). Neurexin-neuroigin signaling in synapse development. *Curr. Opin.*
396 *Neurobiol.* 17, 43–52. doi: 10.1016/j.conb.2007.01.011.
- 397 Dachtler, J., Ivorra, J. L., Rowland, T. E., Lever, C., John Rodgers, R., and Clapcote, S. J. (2015).
398 Heterozygous deletion of α -neurexin I or α -neurexin II results in behaviors relevant to autism and
399 schizophrenia. *Behav. Neurosci.* 129, 765–776. doi: 10.1037/bne0000108.
- 400 Gaare, J. J., Nido, G. S., Sztromwasser, P., Knappskog, P. M., Dahl, O., Lund-Johansen, M., et al.
401 (2018). Rare genetic variation in mitochondrial pathways influences the risk for Parkinson's
402 disease. *Mov. Disord.* 33, 1591–1600. doi: 10.1002/mds.64.
- 403 Heaton, G. R., Landeck, N., Mamais, A., Nalls, M. A., Nixon-Abell, J., Kumaran, R., et al. (2020).
404 Sequential screening nominates the Parkinson's disease associated kinase LRRK2 as a regulator
405 of Clathrin-mediated endocytosis. *Neurobiol. Dis.* 141, 104948. doi: 10.1016/j.nbd.2020.104948.
- 406 Hemmings, S. M. J., Swart, P., Womersely, J. S., Ovenden, E. S., van den Heuvel, L. L., McGregor,
407 N. W., et al. (2022). RNA-seq analysis of gene expression profiles in posttraumatic stress disorder,
408 Parkinson's disease and schizophrenia identifies roles for common and distinct biological
409 pathways. *Discov. Ment. Heal.* 2, 1–18. doi: 10.1007/s44192-022-00009-y.
- 410 Kanehisa, M., Furumichi, M., Sato, Y., Ishiguro-Watanabe, M., and Tanabe, M. (2021). KEGG:
411 Integrating viruses and cellular organisms. *Nucleic Acids Res.* 49, D545–D551. doi:
412 10.1093/nar/gkaa970.
- 413 Kang, Y., Zhang, X., Dobie, F., Wu, H., and Craig, A. M. (2008). Induction of GABAergic
414 postsynaptic differentiation by α -neurexins. *J. Biol. Chem.* 283, 2323–2334. doi:
415 10.1074/jbc.M703957200.
- 416 Krebs, C. E., Karkheiran, S., Powell, J. C., Cao, M., Makarov, V., Darvish, H., et al. (2013). The sac1
417 domain of SYNJ1 identified mutated in a family with early-onset progressive parkinsonism with
418 generalized seizures. *Hum. Mutat.* 34, 1200–1207. doi: 10.1002/humu.22372.
- 419 Kuzniewska, B., Cysewski, D., Wasilewski, M., Sakowska, P., Milek, J., Kulinski, T. M., et al. (2020).
420 Mitochondrial protein biogenesis in the synapse is supported by local translation. *EMBO Rep.* 21,
421 e48882. doi: 10.15252/embr.201948882.
- 422 Liao, Y., Wang, J., Jaehnig, E. J., Shi, Z., and Zhang, B. (2019). WebGestalt 2019: gene set analysis
423 toolkit with revamped UIs and APIs. *Nucleic Acids Res.* 47, W199–W205. doi:
424 10.1093/nar/gkz401.
- 425 Martin, I. (2016). Decoding Parkinson's Disease Pathogenesis: The Role of Deregulated mRNA
426 Translation. *J. Parkinsons. Dis.* 6, 17–27. doi: 10.3233/JPD-150738.
- 427 Missler, M., Zhang, W., Rohlmann, A., Kattenstroth, G., Hammer, R. E., Gottmann, K., et al. (2003).

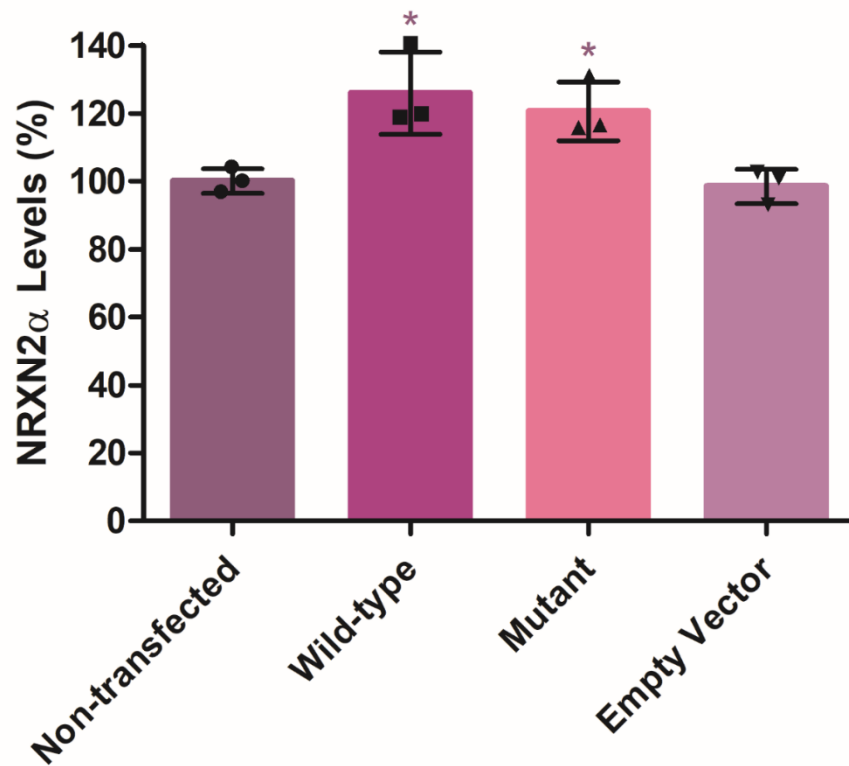
Proteomics analysis of the p.G849D variant in neurexin 2 alpha

- 428 α -neurexins couple Ca²⁺ channels to synaptic vesicle exocytosis. *Nature* 423, 939–948. doi:
429 10.1038/nature01755.
- 430 Müller, S. (2014). In silico analysis of regulatory networks underlines the role of miR-10b-5p and its
431 target BDNF in huntington's disease. *Transl. Neurodegener.* 3, 1–5. doi: 10.1186/2047-9158-3-
432 17.
- 433 Oliveros, J. C. (2015). Venny. An interactive tool for comparing lists with Venn's diagrams.
- 434 Panicker, N., Ge, P., Dawson, V. L., and Dawson, T. M. (2021). The cell biology of Parkinson's
435 disease. *J. Cell Biol.* 220. doi: 10.1083/jcb.202012095.
- 436 Rego, A. C., and Oliveira, C. R. (2003). Mitochondrial dysfunction and reactive oxygen species in
437 excitotoxicity and apoptosis: Implications for the pathogenesis of neurodegenerative diseases.
438 *Neurochem. Res.* 28, 1563–1574. doi: 10.1023/A:1025682611389.
- 439 Searle, B. C. (2010). Scaffold: A bioinformatic tool for validating MS/MS-based proteomic studies.
440 *Proteomics* 10, 1265–1269. doi: 10.1002/pmic.200900437.
- 441 Sebate, B., Cuttler, K., Cloete, R., Britz, M., Christoffels, A., Williams, M., et al. (2021). Prioritization
442 of candidate genes for a South African family with Parkinson's disease using in-silico tools. *PLoS*
443 *One* 16, e0249324. doi: 10.1371/journal.pone.0249324.
- 444 Srinivasan, S., Gal, J., Bachstetter, A., and Nelson, P. T. (2022). Alpha adaptins show isoform-specific
445 association with neurofibrillary tangles in Alzheimer's disease. *Neuropathol. Appl. Neurobiol.* 48,
446 e12776. doi: 10.1111/nan.12776.
- 447 Südhof, T. C. (2008). Neuroligins and neurexins link synaptic function to cognitive disease. *Nature*
448 455, 903–911. doi: 10.1038/nature07456.
- 449 Szklarczyk, D., Gable, A. L., Lyon, D., Junge, A., Wyder, S., Huerta-Cepas, J., et al. (2019). STRING
450 v11: Protein-protein association networks with increased coverage, supporting functional
451 discovery in genome-wide experimental datasets. *Nucleic Acids Res.* 47, D607–D613. doi:
452 10.1093/nar/gky1131.
- 453 The UniProt Consortium (2021). UniProt: The universal protein knowledgebase in 2021. *Nucleic Acids*
454 *Res.* 49, D480–D489. doi: 10.1093/nar/gkaa1100.
- 455 Wang, C., Telpoukhovskaia, M. A., Bahr, B. A., Chen, X., and Gan, L. (2018). Endo-lysosomal
456 dysfunction: a converging mechanism in neurodegenerative diseases. *Curr. Opin. Neurobiol.* 48,
457 52–58. doi: 10.1016/j.conb.2017.09.005.
- 458 Xicoy, H., Wieringa, B., and Martens, G. J. M. (2017). The SH-SY5Y cell line in Parkinson's disease
459 research: a systematic review. *Mol. Neurodegener.* 12, 1–11. doi: 10.1186/s13024-017-0149-0.
- 460 Yakhine-Diop, S., Martínez-Chacón, G., Uribe-Carretero, E., Niso-Santano, M., González-Polo, R.,
461 and Fuentes, J. (2019). The paradigm of protein acetylation in Parkinson's disease. *Neural Regen.*
462 *Res.* 14, 975–976. doi: 10.4103/1673-5374.250575.
- 463

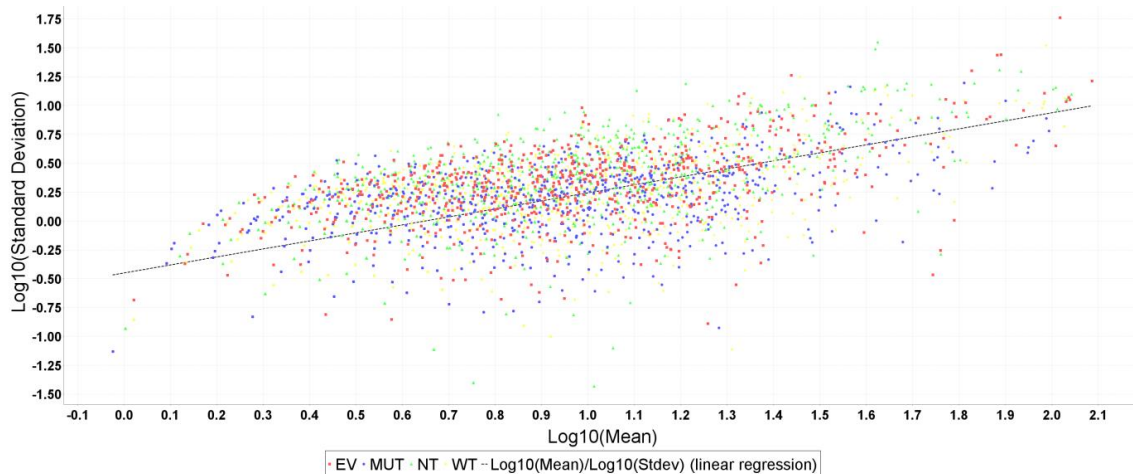
464 **10 Data Availability Statement**

465 The datasets generated for this study will be uploaded to the PRIDE database (www.ebi.ac.uk/pride/).

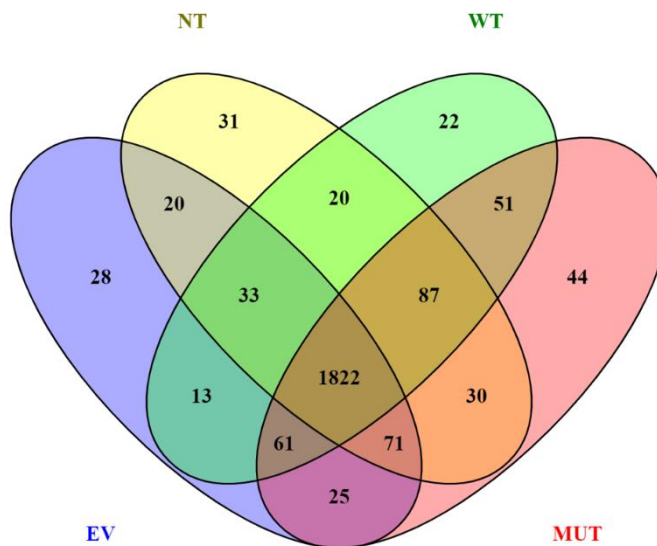
Supplementary Figures



Supplementary Figure S1: Overexpression of wild-type and mutant NRXN2 α in SH-SY5Y cells increases NRXN2 α protein levels. Flow cytometric analysis of NRXN2 α levels shows an increase in NRXN2 α levels in both the wild-type ($p = 0.03$) and mutant ($p = 0.02$) transfected cells when compared to the non-transfected cells. There is no significant change in the empty vector ($p = 0.70$) transfected cells compared to non-transfected cells. $n = 3$; one-way ANOVA and student's t -test.

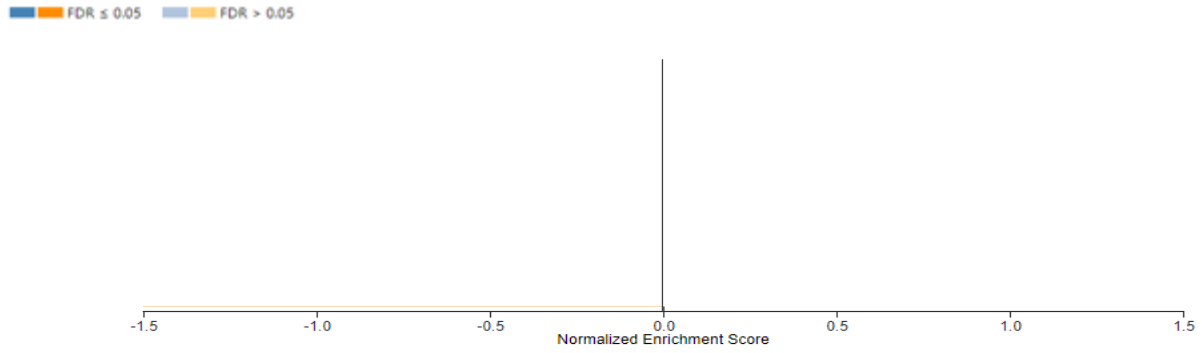


Supplementary Figure S2: Scatterplot of the standard deviation (\log_{10}) vs mean (\log_{10}) shows good clustering of all samples along the linear regression line. Graph generated by Scaffold 1.4.4. Abbreviations: EV: empty vector transfected cells, MUT: mutant transfected cells; NT: non-transfected cells; WT: wild-type transfected cells

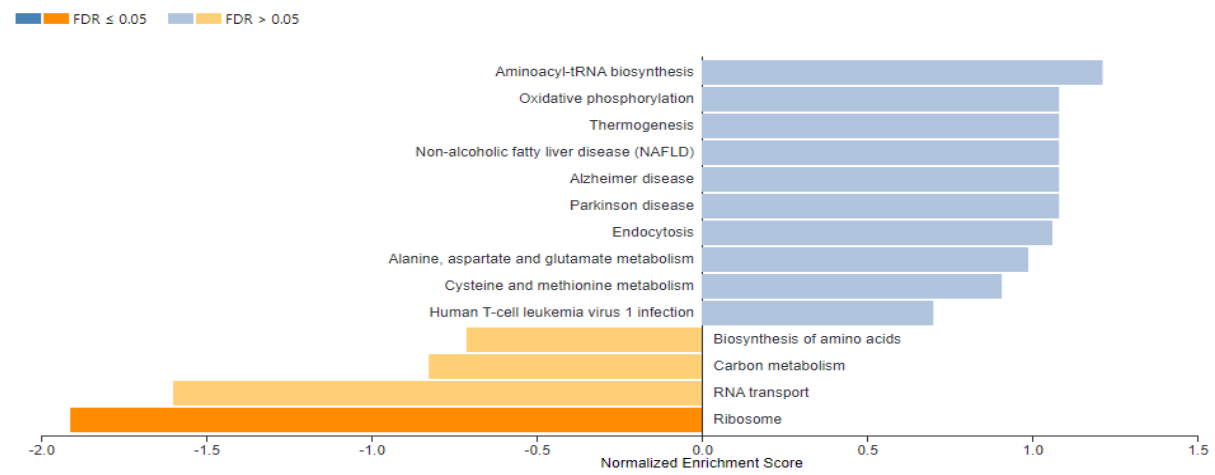


Supplementary Figure S3: Venn diagram of the total proteins identified in each treatment group shows the distribution of shared proteins and numbers of proteins unique to each group. Abbreviations: EV: empty vector transfected cells; NT: non-transfected cells; MUT: mutant transfected cells; WT: wild-type transfected cells. Diagram generated with Venny 2.1 (<https://bioinfogp.cnb.csic.es/tools/venny>) (Oliveros, 2015)

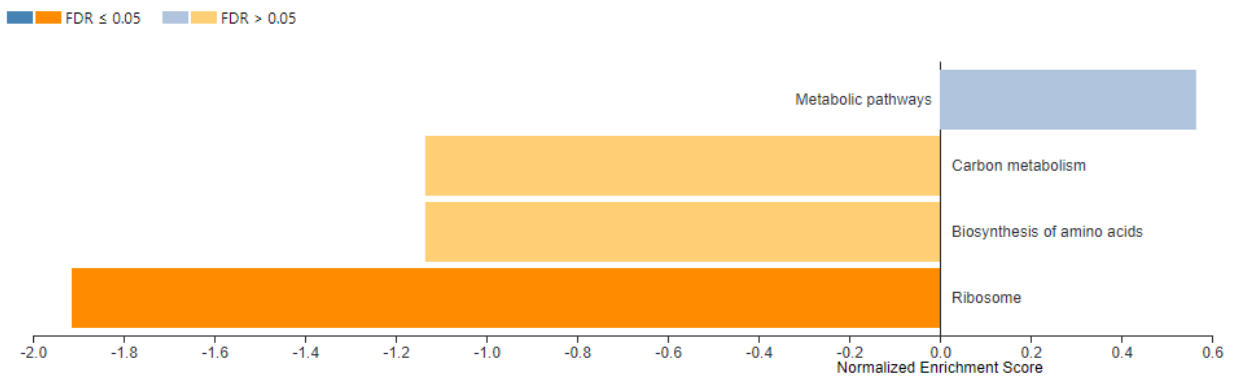
A)



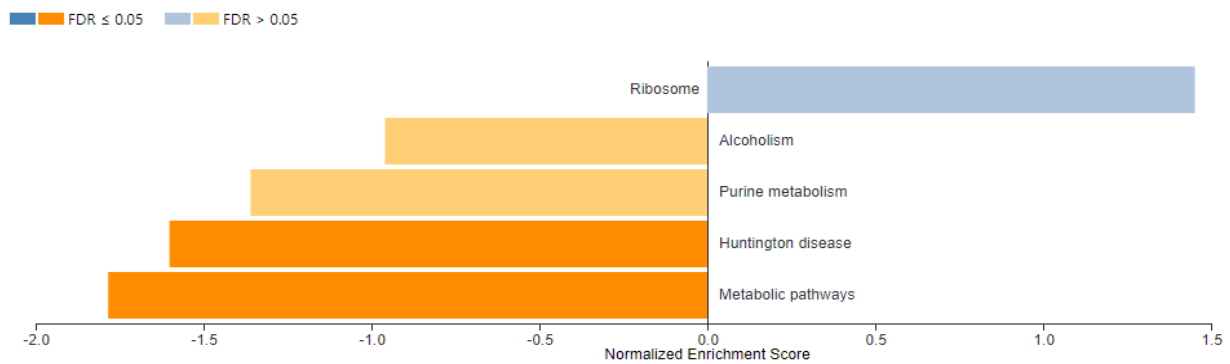
B)



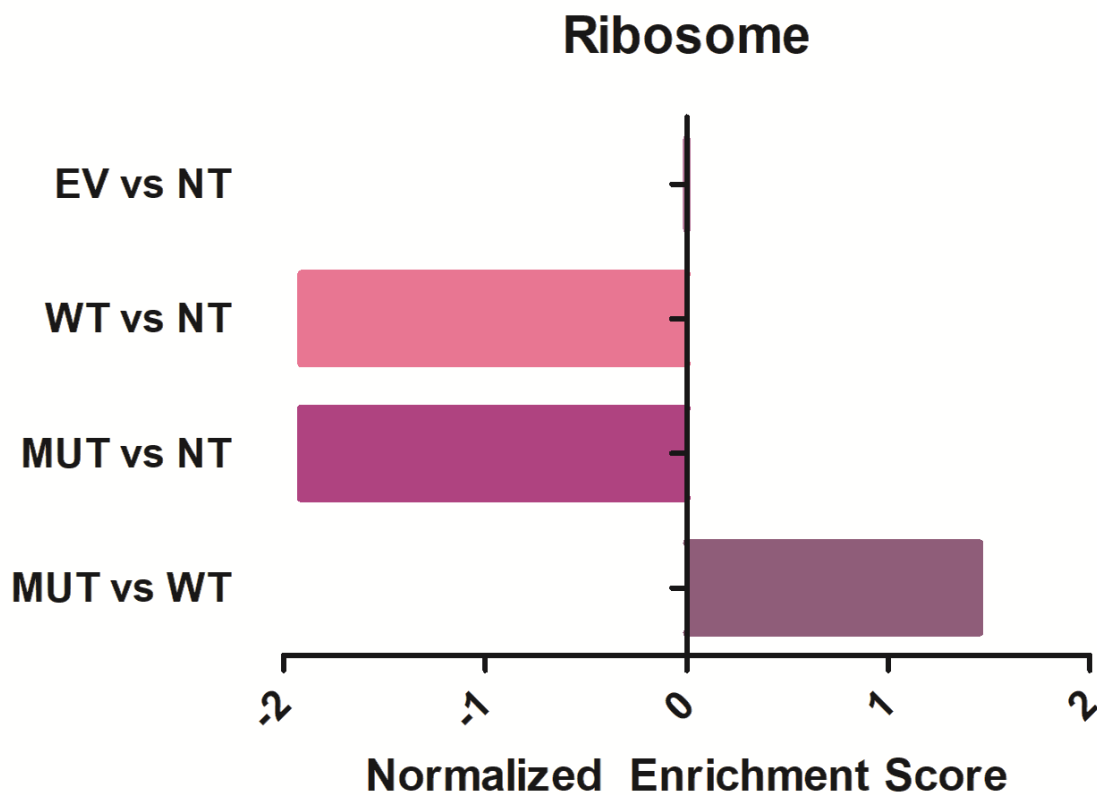
C)



D)



Supplementary Figure S4: Gene set enrichment analysis performed using WebGestalt (<http://www.webgestalt.org>). EV vs NT (a), WT vs NT (b), MUT vs NT (c), and MUT vs WT (d). Gene Ontology terms in orange are negatively enriched, while those in blue are positively enriched. Abbreviations: EV: empty vector transfected cells; FDR: false discovery rate; MUT: mutant transfected cells; NT: non-transfected cells; WT: wild-type transfected cells. WebGestalt: (Liao et al., 2019)



Supplementary Figure S5: Normalized expression scores obtained from WebGestalt (<http://www.webgestalt.org>) for the GO term “ribosome” in each analysis. Abbreviations: EV: empty vector transfected cells; NT: non-transfected cells; MUT: mutant transfected cells; WT: wild-type transfected cells. WebGestalt (Liao et al., 2019)

Supplementary Methods

Plasmids

Site-directed Mutagenesis

In order to generate the p.G849D mutant plasmid (p.G882D in our mouse model (mouse genomic position: 540693_chr19 (GRCm39)), site-directed mutagenesis was performed on the wild-type NRXN2 α -ECFP-N1 plasmid using the Q5 Site-Directed Mutagenesis kit (New England Biolabs) as per the manufacturer's instructions. Briefly, the wild-type plasmid was used as template DNA in a PCR reaction with a mutagenic forward primer, containing the single base pair change that leads to the generation of the G to D substitution, and back-to-back reverse primer. The primer sequences are as follows: Q5 G882D Forward: 5'-GTG TTC AAT GAT CAA CCC TAC ATG GAC C-3'; Q5 G882D Reverse: 5'-CAG CCC ACT CAG GTG CCC-3'. The PCR reaction consisted of an initial denaturation at 98 °C for 30 seconds, followed by 25 cycles of 98 °C for 10 seconds, 69 °C for 30 seconds and 72 °C for 5 minutes, and a final extension at 72 °C for 2 minutes. Following the PCR reaction, the kinase, ligase and DpnI enzyme mixture was added to the PCR product and incubated at room temperature for five minutes. This mixture is used to efficiently phosphorylate, ligate, and circularize the new construct and remove the template construct. After the incubation period, 5 μ l of the reaction mixture was used for bacterial transformation of the NEB 5-alpha competent *E. coli* cells. Confirmation of mutagenesis was performed using Sanger sequencing of plasmid DNA at Stellenbosch University's Central Analytical Facilities (CAF).

Plasmid DNA Isolation

After successful transformation of competent *E. coli*, colonies were inoculated in a 5 ml starter culture of LB media supplemented with 5 μ l kanamycin sulfate (50 mg/ml). The starter culture was incubated at 37 °C for 8 hours in a shaking incubator set at 200 rpm. Thereafter, 100 μ l of the starter culture was added to 100 ml of LB media supplemented with 100 μ l kanamycin sulfate (50 mg/ml). This culture was incubated at 37 °C for 16 hours in a shaking incubator set at 200 rpm. The culture was then centrifuged at 3 400 x g to pellet the cells. Plasmid DNA was isolated from

the bacteria using the ZymoPURE II Plasmid MidiPrep Kit (Zymo Research Corp.) as per the manufacturer's centrifugation protocol. Isolated plasmid DNA was stored at -20 °C until required.

Transfection

SH-SY5Y cells were grown in sterile 25 cm³ flasks until 70% confluent and transfected using Lipofectamine3000 (Invitrogen) as per the manufacturer's instructions Briefly, 5 µg plasmid DNA was added to 10 µl P3000 in 250 µl serum free media (SFM). 7.5 µl Lipofectamine3000 was prepared separately in 250 µl SFM. Thereafter, the two volumes were combined, gently mixed, and incubated for 10-20 minutes at room temperature. DMEM supplemented with 15% FBS without penicillin/streptomycin was then added to each well. The combined transfection reagents were then added dropwise to each flask and the flasks were incubated at 37 °C, 5% CO₂. After 24 hours, the media was removed and replaced with pre-warmed complete media.

NRXN2α Levels

Prior to proteomics analysis, NRXN2α protein levels were determined using immunofluorescent flow cytometry to confirm overexpression of NRXN2α. Briefly, cells were seeded at a density of 500 000 cells per well in a 6-well plate and transfected with the wild-type, mutant, or empty vector plasmids. After 24 hours the media was removed, and cells were trypsinized and transferred to 1.5 ml Eppendorf tubes. Cell pellets were harvested by centrifugation at 438 x g for 10 minutes. The cells were fixed using 3% formaldehyde in PBS for 15 minutes and permeabilized using 0.25% Triton X-100 in PBS for 15 minutes. Cells were then blocked with 0.5% BSA in PBS for 10 minutes and resuspended in 1:100 rabbit anti-NRXN2 primary antibody (Abcam: ab34245) in PBS. These suspensions were incubated overnight at 4 °C. The following morning, the cells were washed in PBS by centrifuging at 2739 x g for 5 minutes and resuspended in 1:100 anti-rabbit Cy3 secondary antibody (Jackson ImmunoResearch Laboratories: 111-165-003) in PBS. These suspensions were incubated in the dark at room temperature for 2 hours. Cells were washed twice in PBS by centrifuging at 2739 x g for 5 minutes and resuspended in deionized water for analysis with the Guava® Muse® Cell Analyzer (Luminex). Unstained, non-transfected cells and stained, non-transfected cells were used to set the gating parameters. Readings were obtained using the

Open Module Red option with 5000 events recorded for each sample. Median fluorescence values were used for analysis of NRXN2 α levels.

Proteomics Analysis

Sample Cleanup

Extraction reagents were removed using a chloroform-methanol-water liquid-liquid extraction method. The samples (100 μ l) were mixed with 400 μ l methanol and thoroughly mixed before the addition of 100 μ l chloroform. Again, the samples were thoroughly mixed before the addition of 400 μ l type I water. After mixing the samples were centrifuged for 3 minutes at 13 000 x g to induce phase separation. The top phase was removed and 400 μ l methanol was added and the sample mixed again. The samples were centrifuged again for 3 minutes at 13 000 x g to pellet the protein wafer that formed during the phase partition.

For the on bead digest, samples were re-suspended in 50 mM NH₄HCO₃ before reduction with 5 mM triscarboxyethyl phosphine (TCEP; Fluka) in 100 mM NH₄HCO₃ for 1 hour at room temperature with agitation. Cysteine residues were thiomethylated with 20 mM S-Methyl methanethiosulfonate (Sigma) in 50 mM NH₄HCO₃ for 30 minutes at room temperature. After thiomethylation the samples were diluted two-fold with binding buffer (100 mM Ammonium acetate, 30% acetonitrile, pH 4.5). The protein solution was added to MagResyn HILIC magnetic particles prepared according to manufacturer's instructions and incubated for 3 hours with rotation. After binding the supernatant was removed and the magnetic particles washed twice with washing buffer (100 mM Ammonium acetate, 95% acetonitrile, pH 4.5). After washing the magnetic particles were suspended in 10 mM NH₄HCO₃ containing trypsin (Pierce) to a final ratio of 1:50. After an overnight incubation at 37 °C the peptides were extracted once with 50 μ l water 1% trifluoroacetic acid (TFA). The samples were dried down and re-suspended in 30 μ l 2% acetonitrile: water; 0.1% formic acid (FA).

Liquid Chromatography

Liquid chromatography was performed on a Thermo Scientific Ultimate 3000 RSLC equipped with a 20 mm x 100 μ m C₁₈ trap column (Thermo Fisher) and a CSH 25 cm x 75 μ m, 1.7 μ m

particle size C₁₈ column (Waters) analytical column. The solvent system employed was loading: 2% acetonitrile: water; 0.1% FA; Solvent A: 2% acetonitrile: water; 0.1% FA and Solvent B: 100% acetonitrile: water. The samples were loaded onto the trap column using loading solvent at a flow rate of 2 µl/min from a temperature controlled autosampler set at 7 °C. Loading was performed for 5 minutes before the sample was eluted onto the analytical column. Flow rate was set to 300 nl/min and the gradient generated as follows: 2% from 0-5 minutes, 2% - 30% from 5 to 65 minutes and 30 - 50% B from 65-80 minutes. Chromatography was performed at 45 °C and the outflow delivered to the mass spectrometer.

CHAPTER 7

Analysis of the Effect of the *NRXN2* p.G849D Variant on its Synaptic Function

This chapter consists of a “submission-ready” manuscript that addressed **Objectives 7-8** of this study. Since *NRXN2α* functions mainly as a synaptic protein, we wanted to evaluate the effect of the p.G849D variant on synapse function. To this end, we created a homology model of *NRXN2α* bound to *NLGN1*. *NRXN2α* is located in the pre-synapse and commonly binds to *NLGN1*, which is located in the post-synapse. We then used GROMACS to perform molecular dynamic (MD) simulations in order to analyze the effect of the mutation on *NRXN2α*-*NLGN1* binding. Thereafter, we wanted to examine synapse formation *in vitro*. To this end, we differentiated SH-SY5Y cells with retinoic acid and transfected them with the wild-type *NRXN2α*-ECFP-N1 and mutant plasmids. We then stained for the pre-synaptic marker, synapsin I, and the post-synaptic marker, PSD-95, using immunofluorescence.

Submission-Ready Article: p.G849D mutant neurexin 2 alpha disrupts the neurexin-neuroigin system *in silico* and synapse formation in SH-SY5Y cells

Authors: Cuttler, K., Hassan, M., Cloete, R., Bardien, S.

Target Journal: European Journal of Neuroscience (Impact Factor: 3.386). Will be submitted.

Supplementary material: This follows directly after the article, in text.

Declarations

Declaration by the candidate

With regard to the submission-ready article constituting Chapter 7 of the dissertation, the nature and scope of my contribution were as follows:

Planned and conducted all experiments, analyzed the experimental data, created all tables, and figures, wrote the first manuscript draft, prepared supplementary material of the article, revised, reviewed and edited the manuscript (extent of contribution = 75%).

The following co-authors have contributed to Chapter 7:

Name	E-mail Address	Nature of Contribution	Extent of Contribution (%)
Maryam Hassan	Hassanmaryam8231@gmail.com	<ul style="list-style-type: none"> Assisted with analysis of molecular dynamics data Manuscript review and editing 	5
Ruben Cloete	ruben@sanbi.ac.za	<ul style="list-style-type: none"> Assisted with analysis of molecular dynamics data Manuscript review and editing Supervision 	10
Soraya Bardien	sbardien@sun.ac.za	<ul style="list-style-type: none"> Research project conception and organization. Manuscript review and editing. Supervision 	10

Signature of candidate:

Date: 07/07/2022

Declaration by co-authors

The undersigned hereby confirm that

1. the declaration above accurately reflects the nature and extent of the contributions of the candidate and the co-authors to Chapter 7,
2. no other authors contributed to Chapter 7, besides those specified above, and
3. potential conflicts of interest have been revealed to all interested parties and that the necessary arrangements have been made to use the material in Chapter 7 of this dissertation.

Name	Signature	Affiliation	Date
Maryam Hassan		South African National Bioinformatics Institute (SANBI), University of the Western Cape, Cape Town, South Africa	07/07/2022
Ruben Cloete		South African National Bioinformatics Institute (SANBI), University of the Western Cape, Cape Town, South Africa	07/07/2022
Soraya Bardien		Stellenbosch University, Cape Town, South Africa	06/07/2022

p.G849D mutant neurexin 2 alpha disrupts the neurexin-neurologin system *in silico*
and alters synapse formation in SH-SY5Y cells

Katelyn Cuttler¹, Maryam Hassan², Ruben Cloete², Soraya Bardien^{1,3}

¹ Division of Molecular Biology and Human Genetics, Faculty of Medicine and Health Sciences,
Stellenbosch University, Cape Town, South Africa

² South African Medical Research Council Bioinformatics Unit, South African National
Bioinformatics Institute, University of the Western Cape, Cape Town, South Africa

³ South African Medical Research Council/Stellenbosch University Genomics of Brain Disorders
Research Unit, Cape Town, South Africa

*E-mail: sbardien@sun.ac.za

Target Journal: European Journal of Neuroscience

Abstract

There is growing evidence implicating synaptic dysfunction as a molecular mechanism underlying Parkinson's disease (PD). In our previous study we identified the p.G849D variant in *neurexin 2* (*NRXN2*), encoding the synaptic protein, NRXN2 α , as a possible causal variant of PD. NRXN2 α is a synaptic maintenance protein embedded in the pre-synaptic membrane that mediates its function via binding to neuroligins (NLGNs) in the post-synaptic membrane. In this study, we aimed to examine the potential effect of the p.G849D variant on the synaptic functioning of NRXN2 α . To this end, we utilized molecular dynamic (MD) simulations to determine the effect of the variant on NRXN2 α -NLGN1 binding. Thereafter, we performed a synapse formation assay *in vitro* by overexpressing NRXN2 α in differentiated SH-SY5Y cells and staining for synaptic markers. Analysis of the MD simulations showed an overall destabilizing effect of the variant on the NRXN2 α -NLGN1 protein system. Therefore, we hypothesized that the variant could disrupt the neurexin-neuroligin system at synapses. Thereafter, following staining for the synaptic markers synapsin I and PSD-95 *in vitro*, we observed an increase in both markers in cells overexpression mutant NRXN2 α . This increase is indicative of an increase in synaptic transmission. Since we saw disruption of the neurexin-neuroligin system, we concluded that this increase may be a compensatory response whereby other cell adhesion molecules at the synapse are attempting to maintain synaptic transmission. Findings from this exploratory study indicate that the p.G849D variant in NRXN2 α may influence its function as a synaptic adhesion protein and that the resultant dysregulated synaptic maintenance could lead to neurodegeneration.

Key Words: neurexin 2 α (*NRXN2*), pG849D, Parkinson's disease, synapse, molecular dynamic simulations, synapsin I, PSD-95

1. Introduction

There is growing evidence implicating synaptic dysfunction in the aetiology of Parkinson's disease (PD) (Torres *et al.*, 2017; Imbriani *et al.*, 2018). Indeed, it has been postulated that synaptopathy is a central event in disease pathogenesis and precedes neuronal damage in PD (Imbriani *et al.*, 2018). Synaptic dysfunction can occur due to mutations that alter the structure and function of synaptic components or abnormal expression levels of a synaptic protein. In a previous study, using molecular modelling and simulation studies we reported that the p.G849D variant in the synaptic protein, neurexin 2 alpha (NRXN2 α) found in a South African multiplex PD family, could play a role in PD development (Sebate *et al.*, 2021). However, that study only looked at the wild-type and mutant NRXN2 α protein structure in isolation from its common binding partner neuroligin 1 (NLGN1). This prompted us to investigate the oligomeric complex of the NRXN2 α protein in complex with NLGN1, which are known to interact at excitatory synapses (Taylor *et al.*, 2009; Reissner *et al.*, 2013). As is known from literature, neurexins are embedded in the presynaptic membrane and are important synaptic maintenance proteins (Craig & Kang, 2007). Therefore, we wanted to examine the effect of the variant on the synaptic functioning of NRXN2 α . Neurexins and neuroligins have been associated with multiple developmental disorders, and there is increasing evidence that they are associated with several neurodegenerative disorders (Fu & Fu, 2015; Goetzl *et al.*, 2018; Lleó *et al.*, 2019) (For Review: Cuttler *et al.*, 2021).

In order to better understand the effect of the p.G849D variant on protein structure and function, we have previously used molecular dynamic (MD) simulations (Sebate *et al.*, 2021). MD simulations play a role in predicting the properties of molecular systems (Geng *et al.*, 2019) and have led to an increased understanding of protein structure-function relationships (Nair & Miners, 2014). Not all genes of interest can be investigated using wet-lab experiments due to the time and costs that arise. In addition, certain protein structures are difficult to resolve experimentally, such as large membranous proteins that are insoluble in water. Therefore, molecular modelling and MD simulations are useful to study structure-function relationships, disease pathways, and drug design (Lemkul, 2019). In PD, in particular, the familial A53T mutation in α -synuclein has been examined using MD simulations (Coskuner & Wise-Scira, 2013). These simulations helped explain the increased α -synuclein aggregation and Lewy body formation observed in individuals with this mutation. It was found that the non-amyloid β component of the protein was more solvent exposed upon introduction of the mutation, contributing to an increased aggregation rate (Coskuner & Wise-Scira, 2013). Other studies utilized MD simulations to understand the role of *DJI*, *VPS35*, and *LRRK2* mutations in PD (Anderson & Daggett, 2008; Zimprich *et al.*, 2011; Guo *et al.*, 2016). These studies show that MD simulations can complement wet-lab experimentation by providing insight into possible mechanisms of PD development which can then be further investigated.

We previously showed through MD simulations that the p.G849D variant is destabilizing to NRXN2 α protein's conformation and has a strong effect on the LNS6 domain (Sebate *et al.*, 2021). The LNS6 domain, in particular, is involved in binding of NRXN2 α to its binding partners and

thus mediates its role in synaptic signalling (Dean & Dresbach, 2006). Therefore, the present study aimed to examine the role of the variant on the synaptic function of NRXN2 α . We did this through a combinatorial approach. First, we performed MD simulations on wild-type and mutant NRXN2 α in complex with a known binding partner, NLGN1 to determine if the synaptic function of NRXN2 α is altered. Thereafter, we examined synapse formation *in vitro* by staining for synaptic markers in differentiated SH-SY5Y cells overexpressing the wild-type or mutant NRXN2 α protein.

2. Materials and Methods

2.1 Ethical Considerations

Ethical approval for the study was obtained from the Health Research Ethics Committee (Protocol numbers 2002/C059 and S20/01/005 PhD) and the Research Ethics Committee: Biological and Environmental Safety (Protocol number BEE-2021-13149), Stellenbosch University, Cape Town, South Africa.

2.2 Generation of the NRXN2-NLGN1 Complex Structure

Since the protein structures of human NRXN2 α and NLGN1 have not yet been solved experimentally, we used homology models. The three dimensional (3D) homology model of NRXN2 α was generated as per Sebate *et al.*, (2021), using PDBID: 3R05 [Laminin neurexin sex hormone binding globulin domains (LNS1-LNS6), with splice insert SS3, *Bos taurus* (cow)] as a template. NLGN1 was extracted from PDBID: 3BIW [Neuroigin-1/Neurexin-1beta synaptic adhesion complex, *Rattus norvegicus* (rat)] by superimposition of the NRXN2 α protein model and using the PyMol align command (DeLano, 2002).

2.3 Molecular Dynamic Simulations

Two simulation systems were prepared, wild-type (WT) NRXN2 in complex with NLGN1 and mutant (MUT) NRXN2 in complex with NLGN1. The two protein structures were prepared for simulation using the CHARMM-GUI solution builder option (www.charmm-gui.org) (Jo *et al.*, 2008; Lee *et al.*, 2016). The systems were solvated with TIP3 water molecules in a rectangular box of at least 10 Å of water between the protein and edges of the box. To neutralize the charge of the systems to 0.15 M concentration, 407 potassium ions and 393 chlorine ions were added to the WT system, while 408 potassium ions and 393 chlorine ions were added to the MUT system using the Monte-Carlo ion placing method. All the simulations were carried out using the GROMACS-5.1 package (Van Der Spoel *et al.*, 2005) along with the CHARMM36M force-field (Huang & Mackerell, 2013). This force-field was used to be consistent with our previous published work

(Sebate *et al.*, 2021) and because it is optimized for proteins, small molecules, nucleotides, and lipid molecules.

Each system underwent 50,000 steps of steepest descents energy minimization to remove steric clashes. The systems then were subjected to a two-step equilibration phase; NVT (constant number of particles, volume and temperature) for 100 ps to stabilize the temperature of the system and a short position restraint NPT (constant number of particles, pressure and temperature) for 100 ps to stabilize the pressure of the system by relaxing the systems and keeping the protein restrained. For the NVT simulation the system was gradually heated by switching on the water bath and the Nose-Hoover coupling method (Rühle, 2007) was used, with constant coupling of 1.0 ps at 303.15 K under a random sampling seed. While for NPT ensemble, the Parrinello-Rahman pressure coupling (Parrinello & Rahman, 1981) was turned on with constant coupling of 1.0 ps at 303.15 K under conditions of position restraints (H-bonds). For both NVT and NPT, electrostatic forces were calculated using Particle Mesh Ewald method (Essmann *et al.*, 1995). Both systems were subjected to a full 200 ns simulation repeated twice to validate the reproducibility of results. The analysis of the trajectory files was done using GROMACS utilities. The root mean square deviation (RMSD) for backbone atoms was calculated using `gmx rmsd`, the root mean square fluctuation (RMSF) average per-residue analysis was calculated using `gmx rmsf`, the change in the solvent accessibility surface area (SASA) for protein atoms was calculated using `gmx sasa`, the radius of gyration for the protein atoms was calculated using `gmx gyrate` and the changes in hydrogen bonds (H-bonds) was calculated using `gmx hbond`. VMD (Humphrey *et al.*, 1996) was used to visually inspect changes in the secondary structural elements and the motion of domains along the trajectory.

2.3.1 Principal Component Analysis (PCA) and Free Energy Surface (FES) Analysis

PCA is a statistical technique that reduces the complexity of a data set and was used here to extract biologically relevant movements of protein domains from irrelevant localized motions of atoms. For PCA analysis, the translational and rotational movements were removed from the system using `gmx covar` from GROMACS to construct a covariance matrix. Next, the eigenvectors and eigenvalues were calculated by diagonalizing the matrix. The eigenvectors that correspond to the largest eigenvalues are called “principal components”, as they represent the largest-amplitude collective motions. We filtered the original trajectory and projected out the part along the most important eigenvectors namely: vector 1 and 2 using `gmx ana eig` from GROMACS utilities. Furthermore, we visualized the sampled conformations in the subspace along the first two eigenvectors using `gmx ana eig` in a two-dimensional projection. The two-dimensional projection of the first two principal components was plotted using Gnuplot version 5.2 (Williams & Kelley, 2019).

Afterwards, we calculated the free energy surface (FES) using `gmx sham` and plotted it using `gmx xpm2ps`. The FES represents all the possible different conformations a protein can adopt during a simulation reported as Gibbs free energy. The molecules free energy was calculated with the formula $\Delta G(r) = -kBT \ln P(x,y)/P_{min}$, where P is the probability distribution of the two variables

Rg and RMSD, Pmin is the maximum probability density function, kB is the Boltzmann constant and T is the temperature of the simulation. Conformations sampled during the simulation are projected on a two-dimensional plane to visualize the reduced free energy surface. The clustering of points in a specific cell represents a possible metastable conformation.

2.4 Cell Culture

SH-SY5Y cells were cultured in DMEM with high glucose (4.5 g/l) and 4 mM L-Glutamine (Lonza). In addition, the media was supplemented with 15% FBS (Gibco) and 1% penicillin/streptomycin (P/S) (Sigma Aldrich). Cells were maintained at 37 °C and 5% CO₂ in a humidified incubator (ESCO Technologies).

2.5 Plasmids

2.5.1 NRXN2 α Wild-type

Since human NRXN2 α cDNA was not available at the time of the study, we used wild type mouse NRXN2 α cDNA instead. The NRXN2 α -ECFP-N1 plasmid was provided by Prof. Ann Marie Craig (University of British Columbia, Canada) and was generated as per Kang et al., (2008). The pECFP-N1 plasmid without an insert (empty vector) was obtained from Prof. Harald Sitte (Medical University of Vienna, Austria).

2.5.2 Site-directed Mutagenesis

In order to generate the p.G849D mutant plasmid (p.G882D in our mouse model (mouse genomic position: 540693_chr19 (GRCm39)), site-directed mutagenesis was performed on the wild-type NRXN2 α -ECFP-N1 plasmid using the Q5 Site-Directed Mutagenesis kit (New England Biolabs) as per the manufacturer's instructions. Briefly, the wild-type plasmid was used as template DNA in a PCR reaction with a mutagenic forward primer, containing the single base pair change that leads to the generation of the G to D substitution, and back-to-back reverse primer. The primer sequences are as follows: Q5 G882D Forward: 5'-GTG TTC AAT GAT CAA CCC TAC ATG GAC C-3'; Q5 G882D Reverse: 5'-CAG CCC ACT CAG GTG CCC-3'. The PCR reaction consisted of an initial denaturation at 98 °C for 30 seconds, followed by 25 cycles of 98 °C for 10 seconds, 69 °C for 30 seconds and 72 °C for 5 minutes, and a final extension at 72 °C for 2 minutes. Following the PCR reaction, the kinase, ligase and DpnI enzyme mixture was added to the PCR product and incubated at room temperature for five minutes. This mixture is used to efficiently phosphorylate, ligate, and circularize the new construct and remove the template construct. After the incubation period, 5 μ l of the reaction mixture was used for bacterial transformation of the NEB 5-alpha competent *E. coli* cells. Confirmation of mutagenesis was performed using Sanger sequencing of plasmid DNA at Stellenbosch University's Central Analytical Facilities (CAF).

2.6 Differentiation of SH-SY5Y Cells

SH-SY5Y cells were maintained in DMEM supplemented with 15% FBS and 1% P/S for 48 hours. Cells were then washed with D-PBS and differentiation media was added (DMEM with 3% FBS, 1% P/S and 10 μ M retinoic acid). The cells were maintained in this differentiation media for 7 days before being used for downstream applications. Confirmation of successful differentiation was determined by examining the cells under an Oxion Inverso Fluo E4 fluorescent microscope (Euromex) at 100x magnification (transmitted light) for the presence of branches and neuronal outgrowths.

2.7 Transfection of SH-SY5Y Cells

The differentiated cells were transfected using TransIT-2020 (Mirus) as per the manufacturer's instructions. The transfection reagents combined with plasmid DNA were added dropwise to each well and the plates were incubated at 37 °C, 5% CO₂. After 24 hours the transfection media was removed and replaced with pre-warmed complete media. The transfection efficiency was determined by examining the cells under an Oxion Inverso Fluo E4 fluorescent microscope (Euromex) at 100x magnification for the presence of cyan fluorescent protein (CFP).

2.8 Fluorescence Microscopy

Differentiated SH-SY5Y cells were seeded onto microscope cover slips within a 6-well plate prior to transfection. After transfection, cells were fixed with 3% formaldehyde in PBS for 20 min at room temperature. Cells were then washed 3 times in 1X PBS, after which they were permeabilized with 0.25% Triton X-100 in PBS for 20 min. Thereafter, cells were washed 3 times in 1X PBS and blocked in 0.5% BSA in PBS for 20 min. Cells were then incubated in primary antibody (1:200 in 0.5% BSA in PBS) overnight at 4 C. Subsequently, the cover slips were washed 3 times with 0.5% BSA in PBS and then incubated with the appropriate secondary antibody (1:500 in 0.5 % BSA in PBS) for 1 h in the dark, at room temperature. The primary and secondary antibodies that were used are listed in **Table 1**. Cover slips were then washed 3 times with PBS. Cover slips were then mounted onto clean microscope slides using Faramount Aqueous Mounting Medium (Dako) and incubated at room temperature for 1.5 h in order to allow the mounting medium to set. Controls were prepared as above, using primary antibodies only and secondary antibodies only.

Confocal microscopy images were acquired at the Central Analytical Facilities of Stellenbosch University with a Zeiss LSM780 confocal microscope. Images were acquired with ZEN 2012 imaging software, using a Plan-Apochromat 20x/0.8 M27 objective. Alexa Fluor 488 was excited with an Argon laser at 488 nm, while Alexa Fluor 568 was excited with a 561 nm laser. Emission was detected from 490-570 nm and 574-712 nm for the respective fluorochromes. Acquired

images were processed in FIJI image analysis software. Channels were separated before the automated thresholding was applied for both the green and red channels. The average intensity of signal above the threshold was measured for each image.

Table 1: Antibodies used for confocal microscopy

Target Protein	Primary Antibody	Secondary Antibody
Synapsin 1	Rabbit anti-Synapsin 1 (Thermo Fisher: 51-200)	Anti-rabbit Alexa Fluor 568 (Thermo Fisher: A-11011)
PSD-95	Mouse anti-PSD-95 (Thermo Fisher MA1046)	Anti-mouse Alexa Fluor 488 (Thermo Fisher: A-11001)

2.9 Graphs and Statistical Analysis

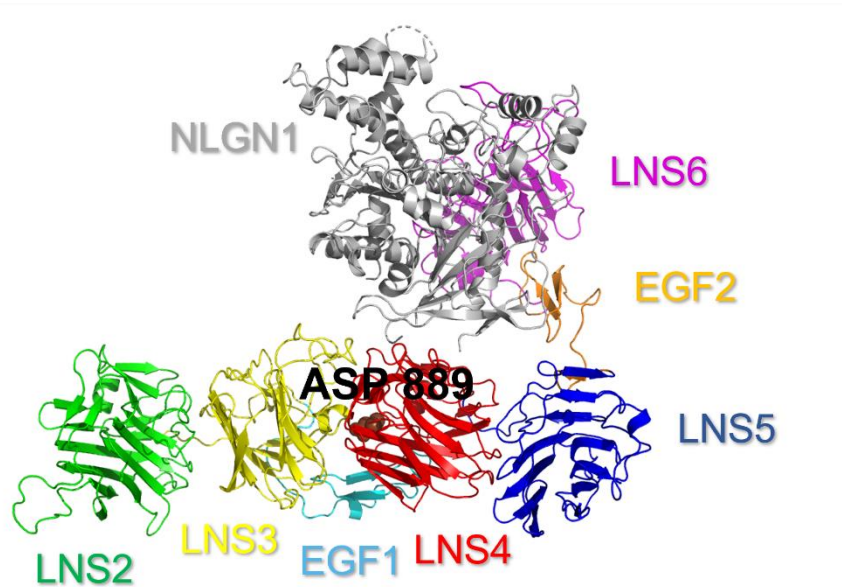
Unless otherwise stated, all MD simulation results were plotted using Gnuplot version 5.2 (Williams & Kelley, 2019). Statistical analysis of the fluorescence microscopy results was performed using GraphPad Prism® 5.02. A one-way ANOVA followed by a two-tailed student's *t*-test, with a confidence interval of 95%, was used as a means of analysing the data, with *p*-values of less than 0.05 considered to be significant.

3. Results

3.1 Generation of the NRXN2 α -NLGN1 Complex Structure

Figure 1A shows the 3D structure generated for NRXN2 α in complex with NLGN1. The NRXN2 α -NLGN1 protein model was superimposed onto the homologous template structure (PDBID: 3BIW). The RMSD value was 0.391 Å which suggests very little deviation in the main chain backbone atoms of the protein model compared to the template. The p.G849D variant (p.G889D in our system) is located in the LNS4 domain and is shown in red spheres (**Figure 1A**). Since our previous studies showed that the variant in the LNS4 domain had an effect on the conformation of the LNS6 domain (Sebate *et al.*, 2021), we also examined this domain in our downstream analysis. **Figure 1B** thus indicates the residue interactions formed between the NRXN2 α LNS6 domain and NLGN1. Four polar contacts were observed in the wild-type structure. The contact residues are also listed in **Table 2**. In the synapse, the LNS6 domain of NRXN2 α is the one that specifically interacts with its binding partners (Dean & Dresbach, 2006). For our MD simulations, we examined (i) total NRXN2 α protein's interaction with NLGN1 and (ii) only the NRXN2 α LNS6 domain's interaction with NLGN1.

A)



B)

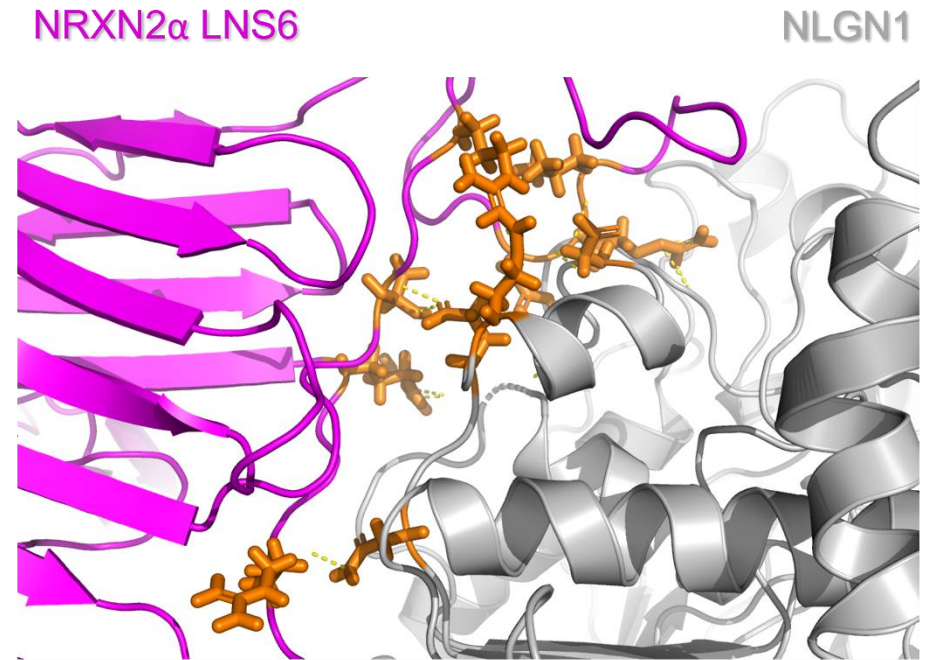


Figure 1: The three-dimensional (3D) structure predicted for NRXN2 α in complex with NLGN1. A) Each domain of NRXN2 α is colour-coded, NLGN1 is shown in grey. The p.G889D mutation is shown in red spheres in the LNS4 domain. B) A zoomed in view of the NRXN2 α LNS6 domain and NLGN1 showing the side chains (orange) potentially forming hydrogen bonds (dotted yellow lines).

Table 2: Residues forming polar contacts between NLGN1 and the LNS6 domain of NRXN2 α

NRXN2 α LNS6	NLGN1
Arg1157	Asp387
Arg1161	Gln395
Arg1284	Glu397
Thr1287	Asn400

Abbreviations: Arg: arginine; Asn: asparagine; Asp: aspartic acid; Gln: glutamine; Glu: glutamic acid; Thr: threonine

3.2 Decreased Stability of MUT NRXN2 α -NLGN1 Complex

Two complex systems were prepared for MD simulations, wild-type (WT) NRXN2 α in complex with NLGN1 and mutant (MUT) NRXN2 α in complex with NLGN1. The kinetic energy and thermodynamic properties were found to fluctuate around stable values. The total energy was stable around -5×10^6 kJ/mol while the potential energy was stable around -6×10^6 kJ/mol for both systems (**Supplementary Figure 1A-B**). In addition, the temperature was stable around 300 K and the pressure was stable around 1 bar for both systems (**Supplementary Figure 1C-D**). Similar values were seen for the 2 repeats (**Supplementary Figure 2A-C, 3A-C**).

3.2.1 Total NRXN2 α Protein in Complex with NLGN1

The results for the total system analysis are shown in **Figure 2**. RMSD graphs show that both systems became stable at approximately 60 ns (**Figure 2A**). When measuring the mean and standard deviation, the RMSD for the MUT is slightly higher ($0.67 \text{ nm} \pm 0.08$) than that of the WT ($0.59 \text{ nm} \pm 0.17$) (**Figure 2A**). A higher RMSD in the MUT vs the WT was also found for the 2 repeats (**Supplementary Figure 2D, 3D**). The Rg values were slightly higher in the MUT ($4.53 \text{ nm} \pm 0.04$) compared to the WT ($4.44 \text{ nm} \pm 0.08$) (**Figure 2B**), as were the SASA values ($696.48 \text{ nm}^2 \pm 7.85$ in the MUT vs $693.42 \text{ nm}^2 \pm 6.22$ in the WT) (**Figure 2C**).

The average RMSF per-residue values were determined for the last 100 ns of the simulations, as this is when the WT reached equilibrium, and are shown for the individual proteins (**Figure 2D-E**). The average RMSF for NRXN2 was slightly higher in the MUT ($0.29 \text{ nm} \pm 0.13$) compared to the WT ($0.20 \text{ nm} \pm 0.09$) (**Figure 2D**), as were the average RMSF values for NLGN1 ($0.17 \text{ nm} \pm 0.05$ in the MUT vs $0.14 \text{ nm} \pm 0.04$ in the WT) (**Figure 2E**). The highly fluctuating residues are labelled on the figures (**Figure 2D-E**). Notably, these residues may be of interest for therapeutic modalities, as they could be potential drug targets to restore the stability of the protein.

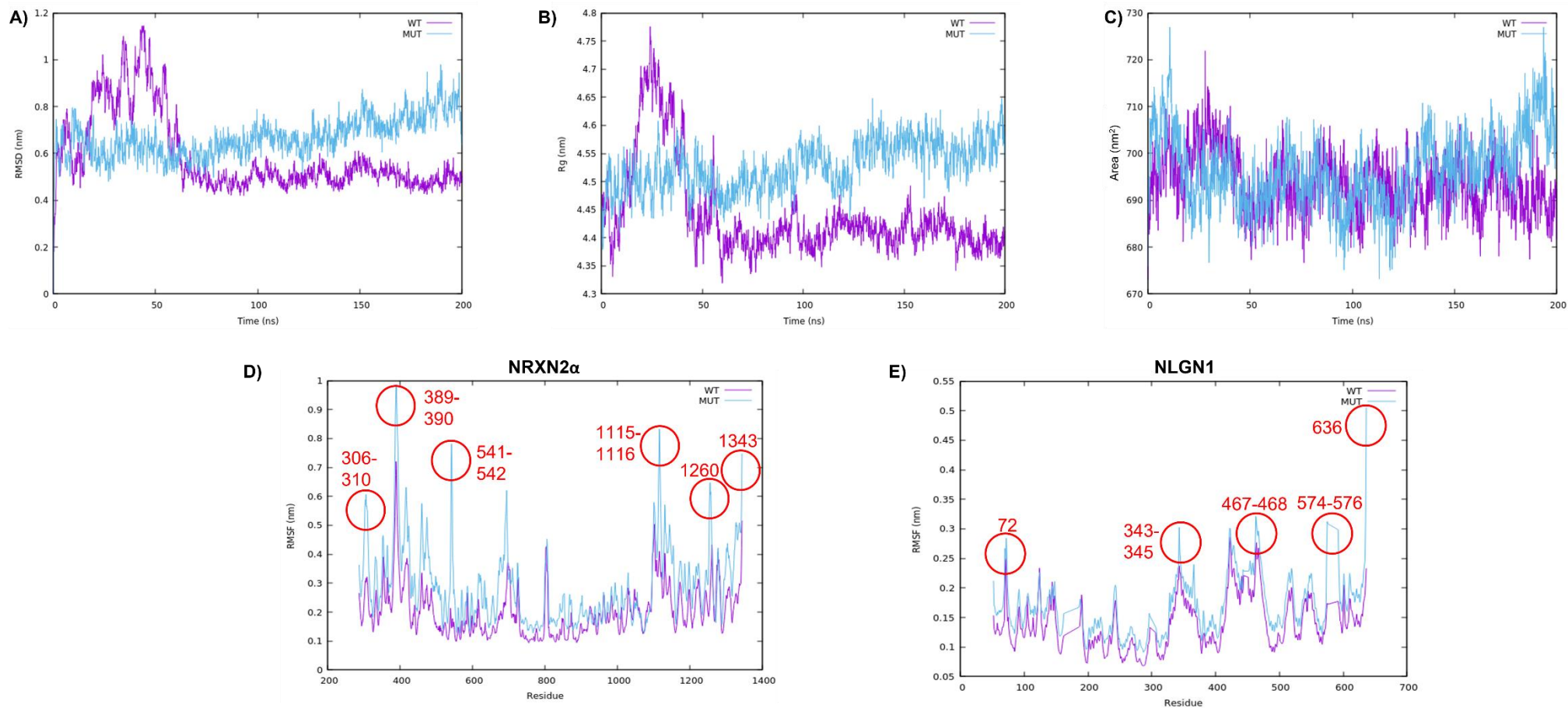


Figure 2: Trajectory analysis of WT and MUT systems for the total protein. A) Root mean square deviation (RMSD) of the backbone atoms. B) Radius of gyration (Rg) of the protein atoms. C) Solvent accessible surface area (SASA) of the protein. D) Root mean square fluctuation (RMSF) for NRXN2 α . E) RMSF for NLGN1.

3.2.2 NRXN2 α LNS6 Domain in Complex with NLGN1

Analysis of the NLGN1 in complex with the LNS6 domain of NRXN2 α showed that the MUT system had a higher RMSD ($0.67 \text{ nm} \pm 0.08$) than the WT system ($0.59 \text{ nm} \pm 0.17$) (**Figure 3A**). In addition, the average number of hydrogen bonds was slightly higher in the MUT system compared to the WT system (535.44 ± 10.50 vs 534.86 ± 10.25) (**Figure 3B**). Although this is not a large difference, there is also a change in the number of hydrogen bonds across the entire 200 ns simulation. The average RMSF for the NRXN2 LNS6 domain was slightly higher in the MUT ($0.24 \text{ nm} \pm 0.11$) compared to the WT ($0.22 \text{ nm} \pm 0.14$) (**Figure 3C**). The average RMSF values for NLGN1 were equal ($0.12 \text{ nm} \pm 0.05$ in the WT vs $0.12 \text{ nm} \pm 0.05$ in the MUT) (**Figure 3D**). However, there are a few residues in NLGN1 with higher fluctuation in the MUT when compared to the WT, namely residues 466 and 636 (**Figure 3D**). Neither these, nor the highly fluctuating residues in NRXN2 (**Figure 3C**), are involved in the hydrogen bonds forming between the LNS6 domain and NLGN1 (**Table 2**). Therefore, the MUT does not seem to have a direct effect on the protein binding. However, the destabilizing values seen previously and the change in the average number of H-bonds over time suggests that these systems are not functioning optimally, which could affect the binding between NRXN2 α and NLGN1. Upon visual inspection of the movement of these domains, the movement of NLGN1 seems to be similar in the WT and MUT systems however, MUT NRXN2 α had more flexible loop regions (**Supplementary Files S1 and S2**: <https://drive.google.com/drive/folders/192Sq7ucYirykkZuYI7P7r2VwFruKtyni?usp=sharing>).

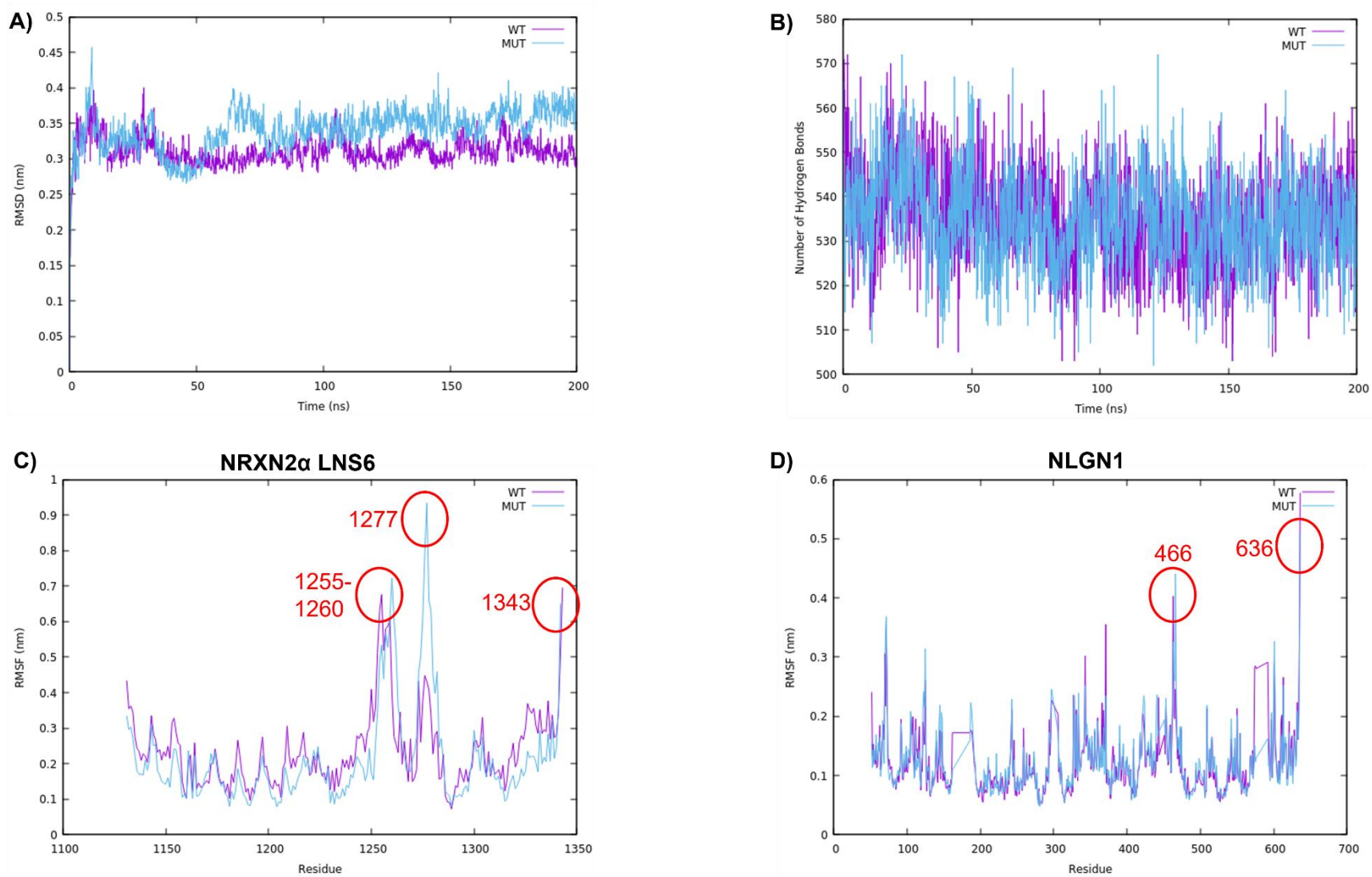


Figure 3: Trajectory analysis of WT and MUT systems for the NRXN2 α LNS6 domain and NLGN1. A) Root mean square deviation (RMSD). B) Number of Hydrogen Bonds. C) Root mean square fluctuation (RMSF) for NRXN2 LNS6 domain. D) RMSF for NLGN1.

3.3 Principal Component Analysis (PCA)

PCA was performed for both the residues of the total protein system and only the NRXN2 α LNS6 domain's residues in conjunction with NLGN1 (**Figure 4**). For the total protein, the covariance matrix was generated using the backbone atoms, whereas the covariance matrix of the NRXN2 α LNS6 domain in conjunction with NLGN1 was generated using the protein atoms. Due to the high computing power required, both analyses were only conducted on the final 10 ns of the simulation during which the systems reached equilibrium.

For the total protein, calculation of the contribution of the principal components (PCs) showed that the first two PCs contributed significantly to the movement of the backbone. PC1 contributed 38% and 37% to the WT and MUT, respectively. PC2 contributed 18% and 6% to the WT and MUT, respectively. 2D projections for the first and second principal components are shown in **Figure 4A**. After diagonalization, the covariance matrix values were calculated for both systems. The covariance matrix values are 111.43 nm² for the WT and 130.90 nm² for the MUT, showing an increase in the MUT system. In agreement with these values, the projection also shows that the MUT system has a more randomised motion compared to the WT system, showing fewer clusters, showing that the MUT system is likely less stable.

For the analysis of the NRXN2 α LNS6 domain in complex with NLGN1, the first two PCs also contributed significantly to the movement of the protein. PC1 contributed 25% and 47% to the WT and MUT, respectively. PC2 contributed 17% and 18% to the WT and MUT, respectively. 2D projections for the first and second principal components are shown in **Figure 4B**. The covariance matrix values are 178.18 nm² for the WT and 212.59 nm² for the MUT, again showing an increase in the MUT system. Again, this shows that the MUT system is likely to be less stable than the WT.

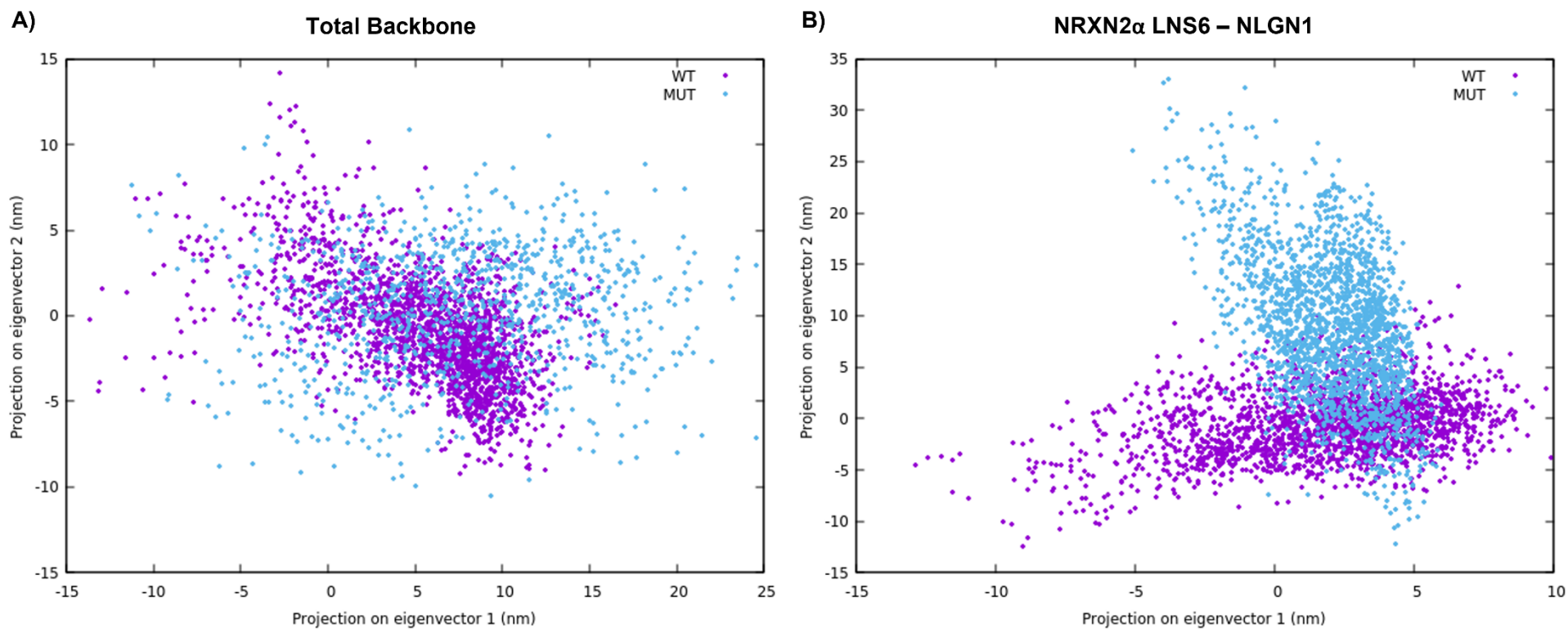


Figure 4: Two-dimensional (2D) projections of the first and second principal components for the WT and MUT systems. A) Total backbone atoms. B) NRXN2 α LNS6 domain in complex with NLGN1.

3.4 Free Energy Surface (FES) Analysis

FES analysis was performed for both the total protein and the NRXN2 α LNS6 domain in complex with NLGN1 (**Figure 5**). For both the total protein (**Figure 5A-B**) and the NRXN2 α LNS6 domain only in complex with NLGN1 (**Figure 5C-D**), the MUT showed only one energy minima state while the WT showed several metastable conformations.

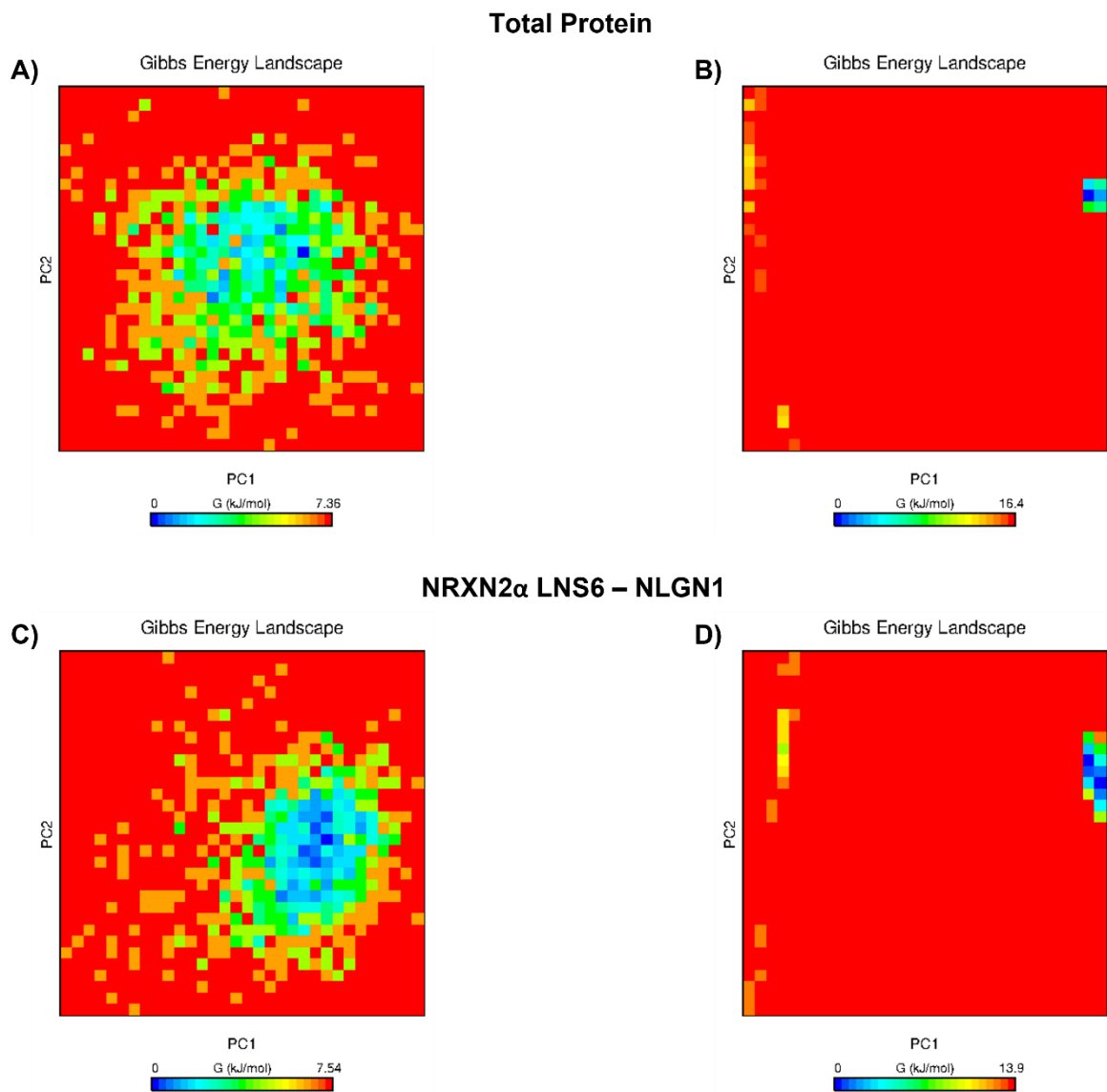


Figure 5: Free energy surface (FES) analysis of the WT and MUT systems. Gibbs free energy of total protein for the WT (A) and MUT (B) systems. Gibbs free energy of the NRXN2 α LNS6 domain in complex with NLGN1 for the WT (C) and MUT (D) systems. Blue regions represent low energy conformational states while red regions indicate high energy states.

3.5 Confirmation of SH-SY5Y Differentiation and Transfection

Figure 6A shows that the SH-SY5Y cells were successfully differentiated after being maintained for 7 days in the differentiation media (DMEM with 3% FBS, 1% P/S and 10 μ M retinoic acid). In comparison to the undifferentiated cells (**Figure 6B**), the differentiated cells are more elongated and have a more branched phenotype.

After confirmation of successful mutagenesis of the mutant plasmid DNA, the wild-type and mutant plasmids, along with the empty vector plasmid (pECFP-N1), were then transfected into the differentiated SH-SY5Y cells. Transfection efficiency, determined by microscopically examining the cells for the presence of CFP-positive cells, was found to be 67% for the wild-type construct, 64% for the mutant construct and 66% for the empty vector construct.

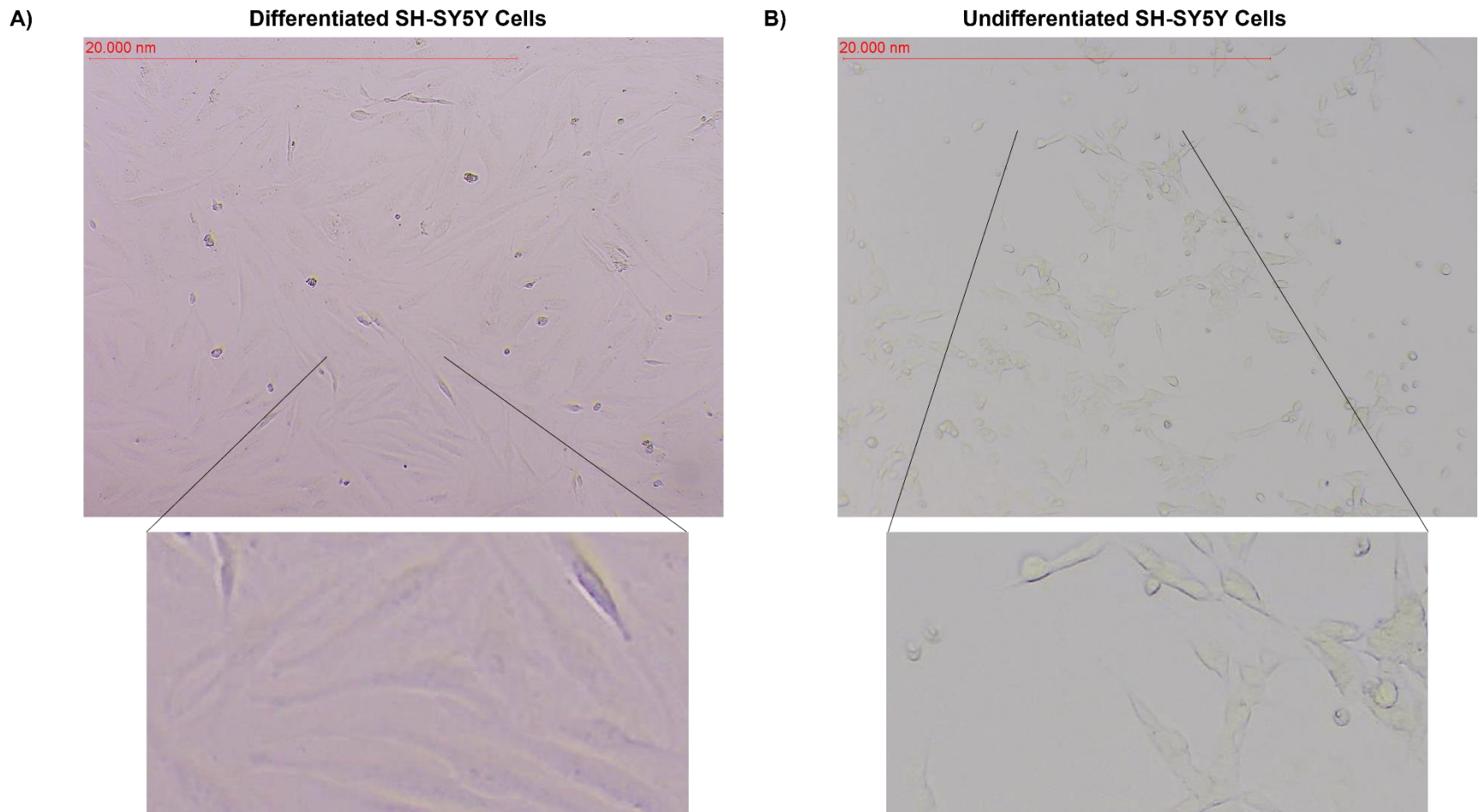


Figure 6: Representative images of SH-SY5Y cells show successful differentiation after 7 days in the differentiation medium.
A) Differentiated SH-SY5Y cells. B) Undifferentiated SH-SY5Y cells.

3.6 Increased Expression of Synapsin I and PSD-95

Synapsin I is a pre-synaptic marker and PSD-95 is a post-synaptic marker of synapse formation in cells. We used immunofluorescent staining and confocal microscopy to examine the levels of these proteins in our samples. **Figure 7A** shows representative images for the different treatments. **Figure 7B** shows a significant increase in synapsin I levels for the wild-type compared to non-transfected cells ($p < 0.0001$) and of the mutant compared to non-transfected cells ($p < 0.0001$). There is also a significant increase in synapsin I levels in the mutant compared to the wild-type samples ($p = 0.03$). Similarly, PSD-95 levels are also significantly increased in the wild-type vs non-transfected cells ($p < 0.01$) and in the mutant vs non-transfected cells ($p < 0.0001$) (**Figure 7C**). Again, a significant increase in PSD-95 levels in the mutant compared to the wild-type samples was observed ($p < 0.01$).

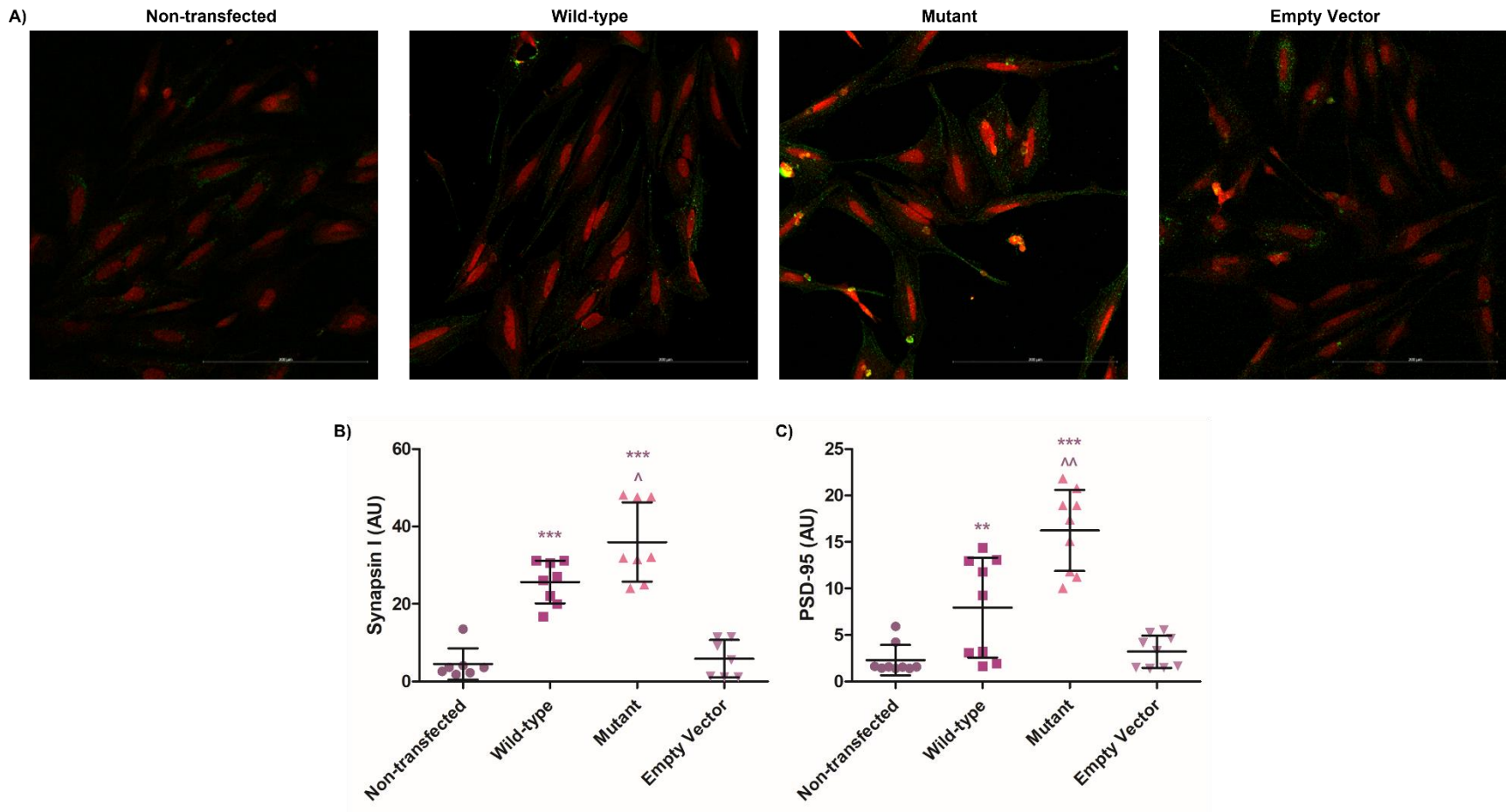


Figure 7: Overexpression of wild-type and mutant NRXN2 α in differentiated SH-SY5Y cells increases synapsin I and PSD-95 levels A) Representative images of synapsin I (red) and PSD-95 (green) staining in the different treatment groups. B) Quantification of synapsin I levels. C) Quantification of PSD-95 levels. $n \geq 9$; one-way ANOVA and student's t -test.

4. Discussion

The aim of the present study was to examine the potential role of the p.G849D variant on the main function of NRXN2 α , namely synapse maintenance and function. To this end, we used a combinatorial approach whereby we examined *in silico* the effect of the variant on the binding of NRXN2 α to its common binding partner, NLGN1, using MD studies, and then examined synapse formation *in vitro* by measuring expression of two synaptic protein markers, synapsin I and PSD-95.

MD Simulations

The p.G849D change in NRXN2 α is from the small non-polar glycine to the much larger, negatively charged aspartic acid. In our previous study, (Sebate *et al.*, 2021) we obtained a deeper insight into the structural implications of this variant on the protein structure. We showed that the variant had an overall destabilizing effect on the protein altering its conformation, and specifically affected the mobility of the LNS6 domain (Sebate *et al.*, 2021). Since the LNS6 domain is mainly involved in the binding of NRXN2 α to its binding partners (Dean & Dresbach, 2006), we predicted that the increased flexibility observed for this domain may affect the binding of neuroligins and thereby potentially the organization of synapses. To this end, we generated a 3D homology model of NRXN2 in complex with NLGN1 and performed MD simulations. Since we were interested in the potential interactions between the LNS6 domain of NRXN2 α and NLGN1, we analyzed the total trajectory of the full protein system as well as the LNS6 domain only in complex with NLGN1.

Trajectory analysis of the total protein system confirmed that the variant had an overall destabilizing effect, as the average RMSD, Rg, SASA and RMSF were all increased in the MUT system when compared to the WT system (**Figure 2**). Trajectory analysis of the LNS6 domain and NLGN1 complex showed similar results whereby the average RMSD and RMSF (NRXN2 α) were both increased in the MUT system (**Figure 3A, C**). However, the average RMSF values for NLGN1 were approximately equal in both systems (**Figure 3D**). Both the LNS6 domain and NLGN1 had a few residues with higher fluctuation values in the MUT when compared to the WT. Interestingly, none of these residues were predicted to be involved in the formation of hydrogen bonds between the LNS6 domain and NLGN1 (**Table 2**). Therefore, the MUT does not seem to have a direct effect on the protein binding with NLGN1. Upon visual inspection of the movement of these domains, MUT NRXN2 α had more flexible loop regions when compared to the WT (**Supplementary Files S1 and S2**). In addition, a change in the number of hydrogen bonds formed between the LNS6 domain and NLGN1 was observed in the MUT (**Figure 3B**). Together with the destabilizing RMSD, Rg and SASA values, this suggests that these systems are not functioning optimally, which could affect the binding between NRXN2 α and NLGN1. Furthermore, future drug development efforts could target the flexible loop regions if there are drug binding pockets nearby to restore stability to the LNS6 domain, and thereby restore binding of the protein to NLGN1. In future, non-bonded interaction energy analysis and docking studies would need to be

done to better understand the binding of NLGN1 to NRXN2 α . This would involve extending the simulations and generating different conformations to assess different binding modes.

PCA and FES Analyses

In order to reduce the complexity of the trajectory data, we utilized PCA and FES analyses. Here, the PCA extracted biologically relevant movements of the protein domains while the FES analysis reports Gibbs free energy and represents all the possible conformations that a protein can adopt during a simulation. Again, these analyses were performed on the total trajectory of the protein system, as well as the LNS6 domain in complex with NLGN1. Due to the size of the system and computational power required, PCA could only be conducted on the protein's backbone atoms for the total protein system. The backbone is generally more stable over the course of the simulation, however here there was still an increase in the covariance matrix values in the MUT system when compared to the WT (**Figure 4A**). The PCA for the LNS6 domain in complex with NLGN1 was able to be performed on the protein residues. Again, the covariance matrix values in the MUT system were higher than those in the WT system (**Figure 4B**). Therefore, both PCAs suggest that the MUT is less stable than the WT.

Following from this, the FES analyses comparing the Gibbs free energy across the top two PCs were performed. For both the total protein system (**Figure 5A-B**) and the LNS6 domain in complex with NLGN1 (**Figure 5C-D**), the MUT showed only one energy minima state while the WT showed several metastable conformations. This provides further evidence that the variant has a destabilizing effect.

Since we had previously used the NRXN2 α homology model to examine the effect of the p.G849D variant on the protein structure (Sebate *et al.*, 2021), we wanted to use the same model to examine the effect of the variant on the binding of NRXN2 α to NLGN1. However, the LNS1 domain of the protein could not be modelled due to the lack of sequence coverage between the target sequence and homologous template structure. A new tool developed by EMBL-EBI, AlphaFold, is able to predict protein structures with high accuracy (Jumper *et al.*, 2021; Varadi *et al.*, 2022). Therefore, it is possible that AlphaFold could be used to predict the full length structure of the human NRXN2 α structure to overcome this limitation. Another limitation is that the 200 ns simulation time may not be sufficient to sample enough of the protein's energy minima landscape or phase space thereby missing important energetic conformations.

NRXN2 α -NLGN1 Function

Neurexins are localized pre-synaptically and are distributed to both excitatory and inhibitory synapses (Krueger *et al.*, 2012). Their functions are mediated by their binding to post-synaptic neuroligins (Craig & Kang, 2007). Together neurexins and neuroligins form trans-synaptic bridges with each other in the synaptic cleft and function in synaptic organization, neuronal cell adhesion, transmembrane signalling and calcium channel regulation (Craig & Kang, 2007). Therefore, the

observed destabilizing effect of the variant on NRXN2 α -NLGN1 binding may negatively affect synaptic transmission efficacy, pre-synaptic vesicular transport, and synaptic plasticity. In the worst-case scenario, the variant could even result in the loss of synaptic regulation leading to the accumulation of metabolic products in the synapse, as has been seen in PD (Fahn, 2010; Schapira & Jenner, 2011; Picconi *et al.*, 2012). Since autophagy and lysosomal clearance is often also impaired in PD (Malik *et al.*, 2019), we speculate that this could worsen this accumulation of toxic metabolites.

Experimental studies have shown that when the function of NRXN2 α is dysregulated there is impairment in synaptic activity and have implicated the protein in another neurological disease, Alzheimer's disease (AD) (Tabuchi & Südhof, 2002; Missler *et al.*, 2003; Brito-Moreira *et al.*, 2017; Naito *et al.*, 2017). Meanwhile, PD animal models have implicated protein complexes at both the pre- and post-synaptic sites as key factors in PD (De La Fuente-Fernández *et al.*, 2004; Roach, 2007; Belluzzi *et al.*, 2012) In addition, studies have shown that the proteins linked to PD, such as SNCA and LRRK2, play a critical role at the pre-synaptic site (Li *et al.*, 2010; Esposito *et al.*, 2012). These studies have demonstrated that PD progression can be affected by the dopamine release into the synaptic cleft which relies on functional pre-synaptic vesicular transport, synaptic vesicle trafficking, and the maintained regulation of pre-synaptic plasticity (Li *et al.*, 2010; Esposito *et al.*, 2012). Therefore, it is plausible that if the neurexin-neuroligin pathway is dysregulated in PD, the resultant synaptic dysregulation could also affect dopamine release into the synaptic cleft.

Synapse Formation

Since we observed a destabilizing effect of the variant on the interaction between NRXN2 α and NLGN1 using MD simulations indicating the potential disruption of the neurexin-neuroligin system, we wanted to examine the effect of the variant on the synaptic function of NRXN2 α *in vitro*. To this end, we transfected differentiated SH-SY5Y cells with plasmids expressing wild-type and mutant NRXN2 α cDNA. Upon differentiation with retinoic acid, SH-SY5Y cells become more neuronal-like with a branched phenotype. They have also previously been shown to form synapses and generate action potentials (Johansson, 1994; Öz & Çelik, 2016). Thereafter, we stained for two synaptic markers, synapsin I and PSD-95. Synapsin I is a pre-synaptic marker used to measure the level of pre-synaptic induction in synaptic vesicles while PSD-95 is a post-synaptic marker used to measure the induction of glutamatergic synapses (Biederer & Scheiffele, 2007). Neurexins are known to induce pre-synaptic differentiation and the differentiation of glutamate post-synaptic specializations *in vitro* through their interactions with neuroligins (Graf *et al.*, 2004). Upon transfection with the wild-type NRXN2 α plasmid, the differentiated SH-SY5Y cells displayed increased levels of both synapsin I and PSD-95 (**Figure 7**). This is indicative of an increase in synaptic transmission and thereby agrees with previously published literature (Graf *et al.*, 2004). At excitatory glutamatergic synapses, neurexins signal to dendrites to trigger the clustering of post-synaptic scaffolding proteins, signal transducing enzymes, and glutamate receptors by causing the aggregation of neuroligins (Graf *et al.*, 2004). It has also been shown that

disruption of this neurexin-neuroigin system results in the loss of glutamate and synaptic transmission (Graf *et al.*, 2004). Interestingly, cells transfected with the mutant plasmid, showed an even greater increase in the levels of these markers (**Figure 7**). Therefore, the mutant appears to be causing an increase in both pre-synaptic and post-synaptic glutamatergic differentiation and, thus, an increase in synaptic transmission. This result was unexpected as we hypothesized that the p.G849D variant would disrupt the neurexin-neuroigin system, leading to a decrease in synaptic transmission. However, it is possible that what we are observing is a compensatory response to the disruption of neurexin-neuroigin signalling. It may be possible that other cell adhesion molecules, such as synaptic cell adhesion molecule (synCAM), synaptic adhesion like molecule (SALM), neural cell adhesion molecule (N-CAM), or neural cadherin (N-Cadherin) are acting to increase synaptic transmission in the absence of wild-type NRXN2 α . SynCAM works to organize excitatory synapses, SALM clusters post-synaptic molecules, N-CAM regulates synaptic plasticity, and N-cadherin modulates synaptic function (Missler *et al.*, 2012). Any of these molecules could therefore increase synaptic transmission if another cell adhesion system was at risk. Therefore, over time, the resultant compensatory mechanisms caused by disruption in neurexin-neuroigin signalling at excitatory glutamatergic synapses may also become disrupted due to the increased pressure to maintain synaptic transmission. Conversely, persistently increased synaptic transmission could also be problematic. Synaptic transmission is initiated when the influx of Ca²⁺ triggers synaptic vesicle exocytosis (Sørensen, 2009). Therefore, repetitive stimulation can lead to the rapid run-down of synaptic output when the readily releasable vesicles are depleted (Sørensen, 2009). Therefore, to better understand the effect of the NRXN2 α variant, it would be important to measure synaptic markers at different time points. It is possible that after the observed increase there could be a rapid loss of synaptic output at a later time point. It would also be pertinent to repeat these experiments using a co-culture model whereby plasmids can be introduced into neuronal cells (Biederer & Scheiffele, 2007; Jiang *et al.*, 2019) allowing synapse formation to be examined in much more detail, in order to determine synaptic vesicle recycling and electrophysiological signal transmission. This would enable a more direct measurement of the actual transmission between synapses. Since neurexins are also able to induce differentiation of GABA post-synaptic specializations (Graf *et al.*, 2004) leading to the formation of inhibitory GABAergic synapses, it would therefore also be interesting to determine the effect of the mutant on these GABAergic synapses in future. This would enable us to determine a ratio between excitatory synaptic output and inhibitory synaptic output to see how the neuronal cells are reacting to the introduction of the variant.

In conclusion, findings from this *in silico* and *in vitro* study point to the fact that the p.G849D variant in NRXN2 α may influence its function as a synaptic adhesion protein. The dysregulated synaptic maintenance as a result could therefore lead to neurodegeneration. However, future studies targeting neurexin-neuroigin binding *in vitro* as well as synaptic formation and electrophysiology experiments are required to better understand the effect of the variant on synaptic transmission.

Acknowledgments

We thank the study participants for their participation in and contribution to this study. The authors would also like to thank Prof. Ann Marie Craig (University of British Columbia, Canada) and Prof. Harald Sitte (Medical University of Vienna, Austria) for the NRXN2 α -ECFP-N1 plasmid and pECFP-N1 plasmid, respectively. We would like to acknowledge the Centre for High Performance Computing (CHPC), Rondebosch, South Africa for allowing us to run our molecular dynamics simulations on their cluster. We additionally acknowledge the support of the DSI-NRF Centre of Excellence for Biomedical Tuberculosis Research, South African Medical Research Council Centre for Tuberculosis Research, Division of Molecular Biology and Human Genetics, Faculty of Medicine and Health Sciences, Stellenbosch University, Cape Town, South Africa.

Conflict of Interest

The authors report no conflicting interests.

Author Contributions

K.C conducted all the experiments, performed all the statistical analyses, and wrote the first draft of the manuscript. M.H and R.C assisted with the running and analysis of the molecular dynamic simulations. R.C conceptualized the study and assisted with generation of the NRXN2-NLGN1 homology model. K.C and S.B conceptualized the study and acquired funding for the study. All authors critically reviewed and edited the manuscript.

Data Availability Statement

Raw data is available from the authors on reasonable request.

Funding

This work is based on the research supported in part by the National Research Foundation of South Africa (NRF) (Grant Number: 129249); the South African Medical Research Council (SAMRC) (self-initiated research grant); the Harry Crossley Foundation and Stellenbosch University, South Africa. SAMRC and The Higher Education Department, Next Generation of Academic Programme (nGAP), provided support for R.C. in the form of a fulltime academic position and salary.

References

- Anderson, P.C. & Daggett, V. (2008) Molecular basis for the structural instability of human DJ-1 induced by the L166P mutation associated with Parkinson's disease. *Biochemistry*, **47**, 9380–9393.
- Belluzzi, E., Greggio, E., & Piccoli, G. (2012) Presynaptic dysfunction in Parkinson's disease: a focus on LRRK2. *Biochem. Soc. Trans.*, **40**, 1111–1116.
- Biederer, T. & Scheiffele, P. (2007) Mixed-culture assays for analyzing neuronal synapse formation. *Nat. Protoc.*, **2**, 670–676.
- Brito-Moreira, J., Lourenco, M. V., Oliveira, M.M., Ribeiro, F.C., Ledo, J.H., Diniz, L.P., Vital, J.F.S., Magdesian, M.H., Melo, H.M., Barros-Aragão, F., De Souza, J.M., Alves-Leon, S. V., Gomes, F.C.A., Clarke, J.R., Figueiredo, C.P., De Felice, F.G., & Ferreira, S.T. (2017) Interaction of amyloid- β ($A\beta$) oligomers with neurexin 2 α and neuroligin 1 mediates synapse damage and memory loss in mice. *J. Biol. Chem.*, **292**, 7327–7337.
- Coskuner, O. & Wise-Scira, O. (2013) Structures and free energy landscapes of the A53T mutant-type α -synuclein protein and impact of A53T mutation on the structures of the wild-type α -synuclein protein with dynamics. *ACS Chem. Neurosci.*, **4**, 1101–1113.
- Craig, A.M. & Kang, Y. (2007) Neurexin-neuroligin signaling in synapse development. *Curr. Opin. Neurobiol.*, **17**, 43–52.
- Cuttler, K., Hassan, M., Carr, J., Cloete, R., & Bardien, S. (2021) Emerging evidence implicating a role for neurexins in neurodegenerative and neuropsychiatric disorders. *Open Biol.*, **11**.
- De La Fuente-Fernández, R., Schulzer, M., Mak, E., Calne, D.B., & Stoessl, A.J. (2004) Presynaptic mechanisms of motor fluctuations in Parkinson's disease: A probabilistic model. *Brain*, **127**, 888–899.
- Dean, C. & Dresbach, T. (2006) Neuroligins and neurexins: Linking cell adhesion, synapse formation and cognitive function. *Trends Neurosci.*, **29**, 21–29.
- DeLano, W. (2002) Pymol: An open-source molecular graphics tool. *CCP4 Newsl. Protein Crystallogr.*, **40**, 82–92.
- Esposito, G., Ana Clara, F., & Verstreken, P. (2012) Synaptic vesicle trafficking and Parkinson's disease. *Dev. Neurobiol.*, **72**, 134–144.
- Essmann, U., Perera, L., Berkowitz, M.L., Darden, T., Lee, H., & Pedersen, L.G. (1995) A smooth particle mesh Ewald method. *J. Chem. Phys.*, **103**, 8577–8593.
- Fahn, S. (2010) Parkinson's disease: 10 years of progress, 1997-2007. *Mov. Disord.*, **25**.

- Fu, L.M. & Fu, K.A. (2015) Analysis of Parkinson's disease pathophysiology using an integrated genomics-bioinformatics approach. *Pathophysiology*, **22**, 15–29.
- Geng, H., Chen, F., Ye, J., & Jiang, F. (2019) Applications of Molecular Dynamics Simulation in Structure Prediction of Peptides and Proteins. *Comput. Struct. Biotechnol. J.*, **17**, 1162–1170.
- Goetzl, E.J., Abner, E.L., Jicha, G.A., Kapogiannis, D., & Schwartz, J.B. (2018) Declining levels of functionally specialized synaptic proteins in plasma neuronal exosomes with progression of Alzheimer's disease. *FASEB J.*, **32**, 888–893.
- Graf, E.R., Zhang, X., Jin, S.X., Linhoff, M.W., & Craig, A.M. (2004) Neurexins induce differentiation of GABA and glutamate postsynaptic specializations via neuroligins. *Cell*, **119**, 1013–1026.
- Guo, Y.B., Chen, J., Zhang, X.D., Xu, S.B., & Liu, H.Y. (2016) Molecular dynamics simulations to understand LRKK2 mutations in Parkinson. *Mol. Simul.*, **42**, 64–70.
- Huang, J. & Mackerell, A.D. (2013) CHARMM36 all-atom additive protein force field: Validation based on comparison to NMR data. *J. Comput. Chem.*, **34**, 2135–2145.
- Humphrey, W., Dalke, A., & Schulten, K. (1996) VMD: Visual molecular dynamics. *J. Mol. Graph.*, **14**, 33–38.
- Imbriani, P., Schirinzi, T., Meringolo, M., Mercuri, N.B., & Pisani, A. (2018) Centrality of early synaptopathy in Parkinson's disease. *Front. Neurol.*, **9**.
- Jiang, W., Gong, J., Rong, Y., & Yang, X. (2019) A new co-culture method for identifying synaptic adhesion molecules involved in synapse formation. *Biophys. Reports*, **5**, 91–97.
- Jo, S., Kim, T., Iyer, V.G., & Im, W. (2008) CHARMM-GUI: A web-based graphical user interface for CHARMM. *J. Comput. Chem.*, **29**, 1859–1865.
- Johannson, S. (1994) Graded action potentials generated by differentiated human neuroblastoma cells. *Acta Physiol. Scand.*, **151**, 331–341.
- Jumper, J., Evans, R., Pritzel, A., Green, T., Figurnov, M., Ronneberger, O., Tunyasuvunakool, K., Bates, R., Žídek, A., Potapenko, A., Bridgland, A., Meyer, C., Kohl, S.A.A., Ballard, A.J., Cowie, A., Romera-Paredes, B., Nikolov, S., Jain, R., Adler, J., Back, T., Petersen, S., Reiman, D., Clancy, E., Zielinski, M., Steinegger, M., Pacholska, M., Berghammer, T., Bodenstein, S., Silver, D., Vinyals, O., Senior, A.W., Kavukcuoglu, K., Kohli, P., & Hassabis, D. (2021) Highly accurate protein structure prediction with AlphaFold. *Nature*, **596**, 583–589.
- Kang, Y., Zhang, X., Dobie, F., Wu, H., & Craig, A.M. (2008) Induction of GABAergic postsynaptic differentiation by α -neurexins. *J. Biol. Chem.*, **283**, 2323–2334.

- Krueger, D.D., Tuffy, L.P., Papadopoulos, T., & Brose, N. (2012) The role of neurexins and neuroligins in the formation, maturation, and function of vertebrate synapses. *Curr. Opin. Neurobiol.*, **22**, 412–422.
- Lee, J., Cheng, X., Swails, J.M., Yeom, M.S., Eastman, P.K., Lemkul, J.A., Wei, S., Buckner, J., Jeong, J.C., Qi, Y., Jo, S., Pande, V.S., Case, D.A., Brooks, C.L., MacKerell, A.D., Klauda, J.B., & Im, W. (2016) CHARMM-GUI Input Generator for NAMD, GROMACS, AMBER, OpenMM, and CHARMM/OpenMM Simulations Using the CHARMM36 Additive Force Field. *J. Chem. Theory Comput.*, **12**, 405–413.
- Lemkul, J. (2019) From Proteins to Perturbed Hamiltonians: A Suite of Tutorials for the GROMACS-2018 Molecular Simulation Package [Article v1.0]. *Living J. Comput. Mol. Sci.*, **1**, 5068–5068.
- Li, X., Wang, J., Yue, Z., Buxbaum, J.D., Elder, G.A., Avshalumov, M. V., Patel, J.C., Rice, M.E., & Nicholson, C. (2010) Enhanced striatal dopamine transmission and motor performance with LRRK2 overexpression in mice is eliminated by familial Parkinson's disease mutation G2019S. *J. Neurosci.*, **30**, 1788–1797.
- Lleó, A., Núñez-Llaves, R., Alcolea, D., Chiva, C., Balateu-Paños, D., Colom-Cadena, M., Gomez-Giro, G., Muñoz, L., Querol-Vilaseca, M., Pegueroles, J., Rami, L., Lladó, A., Molinuevo, J.L., Tainta, M., Clarimón, J., Spires-Jones, T., Blesa, R., Fortea, J., Martínez-Lage, P., Sánchez-Valle, R., Sabidó, E., Bayés, À., & Belbin, O. (2019) Changes in synaptic proteins precede neurodegeneration markers in preclinical Alzheimer's disease cerebrospinal fluid. *Mol. Cell. Proteomics*, **18**, 546–560.
- Malik, B.R., Maddison, D.C., Smith, G.A., & Peters, O.M. (2019) Autophagic and endo-lysosomal dysfunction in neurodegenerative disease. *Mol. Brain*, **12**, 1–21.
- Missler, M., Südhof, T.C., & Biederer, T. (2012) Synaptic cell adhesion. *Cold Spring Harb. Perspect. Biol.*, **4**, a005694.
- Missler, M., Zhang, W., Rohlmann, A., Kattenstroth, G., Hammer, R.E., Gottmann, K., & Südhof, T.C. (2003) α -neurexins couple Ca²⁺ channels to synaptic vesicle exocytosis. *Nature*, **423**, 939–948.
- Nair, P.C. & Miners, J.O. (2014) Molecular dynamics simulations: from structure function relationships to drug discovery. *Silico Pharmacol.*, **2**, 1–4.
- Naito, Y., Tanabe, Y., Lee, A.K., Hamel, E., & Takahashi, H. (2017) Amyloid- β Oligomers Interact with Neurexin and Diminish Neurexin-mediated Excitatory Presynaptic Organization. *Sci. Rep.*, **7**.
- Öz, A. & Çelik, Ö. (2016) Curcumin inhibits oxidative stress-induced TRPM2 channel activation,

- calcium ion entry and apoptosis values in SH-SY5Y neuroblastoma cells: Involvement of transfection procedure. *Mol. Membr. Biol.*, **33**, 76–88.
- Parrinello, M. & Rahman, A. (1981) Polymorphic transitions in single crystals: A new molecular dynamics method. *J. Appl. Phys.*, **52**, 7182–7190.
- Picconi, B., Piccoli, G., & Calabresi, P. (2012) Synaptic dysfunction in Parkinson's disease. In Kreutz, M. & Sala, C. (eds), *Advances in Experimental Medicine and Biology: Synaptic Plasticity*. Springer Vienna, Vienna, pp. 553–572.
- Reissner, C., Runkel, F., & Missler, M. (2013) Neurexins. *Genome Biol.*, **14**, 213.
- Roach, E.S. (2007) Both postsynaptic and presynaptic dysfunction contribute to parkinson disease: Any mechanism will not do. *Arch. Neurol.*, **64**, 143.
- Rühle, V. (2007) Berendsen and Nose-Hoover thermostats. *Am. J. Phys.*, 1–4.
- Schapira, A.H. & Jenner, P. (2011) Etiology and pathogenesis of Parkinson's disease. *Mov. Disord.*, **26**, 1049–1055.
- Sebate, B., Cuttler, K., Cloete, R., Britz, M., Christoffels, A., Williams, M., Carr, J., & Bardien, S. (2021) Prioritization of candidate genes for a South African family with Parkinson's disease using in-silico tools. *PLoS One*, **16**, e0249324.
- Sørensen, J.B. (2009) Vesicle Pools. In Squire, L.R. (ed), *Encyclopedia of Neuroscience*. Elsevier Ltd, Oxford, pp. 99–105.
- Tabuchi, K. & Südhof, T.C. (2002) Structure and evolution of neurexin genes: Insight into the mechanism of alternative splicing. *Genomics*, **79**, 849–859.
- Taylor, P., De Jaco, A., & Comoletti, D. (2009) Neuroligins. In Squire, L.R. (ed), *Encyclopedia of Neuroscience*. Elsevier Ltd, Oxford, pp. 493–496.
- Torres, V.I., Vallejo, D., & Inestrosa, N.C. (2017) Emerging Synaptic Molecules as Candidates in the Etiology of Neurological Disorders. *Neural Plast.*, **2017**, 8081758.
- Van Der Spoel, D., Lindahl, E., Hess, B., Groenhof, G., Mark, A.E., & Berendsen, H.J.C. (2005) GROMACS: Fast, flexible, and free. *J. Comput. Chem.*, **26**, 1701–1718.
- Varadi, M., Anyango, S., Deshpande, M., Nair, S., Natassia, C., Yordanova, G., Yuan, D., Stroe, O., Wood, G., Laydon, A., Zidek, A., Green, T., Tunyasuvunakool, K., Petersen, S., Jumper, J., Clancy, E., Green, R., Vora, A., Lutfi, M., Figurnov, M., Cowie, A., Hobbs, N., Kohli, P., Kleywegt, G., Birney, E., Hassabis, D., & Velankar, S. (2022) AlphaFold Protein Structure Database: Massively expanding the structural coverage of protein-sequence space with high-accuracy models. *Nucleic Acids Res.*, **50**, D439–D444.

Williams, T. & Kelley, C. (2019) gnuplot 5.2: An Interactive Plotting Program.

Zimprich, A., Benet-Pagès, A., Struhal, W., Graf, E., Eck, S.H., Offman, M.N., Haubenberger, D., Spielberger, S., Schulte, E.C., Lichtner, P., Rossle, S.C., Klopp, N., Wolf, E., Seppi, K., Pirker, W., Presslauer, S., Mollenhauer, B., Katzenschlager, R., Foki, T., Hotzy, C., Reinthaler, E., Harutyunyan, A., Kralovics, R., Peters, A., Zimprich, F., Brücke, T., Poewe, W., Auff, E., Trenkwalder, C., Rost, B., Ransmayr, G., Winkelmann, J., Meitinger, T., & Strom, T.M. (2011) A mutation in VPS35, encoding a subunit of the retromer complex, causes late-onset parkinson disease. *Am. J. Hum. Genet.*, **89**, 168–175.

Supplementary Figures

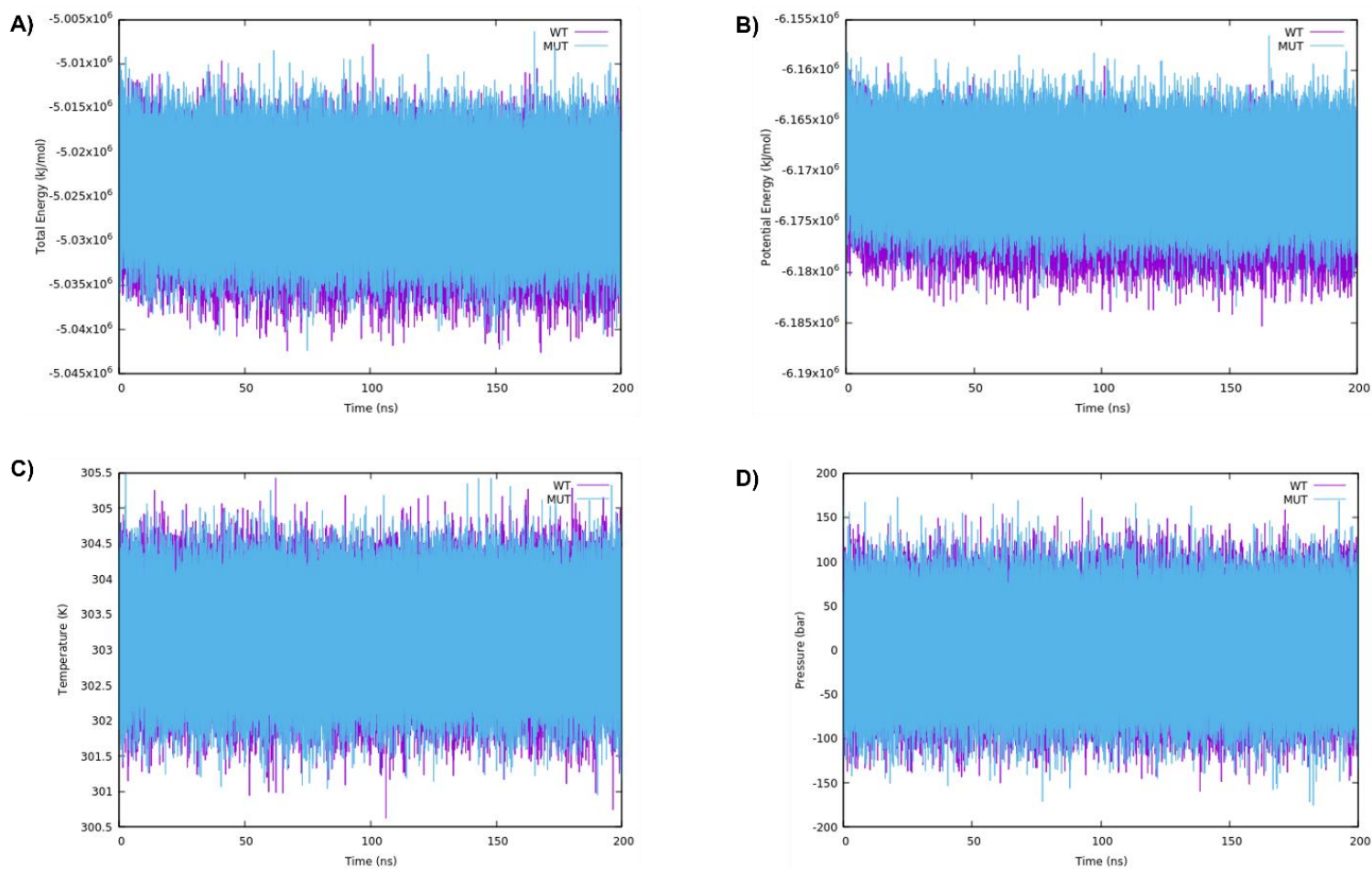


Figure S1: Thermodynamic and kinetic properties of the WT and MUT systems over the 200 ns simulation. A) Total Energy. B) Potential Energy. C) Temperature. D) Pressure.

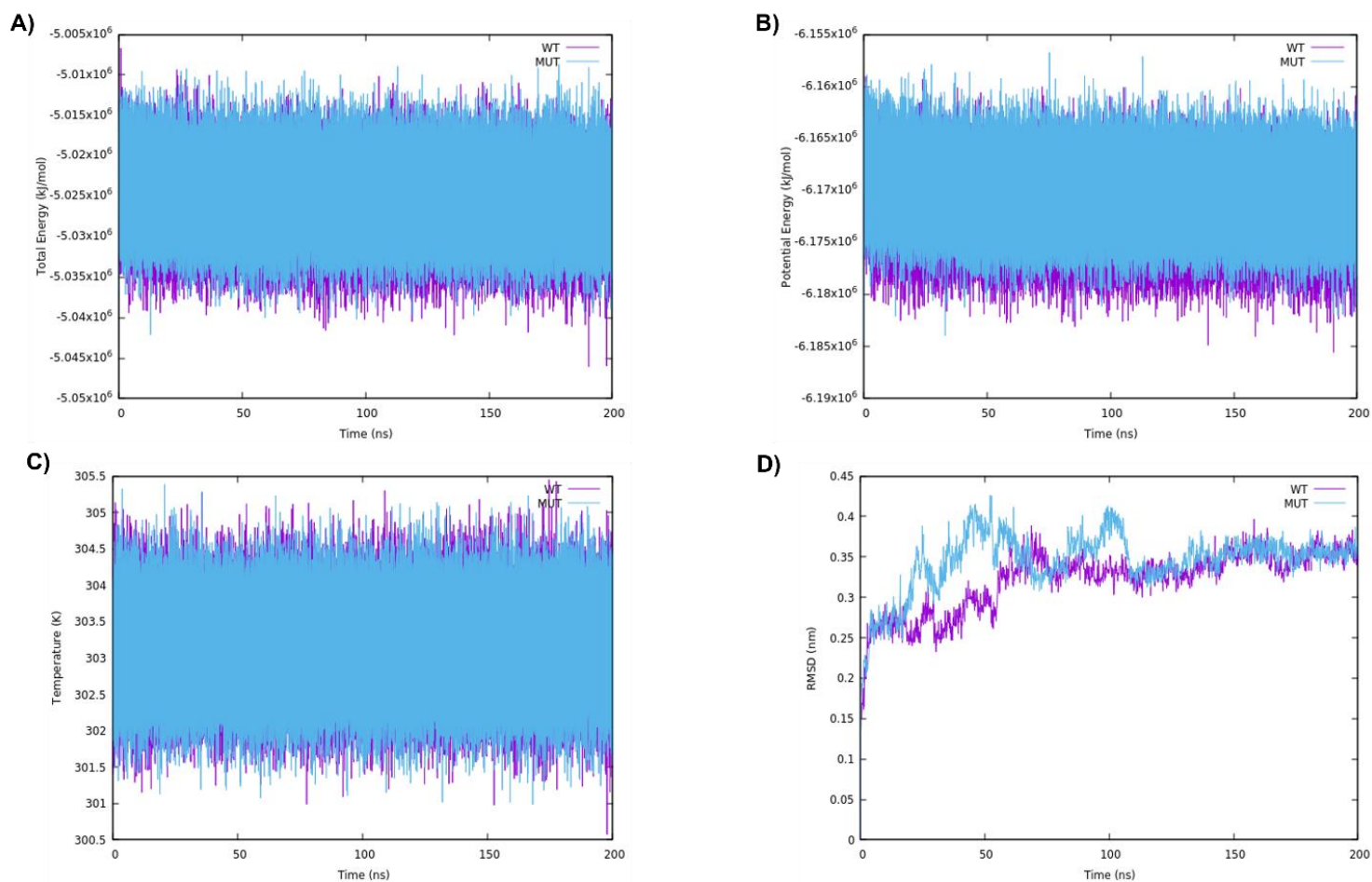


Figure S2: Thermodynamic and kinetic properties of the WT and MUT systems (repeat 1) over the 200 ns simulation. A) Total Energy. B) Potential Energy. C) Temperature. D) Root Mean Square Deviation (RMSD).

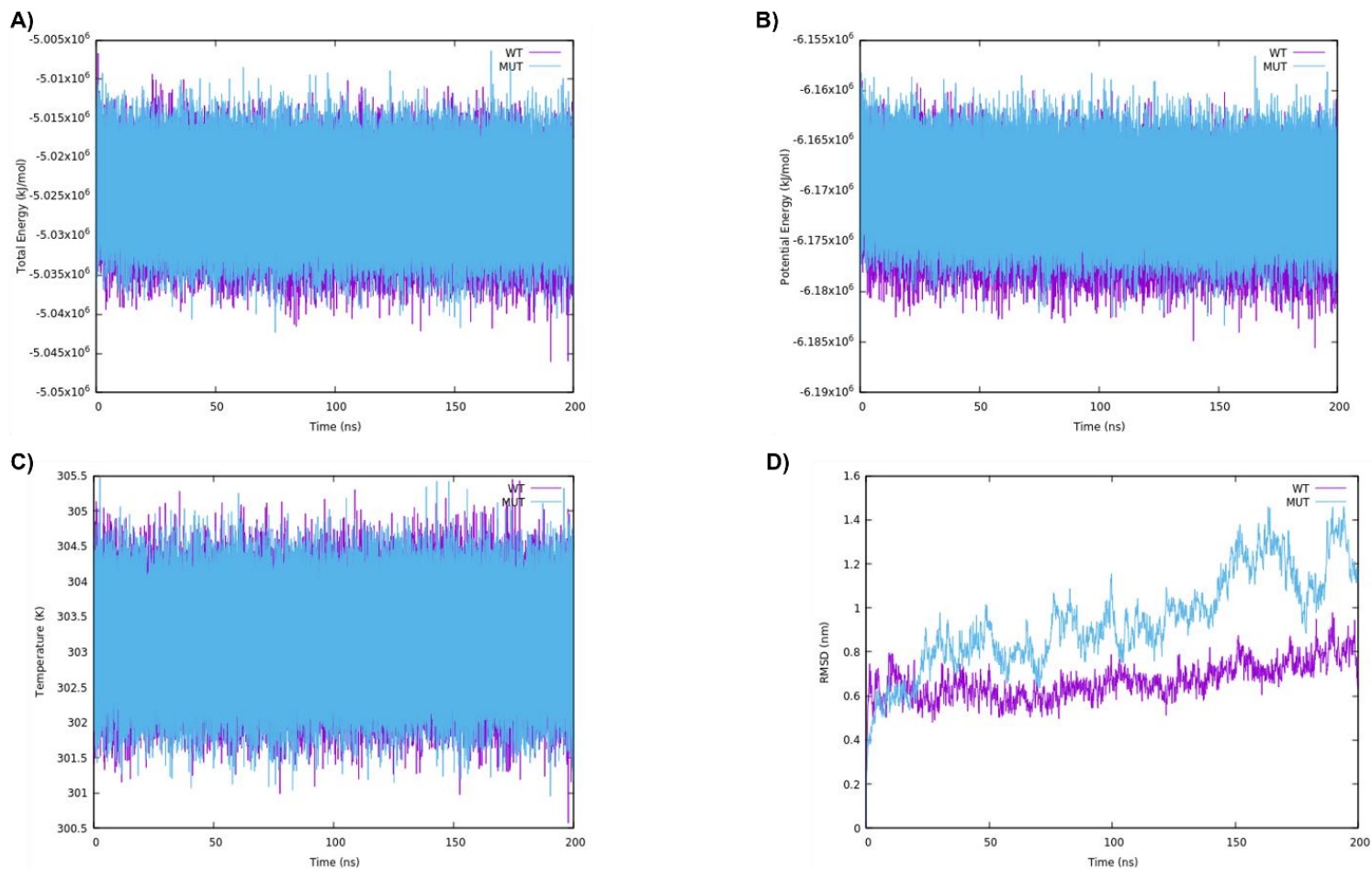


Figure S3: Thermodynamic and kinetic properties of the WT and MUT systems (repeat 2) over the 200 ns simulation. A) Total Energy. B) Potential Energy. C) Temperature. D) Root Mean Square Deviation (RMSD).

CHAPTER 8

Discussion and Conclusion

This final chapter serves to bring together all the different parts of the project and provides insight into the broader significance of the findings.

As previously mentioned, PD is the fastest growing neurological disorder globally, with its prevalence increasing by 118% between 1990 and 2015 (Feigin et al., 2017). However, not much is known about the genetic basis of PD in SSA. Here, as a step towards studying the genetic aetiology of SSA individuals with PD, we identified and recruited a South African (SA) family (ZA253) for genetic studies. This family is of Afrikaner European ancestry and consists of five individuals with PD and four unaffected individuals who consented to take part in this study. After excluding all known causes of PD using a WES approach, we identified a possible causal gene, and performed a literature search to better justify its potential role in the development of PD. In addition, we performed functional studies to better understand how the variant in this gene could result in neuronal death. A summary of these research objectives and their findings is shown in **Figure 8.1**. In brief, WES of three affected members and the subsequent bioinformatic analyses led to prioritization of the p.G849D variant in neurexin 2 (*NRXN2*). Thereafter, we performed a literature review and found that neurexins have in fact been implicated in neuropsychiatric and neurodegenerative disorders. We then decided to perform functional studies on an *in vitro* model of PD, SH-SY5Y cells. We utilized functional assays and proteomics to determine how overexpression of the mutant protein affects the cells and biological pathways. Thereafter, we used a combinatorial study to examine the effect of the mutation on the synaptic functioning of the NRXN2 α protein. Ultimately, our findings indicate that synaptic dysregulation could be linked to mitochondrial dysfunction and may lead to neurodegeneration.

A)

What is the genetic aetiology of Parkinson's disease in family ZA253?

Methods



WES

Results



NRXN2 p.G849D variant

Publication

RESEARCH ARTICLE

Prioritization of candidate genes for a South African family with Parkinson's disease using *in-silico* tools

Boiketlo Sebate¹, Katelyn Cuttler¹, Ruben Cloete^{2*}, Marcell Britz³, Alan Christoffels², Monique Williams⁴, Jonathan Carr⁵, Soraya Bardien^{1*}

Are neurexins implicated in neurodegenerative disorders?

Methods



Literature Search

Results

- established role of neurexins in **neuropsychiatric disorders**
- changes in neurexin expression in several **neurodegenerative disorders**

Publication

Emerging evidence implicating a role for neurexins in neurodegenerative and neuropsychiatric disorders

Katelyn Cuttler¹, Maryam Hassan³, Jonathan Carr^{2,4}, Ruben Cloete³ and Soraya Bardien^{1,4}

Figure 8.1 Schematic diagram summarizing the different parts of the doctoral study and the main findings.

A) Shows the process leading up to the selection of the novel variant. B) Shows the functional studies conducted to study the effect of the variant.

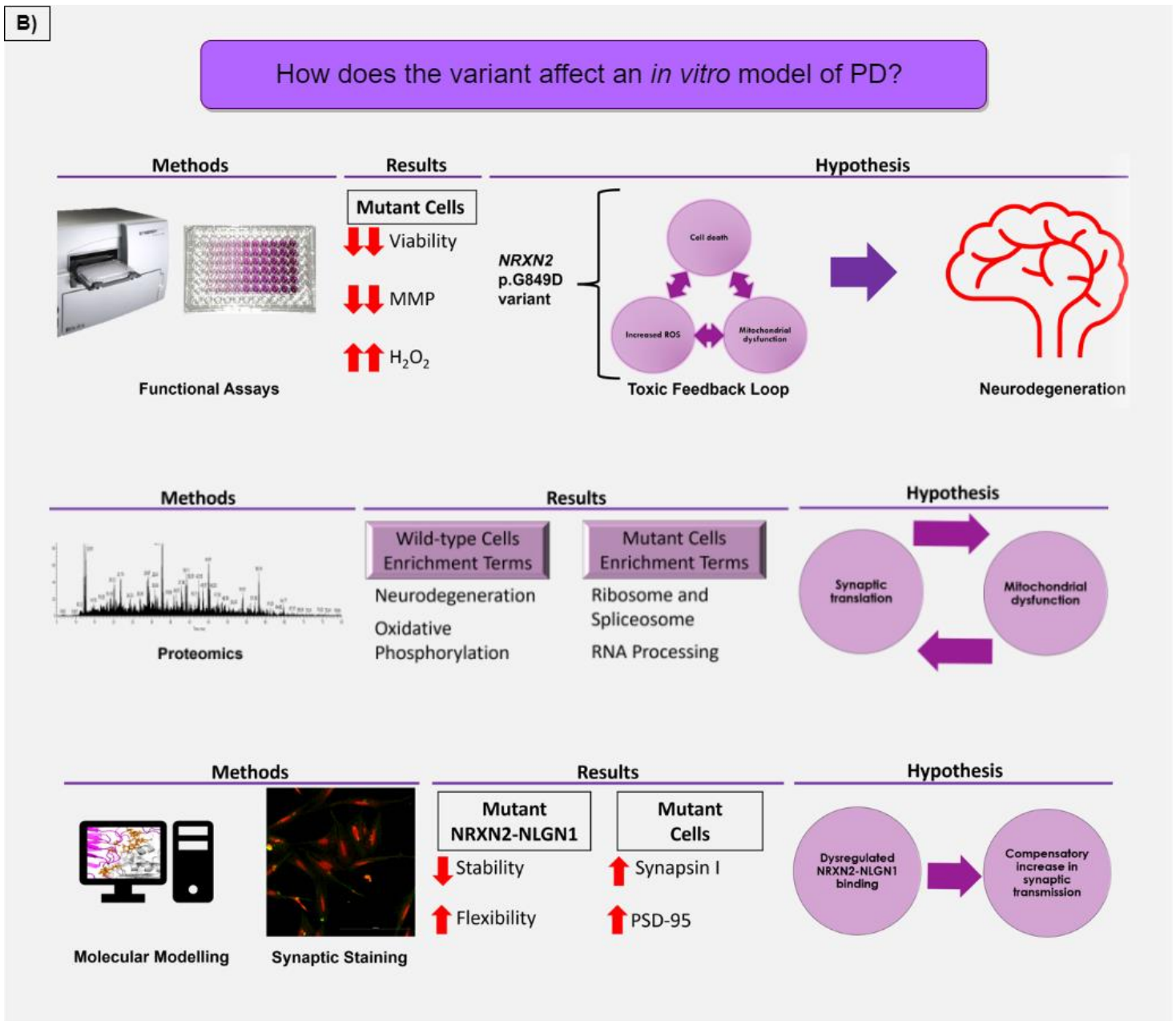


Figure 8.1 Schematic diagram summarizing the different parts of the doctoral study and the main findings *continued*

Abbreviations: *CCNF*: cyclin F; *CFA65*: cilia and flagella associated protein 65; H₂O₂: hydrogen peroxide; MMP: mitochondrial membrane potential; *NRXN2*: neurexin 2 (gene); *NRXN2α*: neurexin 2 alpha (protein); PD: Parkinson’s disease; PSD-95: post-synaptic density protein 95; *RTF1*: requiring fifty-three 1; SH-SY5Y: neuroblastoma cells; *TEP1*: telomerase associated protein; WES: whole exome sequencing (Image created using Microsoft PowerPoint)

8.1 Identification of a Novel Variant in Neurexin 2

Worldwide, the genetic aetiology of PD is still largely unknown, therefore it is necessary to find novel PD-causing genes to help us better understand the pathobiology of the disorder. SSA populations have the potential to facilitate the discovery of novel genes as they have a unique genetic architecture which is distinct from that of other populations outside Africa (Gomez et al., 2014; Lekoubou et al., 2014). It is speculated that due to the rich genetic heterogeneity present in the region, there are unique genotypes, environmental factors, and cultural influences which may affect the disease phenotypes displayed in the region (Gomez et al., 2014; Lekoubou et al., 2014). Therefore, it can be postulated that novel genes discovered in these populations may provide insight to the pathobiology and molecular mechanisms underlying PD.

The family examined in this study, designated as ZA253, has multiple affected individuals as well as unaffected relatives. Therefore, they are a good candidate family to perform co-segregation studies using WES data. Furthermore, this family is of Afrikaner European ancestry, which is a unique genetic group endemic to SA. Their ancestry can be traced back to people of predominantly Dutch ancestry, however, French and German ancestry is also present (Greeff, 2007). In addition, due to the history of population mixing in SA, described as a “melting pot”, the Afrikaner European heritage also includes a component of the indigenous population (Greeff, 2007). Thus, this family is ideal for the potential discovery of novel genes. Consequently, this study’s first objectives were to identify the causal genetic factor of PD in family ZA253.

As per the peer-reviewed original article shown in **Chapter 3** (Sebate, Cuttler et al., 2021), we prioritised the p.G849D variant in *NRXN2* as the potential causal variant of PD in this family. To obtain further evidence that this gene is a good candidate for further studies, we also conducted MD simulations to determine the effect of this variant on the structure of the transcribed protein, *NRXN2 α* and performed a literature review to determine if there was any evidence for the involvement of the larger protein family, the neurexins, in neuronal disorders. To this end, we found that the variant has a destabilizing effect on the protein and results in an extended conformation of the laminin-neurexin-sex hormone binding domain 6 (LNS6), which is responsible for protein binding. In addition, the peer-reviewed review article shown in **Chapter 4** (Cuttler et al., 2021) found that neurexins have been implicated in both neuropsychiatric disorders,

such as autism spectrum disorders and schizophrenia, as well as neurodegenerative disorders, such as AD and PD. In addition, we used the American College of Medical Genetics (ACMG) Guidelines (Richards et al., 2015) to classify the variant as likely pathogenic. The classification table can be found in **Appendix III**.

Therefore, we concluded that *NRXN2* is a good candidate gene for further examination using functional studies.

8.2 Toxic Feedback Loop Hypothesis

The next objectives of the study relate to using wild-type and p.G849D mutant *NRXN2* α plasmids and transfecting them into SH-SY5Y neuroblastoma cells as a cellular model to study the effect of the variant on different aspects of cellular health. The results are presented in an article currently under review with Journal of Neural Transmission (**Chapter 5**).

We found that overexpression of the mutant protein decreased cellular viability and MMP, and increased H_2O_2 levels, which is indicative of an increase in ROS. We thus hypothesized that it may be involved in a toxic feedback loop which could result in neurodegeneration (**Figure 8.1**). In this loop, neuronal cell death could lead to mitochondrial dysfunction which increases ROS generation and thus would result in more neuronal cell death, thereby continuing the loop. This toxic feedback loop is a well-known phenomenon. Indeed, regulation of cell death has emerged as the second major function of mitochondria since they provide the main intracellular source of ROS (Ott et al., 2007). Excessive ROS production is implicated in mtDNA mutations, ageing, and cell death (Ott et al., 2007). Several disorders have thus been linked to the dysfunction of these systems, including AD and various cancers (Hu et al., 2017; Wang et al., 2017).

While the experiments performed do not provide clear evidence of which event may set off the loop, there is recent research which suggests that synaptic dysfunction can cause mitochondrial dysfunction (Kuzniewska et al., 2020; Plum et al., 2020). Kuzniewska et al., (2020) found that dysregulated synaptic translation can lead to altered mitochondrial physiology, while Plum et al., (2020) showed that synaptosomes present in PD have altered mitochondrial translation. Therefore, we propose that an aberrant synaptic protein, such as mutant *NRXN2* α , could first cause

mitochondrial damage which would then initiate this feedback loop. Over time, the excess neuronal cell death caused by this toxic loop could lead to the degeneration observed in PD and other neurodegenerative disorders. This work therefore serves to provide more evidence to connect synaptic dysfunction and mitochondrial dysfunction in the aetiology of PD.

8.3 Dysregulation of Pathways

To further understand the effect of the variant, the next objective was to investigate the dysregulated biological pathways caused by the variant using proteomics analysis. To this end we examined the effect of overexpression of both the wild-type and mutant protein using a hypothesis-free approach and the results are presented as an article currently under review with *Frontiers in Aging Neuroscience* (**Chapter 6**).

In complex diseases, various causal genes and genetic factors can often lead to similar phenotypes (Kim et al., 2011). On a molecular level, these perturbations often operate on similar cellular pathways (Sieberts and Schadt, 2007; Schadt, 2009), as is seen in PD whereby there are only a handful of known pathways implicated in development of the disorder (**Figure 1.2**). Therefore, a better understanding of dysregulated pathways is fundamental to understand the mechanisms underlying these disorders.

In our analysis, overexpression of the wild-type protein led to the enrichment of proteins involved in neurodegenerative diseases (**Figure 8.1**). These proteins were shown to have functions related to mitochondria and lysosomes, which are known to be dysregulated in PD (Rego and Oliveira, 2003; Wang et al., 2018). This shows that wild-type NRXN2 α could be involved in neurodegeneration, and possibly provides further evidence implicating synaptic proteins in the pathobiology of PD. Interestingly, overexpression of the mutant protein led to the decline of proteins involved in ribosomal functions (**Figure 8.1**), both in the cytoplasm and in mitochondria. Since the main function of the ribosome is translation of mRNA into protein, dysregulated translation could be implicated as a biological process involved in neurodegeneration, and hints at a possible mode of action for the p.G849D variant. We therefore hypothesized that dysregulated synaptic function and dysregulated mitochondrial functioning are linked, with one possibly leading

to the other. Indeed, it has been shown that if synaptic translation is dysregulated, mitochondrial physiology can be altered (Kuzniewska et al., 2020). Therefore, we hypothesize that the mutant NRXN2 α could cause disruption of translation at the synapses and that this may affect mitochondrial physiology. The altered mitochondria could result in their dysfunction which is known to be linked to neurodegenerative disorders. Therefore, this work shows that biological processes related to the ribosome, translation and tRNA, specifically at the synapse, could be an important mechanism in PD pathobiology.

8.4 Interaction with Neuroligin

The final study objectives involved investigating the effect of the variant on the primary function of the protein. These results are presented in **Chapter 7** as a “submission-ready” manuscript prepared for the European Journal of Neuroscience. In this case, NRXN2 α is a synaptic regulation protein, so we wanted to examine the effect of the variant on its synaptic functioning. To this end, we first utilized *in silico* MD simulations to examine the effect of the variant on NRXN2 α binding to NLGN1, since these proteins function together at the synaptic cleft to mediate synaptic functions (Craig and Kang, 2007).

These simulations showed an overall destabilizing effect of the mutant on the NRXN2 α -NLGN1 protein system (**Figure 8.1**). We also observed a change in hydrogen bonds between the LNS6 domain of NRXN2 α (the domain responsible for protein binding) and NLGN1. In addition, the loop regions of the LNS6 domain were more flexible in the mutant when compared to the wild-type protein system (**Figure 8.1**). Together neurexins and neuroligins form synaptic complexes in the synaptic cleft and function in synaptic organization, neuronal cell adhesion, transmembrane signalling and calcium channel regulation (Craig and Kang, 2007). At the synapse, neurexins and neuroligins form a trans-synaptic bridge whereby neurexins signal dendrites to aggregate neuroligins (Graf et al., 2004). This results in the clustering of post-synaptic scaffold proteins, signal transducing enzymes, and glutamate receptors leading to synaptic transmission and vesicular transport (Graf et al., 2004). Therefore, the observed destabilizing effect of the variant on NRXN2 α -NLGN1 binding may negatively affect synaptic transmission efficacy, pre-synaptic

vesicular transport, and synaptic plasticity. Furthermore, PD progression is affected by the release of dopamine into the synaptic cleft which relies on functional pre-synaptic vesicular transport, synaptic vesicle trafficking, and the maintained regulation of pre-synaptic plasticity (Li et al., 2010; Esposito et al., 2012). Therefore, it is plausible that if the neurexin-neuroligin pathway is dysregulated in PD, the resultant synaptic dysregulation could also affect dopamine release into the synaptic cleft.

8.5 Dysregulation of Synaptic Function

In order to further examine the effect of the variant on synaptic functioning, we used an *in vitro* model to stain for markers of synapse formation, namely the pre-synaptic marker synapsin I and the post-synaptic marker PSD-95. Again, these results are presented in **Chapter 7** as a “submission-ready” manuscript.

Interestingly, overexpression of mutant NRXN2 α *in vitro* showed an increase in both synaptic markers (**Figure 8.1**). This is indicative of an increase in synaptic differentiation and transmission (Graf et al., 2004). Neurexins are known to induce pre-synaptic differentiation and the differentiation of glutamate post-synaptic specializations *in vitro* through their interactions with neuroligins, which results in increased synaptic transmission (Graf et al., 2004). This result was unexpected as the MD simulations showed that the mutation may disrupt the neurexin-neuroligin system, and thus we expected a decrease in synaptic transmission. While persistently increased synaptic transmission is also problematic since it depletes readily releasable vesicles (Sørensen, 2009), we propose that this increased transmission is a compensatory mechanism. Indeed, there are multiple synaptic cell adhesion molecules present which have functions that overlap those of neurexins (Missler et al., 2012). Therefore, it is possible that one or more of these molecules may be able to take over this function for a time and increase the synaptic output. However, since PD and other neurodegenerative disorders are age-related, we propose that, over time, the reliance on these other systems may strain the system, and result in overall disruption of synaptic maintenance. Therefore, these results indicate that the variant may impact NRXN2 α 's function as a synaptic cell adhesion protein.

8.6 Overall Hypothesis

As previously mentioned, NRXN2 α is a synaptic maintenance protein with functions in neuronal cell-cell adhesion, neurotransmitter secretion regulation, and synaptic regulation, amongst others. This dissertation has shown that NRXN2 α , and its larger protein family, the neurexins, are good candidates for further studies. Overall, we postulate that the disruption of NRXN2 α and synaptic dysregulation could potentially lead to neurodegeneration. The results from our functional studies implicate a toxic feedback loop in PD involving mitochondria, ROS, and cell death. While the results from the proteomics analysis show that dysregulated synaptic translation could be the cause of mitochondrial dysfunction. Furthermore, the variant was shown to have an effect on the synaptic function of NRXN2 α . Therefore, this dissertation provides evidence that mutant NRXN2 α could result in neurodegeneration and links synaptic dysfunction and mitochondrial dysfunction as two aetiologies of PD (**Figure 8.2**).

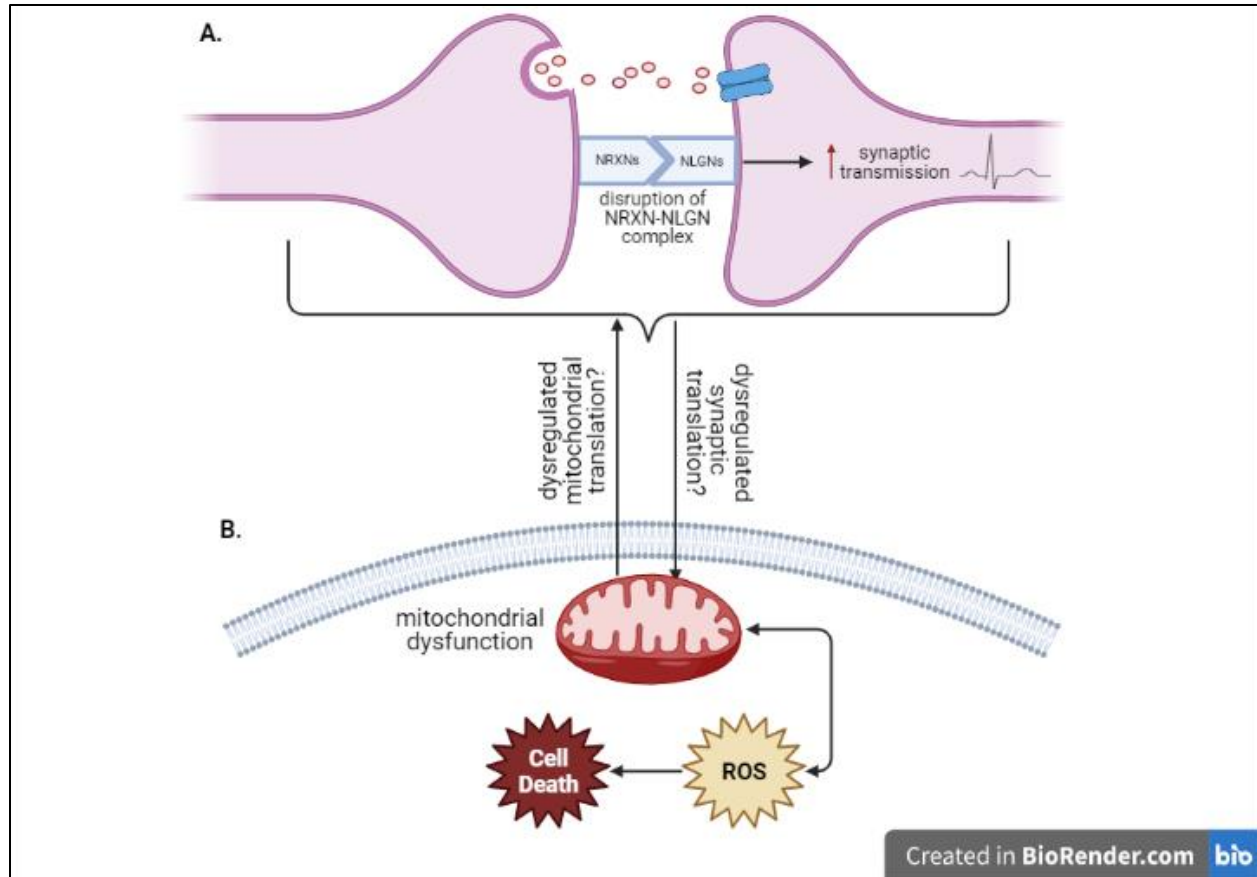


Figure 8.2: Proposed schema of how the p.G849D variant in *NRXN2* can lead to Parkinson's disease. A) At the synaptic cleft, the variant could result in a disruption of the neurexin-neuroligin complex which results in a compensatory increase in synaptic transmission. Over time, the reliance on these other systems may strain the system, and result in overall disruption of synaptic maintenance. B) In the cytoplasm, it has been shown that disrupted mitochondrial translation can negatively affect synaptic function (Plum et al., 2020), while we propose that dysregulated synaptic translation caused by the variant can result in mitochondrial dysfunction. Overall, the resultant dysfunctional mitochondria can lead to an increase in ROS which causes neuronal cell death and can ultimately lead to neurodegeneration. Abbreviations: NLGN: neuroligin, NRXN: neurexin, ROS: reactive oxygen species. (Image created in BioRender.com)

8.7 Study Limitations

For the first part of this study, the main limitation is the inability of WES to accurately detect copy number (Fromer et al., 2012; Krumm et al., 2012) and non-coding variants (Botstein and Risch, 2003). However, WES is well-suited for identifying SNPs in coding regions, as 80-85% of pathogenic mutations in genetic disorders to date are exonic (Ku et al., 2017). Indeed, several PD-associated genes have been identified through familial co-segregation studies as well as WES (Lill, 2016; Puschmann, 2017; Pillay et al., 2022).

When using *in silico* tools for analyses, such as using tools for pathogenicity predictions, each tool has their own algorithm which can provide inaccurate results. To this end, whenever we used *in silico* tools, we tried to account for this by comparing results between at least two different tools.

For the functional studies, the major limitations are the use of an overexpression model in a commercialized cell line. In the family, the p.G849D variant in NRXN2 α is heterozygous, therefore NRXN2 α cDNA in a plasmid is only a model in an attempt to understand the possible functional impact of the variant. Also, since this study was explorative, we utilized SH-SY5Y neuroblastoma cells. While SH-SY5Y cells are a relatively good *in vitro* model of PD, since they are dopaminergic and catecholaminergic (Xicoy et al., 2017), the findings would need to be validated using other models of PD, such as a mouse model or induced pluripotent stem cells (iPSCs).

For the MD simulations, a limitation is that we were unable to model the LNS1 domain of NRXN2 α , as there was insufficient sequence coverage between the target sequence and the homologous template (PDBID: 3R05). Since there is no experimental model for the structure of human NRXN2 α , there was no way to overcome this limitation. However, new technologies, such as AlphaFold (Jumper et al., 2021; Varadi et al., 2022), may now enable better modelling of protein structures.

8.8 Future Work

This study is one of the first, to our knowledge, to potentially implicate NRXN2 α and synaptic dysfunction in PD. As such, this study has been largely explorative, whereby we attempted to elucidate potential mechanisms by which the p.G849D variant could lead to PD. Interestingly, the results link both mitochondrial dysfunction and dysregulated synaptic translation and transmission to this disorder.

However, these experiments were performed using SH-SY5Y cells as an *in vitro* model of PD. Therefore, in future, these results would need to be confirmed and validated in better models of PD and/or neurodegeneration. To this end, mice models could be used to model PD pathobiology in the brain. One could use a mouse model to overexpress NRXN2 α with a brain specific promoter enabling NRXN2 α levels to be overexpressed only in the brain. This would allow for the measurement of brain specific NRXN2 α transcripts and their effect on neurodegeneration. Knockdown of NRXN2 α in a mouse model is also an option and would allow definitive validation that the protein can lead to neurodegeneration. Alternatively, a transgenic mouse model could be developed whereby the p.G849D variant was expressed in a heterozygous manner, as was seen in the original family (Sebate et al., 2021). This would provide a more accurate representation of their exact disease state.

Another option would be to use iPSCs developed from fibroblasts taken from family members. These iPSCs could be differentiated into dopaminergic neurons and would therefore be characteristic of the disease state of the individuals and their genetic backgrounds. Indeed, researchers have recently developed a method to differentiate iPSCs in A9 dopaminergic neurons, with A9 neurons being the ones found to be most affected in PD (Li et al., 2022). This would enable better measurements of the effect of the variant. The iPSCs can also be differentiated into multiple other cell lines, enabling a multitude of options for further research. Taken further, iPSCs can be used to construct brain organoids which will mimic the neuronal environment whereby the disease is present. This would allow experiments which are normally performed *in vivo* to be performed on material obtained from the PD patients.

It is noted that while these types of experiments will be better able to determine the role of the *NRXN2α* variant, they would not suffice to solve the pathobiology of PD. Ultimately, what is needed is a systems biology approach whereby genetics, transcriptomics and proteomics data would be integrated to fully understand the functional consequence of this and other variants. If indeed, mitochondrial dysfunction and synaptic dysfunction are linked in neurodegeneration, systems biology approaches may be able to elucidate the mechanisms behind this dysfunction. These approaches can be used to help decipher underlying mechanisms in a tissue- or even cell-specific manner in material derived from individuals with PD. This could provide targets for further research and/or therapeutic intervention.

8.9 Conclusion

PD is a complex neurodegenerative disorder whose genetic basis is poorly understood in Sub-Saharan Africa (SSA). Given that population-specific genetic variation can greatly impact disease risk, as well as drug metabolism and efficacy (Siddiqi and Koemeter-Cox, 2021), it is important to investigate the potential genetic causes in SSA populations. In this study, a novel variant, p.G849D in *NRXN2*, was identified in a South African Afrikaner European family. However, it is not sufficient to only identify candidate genes, it is also important to perform functional studies to validate them, as they could aid in improving our understanding of the pathways involved in PD. Indeed, this exploratory study has shown that synaptic dysfunction and mitochondrial dysfunction could be linked and that this may result in neurodegeneration, thereby providing an interesting area for future research.

Therefore, in conclusion, this study has shown that it is important to look at the genetics of PD underrepresented populations and to validate potential causative variants with functional studies. Indeed, examination of the single variant identified in family ZA253 has potentially linked two PD pathologies, synaptic dysfunction and mitochondrial dysfunction, to the onset of neurodegeneration. Therefore, these types of studies can provide insight to the mechanisms underlying PD. Ultimately this knowledge can help us to painstakingly piece together the complex puzzle that is PD.

References

- Antony, P. M. A., Diederich, N. J., Krüger, R., and Balling, R. (2013). The hallmarks of Parkinson's disease. *FEBS J.* 280, 5981–5993. doi: 10.1111/febs.12335.
- Armstrong, M. J., and Okun, M. S. (2020). Diagnosis and Treatment of Parkinson Disease: A Review. *JAMA - J. Am. Med. Assoc.* 323, 548–560. doi: 10.1001/jama.2019.22360.
- Bardien, S., Keyser, R., Yako, Y., Lombard, D., and Carr, J. (2009). Molecular analysis of the parkin gene in South African patients diagnosed with Parkinson's disease. *Park. Relat. Disord.* 15, 116–121. doi: 10.1016/j.parkreldis.2008.04.005.
- Bardien, S., Marsberg, A., Keyser, R., Lombard, D., Lesage, S., Brice, A., et al. (2010). LRRK2 G2019S mutation: Frequency and haplotype data in South African Parkinson's disease patients. *J. Neural Transm.* 117, 847–853. doi: 10.1007/s00702-010-0423-6.
- Belin, A. C., and Westerlund, M. (2008). Parkinson's disease: A genetic perspective. *FEBS J.* 275, 1377–1383. doi: 10.1111/j.1742-4658.2008.06301.x.
- Bernal-Pacheco, O., Limotai, N., Go, C. L., and Fernandez, H. H. (2012). Nonmotor manifestations in parkinson disease. *Neurologist* 18, 1–16. doi: 10.1097/NRL.0b013e31823d7abb.
- Blanckenberg, J., Bardien, S., Glanzmann, B., Okubadejo, N. U., and Carr, J. A. (2013). The prevalence and genetics of Parkinson's disease in sub-Saharan Africans. *J. Neurol. Sci.* 335, 22–25. doi: 10.1016/j.jns.2013.09.010.
- Blanckenberg, J., Ntsapi, C., Carr, J. A., and Bardien, S. (2014). EIF4G1 R1205H and VPS35 D620N mutations are rare in Parkinson's disease from South Africa. *Neurobiol. Aging* 35, 445.e1-445.e3. doi: 10.1016/j.neurobiolaging.2013.08.023.
- Blauwendraat, C., Heilbron, K., Vallerga, C. L., Bandres-Ciga, S., von Coelln, R., Pihlstrøm, L., et al. (2019). Parkinson's disease age at onset genome-wide association study: Defining heritability, genetic loci, and α -synuclein mechanisms. *Mov. Disord.* 34, 866–875. doi: 10.1002/mds.27659.

- Bonifati, V., Rizzu, P., Van Baren, M. J., Schaap, O., Breedveld, G. J., Krieger, E., et al. (2003). Mutations in the DJ-1 gene associated with autosomal recessive early-onset parkinsonism. *Science* (80-.). 299, 256–259. doi: 10.1126/science.1077209.
- Botstein, D., and Risch, N. (2003). Discovering genotypes underlying human phenotypes: Past successes for mendelian disease, future approaches for complex disease. *Nat. Genet.* 33, 228–237. doi: <https://doi.org/10.1038/ng1090>.
- Bower, J. H. (2017). Understanding Parkinson disease in sub Saharan Africa: A call to action for the international neurologic community. *Park. Relat. Disord.* 41, 1–2. doi: 10.1016/j.parkreldis.2017.05.008.
- Brito-Moreira, J., Lourenco, M. V, Oliveira, M. M., Ribeiro, F. C., Ledo, J. H., Diniz, L. P., et al. (2017). Interaction of amyloid- β (A β) oligomers with neurexin 2 α and neuroligin 1 mediates synapse damage and memory loss in mice. *J. Biol. Chem.* 292, 7327–7337. doi: <https://doi.org/10.1074/jbc.M116.761189>.
- Chartier-Harlin, M. C., Dachsel, J. C., Vilarino-Güell, C., Lincoln, S. J., Leprêtre, F., Hulihan, M. M., et al. (2011). Translation initiator EIF4G1 mutations in familial parkinson disease. *Am. J. Hum. Genet.* 89, 398–406. doi: 10.1016/j.ajhg.2011.08.009.
- Chen, L. Y., Jiang, M., Zhang, B., Gokce, O., and Südhof, T. C. (2017). Conditional Deletion of All Neurexins Defines Diversity of Essential Synaptic Organizer Functions for Neurexins. *Neuron* 94, 611-625.e4. doi: 10.1016/j.neuron.2017.04.011.
- Cilia, R., Sironi, F., Akpalu, A., Cham, M., Sarfo, F. S., Brambilla, T., et al. (2012). Screening LRRK2 gene mutations in patients with Parkinson's disease in Ghana. *J. Neurol.* 259, 569–570. doi: 10.1007/s00415-011-6210-y.
- Connolly, B. S., and Lang, A. E. (2014). Pharmacological treatment of Parkinson disease: A review. *JAMA - J. Am. Med. Assoc.* 311, 1670–1683. doi: 10.1001/jama.2014.3654.
- Craig, A. M., and Kang, Y. (2007). Neurexin-neuroligin signaling in synapse development. *Curr. Opin. Neurobiol.* 17, 43–52. doi: 10.1016/j.conb.2007.01.011.
- Cuttler, K., Hassan, M., Carr, J., Cloete, R., and Bardien, S. (2021). Emerging evidence implicating a role for neurexins in neurodegenerative and neuropsychiatric disorders. *Open*

Biol. 11. doi: 10.1098/RSOB.210091.

- Dachtler, J., Glasper, J., Cohen, R. N., Ivorra, J. L., Swiffen, D. J., Jackson, A. J., et al. (2014). Deletion of α -neurexin II results in autism-related behaviors in mice. *Transl. Psychiatry* 4. doi: 10.1038/tp.2014.123.
- Dachtler, J., Ivorra, J. L., Rowland, T. E., Lever, C., John Rodgers, R., and Clapcote, S. J. (2015). Heterozygous deletion of α -neurexin I or α -neurexin II results in behaviors relevant to autism and schizophrenia. *Behav. Neurosci.* 129, 765–776. doi: 10.1037/bne0000108.
- Dauer, W., and Przedborski, S. (2003). Parkinson's disease: mechanisms and models. *Neuron* 39, 889–909. doi: 10.1016/S0896-6273(03)00568-3.
- de Wit, J., Sylwestrak, E., O'Sullivan, M. L., Otto, S., Tiglio, K., Savas, J. N., et al. (2009). LRRTM2 Interacts with Neurexin1 and Regulates Excitatory Synapse Formation. *Neuron* 64, 799–806. doi: 10.1016/j.neuron.2009.12.019.
- Dekker, M. C. J., Coulibaly, T., Bardien, S., Ross, O. A., Carr, J., and Komolafe, M. (2020). Parkinson's Disease Research on the African Continent: Obstacles and Opportunities. *Front. Neurol.* 11, 512. doi: 10.3389/fneur.2020.00512.
- DeLano, W. (2002). Pymol: An open-source molecular graphics tool. *CCP4 Newsl. Protein Crystallogr.* 40, 82–92.
- Deng, H. X. H., Shi, Y., Yang, Y., Ahmeti, K. B., Miller, N., Huang, C., et al. (2016). Identification of TMEM230 mutations in familial Parkinson's disease. *Nat. Genet.* 48, 733–739. doi: <https://doi.org/10.1038/ng.3589>.
- Di Monte, D. A., Lavasani, M., and Manning-Bog, A. B. (2002). Environmental Factors in Parkinson's Disease. *Neurotoxicology* 23, 487–502. doi: 10.1016/S0161-813X(02)00099-2.
- Docampo, E., Ribasés, M., Gratacòs, M., Bruguera, E., Cabezas, C., Sánchez-Mora, C., et al. (2012). Association of Neurexin 3 polymorphisms with smoking behavior. *Genes, Brain Behav.* 11, 704–711. doi: 10.1111/j.1601-183X.2012.00815.x.
- Dorsey, E. R., Elbaz, A., Nichols, E., Abd-Allah, F., Abdelalim, A., Adsuar, J. C., et al. (2018). Global, regional, and national burden of Parkinson's disease, 1990–2016: a systematic

- analysis for the Global Burden of Disease Study 2016. *Lancet Neurol.* 17, 939–953. doi: 10.1016/S1474-4422(18)30295-3.
- Esposito, G., Ana Clara, F., and Verstreken, P. (2012). Synaptic vesicle trafficking and Parkinson's disease. *Dev. Neurobiol.* 72, 134–144. doi: 10.1002/dneu.20916.
- Feigin, V. L., Krishnamurthi, R. V., Theadom, A. M., Abajobir, A. A., Mishra, S. R., Ahmed, M. B., et al. (2017). Global, regional, and national burden of neurological disorders during 1990–2015: a systematic analysis for the Global Burden of Disease Study 2015. *Lancet Neurol.* 16, 877–897. doi: 10.1016/S1474-4422(17)30299-5.
- Finberg, J. P. M. (2019). Inhibitors of MAO-B and COMT: their effects on brain dopamine levels and uses in Parkinson's disease. *J. Neural Transm.* 126, 433–448. doi: 10.1007/s00702-018-1952-7.
- Fonzo, A. D., Dekker, M. C. J., Montagna, P., Baruzzi, A., Yonova, E. H., Guedes, L. C., et al. (2009). FBXO7 mutations cause autosomal recessive, early-onset parkinsonian- pyramidal syndrome. *Neurology* 72, 240–245. doi: 10.1212/01.wnl.0000338144.10967.2b.
- Fromer, M., Moran, J. L., Chambert, K., Banks, E., Bergen, S. E., Ruderfer, D. M., et al. (2012). Discovery and statistical genotyping of copy-number variation from whole-exome sequencing depth. *Am. J. Hum. Genet.* 91, 597–607. doi: <https://doi.org/10.1016/j.ajhg.2012.08.005>.
- Funayama, M., Ohe, K., Amo, T., Furuya, N., Yamaguchi, J., Saiki, S., et al. (2015). CHCHD2 mutations in autosomal dominant late-onset Parkinson's disease: A genome-wide linkage and sequencing study. *Lancet Neurol.* 14, 274–282. doi: [https://doi.org/10.1016/S1474-4422\(14\)70266-2](https://doi.org/10.1016/S1474-4422(14)70266-2).
- Galvan, A., and Wichmann, T. (2008). Pathophysiology of Parkinsonism. *Clin. Neurophysiol.* 119, 1459–1474. doi: 10.1016/j.clinph.2008.03.017.
- Gökçal, E., Gür, V. E., Selvitop, R., Babacan Yildiz, G., and Asil, T. (2017). Motor and non-motor symptoms in parkinson's disease: Effects on quality of life. *Noropsikiyatri Ars.* 54, 143–148. doi: 10.5152/npa.2016.12758.
- Gomez, F., Hirbo, J., and Tishkoff, S. A. (2014). Genetic variation and adaptation in Africa:

- Implications for human evolution and disease. *Cold Spring Harb. Perspect. Biol.* 6. doi: 10.1101/cshperspect.a008524.
- Graf, E. R., Zhang, X., Jin, S. X., Linhoff, M. W., and Craig, A. M. (2004). Neurexins induce differentiation of GABA and glutamate postsynaptic specializations via neuroligins. *Cell* 119, 1013–1026. doi: 10.1016/j.cell.2004.11.035.
- Greeff, J. M. (2007). Deconstructing Jaco: Genetic heritage of an Afrikaner. *Ann. Hum. Genet.* 71, 674–688. doi: <https://doi.org/10.1111/j.1469-1809.2007.00363.x>.
- Grosch, J., Winkler, J., and Kohl, Z. (2016). Early degeneration of both dopaminergic and serotonergic axons – a common mechanism in parkinson’s disease. *Front. Cell. Neurosci.* 10, 293. doi: 10.3389/fncel.2016.00293.
- Hu, H., Tan, C. C., Tan, L., and Yu, J. T. (2017). A Mitocentric View of Alzheimer’s Disease. *Mol. Neurobiol.* 54, 6046–6060. doi: 10.1007/s12035-016-0117-7.
- Jankovic, J. (2008). Parkinson’s disease: clinical features and diagnosis. *J. Neurol. Neurosurg. Psychiatry* 79, 368–375. doi: 10.1136/jnnp.2007.131045.
- Jansen van Rensburg, Z., Abrahams, S., Chetty, D., Step, K., Acker, D., Lombard, C. J., et al. (2022). The South African Parkinson’s Disease Study Collection. *Mov. Disord.* 37, 230–232. doi: 10.1002/mds.28828.
- Jumper, J., Evans, R., Pritzel, A., Green, T., Figurnov, M., Ronneberger, O., et al. (2021). Highly accurate protein structure prediction with AlphaFold. *Nature* 596, 583–589. doi: 10.1038/s41586-021-03819-2.
- Kanehisa, M., Furumichi, M., Sato, Y., Ishiguro-Watanabe, M., and Tanabe, M. (2021). KEGG: Integrating viruses and cellular organisms. *Nucleic Acids Res.* 49, D545–D551. doi: 10.1093/nar/gkaa970.
- Keyser, R. J., Lesage, S., Brice, A., Carr, J., and Bardien, S. (2010). Assessing the prevalence of PINK1 genetic variants in South African patients diagnosed with early- and late-onset Parkinson’s disease. *Biochem. Biophys. Res. Commun.* 398, 125–129. doi: 10.1016/j.bbrc.2010.06.049.

- Keyser, R. J., van der Merwe, L., Venter, M., Kinnear, C., Warnich, L., Carr, J., et al. (2009). Identification of a novel functional deletion variant in the 5'-UTR of the DJ-1 gene. *BMC Med. Genet.* 10, 105. doi: 10.1186/1471-2350-10-105.
- Kim, Y. A., Wuchty, S., and Przytycka, T. M. (2011). Identifying causal genes and dysregulated pathways in complex diseases. *PLoS Comput. Biol.* 7, e1001095. doi: 10.1371/journal.pcbi.1001095.
- Kitada, T., Asakawa, S., Hattori, N., Matsumine, H., Yamamura, Y., Minoshima, S., et al. (1998). Mutations in the parkin gene cause autosomal recessive juvenile parkinsonism. *Nature* 392, 605–608. doi: 10.1038/33416.
- Klein, C., and Westenberger, A. (2012). Genetics of Parkinson's Disease. *Cold Spring Harb. Perspect. Med.* 2. doi: 10.1101/cshperspect.a008888.
- Ko, J., Fuccillo, M. V., Malenka, R. C., and Südhof, T. C. (2009). LRRTM2 Functions as a Neurexin Ligand in Promoting Excitatory Synapse Formation. *Neuron* 64, 791–798. doi: 10.1016/j.neuron.2009.12.012.
- Koks, S., Pfaff, A. L., Bubb, V. J., and Quinn, J. P. (2022). Longitudinal intronic RNA-Seq analysis of Parkinson's disease patients reveals disease-specific nascent transcription. *Exp. Biol. Med.*, 15353702221081028. doi: 10.1177/15353702221081027.
- Krebs, C. E., Karkheiran, S., Powell, J. C., Cao, M., Makarov, V., Darvish, H., et al. (2013). The sac1 domain of SYNJ1 identified mutated in a family with early-onset progressive parkinsonism with generalized seizures. *Hum. Mutat.* 34, 1200–1207. doi: 10.1002/humu.22372.
- Krumm, N., Sudmant, P. H., Ko, A., O'Roak, B. J., Malig, M., Coe, B. P., et al. (2012). Copy number variation detection and genotyping from exome sequence data. *Genome Res.* 22, 1525–1532. doi: <https://doi.org/10.1101/gr.138115.112>.
- Ku, C. S., Cooper, D. N., and Patrinos, G. P. (2017). The Rise and Rise of Exome Sequencing. *Public Health Genomics* 19, 315–324. doi: 10.1159/000450991.
- Kuzniewska, B., Cysewski, D., Wasilewski, M., Sakowska, P., Milek, J., Kulinski, T. M., et al. (2020). Mitochondrial protein biogenesis in the synapse is supported by local translation.

- EMBO Rep.* 21, e48882. doi: 10.15252/embr.201948882.
- Langston, J. W. (2006). The parkinson's complex: Parkinsonism is just the tip of the iceberg. *Ann. Neurol.* 59, 591–596. doi: 10.1002/ana.20834.
- Lekoubou, A., Echouffo-Tcheugui, J. B., and Kengne, A. P. (2014). Epidemiology of neurodegenerative diseases in sub-Saharan Africa: A systematic review. *BMC Public Health* 14, 1–32. doi: 10.1186/1471-2458-14-653.
- Lesage, S., and Brice, A. (2009). Parkinson's disease: From monogenic forms to genetic susceptibility factors. *Hum. Mol. Genet.* 18. doi: 10.1093/hmg/ddp012.
- Lesage, S., Drouet, V., Majounie, E., Deramecourt, V., Jacoupy, M., Nicolas, A., et al. (2016). Loss of VPS13C Function in Autosomal-Recessive Parkinsonism Causes Mitochondrial Dysfunction and Increases PINK1/Parkin-Dependent Mitophagy. *Am. J. Hum. Genet.* 98, 500–513. doi: <https://doi.org/10.1016/j.ajhg.2016.01.014>.
- Li, H., Jiang, H., Li, H., Li, L., Yan, Z., and Feng, J. (2022). Generation of human A9 dopaminergic pacemakers from induced pluripotent stem cells. *Mol. Psychiatry*, 1–12. doi: 10.1038/s41380-022-01628-1.
- Li, X., Wang, J., Yue, Z., Buxbaum, J. D., Elder, G. A., Avshalumov, M. V., et al. (2010). Enhanced striatal dopamine transmission and motor performance with LRRK2 overexpression in mice is eliminated by familial Parkinson's disease mutation G2019S. *J. Neurosci.* 30, 1788–1797. doi: 10.1523/JNEUROSCI.5604-09.2010.
- Liao, Y., Wang, J., Jaehnig, E. J., Shi, Z., and Zhang, B. (2019). WebGestalt 2019: gene set analysis toolkit with revamped UIs and APIs. *Nucleic Acids Res.* 47, W199–W205. doi: 10.1093/nar/gkz401.
- Lill, C. M. (2016). Genetics of Parkinson's disease. *Mol. Cell. Probes* 3, 386–396. doi: <https://doi.org/10.1016/j.mcp.2016.11.001>.
- Lim, S. Y., Fox, S. H., and Lang, A. E. (2009). Overview of the extranigral aspects of parkinson disease. *Arch. Neurol.* 66, 167–172. doi: 10.1001/archneurol.2008.561.
- Mazzoni, P., Shabbott, B., and Cortés, J. C. (2012). Motor control abnormalities in Parkinson's

- disease. *Cold Spring Harb. Perspect. Med.* 2, a009282. doi: 10.1101/cshperspect.a009282.
- Missler, M., and Südhof, T. C. (1998). Neurexins: Three genes and 1001 products. *Trends Genet.* 14, 20–26. doi: 10.1016/S0168-9525(97)01324-3.
- Missler, M., Südhof, T. C., and Biederer, T. (2012). Synaptic cell adhesion. *Cold Spring Harb. Perspect. Biol.* 4, a005694. doi: 10.1101/cshperspect.a005694.
- Missler, M., Zhang, W., Rohlmann, A., Kattenstroth, G., Hammer, R. E., Gottmann, K., et al. (2003). α -neurexins couple Ca²⁺ channels to synaptic vesicle exocytosis. *Nature* 423, 939–948. doi: 10.1038/nature01755.
- Mitchell, K. T., and Ostrem, J. L. (2020). Surgical Treatment of Parkinson Disease. *Neurol. Clin.* 38, 293–307. doi: 10.1016/j.ncl.2020.01.001.
- Møller, R. S., Weber, Y. G., Klitten, L. L., Trucks, H., Muhle, H., Kunz, W. S., et al. (2013). Exon-disrupting deletions of NRXN1 in idiopathic generalized epilepsy. *Epilepsia* 54, 256–264. doi: 10.1111/epi.12078.
- Mukherjee, K., Sharma, M., Urlaub, H., Bourenkov, G. P., Jahn, R., Südhof, T. C., et al. (2008). CASK Functions as a Mg²⁺-Independent Neurexin Kinase. *Cell* 133, 328–339. doi: 10.1016/j.cell.2008.02.036.
- Naito, Y., Tanabe, Y., Lee, A. K., Hamel, E., and Takahashi, H. (2017). Amyloid- β Oligomers Interact with Neurexin and Diminish Neurexin-mediated Excitatory Presynaptic Organization. *Sci. Rep.* 7. doi: <https://doi.org/10.1038/srep42548>.
- Okubadejo, N., Britton, A., Crews, C., Akinyemi, R., Hardy, J., Singleton, A., et al. (2008). Analysis of Nigerians with apparently sporadic Parkinson disease for mutations in LRRK2, PRKN and ATXN3. *PLoS One* 3. doi: 10.1371/journal.pone.0003421.
- Oliveros, J. C. (2015). Venny. An interactive tool for comparing lists with Venn’s diagrams.
- Ott, M., Gogvadze, V., Orrenius, S., and Zhivotovsky, B. (2007). Mitochondria, oxidative stress and cell death. *Apoptosis* 12, 913–922. doi: 10.1007/s10495-007-0756-2.
- Ovallath, S., and Deepa, P. (2013). The history of parkinsonism: Descriptions in ancient Indian medical literature. *Mov. Disord.* 28, 566–568. doi: 10.1002/mds.25420.

- Parkinson, J. (2002). An essay on the shaking palsy. 1817. *J. Neuropsychiatry Clin. Neurosci.* 14. doi: 10.1176/jnp.14.2.223.
- Perier, C., Bové, J., and Vila, M. (2011). Mitochondria and Programmed Cell Death in Parkinson's Disease: Apoptosis and Beyond. *Antioxid. Redox Signal.* 16, 883–895. doi: 10.1089/ars.2011.4074.
- Pillay, N. S., Ross, O. A., Christoffels, A., and Bardien, S. (2022). Current Status of Next-Generation Sequencing Approaches for Candidate Gene Discovery in Familial Parkinson's Disease. *Front. Genet.* 13, 106. doi: 10.3389/fgene.2022.781816.
- Plum, S., Eggers, B., Helling, S., Stepath, M., Theiss, C., Leite, R. E. P., et al. (2020). Proteomic Characterization of Synaptosomes from Human Substantia Nigra Indicates Altered Mitochondrial Translation in Parkinson's Disease. *Cells* 9, 2580. doi: 10.3390/cells9122580.
- Poewe, W. (2008). Non-motor symptoms in Parkinson's disease. *Eur. J. Neurol.* 15, 14–20. doi: 10.1111/j.1468-1331.2008.02056.x.
- Polymeropoulos, M. H., Lavedan, C., Leroy, E., Ide, S. E., Dehejia, A., Dutra, A., et al. (1997). Mutation in the alpha-synuclein gene identified in families with Parkinson's disease. *Science* 276, 2045–2047. doi: 10.1126/SCIENCE.276.5321.2045.
- Puschmann, A. (2017). New Genes Causing Hereditary Parkinson's Disease or Parkinsonism. *Curr. Neurol. Neurosci. Rep.* 17, 66. doi: <https://doi.org/10.1007/s11910-017-0780-8>.
- Quadri, M., Mandemakers, W., Grochowska, M. M., Masius, R., Geut, H., Fabrizio, E., et al. (2018). LRP10 genetic variants in familial Parkinson's disease and dementia with Lewy bodies: a genome-wide linkage and sequencing study. *Lancet Neurol.* 17, 597–608. doi: [https://doi.org/10.1016/S1474-4422\(18\)30179-0](https://doi.org/10.1016/S1474-4422(18)30179-0).
- Rego, A. C., and Oliveira, C. R. (2003). Mitochondrial dysfunction and reactive oxygen species in excitotoxicity and apoptosis: Implications for the pathogenesis of neurodegenerative diseases. *Neurochem. Res.* 28, 1563–1574. doi: 10.1023/A:1025682611389.
- Richards, S., Aziz, N., Bale, S., Bick, D., Das, S., Gastier-Foster, J., et al. (2015). Standards and guidelines for the interpretation of sequence variants: A joint consensus recommendation of

- the American College of Medical Genetics and Genomics and the Association for Molecular Pathology. *Genet. Med.* 17, 405–424. doi: 10.1038/gim.2015.30.
- Rudenko, G., Hohenester, E., and Muller, Y. A. (2001). LG/LNS domains: Multiple functions - One business end? *Trends Biochem. Sci.* 26, 363–368. doi: 10.1016/S0968-0004(01)01832-1.
- Rudenko, G., Nguyen, T., Chelliah, Y., Su, T. C., Deisenhofer, J., and Hughes, H. (1999). The Structure of the Ligand-Binding Domain of Neurexin I β : Regulation of LNS Domain Function. *Cell* 99, 93–101.
- Schaaf, C. P., Boone, P. M., Sampath, S., Williams, C., Bader, P. I., Mueller, J. M., et al. (2012). Phenotypic spectrum and genotype-phenotype correlations of NRXN1 exon deletions. *Eur. J. Hum. Genet.* 20, 1240–1247. doi: 10.1038/ejhg.2012.95.
- Schadt, E. E. (2009). Molecular networks as sensors and drivers of common human diseases. *Nature* 461, 218–223. doi: 10.1038/nature08454.
- Schreiner, D., Nguyen, T.-M., Russo, G., Heber, S., Patrignani, A., Ahrné, E., et al. (2014). Targeted Combinatorial Alternative Splicing Generates Brain Region-Specific Repertoires of Neurexins. *Neuron* 84, 386–698. doi: <https://doi.org/10.1016/j.neuron.2014.09.011>.
- Schreiner, D., Simicevic, J., Ahrné, E., Ahrné, A., Schmidt, A., and Scheiffele, P. (2015). Quantitative isoform-profiling of highly diversified recognition molecules. *Elife* 4. doi: 10.7554/eLife.07794.001.
- Schumacher-Schuh, A. F., Bieger, A., Okunoye, O., Mok, K., Lim, S.-Y., Bardien, S., et al. (2022). Underrepresented Populations in Parkinson’s Genetics Research: Current Landscape and Future Directions. *Mov. Disord.*, 2021.12.07.21266995. doi: 10.1002/MDS.29126.
- Sebate, B., Cuttler, K., Cloete, R., Britz, M., Christoffels, A., Williams, M., et al. (2021). Prioritization of candidate genes for a South African family with Parkinson’s disease using in-silico tools. *PLoS One* 16, e0249324. doi: 10.1371/journal.pone.0249324.
- Seppi, K., Ray Chaudhuri, K., Coelho, M., Fox, S. H., Katzenschlager, R., Perez Lloret, S., et al. (2019). Update on treatments for nonmotor symptoms of Parkinson’s disease—an evidence-

- based medicine review. *Mov. Disord.* 34, 180–198. doi: 10.1002/mds.27602.
- Siddiqi, B., and Koemeter-Cox, A. (2021). A Call to Action: Promoting Diversity, Equity, and Inclusion in Parkinson’s Research and Care. *J. Parkinsons. Dis.* 11, 905–908. doi: 10.3233/JPD-212593.
- Siddiqui, T. J., Pancaroglu, R., Kang, Y., Rooyakkers, A., and Craig, A. M. (2010). LRRTMs and Neuroligins Bind Neurexins with a Differential Code to Cooperate in Glutamate Synapse Development. *J. Neurosci.* 30, 7495–7506. doi: 10.1523/jneurosci.0470-10.2010.
- Sidransky, E., Nalls, M. A., Aasly, J. O., Aharon-Peretz, J., Annesi, G., Barbosa, E. R., et al. (2009). Multicenter Analysis of Glucocerebrosidase Mutations in Parkinson’s Disease. *N. Engl. J. Med.* 361, 1651–1661. doi: 10.1056/nejmoa0901281.
- Sieberts, S. K., and Schadt, E. E. (2007). Moving toward a system genetics view of disease. *Mamm. Genome* 18, 389–401. doi: 10.1007/s00335-007-9040-6.
- Sørensen, J. B. (2009). “Vesicle Pools,” in *Encyclopedia of Neuroscience*, ed. L. R. Squire (Oxford: Elsevier Ltd), 99–105. doi: 10.1016/B978-008045046-9.01384-X.
- Suchowersky, O. (2002). Parkinson’s disease: medical treatment of moderate to advanced disease. *Curr. Neurol. Neurosci. Rep.* 2, 310–316. doi: 10.1007/s11910-002-0006-5.
- Sulzer, D., and Surmeier, D. J. (2013). Neuronal vulnerability, pathogenesis, and Parkinson’s disease. *Mov. Disord.* 28, 41–50. doi: 10.1002/mds.25095.
- Szklarczyk, D., Gable, A. L., Lyon, D., Junge, A., Wyder, S., Huerta-Cepas, J., et al. (2019). STRING v11: Protein-protein association networks with increased coverage, supporting functional discovery in genome-wide experimental datasets. *Nucleic Acids Res.* 47, D607–D613. doi: 10.1093/nar/gky1131.
- Tabuchi, K., and Südhof, T. C. (2002). Structure and evolution of neurexin genes: Insight into the mechanism of alternative splicing. *Genomics* 79, 849–859. doi: 10.1006/geno.2002.6780.
- The UniProt Consortium (2021). UniProt: The universal protein knowledgebase in 2021. *Nucleic Acids Res.* 49, D480–D489. doi: 10.1093/nar/gkaa1100.

- Uemura, T., Lee, S. J., Yasumura, M., Takeuchi, T., Yoshida, T., Ra, M., et al. (2010). Trans-synaptic interaction of GluR δ 2 and neurexin through Cbln1 mediates synapse formation in the cerebellum. *Cell* 141, 1068–1079. doi: 10.1016/j.cell.2010.04.035.
- Ullrich, B., Ushkaryov, Y. A., and Südhof, T. C. (1995). Cartography of neurexins: More than 1000 isoforms generated by alternative splicing and expressed in distinct subsets of neurons. *Neuron* 14, 497–507. doi: 10.1016/0896-6273(95)90306-2.
- Ushkaryov, Y. A., Petrenko, A. G., Geppert, M., and Südhof, T. C. (1992). Neurexins: Synaptic cell surface proteins related to the α -latrotoxin receptor and laminin. *Science* (80-.). 257, 50–56. doi: 10.1126/science.1621094.
- Vaags, A. K., Lionel, A. C., Sato, D., Goodenberger, M., Stein, Q. P., Curran, S., et al. (2012). Rare deletions at the neurexin 3 locus in autism spectrum disorder. *Am. J. Hum. Genet.* 90, 133–141. doi: 10.1016/j.ajhg.2011.11.025.
- Valente, E. M., Abou-Sleiman, P. M., Caputo, V., Muqit, M. M. K., Harvey, K., Gispert, S., et al. (2004). Hereditary early-onset Parkinson’s disease caused by mutations in PINK1. *Science* (80-.). 304, 1158–1160. doi: 10.1126/science.1096284.
- van der Merwe, C., Carr, J., Glanzmann, B., and Bardien, S. (2016). Exonic rearrangements in the known Parkinson’s disease-causing genes are a rare cause of the disease in South African patients. *Neurosci. Lett.* 619, 168–171. doi: 10.1016/j.neulet.2016.03.028.
- Van Der Spoel, D., Lindahl, E., Hess, B., Groenhof, G., Mark, A. E., and Berendsen, H. J. C. (2005). GROMACS: Fast, flexible, and free. *J. Comput. Chem.* 26, 1701–1718. doi: <https://doi.org/10.1002/jcc.20291>.
- Varadi, M., Anyango, S., Deshpande, M., Nair, S., Natassia, C., Yordanova, G., et al. (2022). AlphaFold Protein Structure Database: Massively expanding the structural coverage of protein-sequence space with high-accuracy models. *Nucleic Acids Res.* 50, D439–D444. doi: 10.1093/nar/gkab1061.
- Velkoff, V. A., and Kowal, P. R. (2006). “Aging in sub-Saharan Africa: the changing demography of the region,” in *Aging in Sub-Saharan Africa: Recommendations for Furthering Research*, eds. B. Cohen and J. Menken (Washington, D.C.: The National

Academies Press), 55–91.

- Vilariño-Güell, C., Wider, C., Ross, O. A., Dachsel, J. C., Kachergus, J. M., Lincoln, S. J., et al. (2011). VPS35 Mutations in Parkinson Disease. *Am. J. Hum. Genet.* 89, 162–167. doi: 10.1016/J.AJHG.2011.06.001.
- Wang, C., Telpoukhovskaia, M. A., Bahr, B. A., Chen, X., and Gan, L. (2018). Endo-lysosomal dysfunction: a converging mechanism in neurodegenerative diseases. *Curr. Opin. Neurobiol.* 48, 52–58. doi: 10.1016/j.conb.2017.09.005.
- Wang, Q., Huang, L., and Yue, J. (2017). Oxidative stress activates the TRPM2-Ca²⁺-CaMKII-ROS signaling loop to induce cell death in cancer cells. *Biochim. Biophys. Acta - Mol. Cell Res.* 1864, 957–967. doi: 10.1016/j.bbamcr.2016.12.014.
- Warde-Farley, D., Donaldson, S. L., Comes, O., Zuberi, K., Badrawi, R., Chao, P., et al. (2010). The GeneMANIA prediction server: Biological network integration for gene prioritization and predicting gene function. *Nucleic Acids Res.* 38, W214–W220. doi: 10.1093/nar/gkq537.
- Williams, U., Bandmann, O., and Walker, R. (2018). Parkinson’s Disease in Sub-Saharan Africa: A Review of Epidemiology, Genetics and Access to Care. *J. Mov. Disord.* 11, 53–64. doi: 10.14802/jmd.17028.
- Winklhofer, K. F., and Haass, C. (2010). Mitochondrial dysfunction in Parkinson’s disease. *Biochim. Biophys. Acta - Mol. Basis Dis.* 1802, 29–44. doi: <https://doi.org/10.1016/j.bbadis.2009.08.013>.
- Xicoy, H., Wieringa, B., and Martens, G. J. M. (2017). The SH-SY5Y cell line in Parkinson’s disease research: a systematic review. *Mol. Neurodegener.* 12, 1–11. doi: 10.1186/s13024-017-0149-0.
- Yangngam, S., Plong-On, O., Sripo, T., Roongpraiwan, R., Hansakunachai, T., Wirojanan, J., et al. (2014). Mutation Screening of the Neurexin 1 Gene in Thai Patients with Intellectual Disability and Autism Spectrum Disorder. *Genet. Test. Mol. Biomarkers* 18, 510–515. doi: 10.1089/gtmb.2014.0003.
- Yasuda, T., and Mochizuki, H. (2010). The regulatory role of α -synuclein and parkin in neuronal

cell apoptosis; Possible implications for the pathogenesis of Parkinson's disease. *Apoptosis* 15, 1312–1321. doi: 10.1007/s10495-010-0486-8.

Yonova-Doing, E., Atadzhanov, M., Quadri, M., Kelly, P., Shawa, N., Musonda, S. T. S., et al. (2012). Analysis of LRRK2, SNCA, Parkin, PINK1, and DJ-1 in Zambian patients with Parkinson's disease. *Park. Relat. Disord.* 18, 567–571. doi: 10.1016/j.parkreldis.2012.02.018.

Zhang, Z. X., Dong, Z. H., and Román, G. C. (2006). Early descriptions of Parkinson disease in ancient China. *Arch. Neurol.* 63, 782–784. doi: 10.1001/archneur.63.5.782.

Zimprich, A., Benet-Pagès, A., Struhal, W., Graf, E., Eck, S. H., Offman, M. N., et al. (2011). A mutation in VPS35, encoding a subunit of the retromer complex, causes late-onset parkinson disease. *Am. J. Hum. Genet.* 89, 168–175. doi: <https://doi.org/10.1016/j.ajhg.2011.06.008>.

Zimprich, A., Biskup, S., Leitner, P., Lichtner, P., Farrer, M., Lincoln, S., et al. (2004). Mutations in LRRK2 cause autosomal-dominant parkinsonism with pleomorphic pathology. *Neuron* 44, 601–607. doi: 10.1016/j.neuron.2004.11.005.

Appendices

Appendix I: Standard Operating Procedures



SUN Host Genetics Research Group

Division Molecular Biology and Human Genetics

Laboratory Standard Operating Procedures

DNA Isolation using the NucleoSpin® Blood XL Kit			
SOP:LM-018	Version #: 3.0	Effective Date: 26 Nov 2019	Page 1 of 7
Prepared by: Digitally signed by Sihaam Boolay SU Date: 2019.11.26 15:44:05 +02'00' Dr Sihaam Boolay Lab Manager	Approved by QA: Digitally signed by Craig Kinnear Date: 2019.11.27 09:38:44 +02'00' Prof Craig Kinnear Quality Assurer	Principal Investigator: Digitally signed by Marlo Möller Date: 2019.11.26 16:10:27 +02'00' X Prof Marlo Möller Principle Investigator	

TABLE OF CONTENTS

PAGE

1	SCOPE	2
2	RESPONSIBILITY	2
3	SAFETY WARNINGS AND PRECAUTIONS.....	2
4	BACKGROUND	2
5	LABORATORY PROCEDURE FOR DNA EXTRACTION	2
5.1	Reagents and Equipment.....	2
5.2	Preparations.....	3
5.3	Genomic DNA purification with NucleoSpin® Blood XL.....	3
	Lyse the Blood Sample	3
	Bind DNA	4
	Wash silica membrane	4
	Elute highly pure DNA	5
6	QUANTIFICATION and STORAGE OF DNA.....	5
7	REFERENCES	5
8	SUPPORTING DOCUMENTS	5
9	AVAILABILITY	6
10	DOCUMENT HISTORY.....	7

DNA Isolation using the NucleoSpin® Blood XL Kit			
SOP: LM-018	Version #: 3.0	Effective Date: 26 Nov 2019	Page 2 of 7

1 SCOPE

This standard operating procedure defines the processing of Genomic DNA extraction from whole blood using the NucleoSpin® Blood XL kit.

2 RESPONSIBILITY

Blood shall be processed only by staff members who are trained in these procedures as well as laboratory health and safety procedures for working with human blood.

3 SAFETY WARNINGS AND PRECAUTIONS

All human biological material should be considered biohazardous and handled using universal clinical and personal safety precautions.

All chemicals should be considered as potentially hazardous and should be used in accordance with the principles of GLP.

4 BACKGROUND

- The NucleoSpin® Blood method, allows the preparation of genomic DNA from whole blood, cultured cells, serum, plasma, or other body fluids.
- By incubating the whole blood in a solution containing large amounts of chaotropic ions in the presence of Proteinase K, lysis is achieved.
- Ethanol is then added to the lysate, which creates the ideal conditions for binding of DNA to the silica membrane of the corresponding NucleoSpin® Blood Columns. The binding process is reversible and specific to nucleic acids.
- Subsequent washing steps aid in efficiently removing contaminants. Finally, pure genomic DNA is eluted under low ionic strength conditions in a slightly alkaline elution buffer.
- The NucleoSpin® Blood L / XL kits allow purification of highly pure genomic DNA with an A260 / A280 ratio between 1.60 and 1.90 and a typical concentration 200–300 ng/μL.

5 LABORATORY PROCEDURE FOR DNA EXTRACTION

5.1 Reagents and Equipment

- NucleoSpin® Blood XL kit by Macherey-Nagel (Separations)
- Water bath/ Air incubator or dry bath able to reach 56°C.
- 50ml Conical Tubes
- Variable volume pipettes and Pipette-man
- 10 and 25ml Serological pipettes

DNA Isolation using the NucleoSpin® Blood XL Kit			
SOP: LM-018	Version #: 3.0	Effective Date: 26 Nov 2019	Page 3 of 7

- Centrifuge (4,000–4,500 x g)
- 1.5/2ml Eppendorf tubes

5.2 Preparations

Samples should be processed as soon as possible or stored at 4°C for 1-3 days or -80°C (long-term).

NOTE: Do not store samples at -20°C before processing

- 1) Prepare the Wash Buffer BQ2 by adding the indicated volume of absolute ethanol (Volume is indicated on the Wash Buffer BQ2 bottle). Label the bottle with a date to indicate when the ethanol was added. Store Wash Buffer BQ2 at room temperature (18–25 °C) for up to one year.
- 2) Prepare Proteinase K by adding the indicated volume of Proteinase Buffer PB to the Lyophilized powder. Proteinase K solution is stable at -20 °C for up to 6 months (Volume is indicated on the lyophilized Proteinase K bottle).
- 3) Set an incubator or water bath to 56 °C.
- 4) Preheat Elution Buffer BE to 70 °C in a dry bath.
- 6) For centrifugation, a centrifuge with a swing-out rotor and appropriate buckets capable of reaching 4,000–4,500 x g is required.

5.3 Genomic DNA purification with NucleoSpin® Blood XL

NOTE: If samples are being stored at -80°C, rapidly defrost at 37°C and keep on ice till DNA extraction is started.

Lyse the Blood Sample

- 1) Pipette up to 10 mL blood sample (equilibrated to room temperature) into a 50 mL tube.
 - a) Vigorous mixing is important to obtain high yield and purity of DNA.
- 2) Add 10 mL Buffer BQ1 and 500µl Proteinase K to the samples and vortex the mixture vigorously for 10 sec.
 - b) If processing less than 10 mL blood, adjust to one volume of Buffer BQ1
- 3) Incubate samples at 56 °C for 20 min. During 5 min intervals vortex samples vigorously.
 - c) The lysate should become brownish during incubation with Buffer BQ1.
 - d) Let the lysate cool down to RT before adding the ethanol.

DNA Isolation using the NucleoSpin® Blood XL Kit			
SOP: LM-018	Version #: 3.0	Effective Date: 26 Nov 2019	Page 4 of 7

- 4) Add 10 mL absolute ethanol to each sample and mix by inverting the tube 10 times (if processing less than 10 mL blood, add one volume of ethanol).

NOTE: High local ethanol concentration must be avoided, by immediate mixing after addition.

- 5) Ensure that the lysate has cooled down to RT (about 10-15 min) before loading it onto the columns. Loading of hot lysate may lead to diminished yields.

Bind DNA

- 6) For each preparation, take one NucleoSpin® Blood XL Column placed in a Collection Tube and load 15 mL of lysate. Do not moisten the rim of the column. Close the tubes with screw caps and centrifuge for 3 min at 3220 x g.
- 7) Discard flow-through. Keep the tube with column upright to avoid contact of flow-through with the column outlet. Keep NucleoSpin® Blood XL Column in an upright position as liquid may pass through the ventilation slots on the rim of the column even if the caps are closed.
- 8) Load 15 mL of the remaining lysate to the respective NucleoSpin® Blood XL Column. Centrifuge for 3 min at 3220 x g. Discard the flow through and place the column back into the Collection Tube.
- 9) **Additional Wash Step.** Only perform this step if the blood has been stored for long periods at -20° or -80°C, has clots in them or the lysate is very dark brown.
- Prepare a solution of 1:1:1 with autoclaved water: BQ1: absolute ethanol.
 - Add 10 ml of this buffer to the column. Centrifuge at 3220x g for 3 min.

Wash silica membrane

- 10) 1st wash: Add 7.5 mL Buffer BQ2 to the NucleoSpin® Blood XL Column. Centrifuge for 3 min at 3220 x g. It is not necessary to discard the flow-through after the first washing step.
- 11) 2nd Wash: Add 7.5 mL Buffer BQ2. Centrifuge for 12 min at 3220 x g. Remove the column carefully from the rotor to avoid that flow-through gets in contact with the column outlet. The drying of the NucleoSpin® Blood XL Column is performed by prolonged centrifugation time (12 min) in the 2nd wash step.

DNA Isolation using the NucleoSpin® Blood XL Kit			
SOP: LM-018	Version #: 3.0	Effective Date: 26 Nov 2019	Page 5 of 7

Elute highly pure DNA

- 12) Insert the column into a new NucleoSpin® Blood XL Collection Tube (50 mL) and apply 1000 µL of preheated Buffer BE (70 °C) directly to the center of the silica membrane.
- 13) Incubate at RT for 2 min.
- 14) Centrifuge at 3220 x g for 2 min.
- 15) **Additional elution step:** Reapply the 1000 µL of eluant to the membrane.
- 16) Incubate at RT for 2 min.
- 17) Centrifuge at 3220 x g for 2 min.

6 QUANTIFICATION AND STORAGE OF DNA

- 1) Incubate the DNA at 4°C overnight
- 2) Determine the concentration and purity of the DNA by using a Nanodrop™ Spectrophotometer or the Multiskan.
 - a. *A ratio of absorbance (A260/280) of 1.8 is used to assess the purity of the DNA and a lower ratio would indicate protein contamination.*
 - b. *A260/A230 ratio of 2 is indicative of good quality DNA but a ratio which is considerably lower could indicate contamination with salts and solvents, which absorbs at A230.*
- 3) Quantification of dsDNA is determined using the Qubit Fluorometer, when required.
- 4) Prepare 2-3 aliquots of DNA
- 5) DNA will be stored long term, at 4°C or at -80 °C, depending on the Study requirement.

7 REFERENCES

- NucleoSpin® Blood MACHEREY-NAGEL product book -06/2014, Rev14 (www.mn-net.com)
- All technical literature is available on the internet at www.mn-net.com.
- <http://www.mnnet.com/Products/DNAandRNAPurification/GenomicDNA/DNAfrombloodandbiologicalfluids/NucleoSpinBloodLXL/tabid/1349/language/en-US/Default.aspx>

8 SUPPORTING DOCUMENTS

- FM-013: Formulation Method for NucleoSpin® Blood XL.
- LM-016: Qubit Fluorometer Analysis

DNA Isolation using the NucleoSpin ® Blood XL Kit			
SOP: LM-018	Version #: 3.0	Effective Date: 26 Nov 2019	Page 6 of 7

9 AVAILABILITY

The original signed version of this document is kept by the Quality Assurance Officer. A copy of the document can be found on the document management system ALFRESCO.

DNA Isolation using the NucleoSpin® Blood XL Kit			
SOP: LM-018	Version #: 3.0	Effective Date: 26 Nov 2019	Page 7 of 7

10 DOCUMENT HISTORY

Version No.	Date Approved/ Reviewed	Location of Change History	Author	Approving Official	Next Review Date
1.0		<i>New SOP</i>	J Theys	M. Möller	April 2018
1.1	10 April 2018	<i>Section 4.3: Missing information added Headings were changed</i>	J Theys	S. Boolay	May 2018
1.2	9 May 2018	<i>Section 5: Additional info added Heading were changed</i>	J Theys	M. Möller	May 2018
1.3	14 May 2018	<i>Section 4.2: "Short term" and "Ethanol" corrected</i>	J Theys	M. Möller	15 May 2018
2.0	15 May 2018	<i>Minor Typo errors corrected</i>	S Boolay	M. Möller	25 Nov 2019
2.1	25 Nov 2019	<i>Title changed Section 3: Safety warnings and precautions added. Section 5.3. Note added Section 5.2: Multiskan info added Section 5.3.9 Additional Wash clarified Section 5.3.15: Additional elution step changed. Section 6 Multiskan added Throughout document, centrifugation step changed from 4000xg to 3220xg and time changed, to accommodate for the centrifuge being used.</i>	S. Boolay	M. Möller	



SUN MAGIC Lab Research Group
Division Molecular Biology and Human Genetics
Laboratory Standard Operating Procedures




SITE-DIRECTED MUTAGENESIS USING THE Q5® KIT			
SOP#: LM-030	Version #: 1.0	Effective Date: 2020/04/22	Page 1 of 6
Prepared by: Katelyn Cuttler (Signature & Date)		Approved by Principal Investigator: Prof. Soraya Bardin (Signature & Date)	
 22/04/2020		 22/04/2020	

TABLE OF CONTENTS

1	SCOPE	2
2	RESPONSIBILITIES	2
3	SAFETY WARNINGS AND PRECAUTIONS	2
4	CRITICAL PARAMETERS	2
5	BACKGROUND	2
6	PROCEDURE	2
	6.1 EQUIPMENT, REAGENTS AND CONSUMABLES REQUIRED	2
	6.2 PREPARATION OF SOLUTIONS	3
	6.3 STORAGE OF SOLUTIONS AND MATERIALS	3
	6.4 PROTOCOL	3
	6.5 GENERAL GUIDELINES	5
7	DEFINITIONS	5
8	REFERENCES	5
9	SUPPORTING DOCUMENTS	5
10	AVAILABILITY	6
11	DOCUMENT HISTORY	6

 SUN MAGIC Lab Research Group Division Molecular Biology and Human Genetics Laboratory Standard Operating Procedures	SITE-DIRECTED MUTAGENESIS USING THE Q5® KIT		
	SOP#: LM-030	Version #: 1.0	Effective Date: 2020/04/22

1 SCOPE

This standard operating procedure defines the processing of site-directed mutagenesis via the Q5® Site-Directed Mutagenesis kit. Please note that bacterial transformation (LM-029) and plasmid miniprep (LM-031) may need to be done prior to this technique.

2 RESPONSIBILITIES

No specific training or precautions are required for this SOP.

3 SAFETY WARNINGS AND PRECAUTIONS

No dangerous chemicals or materials are used in this SOP. However, all chemicals and materials should be used in accordance with the GLP principles. proper PPE (labcoat and gloves) must be worn at all times

4 CRITICAL PARAMETERS

None

5 BACKGROUND

The Q5® Site-Directed Mutagenesis Kit enables rapid, site-specific mutagenesis of double-stranded plasmid DNA in less than 2 hours.


The kit utilizes the robust Q5 Hot Start High-Fidelity DNA Polymerase along with custom-designed mutagenic primers to create insertions, deletions and substitutions in a wide variety of plasmids. After PCR, the amplified material is added directly to a unique KLD enzyme mix for rapid circularization and template removal.

Transformation into high-efficiency NEB 5-alpha Competent *E. coli* ensures robust results with plasmids up to 20 kb in length.

6 PROCEDURE

6.1 EQUIPMENT, REAGENTS AND CONSUMABLES REQUIRED

- Q5 Hot Start High-Fidelity 2X Master Mix
- Forward Primer & Reverse Primer
- Template DNA (plasmid DNA)

 SUN MAGIC Lab Research Group Division Molecular Biology and Human Genetics Laboratory Standard Operating Procedures	SITE-DIRECTED MUTAGENESIS USING THE Q5[®] KIT		
	SOP#: LM-030	Version #: 1.0	Effective Date: 2020/04/22

- Nuclease-free water
- 2X KLD Reaction Buffer
- 10X KLD Enzyme Mix
- NEB 5-alpha competent Escherichia coli cells
- LB agar
- Petri dishes
- Thermocycler

6.2 PREPARATION OF SOLUTIONS

- Forward and reverse primers: resuspend primers in dH₂O as per manufacturer's instructions
- LB agar: 5g Bacto-tryptone, 2.5g yeast extract, 5g NaCl, 7.5g agar in 500 ml dH₂O
- LB agar with selected antibiotic: Autoclave LB agar. Once it has cooled down to ± 55 °C add antibiotic to suggested concentration (ampicillin: 25 μ g/ml; kanamycin: 100 μ g/ml)

6.3 STORAGE OF SOLUTIONS AND MATERIALS


- Store Q5 Hot Start High-Fidelity 2X Master Mix, 2X KLD Reaction Buffer and 10X KLD Enzyme Mix at 4 °C
- Store nuclease free water at 4 °C
- Store template DNA at 4 °C
- Store resuspended forward and reverse primers at 4 °C
- LB agar plates must be stored at 4 °C
- NEB 5-alpha E. coli cells are stored at -80 °C when not in use

6.4 PROTOCOL

A. Exponential Amplification (PCR)

1. Assemble the following reagents in a thin-walled PCR tube:

	25 μl RXN	FINAL CONC.
Q5 Hot Start High-Fidelity 2X Master Mix	12.5 μ l	1X
10 μ M Forward Primer	1.25 μ l	0.5 μ M
10 μ M Reverse Primer	1.25 μ l	0.5 μ M

 SUN MAGIC Lab Research Group Division Molecular Biology and Human Genetics Laboratory Standard Operating Procedures	SITE-DIRECTED MUTAGENESIS USING THE Q5® KIT			
	SOP#: LM-030	Version #: 1.0	Effective Date: 2020/04/22	Page 4 of 6

Template DNA (1–25 ng/μl)	1 μl	1-25 ng
Nuclease-free water	9.0 μl	

2. Mix reagents by aspiration, then transfer to a thermocycler.

3. Perform the following cycling conditions:

STEP	TEMP	TIME
Initial Denaturation	98°C	30 seconds
25 Cycles	98°C	10 seconds
	50–72°C*	10–30 seconds
	72°C	20–30 seconds/kb
Final Extension	72°C	2 minutes
Hold	4–10°C	

B. Kinase, Ligase & DpnI (KLD) Treatment


1. Assemble the following reagents:

	VOLUME	FINAL CONC.
PCR Product	1 μl	
2X KLD Reaction Buffer	5 μl	1X
10X KLD Enzyme Mix	1 μl	1X
Nuclease-free Water	3 μl	

2. Mix well by pipetting up and down and incubate at room temperature for 5 minutes.

C. Transformation

1. Thaw a tube of NEB 5-alpha Competent *E. coli* cells on ice.
2. Add 5 μl of the KLD mix from Step B above to the tube of thawed cells. Carefully flick the tube 4-5 times to mix. Do not vortex.
3. Place the mixture on ice for 30 minutes.

 SUN MAGIC Lab Research Group Division Molecular Biology and Human Genetics Laboratory Standard Operating Procedures	SITE-DIRECTED MUTAGENESIS USING THE Q5® KIT			
	SOP#: LM-030	Version #: 1.0	Effective Date: 2020/04/22	Page 5 of 6

4. Heat shock at 42°C for 30 seconds.
5. Place on ice for 5 minutes.
6. Pipette 950 µl of room temperature SOC into the mixture.
7. Incubate at 37°C for 60 minutes with shaking (250 rpm).
8. Mix the cells thoroughly by flicking the tube and inverting, then spread 50-100 µl onto a LB agar plate with the appropriate antibiotic (ampicillin, kanamycin etc.) and incubate overnight at 37°C.

6.5 GENERAL GUIDELINES

- For a Q5-optimized annealing temperature of mutagenic primers, please use NEBaseChanger™, the online NEB primer design software. For pre-designed, back-to-back primer sets, a $T_a = T_m + 3$ rule can be applied, but optimization may be necessary.
- When plating cells (step 8), it may be necessary (particularly for simple substitution and deletion experiments) to make a 10- to 40-fold dilution of the transformation mix in SOC prior to plating, to avoid a lawn of colonies.

7 DEFINITIONS

NEB	New England Biolabs
E. coli	Escherichia coli
PCR	polymerase chain reaction
KLD	kinase, ligase and Dpu I
dH ₂ O	distilled water
LB agar	Luria-Bertani agar
SOC	super optimal broth with catabolite repression


8 REFERENCES

Q5® Site-Directed Mutagenesis Kit (New England Biolabs)

9 SUPPORTING DOCUMENTS

LM-029: Bacterial Transformation of E. coli DH5α cells

LM-031: Plasmid Miniprep using the Zyppy™ Plasmid Miniprep Kit

 SUN MAGIC Lab Research Group Division Molecular Biology and Human Genetics Laboratory Standard Operating Procedures	SITE-DIRECTED MUTAGENESIS USING THE Q5® KIT			
	SOP#: LM-030	Version #: 1.0	Effective Date: 2020/04/22	Page 6 of 6

10 AVAILABILITY

The original signed version of this document is kept by the Laboratory Manager. A copy of the document can be found on the document management system ALFRESCO.

11 DOCUMENT HISTORY

Version No.	Date Approved	Location of Change/ History	Author/ Reviewer	Approving Official	Next Review Date
1.0	22/04/2020	<i>New SOP</i>	Katelyn Cuttler	Prof Soraya Bardien	As required



SUN Host Genetics Research Group
Division Molecular Biology and Human Genetics
Laboratory Standard Operating Procedures

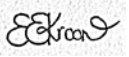



CONFOCAL ANTIBODY STAINING PROTOCOL			
SOP# LM-048	Version #: 1.0	Effective Date: 21 October 2020	Page 1 of 11
Prepared by: Elouise Kroon (Allison Seeger UCT)		Approved by QA: Dr Marlo Möller	Approved by Principal Investigator: Prof Eileen Hoal
(Signature & Date)  21 October 2020		(Signature & Date)  21 October 2020	(Signature & Date)  21 October 2020

TABLE OF CONTENTS

1. SCOPE.....	2
2. RESPONSIBILITIES	2
3. BACKGROUND	2
4. PROCEDURE	3
4.1. Antibody Staining Protocol.....	3
4.1.1 Antibody Staining METHOD	3
4.1.1.1. <i>Reagents and Hardware</i>	3
4.1.1.2. <i>Method for Perm/Quench Buffer preparation</i>	3
4.1.2. Auramine Staining Protocol.....	5
5. DEFINITIONS	5
6. REFERENCES	5
7. SUPPORTING DOCUMENTS.....	5
8. AVAILABILITY.....	6
9. DOCUMENT HISTORY	7

 SUN Host Genetics Research Group Division Molecular Biology and Human Genetics Laboratory Standard Operating Procedures	CONFOCAL ANTIBODY STAINING PROTOCOL		
	SOP#:	Version #: <i>1.0</i>	Effective Date: 21 October 2020

1. SCOPE


The aim of this standard operating procedure (SOP) is to describe the antibody staining steps for the fixed (4% PFA or 4% Formaldehyde if PFA was not available) neutrophils for downstream confocal microscopy.

2. RESPONSIBILITIES

- 1) It is the responsibility of the lab personnel to follow this SOP as written.
- 2) It is the responsibility of the lab personnel to follow the necessary safety precautions when handling blood and related products during this process.
- 3) It is the responsibility of lab management to ensure this laboratory procedure is appropriate for their intended use and that all personnel involved in this process are appropriately trained before processing any project related samples.

3. BACKGROUND

None

 SUN Host Genetics Research Group Division Molecular Biology and Human Genetics Laboratory Standard Operating Procedures	CONFOCAL ANTIBODY STAINING PROTOCOL		
	SOP#:	Version #: <i>1.0</i>	Effective Date: 21 October 2020

4. PROCEDURE

4.1. Antibody Staining Protocol

4.1.1 Antibody Staining METHOD

4.1.1.1. *Reagents and Hardware*

- P1000, P200, P20 Pipettes and tips
- Multi-channel Pipette
- 15/50ml sterile centrifuge tubes
- Perm/Quench Buffer (*stock made in lab- see 4.1.1.2 for Perm/Quench Buffer preparation)
- PGAS Buffer (*stock made in lab- see 4.1.1.2 for PGAS Buffer preparation)
- Poli-L-Lysine
- PBS
- Reservoir wells, foil
- Primary and Secondary Antibodies needed
- Auramine Stain
- diH₂O

4.1.1.2. *Method for Perm/Quench Buffer preparation*


Note: This makes 1Litre. Wrap in foil and store in the dark.

- 1) Combine the following reagents:
 - 2.8g Ammonium chloride (NH₄Cl) (50mM)
 - 0.2% Saponin (Dissolve 2g in 1L PBS)
- 2) NH₄Cl and Saponin are dissolved in 1L PBS. (Can add 1.4g NH₄CL and 1g Saponin to 500ml PBS for smaller batch- either directly to PBS in manufacturer's bottle or in sterile glass.)
- 3) Store in dark and 4°C.

4.1.1.3. *Method for PGAS Buffer preparation*

Note: This makes 1Litre. Wrap in foil and store in the dark.

- 1) Combine the following reagents:
 - 0.2% BSA (20g)
 - 0.2% Saponin (Or 1ml of 20% Saponin {20g in 100ml PBS})
 - 0.2% NaN₃ (Azide) (0.2g or 1ml of 20% NaN₃)

 SUN Host Genetics Research Group Division Molecular Biology and Human Genetics Laboratory Standard Operating Procedures	CONFOCAL ANTIBODY STAINING PROTOCOL		
	SOP#:	Version #: <i>1.0</i>	Effective Date: 21 October 2020

- 2) Combine all in 1L PBS and wrap in foil. (Can also make 500ml mixture as above.)
- 3) Store in dark.

4.1.1.4. Prepare 1 and 2 antibody cocktails for each staining protocol

Note: Calculate the number of wells needed to stain for each plate and make up the antibody cocktails in 10ml sterile centrifuge tube. Wrap tube in foil and keep on ice. Once cocktails made, return the antibodies the fridge(4°C).

Staining Protocol 1:


- 1° Ab cocktail #1
 1:500 H2A-H2B (decondensed chromatin)
 1:500 MRP-8 (calprotectin)
 in PGAS Buffer (100µl/well)
- 2° Ab cocktail #1
 1:1000 α-mouse-Cy3
 1:500 α-rabbit-AF647
 10µg/ml Hoechst 33342
 in PGAS Buffer (100µl/well)

Staining Protocol 2:

- 1° Ab cocktail #2
 1:500 H2A-H2B (decondensed chromatin)
 1:200 MMP-8
 1:200 NE (neutrophil elastase)
 in PGAS Buffer (100µl/well)
- 2° Ab cocktail #2
 1:500 α-mouse-AF405
 1:1000 α-rabbit-Cy3
 1:500 α-goat-PerCP
 in PGAS Buffer (100µl/well)

4.1.1.5. Method for antibody staining

- 1) Using multi-channel pipette, remove PBS from all wells
- 2) Add 100µl Perm/Quench Buffer to each well using multi-channel pipette and incubate at room temperature for 15min
- 3) Discard Perm/Quench Buffer using multi-channel pipette
- 4) Add 100µl PGAS Buffer to each well using multi-channel pipette and incubate at room temperature for 5min
- 5) Discard PGAS Buffer using multi-channel pipette
- 6) Add 100µl 1°Ab cocktail and incubate overnight at 4°C
- 7) Discard 1° Ab cocktail using multi-channel pipette
- 8) Wash 2X by adding 100µl PGAS Buffer with multi-channel pipette, pipetting up and down twice and then discarding

 SUN Host Genetics Research Group Division Molecular Biology and Human Genetics Laboratory Standard Operating Procedures	CONFOCAL ANTIBODY STAINING PROTOCOL		
	SOP#:	Version #: <i>1.0</i>	Effective Date: 21 October 2020

- 9) Add 100µl 2° Ab cocktail and incubate at room temperature for 1h in the dark
- 10) Wash 3X by adding 100µl PGAS Buffer with multi-channel pipette, pipetting up and down twice and then discarding
- 11) Add PGAS Buffer to the brim (about 300µl per well), cover plate with a foil cover, place in a zip-lock bag and store at 4°C until ready for microscopy

4.1.2. Auramine Staining Protocol

- 1) Discard PGAS Buffer using multi-channel pipette
- 2) Add 100µl phenolic auramine and incubate at room temperature for 15min
- 3) Discard phenolic auramine using multi-channel pipette
- 4) Add 100µl diH₂O and remove immediately
- 5) Add 100µl acid alcohol and incubate at room temperature for 2min
- 6) Discard acid alcohol using multi-channel pipette
- 7) Add 100µl diH₂O and remove immediately
- 8) Add 100µl potassium permanganate and incubate at room temperature for 3min
- 9) Discard potassium permanganate with multi-channel pipette
- 10) Add 100µl diH₂O and remove immediately
- 11) Add PGAS Buffer to the brim (about 300µl per well), cover plate with a foil cover, place in a zip-lock bag and store at 4°C until ready for microscopy

5. DEFINITIONS


°C	Degrees Celsius
diH ₂ O	Distilled Water
mL	millilitre
PBS	Phosphate buffered saline
SOP	Standard Operating Procedure
µL	microlitre
Ab	Antibody

6. REFERENCES

Allison Seeger-UCT Antibody Staining Protocol


7. SUPPORTING DOCUMENTS

None

 SUN Host Genetics Research Group Division Molecular Biology and Human Genetics Laboratory Standard Operating Procedures	CONFOCAL ANTIBODY STAINING PROTOCOL		
	SOP#:	Version #: <i>1.0</i>	Effective Date: 21 October 2020

8. AVAILABILITY

The original signed version of this document is kept by the Quality Assurance Officer. A copy of the document can be found on the document management system ALFRESCO.

 SUN Host Genetics Research Group Division Molecular Biology and Human Genetics Laboratory Standard Operating Procedures	CONFOCAL ANTIBODY STAINING PROTOCOL		
	SOP#:	Version #: <i>1.0</i>	Effective Date: 21 October 2020

9. DOCUMENT HISTORY

Version No.	Date Approved	Location of Change History	Author/Reviewer	Approving Official	Next Review Date
0.1	13 April 2018	<i>UCT Antibody SOP by Allison Seeger</i>	EE Kroon		
1.0	21 October 2020	<i>Adapted from UCT Antibody SOP by Allison Seeger</i>	EE Kroon	M Möller	

SUN Magic Lab Research Group
Division Molecular Biology and Human Genetics
Laboratory Standard Operating Procedures

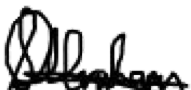

Culturing of Eukaryotic Cell Lines: SH-SY5Y, HEK and fibroblast cells			
SOP#: TC_LM-001	Version #: 1.0	Effective Date: 2020/04/28	Page 1 of 11
Prepared by: (Signature & Date)  28 / 04 / 2020		Approved by Principal Investigator: (Signature & Date)  28/04/2020	
Dr Shameemah Abrahams Postdoctoral Researcher		Prof Soraya Bardien Principal Investigator	

TABLE OF CONTENTS

1	SCOPE.....	2
2	RESPONSIBILITIES	2
3	SAFETY WARNINGS AND PRECAUTIONS	2
4	BACKGROUND	2
5	LABORATORY PROCEDURE FOR CELL CULTURING	3
5.1	EQUIPMENT AND CONSUMABLES REQUIRED	3
5.2	PREPARATION OF SOLUTIONS	3
5.3	TISSUE CULTURING PROTOCOL	4
5.3.1	Culturing Human Fibroblasts from the Skin Biopsy	4
5.3.2	Subculturing of Human Fibroblasts, SH-SY5Y and HEK293 Cells	4
	Subculturing/splitting cells	5
5.3.4	Seeding Cells for Downstream Experiments	6
5.3.5	Lysates for Protein and DNA Extraction Experiments.....	7
5.4	GENERAL GUIDELINES	7
6	STORAGE AND STABILITY	8
7	DEFINITIONS.....	8
8	REFERENCES	8
9	SUPPORTING DOCUMENTS	9
10	AVAILABILITY	9
11	DOCUMENT HISTORY.....	9

1 SCOPE

This Standard Operating Procedure (SOP) outlines the procedure for growing dermal fibroblasts from skin biopsies and culturing of neuroblastoma SH-SY5Y, human kidney HEK293 and dermal fibroblast cells.

2 RESPONSIBILITIES

Cell culturing will only be processed and handled by those trained in these specific procedures, as well as the general tissue culture laboratory safety and training procedures.

3 SAFETY WARNINGS AND PRECAUTIONS

- All human biological material should be considered biohazardous and handled using universal clinical and personal safety precautions, and personal protective equipment or PPE (where necessary).
- Always check MSDS or data safety sheets of the listed chemicals before starting a protocol. All chemicals should be considered potentially hazardous and should be used in accordance with the principles of good laboratory practice (GLP).

NB: Trypan blue solution is considered a respiratory irritant and suspected carcinogenic, please use appropriate PPE (e.g. gloves and face mask).

4 BACKGROUND

- This is an SOP regarding the culturing and handling of different cell types, specifically dermal fibroblast, SH-SY5Y neuroblastoma and HEK293 human kidney cells.
- Dermal fibroblasts are cultured from a skin biopsy (will not be discussed here) collected from participants by a trained physician/nurse and are considered primary, nonimmortalized cells.
- The SH-SY5Y and HEK293 cells are immortalized human cell lines purchased from commercial vendors and originally derived from a human bone marrow biopsy and embryonic kidney cells, respectively.
- Human dermal fibroblasts are often used as *ex vivo* models of disease especially diseases with a genetic contribution, due to the patient fibroblasts carrying disease-associated mutations. The SH-SY5Y cells are commonly used when investigating neurological disorders, due to its neuron-like features after differentiation. Finally, HEK293 cells are used in cancer biology and gene therapy due its robust growth and ease of transfecting with viral vectors.

5 LABORATORY PROCEDURE FOR CELL CULTURING

5.1 EQUIPMENT AND CONSUMABLES REQUIRED

The materials, equipment and forms listed are recommendations only and alternative products as suitable may be substituted for the site-specific task or procedure.

- Cell culture facilities and equipment
- Cell culture growth media (DMEM + 1% Pen/Strep + 10% FBS)
- Cell culture freezing media
- Culture flasks; 25 cm³ (T25) and/or 75 cm³ (T75) flasks, as needed
- Cryovials (for storage)
- Cryonic freezing container with isopropanol, e.g. Mr. Frosty (Thermo Scientific) or Cool Cell
- -80 °C freezer
- Liquid nitrogen facilities
- Other reagents (see section 5.2)

5.2 PREPARATION OF SOLUTIONS

- Culture Growth Medium (keep at 4 °C):
 - A. 500ml DMEM with 4.5g/L glucose & L-glutamine
 - B. 10% FBS
 - C. 1% Pen/Strep (10 000 U/ml)

Total volume of 500ml, use 445 ml DMEM, 50ml FBS and 5ml Pen/Strep or if 15% FBS is required, then use 420ml DMEM, 75ML FBS and 5ml Pen/Strep

- Freezing Medium (keep at 4 °C):
 - A. 90% FBS
 - B. 10% DMSO

In 50ml aliquot, use 45ml FBS and 5ml DMSO

- Fibroblast Isolation Medium:
 - A. 95ml Amniochrome II complete media
 - B. 95ml Chang Medium® D
 - C. 5ml Non-essential amino acids (NEAA)
 - D. 5ml Pen/Strep

Pre-warm to 37°C before use. Store at 4°C.

- Passive Lysis Buffer
 - A. 5ml Tris- HCl (1M, pH 7.4)
 - B. 3ml NaCl (5M)
 - C. 1% Triton-x
 - D. 150µl MgCl₂ (1M)
 - E. 150ml ddH₂O

Add on day of lysis:

- F. 0.1% β -mercapto-ethanol
- G. 1% Halt™ Protease and Phosphatase Inhibitor Cocktail (100x)

- Other reagents used:
 - PBS
 - Trypan Blue solution
 - Trypsin/EDTA
 - 70% Ethanol

5.3 TISSUE CULTURING PROTOCOL

5.3.1 Culturing Human Fibroblasts from the Skin Biopsy

This section only pertains to dermal fibroblasts.

- 1) After the skin punch biopsy, insert the piece of skin into a volume of 300 μ l collagenase (Sigma-Aldrich, United States) per 1ml culture growth media in a 15ml polypropylene tube.
- 2) Incubate the skin biopsy suspension for one hour at 37°C with manual agitation in a shaker incubator.
- 3) The suspension is centrifuged at 160 x g (1200rpm) for 10 minutes.
- 4) The supernatant is discarded while the pellet is resuspended in 5ml of fibroblast isolation media.
- 5) The suspension is transferred to a CellBind® T25 tissue culture flask (Corning Inc., United States).
- 6) Culture flasks are incubated at 37°C in a 5% CO₂ humidified incubator.
- 7) Subculturing of fibroblasts until sufficient confluency and frozen, as appropriate.

5.3.2 Subculturing of Human Fibroblasts, SH-SY5Y and HEK293 Cells

The subsequent sections 5.3.2 – 5.3.5 pertains to dermal fibroblasts, SH-SY5Y and HEK293 cells.

Growing cells from frozen

- 1) Take vial with frozen fibroblasts out of the liquid nitrogen and keep on ice until ready to be plated.
- 2) Prepare culture growth media and warm media to 37°C.
- 3) Once media has warmed, add ~3ml to a T25 culture flask ('small') and 1ml directly to the vial with frozen cells.

- 4) At this point the vial can be briefly warmed in the water bath, under sterile conditions, to ensure that the thawing proceeds as quickly as possible and warm media can be added to the vial to thaw completely.
- 5) The next 2 steps can be performed depending if the cell line is very robust (e.g. HEK cells)
 - a. Transfer the contents of the vial to a 15ml centrifuge tube and slowly add 510ml warm media to the tube.
 - b. Centrifuge for 2min at 252 x g (1500rpm) and discard the supernatant.
- 6) Dilute the cell pellet in 1ml media and transfer the contents to the culture flask (total volume = ~5ml) and incubate at 37°C and 5% CO₂.
- 7) Replace the culture media the next day to rid the growth environment of cell debris, unattached cells and any traces of DMSO leftover from the freezing media. (Note for adherent cells: check cells first & change only if no cells are in suspension)
- 8) Thereafter, replace the media every 2-4 days. Add media when the levels are low, before the weekend or media colour change (~1ml for T25, ~2-3ml for T75).
 - a. Timeframe:
 - i. Dermal fibroblasts = 3-5 days
 - ii. SH-SY5Y = 2-3 days
 - iii. HEK293 = 1-3 days
 - b. Do not replace the media too often as the cells rely on growth factors produced into the media.

Subculturing/splitting cells

- 9) At 80-90% confluency cells can be split and seeded into new flasks. This process is repeated until required cell concentrations are reached for experimental purposes, or until cells are frozen down for stock amplification purposes
- 10) Remove media and rinse with PBS to the side rather directly on the cells.
 - a. If a T25 flask is used, add 3ml PBS
 - b. If a T75 flask, add 5ml PBS.
- 11) Remove PBS and add Trypsin/EDTA.
 - a. If a T25 flask is used, add 3ml Trypsin/EDTA,
 - b. If T75 flask, add 5ml Trypsin/EDTA
- 12) Incubate flasks at 37°C for 4-7 minutes or once the cells round up and detach from the surface.
- 13) Tap the sides to lift remaining cells and examine under microscope to check that all cells are detached. If cells remain, incubate for an additional 1-2 minutes or use a cell scraper.
- 14) Add growth media to inactivate the Trypsin/EDTA and mix gently.
 - a. If a T25 flask is used, add 3ml growth medium,
 - b. If a T75 flask, add 5ml growth medium
- 15) Timeframes between subcultures depends on cell line:
 - a. Most cell lines require sub-culturing every 5-7 days.
 - b. If longer than 5 days. Change medium every 3-4 days

5.3.3 Freezing Down Procedure for Human Fibroblasts, SH-SY5Y and HEK293 Cells

- 1) Ideally, a cryonic freezing container with isopropanol, such as a Mr. Frosty (Thermo Scientific), should be used to ensure that the freezing process is as slow and gentle as possible. If the Mr. Frosty is at room temperature, put it in the -20°C freezer during the sample prep for freezing.
- 2) Follow steps 10 – 13 under section 5.3.2 (above).
- 3) Discard the supernatant and resuspend the cell pellet gently in 1ml warmed freezing media (Section 5.2) and transfer cell mixture to a cryonic freezer vial.
- 4) Place the vial inside the Mr. Frosty and put the Mr. Frosty in the -80°C freezer.
- 5) Cell samples can be removed from the Mr. Frosty the next day and put into liquid nitrogen for long-term storage. Alternatively, samples can be left at -80°C for shortterm storage (~4 months).

5.3.4 Seeding Cells for Downstream Experiments

- 1) Follow steps 10-13 from section 5.3.2, above.
- 2) Add 1-2ml of media to the pellet and dissolve completely.
- 3) Count the cell density either using the haemocytometer or automated cell counter.
 - a. Counting cells using the haemocytometer:

The haemocytometer is a specialized glass slide with nine squares of 1 mm x 1 mm. The four squares at each corner are subdivided into a 4 x 4 grid and are used for counting most cell types, except very small and abundant cell populations (e.g. red blood cells).

NB: Always clean cover slip and haemocytometer with ethanol before and after use.

- Dissolve an aliquot of the cell suspension in trypan blue solution and add this carefully between the haemocytometer and cover slip (e.g. 1 µl of the cell suspension to 9 µl of trypan blue to produce a 1:10 ratio).
- Using a light microscope, count the cells without trypan blue (viable) within the four squares at each corner of the haemocytometer.

- Calculation:

$(\text{Count 1} + \text{Count 2} + \text{Count 3} + \text{Count 4})/4 = \text{Average count of cells for all 4 squares}$

$*(\text{Average count} \times 10^4) \times \text{Dilution factor} = \text{Viable count in cells/ml}$

$(\text{Viable cells/ml}) / 1000 = \text{Viable count (in cells/}\mu\text{l)}$

*Note: The value 10^4 ml refers to the volume between the haemocytometer and cover slip. Dilution factor refers to the ratio of the cell suspension to trypan blue

(e.g. for 1:10 one would need to multiply by 10)

b. Counting cells using an automated cell counter (refer to protocol EM-003)

5.3.5 Lysates for Protein and DNA Extraction Experiments

- 1) Cell lysates are required to obtain protein or DNA from cultured cells for subsequent experiments, including western blot, co-immunoprecipitation, genetic mutation confirmatory.
- 2) Follow steps 10-13 from section 5.3.2. (Note: Cell flasks or plates can be used whichever is appropriate for the desired cell number and experimental design.)
- 3) After trypsinization, cells are removed using a cell scraper (Note: Maintain sterile use of cell scrapers to avoid cross contamination between different treatment/study/cell types).
- 4) Cell suspension is transferred to a 15ml polypropylene tube containing 3-5ml growth media. The suspension is centrifuged for 3min at $1006 \times g$ (3000rpm) at 4°C .
 - a. For cells cultured in six-well tissue culture plates, cells treated similarly from separate wells are pooled in either 15 or 50ml polypropylene tubes.
- 5) After the supernatant is discarded, the pellet is resuspended in 1ml of PBS and the suspension is transferred to a sterile 2ml microcentrifuge tube.
- 6) The 2ml suspension is re-pelleted by centrifugation for 1min at $7245 \times g$ (9000rpm) in a microcentrifuge.
- 7) After the supernatant is discarded, the cell pellet can either be frozen (-80°C) for future use or lysed as follows.
- 8) The pellet is resuspended in 50-300 μl ice-cold passive lysis buffer (Section 5.2), depending on pellet size, and incubated on ice for 30min.
- 9) Cells are centrifuged at $15\ 115 \times g$ (13 000rpm) for 15min at 4°C in a microcentrifuge and the supernatant is transferred to a sterile 1.5ml microcentrifuge tube.
- 10) Cell lysates are either used immediately for downstream applications or stored at 80°C .
- 11) For protein extraction from cell lysates, please refer to the SOPs LM-032 and LM033.
- 12) For DNA and RNA extraction from cell lysates, please refer to the SOPs LM-036 and LM-037.

5.4 GENERAL GUIDELINES

- Sterile conditions while working (spraying surfaces with 70% ethanol), frequent cleaning of the tissue culture laboratory (70% ethanol, virucidal

detergents) and monitoring for mycoplasma infection must be observed to ensure stable cell growth and prevent contamination.

- Always ensure the incubator is set at a temperature of 37°C and 5% CO₂ levels for optimal cell growth.
- It is good practice to culture sufficient cells to ensure multiple aliquots of cells per passage can be stored.
- It important to note the passage number of cell samples after each subculture and when freezing down cells.
- Centrifugation steps are performed in a 1.5-2L benchtop centrifuge (e.g. Heraeus Megafuge 16, ThermoFisher Sci), unless otherwise specified.
- Media should be red in color (if using standard DMEM media), if media is yellow the nutrients are depleted or possible contamination. Replenish with fresh media and ensure no visible contamination present.
- If cells struggle to grow, the possible causes are:
 1. Cells have been passaged too many times/frequent subculturing
 2. Cells are contaminated
 3. Undergone stress during the thawing process or similar mechanical stressor

Possible troubleshooting suggestions:

1. Use cells of a lower passage number or try to subculture the same batch of cells less frequently
2. Discard and grow up cells from a sterile batch
3. Increase FBS content in the growth media and/or change media less frequently

6 STORAGE AND STABILITY

- Cryopreserve cells in appropriate cryovial tubes, preferably 1.5-2ml.
- Frozen cells can be temporarily (~4 months) stored at -80 °C or long-term in liquid nitrogen.
- Always freeze cells using freezing media and a cryonic freezing container with isopropanol, such as a Mr. Frosty.

7 DEFINITIONS

DMEM	Dulbecco's Modified Eagle Medium
DMSO	Dimethyl Sulfoxide
EDTA	Ethylenediaminetetraacetic Acid
FBS	Fetal Bovine Serum
PBS	Phosphate Buffered Saline
Pen/Strep	Penicillin and Streptomycin

8 REFERENCES

Neethling, A. 2017. Functional characterization of sequence variants in leucine-rich repeat kinase 2 (*LRRK2*) and its possible interaction with the translocase of outer mitochondrial membrane (TOM) protein complex. [Dissertation]

Haylett, WL. 2015. Identification of parkin interactions: Implications for Parkinson's disease

[Dissertation]

MRC Flagship, Shared Roots. Standard Operating Procedures SOP_ShR4: Obtaining Skin Biopsies and Culturing Fibroblasts.

9 SUPPORTING DOCUMENTS

- FM-042: Formulation Method for Culturing Eukaryotic Cells
- EM-003: Counting Fibroblasts Using the Automated Countess
- LM-032: Intracellular Protein Extraction
- LM-033: Bradford Assay
- LM-036: DNA Extraction from Cultured Cells
- LM-037: RNA Extraction from Cultured Cells
- TC_LM-008: Transportation of Cells

10 AVAILABILITY

The original signed version of this document is kept by the Laboratory Manager. A copy of the document can be found on the document management system ALFRESCO.

11 DOCUMENT HISTORY

Version No.	Date	Location of Change History	Author	Approving Official	Date Approved	Next Review Date
1.0	28 April 2020	<i>New SOP</i>	Dr Shameemah Abrahams	Prof Soraya Bardien	28 April 2020	As needed



SUN MAGIC Lab Research Group
Division Molecular Biology and Human Genetics
Laboratory Standard Operating Procedures




Transfection of plasmid DNA into eukaryotic cells			
SOP#: TC_LM-002	Version #: 1.0	Effective Date: 2020/03/27	Page 1 of 5
Prepared by: Devina Chetty		Approved by Principal Investigator: Soraya Bardien	
(Signature & Date)  Digitally signed by Devina Chetty Date: 2020.04.21 19:37:28 +02'00'		(Signature & Date)  21/04/2020	

TABLE OF CONTENTS

1	SCOPE	2
2	RESPONSIBILITIES	2
3	SAFETY WARNINGS AND PRECAUTIONS	2
4	BACKGROUND	2
5	PROCEDURE	2
5.1	EQUIPMENT AND CONSUMABLES REQUIRED	2
5.2	PREPARATIONS	3
5.3	STORAGE OF SOLUTIONS	3
5.4	Transfection of plasmid DNA into eukaryotic cells	3
A.	HEK293 cells.....	3
B.	COS7 cells	4
C.	Storage	4
5.5	GENERAL GUIDELINES	4
6	DEFINITIONS	4
7	REFERENCES	4
8	SUPPORTING DOCUMENTS	4
9	AVAILABILITY	5
10	DOCUMENT HISTORY	5

 UNIVERSITEIT STELLENBOSCH UNIVERSITY SUN MAGIC Lab Research Group Division Molecular Biology and Human Genetics Laboratory Standard Operating Procedures	TRANSFECTION OF PLASMID DNA INTO EUKARYOTIC CELLS		
	SOP#: TC_LM-002	Version #: 1.0	Effective Date: 2020/03/27

1 SCOPE

This standard operating procedure defines the transfection of plasmids into eukaryotic cells. Please refer to bacterial transformation protocol (SOP number: LM-029) before performing this SOP.

2 RESPONSIBILITIES

Cells in tissue culture (Wickremaratchi *et al.*) shall be processed only by students and staff members who are trained in these procedures.

3 SAFETY WARNINGS AND PRECAUTIONS

All chemicals should be considered as potentially hazardous and should be used in accordance with the principles of GLP.

All human and animal biological material (e.g. eukaryotic cells and viral vectors) should be considered biohazardous and handled using universal clinical and personal safety precautions.


4 BACKGROUND

- This protocol allows for plasmid transfection into HEK293 cells and COS7 cells.
- Seeding cells at optimized densities for specific sterile cell culture plates and using optimized transfection is important to ensure experimental efficiency and reproducibility.
- Serum-free media enables enhanced growth and viability of cells, as well as easier downstream processing and better control of physiological responsiveness.

5 PROCEDURE

5.1 EQUIPMENT AND CONSUMABLES REQUIRED

- Sterile cell culture plates (96-, 24- or 6-well)
- Lipofectamine 2000 (Invitrogen™, United States)
- DMRIE-C transfection reagent (Invitrogen™, United States)
- Serum free media
- Complete media i.e. DMEM (Lonza™)
- Variable volume pipettes
- Humidified incubator (37°C, 5% CO₂)

 UNIVERSITEIT STELLENBOSCH UNIVERSITY SUN MAGIC Lab Research Group Division Molecular Biology and Human Genetics Laboratory Standard Operating Procedures	TRANSFECTION OF PLASMID DNA INTO EUKARYOTIC CELLS		
	SOP#: TC_LM-002	Version #: 1.0	Effective Date: 2020/03/27

- 1.5/2ml Eppendorf tubes

5.2 PREPARATIONS

- Serum free media (DMEM without FBS)
- Complete media (DMEM with FBS and P/S)

5.3 STORAGE OF SOLUTIONS

All prepared solutions must be stored until use at 4°C.

5.4 Transfection of plasmid DNA into eukaryotic cells


A. HEK293 cells

- 1) Seed HEK293 cells at optimized density in specific cell culture plates:
 - a) 20 000 cells/well for a 96-well plate
 - b) 100 000 cells/well for a 24-well plate
 - c) 500 000 cells/well for a 6-well plate
- 2) Based on the volume of the culture plate, separately incubate optimized volumes of Lipofectamine 2000 (Table 1; column 2) and concentrations of plasmid DNA (Table 1 below; column 4) in a pre-determined volume of serum-free media (SFM) (Table 1; columns 3 and 5) for 5 minutes at room temperature.
 - a) For example, when using a 96-well plate, separately incubate 0.6µl Lipofectamine2000 and 0.4µg plasmid DNA in 20µl SFM.

Table 1 Transfection of HEK293 cells with Lipofectamine 2000 transfection reagent

Plate	Lipo	SFM	Plasmid DNA	SFM	Transfection mixture volume	Total well volume
96-well	0.6 µl	20 µl	0.4 µg	20 µl	40 µl	200 µl
24-well	1 µl	25 µl	0.6 µg	25 µl	50 µl	400 µl
6-well	8 µl	200 µl	3 µg	200 µl	400 µl	2 ml

- 3) Combine the two volumes (SFM-Lipofectamine 2000 mixture and SFM-plasmid DNA mixture) and gently mix to form transfection mixture.
- 4) Incubate the transfection mixture for 20 minutes at room temperature.
- 5) Remove a volume equal to the volume of the transfection mixture from each well.
- 6) Add transfection mixture dropwise to each well.
- 7) Incubate plates at 37°C, 5% CO₂ for six hours.
- 8) After incubation, remove media and replace with pre-warmed complete media.
- 9) Incubate cells overnight.

 UNIVERSITEIT STELLENBOSCH UNIVERSITY SUN MAGIC Lab Research Group Division Molecular Biology and Human Genetics Laboratory Standard Operating Procedures	TRANSFECTION OF PLASMID DNA INTO EUKARYOTIC CELLS		
	SOP#: TC_LM-002	Version #: 1.0	Effective Date: 2020/03/27

B. COS7 cells

- 1) Seed COS7 cells at optimized density in specific cell culture plates e.g. 50 000 cells/well for a 24-well plate.
- 2) Incubate 1 µg of plasmid DNA and 0.7 µl of DMRIE-C transfection reagent separately with 75 µl of SFM for 30 minutes at room temperature.
- 3) After incubation, combine the two volumes and gently mix to form 150 µl transfection mixture.
- 4) Incubate the transfection mixture again for 30 minutes at room temperature.
- 5) Remove all the media from the 24-well culture plates and replace with 150 µl transfection mixture.
- 6) Incubate plates at 37°C, 5% CO₂ for four to five hours.
- 7) Following incubation, remove transfection media and replace with pre-warmed complete media.
- 8) Incubate overnight at 37°C, 5% CO₂.

C. Storage

- 1) Plasmid DNA may be stored in Eppendorf tubes at -80°C for later transfection of eukaryotic cells.

5.5 GENERAL GUIDELINES

Transfections may require optimization for each cell type and plasmid used.

6 DEFINITIONS AND ABBREVIATIONS


HEK-293 cells	Human embryonic kidney cells
COS7 cells	African green monkey kidney fibroblast-like cells
SFM	Serum-free media (SFM) is that which does not contain any animal-derived growth-promoting serum
Lipo	Lipofectamine

7 REFERENCES

NEETHLING, A. 2017. *Functional characterization of sequence variants in leucine-rich repeat kinase 2 (LRRK2) and its possible interaction with the translocase of outer mitochondrial membrane (TOM) protein complex* PhD, Stellenbosch University.

8 SUPPORTING DOCUMENTS

N/A

 UNIVERSITEIT STELLENBOSCH UNIVERSITY SUN MAGIC Lab Research Group Division Molecular Biology and Human Genetics Laboratory Standard Operating Procedures	TRANSFECTION OF PLASMID DNA INTO EUKARYOTIC CELLS			
	SOP#: TC_LM-002	Version #: 1.0	Effective Date: 2020/03/27	Page 5 of 5

9 AVAILABILITY

The original signed version of this document is kept by the Laboratory Manager. A copy of the document can be found on the document management system ALFRESCO.

10 DOCUMENT HISTORY

Version No.	Date Approved	Location of Change/ History	Author/ Reviewer	Approving Official	Next Review Date
1.0	21/04/2020	<i>New SOP</i>	D Chetty	S Bardien	As required



SUN MAGIC Lab Research Group
Division Molecular Biology and Human Genetics
Laboratory Standard Operating Procedures




DIFFERENTIATION OF SH-SY5Y CELLS USING RETINOIC ACID			
SOP#: TC_LM-004	Version #: 1.0	Effective Date: 2020/04/22	Page 1 of 4
Prepared by: Katelyn Cuttler (Signature & Date)		Approved by Principal Investigator: Prof. Soraya Barden (Signature & Date)	
 22/04/2020		 22/04/2020	

TABLE OF CONTENTS

1	SCOPE	2
2	RESPONSIBILITIES	2
3	SAFETY WARNINGS AND PRECAUTIONS	2
4	CRITICAL PARAMETERS	2
5	BACKGROUND	2
6	PROCEDURE	2
	6.1 EQUIPMENT AND REAGENTS REQUIRED	2
	6.2 PREPARATION OF SOLUTIONS	3
	6.3 STORAGE OF SOLUTIONS AND MATERIALS	3
	6.4 PROTOCOL	3
	6.5 GENERAL GUIDELINES	3
7	DEFINITIONS	3
8	REFERENCES	4
9	SUPPORTING DOCUMENTS	4
10	AVAILABILITY	4
11	DOCUMENT HISTORY	4

 UNIVERSITEIT STELLENBOSCH UNIVERSITY SUN MAGIC Lab Research Group Division Molecular Biology and Human Genetics Laboratory Standard Operating Procedures	DIFFERENTIATION OF SH-SY5Y CELLS USING RETINOIC ACID		
	SOP#: TC_LM-004	Version #: 1.0	Effective Date: 2020/04/22

1 SCOPE

This SOP describes the differentiation of SH-SY5Y cells using retinoic acid.

2 RESPONSIBILITIES

Only trained personnel can use this SOP. Standard cell culture training is required to perform this assay. Standard biohazardous safety precautions need to be taken.

3 SAFETY WARNINGS AND PRECAUTIONS

Retinoic acid is a skin irritant. Wear gloves at all times when handling.

All chemicals and materials should be used in accordance with the GLP principles. Proper PPE (labcoat and gloves) must be worn at all times.

4 CRITICAL PARAMETERS

Cell culture is performed in a Biohazard BSL II cabinet

5 BACKGROUND


This method permits the differentiation of neuroblastoma SH-SY5Y cells into a neuronal-like phenotype.

This is done by decreasing serum FBS levels and adding retinoic acid to the cell culture media. Retinoic acid induces differentiation by activating the PI3K/ Akt pathway and modulating the levels of certain transcription factors. The decreased FBS levels prevent growth hormones present in FBS from interrupting this procedure.

6 PROCEDURE

6.1 EQUIPMENT AND REAGENTS REQUIRED

- SH-SY5Y cells
- DMEM 4.5 g/l glucose with L-glutamine
- FBS
- P/S
- D-PBS
- humidified incubator

 UNIVERSITEIT STELLENBOSCH UNIVERSITY SUN MAGIC Lab Research Group Division Molecular Biology and Human Genetics Laboratory Standard Operating Procedures	DIFFERENTIATION OF SH-SY5Y CELLS USING RETINOIC ACID		
	SOP#: TC_LM-004	Version #: 1.0	Effective Date: 2020/04/22

6.2 PREPARATION OF SOLUTIONS

- Cell culture media: Add 45 ml FBS and 5 ml P/S to 450 ml DMEM
- Differentiation media: Add 1.5 ml FBS, 0.5 ml P/S and 10 μ M retinoic acid to 48 ml DMEM
- 10 μ M retinoic acid: Dissolve retinoic acid powder in DMSO to a concentration of 10 μ M

6.3 STORAGE OF SOLUTIONS AND MATERIALS

- Store all solutions at 4 °C
- Store retinoic acid powder at 4 °C
- Cover retinoic acid with foil as it is sensitive to light

6.4 PROTOCOL


1. Grow SH-SY5Y cells in cell culture media (DMEM with 10% FBS and 1% P/S) for 48 hours in a humidified incubator (see TC_LM-001)
2. Wash cells with 1X D-PBS
3. Add differentiation media (DMEM with 3% FBS, 1% P/S and 10 μ M retinoic acid)
4. Maintain cells in differentiation media for 7 days by changing media when required and keeping cells in a humidified incubator
5. After 7 days the cells are considered fully differentiated and can be used for downstream experimentation

6.5 GENERAL GUIDELINES

- Successful differentiation can be observed by the change in cell morphology
- However, a western blot may need to be performed in order to confirm differentiation of the cells by measuring levels of differentiation proteins (see LM_034: Western Blotting)

7 DEFINITIONS

DMEM	Dulbecco's Modified Eagle Medium
FBS	foetal bovine serum
P/S	penicillin/ streptomycin solution

 UNIVERSITEIT STELLENBOSCH UNIVERSITY SUN MAGIC Lab Research Group Division Molecular Biology and Human Genetics Laboratory Standard Operating Procedures	DIFFERENTIATION OF SH-SY5Y CELLS USING RETINOIC ACID			
	SOP#: TC_LM-004	Version #: 1.0	Effective Date: 2020/04/22	Page 4 of 4
DMSO	dimethyl sulfoxide			
D-PBS	Dulbecco's phosphate buffered saline			

8 REFERENCES

Cheung Y., Lau WK, Yu M, Lai CS, Yeung S, So K, Chang RC (2009) Effects of all-*trans*-retinoic acid on human SH-SY5Y neuroblastoma as an *in vitro* model of neurotoxicity research. *NeuroToxicology*. 30: 127-135.

9 SUPPORTING DOCUMENTS

TC_LM-001: Culturing of Eukaryotic Cell Lines: SH-SY5Y, HEK and fibroblasts cells
 LM_034: Western Blotting

10 AVAILABILITY

The original signed version of this document is kept by the Laboratory Manager. A copy of the document can be found on the document management system ALFRESCO.

11 DOCUMENT HISTORY

Version No.	Date Approved	Location of Change/ History	Author/ Reviewer	Approving Official	Next Review Date
1.0	22/04/2020	<i>New SOP</i>	Katelyn Cuttler	Prof Soraya Bardien	As required

Appendix II: Chapter 6 Supplementary Tables**Supplementary Table S1: List of unique proteins in wild-type transfected cells**

Protein	Name	Function
sp P0DTE8 AMY1C_HUMAN	Alpha-amylase 1C	Calcium-binding enzyme that initiates starch digestion in the oral cavity.
sp Q9HD20 AT131_HUMAN	Endoplasmic reticulum transmembrane helix translocase	Endoplasmic reticulum translocase required to remove mitochondrial transmembrane proteins mistargeted to the endoplasmic reticulum .
sp O60885 BRD4_HUMAN	Bromodomain-containing protein 4	Chromatin reader protein that recognizes and binds acetylated histones and plays a key role in transmission of epigenetic memory across cell divisions and transcription regulation.
sp Q9Y315 DEOC_HUMAN	Deoxyribose-phosphate aldolase	Catalyses a reversible aldol reaction between acetaldehyde and D-glyceraldehyde 3-phosphate to generate 2-deoxy-D-ribose 5-phosphate. Participates in stress granule (SG) assembly. May allow ATP production from extracellular deoxyinosine in conditions of energy deprivation.
sp O60610 DIAP1_HUMAN	Protein diaphanous homolog 1	Actin nucleation and elongation factor required for the assembly of F-actin structures, such as actin cables and stress fibres.
sp Q9H4M9 EHD1_HUMAN	EH domain-containing protein 1	ATP- and membrane-binding protein that controls membrane reorganization/tubulation upon ATP hydrolysis.
sp Q96A65 EXOC4_HUMAN	Exocyst complex component 4	Component of the exocyst complex involved in the docking of exocytic

Protein	Name	Function
		vesicles with fusion sites on the plasma membrane.
sp Q9UJY5 GGA1_HUMAN	ADP-ribosylation factor-binding protein GGA1	Plays a role in protein sorting and trafficking between the trans-Golgi network (TGN) and endosomes.
sp P04899 GNAI2_HUMAN	Guanine nucleotide-binding protein G	Guanine nucleotide-binding proteins (G proteins) are involved as modulators or transducers in various transmembrane signaling systems.
sp Q8NBJ5 GT251_HUMAN	Procollagen galactosyltransferase 1	Beta-galactosyltransferase that transfers beta-galactose to hydroxylysine residues of type I collagen.
sp Q9BZE4 GTPB4_HUMAN	GTP-binding protein 4	Involved in the biogenesis of the 60S ribosomal subunit.
sp Q12907 LMAN2_HUMAN	Vesicular integral-membrane protein VIP36	Plays a role as an intracellular lectin in the early secretory pathway.
sp Q5VWZ2 LYPL1_HUMAN	Lysophospholipase-like protein	Has depalmitoylating activity toward KCNMA1. Able to hydrolyse only short chain substrates due to its shallow active site.
sp Q86U44 MTA70_HUMAN	N6-adenosine-methyltransferase catalytic subunit	The METTL3-METTL14 heterodimer forms a N6-methyltransferase complex that methylates adenosine residues at the N(6) position of some RNAs and regulates various processes such as the circadian clock, differentiation of embryonic and hematopoietic stem cells, cortical neurogenesis, response to DNA damage, differentiation of T-cells and primary miRNA processing.
sp O60287 NPA1P_HUMAN	Nucleolar pre-ribosomal-associated protein 1	Involved in RNA binding.

Protein	Name	Function
sp Q8WVJ2 NUDC2_HUMAN	NudC domain-containing protein 2	May regulate the LIS1/dynein pathway by stabilizing LIS1 with Hsp90 chaperone.
sp O60313 OPA1_HUMAN	Dynamin-like 120 kDa protein, mitochondrial	Dynamin-related GTPase that is essential for normal mitochondrial morphology by regulating the equilibrium between mitochondrial fusion and mitochondrial fission.
sp O43913 ORC5_HUMAN	Origin recognition complex subunit 5	Component of the origin recognition complex (ORC) that binds origins of replication.
sp O15428 PINL_HUMAN	Putative PIN1-like protein	Enzyme with peptidyl-prolyl cis-trans isomerase activity.
sp Q9UKA9 PTBP2_HUMAN	Polypyrimidine tract-binding protein 2	RNA-binding protein which binds to intronic polypyrimidine tracts and mediates negative regulation of exons splicing.
sp Q02127 PYRD_HUMAN	Dihydroorotate dehydrogenase	Catalyses the conversion of dihydroorotate to orotate with quinone as electron acceptor.
sp P20742 PZP_HUMAN	Pregnancy zone protein	Is able to inhibit all four classes of proteinases by a unique 'trapping' mechanism.

Supplementary Table S2: List of unique proteins in mutant transfected cells

Protein	Name	Function
sp P05067 A4_HUMAN	Amyloid-beta precursor protein	Functions as a cell surface receptor and performs physiological functions on the surface of neurons relevant to neurite growth, neuronal adhesion and axonogenesis. Interaction between APP molecules on neighbouring cells promotes synaptogenesis.
sp O94805 ACL6B_HUMAN	Actin-like protein 6B	Involved in transcriptional activation and repression of select genes by chromatin remodelling (alteration of DNA-nucleosome topology).
sp O60678 ANM3_HUMAN	Protein arginine N-methyltransferase 3	Protein-arginine N-methyltransferase that catalyses both the monomethylation and asymmetric dimethylation of the guanidino nitrogens of arginine residues in target proteins, and therefore falls into the group of type I methyltransferase. May regulate retinoic acid synthesis and signaling by inhibiting ALDH1A1 retinal dehydrogenase activity.
sp Q13873 BMPR2_HUMAN	Bone morphogenetic protein receptor type-2	On ligand binding, forms a receptor complex consisting of two type II and two type I transmembrane serine/threonine kinases. Type II receptors phosphorylate and activate type I receptors which autophosphorylate, then bind and activate SMAD transcriptional regulators.

Protein	Name	Function
sp Q15059 BRD3_HUMAN	Bromodomain-containing protein 3	Chromatin reader that recognizes and binds hyperacetylated chromatin and plays a role in the regulation of transcription, probably by chromatin remodelling and interaction with transcription factors. Regulates transcription by promoting the binding of the transcription factor GATA1 to its targets.
sp Q9HC52 CBX8_HUMAN	Chromobox protein homolog 8	Component of a Polycomb group (PcG) multiprotein PRC1-like complex, a complex class required to maintain the transcriptionally repressive state of many genes, including Hox genes, throughout development. PcG PRC1 complex acts via chromatin remodelling and modification of histones; it mediates monoubiquitination of histone H2A 'Lys-119', rendering chromatin heritably changed in its expressibility.
sp Q96CT7 CC124_HUMAN	Coiled-coil domain-containing protein 124	Required for proper progression of late cytokinetic stages.
sp O76031 CLPX_HUMAN	ATP-dependent Clp protease ATP-binding subunit clpX-like, mitochondrial	ATP-dependent specificity component of the Clp protease complex. Targets specific substrates for degradation by the Clp complex.
sp Q5JTJ3 COA6_HUMAN	Cytochrome c oxidase assembly facto 6 homolog	Involved in the maturation of the mitochondrial respiratory chain complex IV subunit MT-CO2/COX2. Thereby, may regulate early steps of complex IV assembly.
sp P67870 CSK2B_HUMAN	Casein kinase II subunit beta	Regulatory subunit of casein kinase II/CK2. As part of the

Protein	Name	Function
		kinase complex regulates the basal catalytic activity of the alpha subunit a constitutively active serine/threonine-protein kinase that phosphorylates a large number of substrates containing acidic residues C-terminal to the phosphorylated serine or threonine.
sp Q13616 CUL1_HUMAN	Cullin-1	Core component of multiple cullin-RING-based SCF (SKP1-CUL1-F-box protein) E3 ubiquitin-protein ligase complexes, which mediate the ubiquitination of proteins involved in cell cycle progression, signal transduction and transcription.
sp O60231_DHX16_HUMAN	Pre-mRNA-splicing factor ATP-dependent RNA helicase DHX16	Required for pre-mRNA splicing as component of the spliceosome.
sp P09884 DPOA_HUMAN	DNA polymerase alpha catalytic subunit	Catalytic subunit of the DNA polymerase alpha complex (also known as the alpha DNA polymerase-primase complex) which plays an essential role in the initiation of DNA synthesis.
sp Q5T1H1 EYS_HUMAN	Protein eyes shut homology	Required to maintain the integrity of photoreceptor cells.
sp Q8WXD5 GEMI6_HUMAN	Gem-associated protein 6	The SMN complex catalyses the assembly of small nuclear ribonucleoproteins (snRNPs), the building blocks of the spliceosome, and thereby plays an important role in the splicing of cellular pre-mRNAs.
sp Q9H3K2 GHITM_HUMAN	Growth hormone-inducible transmembrane protein	Required for the mitochondrial tubular network and cristae

Protein	Name	Function
		organization. Involved in apoptotic release of cytochrome c.
sp P34931 HS71L_HUMAN	Heat shock 70 kDa protein 1-like	Molecular chaperone implicated in a wide variety of cellular processes, including protection of the proteome from stress, folding and transport of newly synthesized polypeptides, activation of proteolysis of misfolded proteins and the formation and dissociation of protein complexes. Plays a pivotal role in the protein quality control system, ensuring the correct folding of proteins, the re-folding of misfolded proteins and controlling the targeting of proteins for subsequent degradation.
sp Q9NX55 HYPK_HUMAN	Huntingtin-interacting protein K	Component of several N-terminal acetyltransferase complexes.
sp Q9HA64 KT3K_HUMAN	Ketosamine-3-kinase	Ketosamine-3-kinase involved in protein deglycation by mediating phosphorylation of ribuloselysine and psicoselysine on glycosylated proteins, to generate ribuloselysine-3 phosphate and psicoselysine-3 phosphate, respectively. Ribuloselysine-3 phosphate and psicoselysine-3 phosphate adducts are unstable and decompose under physiological conditions.
sp Q9H9P8 L2HDH_HUMAN	L-2-hydroxyglutarate dehydrogenase, mitochondrial	Mitochondrial enzyme with (S)-2-hydroxy-acid oxidase activity and 2-hydroxyglutarate dehydrogenase activity.
sp Q9NX58 LYAR_HUMAN	Cell growth-regulating nucleolar protein	Plays a role in the maintenance of the appropriate processing of

Protein	Name	Function
		47S/45S pre-rRNA to 32S/30S pre-rRNAs and their subsequent processing to produce 18S and 28S rRNAs. Also acts at the level of transcription regulation.
sp Q9H0A0 NAT10_HUMAN	RNA cytidine acetyltransferase	RNA cytidine acetyltransferase that catalyses the formation of N(4)-acetylcytidine (ac4C) modification on mRNAs, 18S rRNA and tRNAs. Catalyses ac4C modification of a broad range of mRNAs, enhancing mRNA stability and translation.
sp O00712 NFIB_HUMAN	Nuclear factor 1 B-type	Transcriptional activator of GFAP, essential for proper brain development.
sp Q9BVI4 NOC4L_HUMAN	Nucleolar complex protein 4 homology	Involved in RNA binding.
sp Q96P11 NSUN5_HUMAN	28s rRNA (cytosine-C(5))-methyltransferase	S-adenosyl-L-methionine-dependent methyltransferase that specifically methylates the C(5) position of cytosine 3782 (m5C3782) in 28S rRNA. m5C3782 promotes protein translation without affecting ribosome biogenesis and fidelity.
sp P13674 P4HA1_HUMAN	Prolyl 4-hydroxylase subunit alpha-1	Catalyses the post-translational formation of 4-hydroxyproline in -Xaa-Pro-Gly- sequences in collagens and other proteins.
sp P51003 PAPOA_HUMAN	Poly(A) polymerase alpha	Polymerase that creates the 3'-poly(A) tail of mRNAs. Also required for the endoribonucleolytic cleavage reaction at some polyadenylation sites.
sp Q9NTI5 PDS5B_HUMAN	Sister chromatid cohesion protein PDS5 homolog B	Regulator of sister chromatid cohesion in mitosis which may stabilize cohesin complex

Protein	Name	Function
		association with chromatin. May couple sister chromatid cohesion during mitosis to DNA replication. Cohesion ensures that chromosome partitioning is accurate in both meiotic and mitotic cells and plays an important role in DNA repair.
sp Q63HM9 PLCX3_HUMAN	PI-PLC X domain-containing protein 3	Enzyme with phosphoric diester hydrolase activity.
sp Q86TP1 PRUN1_HUMAN	Exopolyphosphatase PRUNE1	Phosphodiesterase (PDE) that has higher activity toward cAMP than cGMP, as substrate. Plays a role in cell proliferation, migration, and differentiation, and acts as a negative regulator of NME1.
sp Q15269 PWP2_HUMAN	Periodic tryptophan protein 2 homology	Involved in RNA binding.
sp P20338 RAB4A_HUMAN	Ras-related protein Rab-4A	Small GTPase which cycles between an active GTP-bound and an inactive GDP-bound state. Involved in protein transport and in vesicular traffic.
sp Q9H5N1 RABE2_HUMAN	Rab GTPase-binding effector protein 2	Plays a role in membrane trafficking and in homotypic early endosome fusion.
sp P35251 RFC1_HUMAN	Replication factor C subunit 1	The elongation of primed DNA templates by DNA polymerase delta and epsilon requires the action of the accessory proteins PCNA and activator 1. This subunit binds to the primer-template junction.
sp P19388 RPAB1_HUMAN	DNA-directed RNA polymerases I, II, and III subunit RPABC1	DNA-dependent RNA polymerase catalyses the transcription of DNA into RNA using the four ribonucleoside triphosphates as substrates. Common component of RNA

Protein	Name	Function
		polymerases I, II and III which synthesize ribosomal RNA precursors, mRNA precursors and many functional non-coding RNAs, and small RNAs, such as 5S rRNA and tRNAs, respectively.
sp Q9Y399}RT02_HUMAN	28S ribosomal protein S2, mitochondrial	Required for mitoribosome formation and stability, and mitochondrial translation.
sp Q9UBV2 SE1L1_HUMAN	Protein sel-1 homolog 1	Plays a role in the endoplasmic reticulum quality control (ERQC) system also called ER-associated degradation (ERAD) involved in ubiquitin-dependent degradation of misfolded endoplasmic reticulum proteins.
sp Q8WVK2 SNR27_HUMAN	U4/U6.U5 small nuclear ribonucleoprotein 27 kDa protein	May play a role in mRNA splicing.
sp P08240 SRPRA_HUMAN	Signal recognition particle receptor subunit alpha	Component of the signal recognition particle (SRP) complex receptor (SR). Ensures, in conjunction with the SRP complex, the correct targeting of the nascent secretory proteins to the endoplasmic reticulum membrane system.
sp Q13033 STRN3_HUMAN	Striatin-3	Binds calmodulin in a calcium dependent manner. May function as scaffolding or signaling protein.
sp O60220 TIM8A_HUMAN	Mitochondrial import inner membrane translocase subunit Tim8 A	Mitochondrial intermembrane chaperone that participates in the import and insertion of some multi-pass transmembrane proteins into the mitochondrial inner membrane.

Protein	Name	Function
sp Q56UQ5 TPT1L_HUMAN	TPT1-lik protein	Involved in calcium ion binding.
sp O75152 ZC11A_HUMAN	Zinc finger CCCH domain-containing protein 11A	RNA-binding protein that interacts with purine-rich sequences and is involved in nuclear mRNA export; probably mediated by association with the TREX complex.
sp Q96ME7 ZN512_HUMAN	Zinc finger protein 512	May be involved in transcriptional regulation.

Supplementary Table S3: List of unique proteins in non-transfected cells

Protein	Name	Function
sp Q9ULX6 AKP8L_HUMAN	A-kinase anchor protein 8-like	Could play a role in constitutive transport element (CTE)-mediated gene expression by association with DHX9.
sp Q75179 ANR17_HUMAN	Ankyrin repeat domain-containing protein 2	Could play pivotal roles in cell cycle and DNA regulation.
sp Q6PL18 ATAD2_HUMAN	ATPase family AAA domain-containing protein 2	May be a transcriptional coactivator of the nuclear receptor ESR1 required to induce the expression of a subset of oestradiol target genes, such as CCND1, MYC and E2F1.
sp P55957 BID_HUMAN	BH3-interacting domain death agonist	Induces caspases and apoptosis .
sp Q8WUQ7 CATIN_HUMAN	Cactin	Involved in the regulation of innate immune response. Acts as negative regulator of Toll-like receptor, interferon-regulatory factor (IRF) and canonical NF-kappa-B signaling pathways.
sp P09669 COX6C_HUMAN	Cytochrome c oxidase subunit 6C	Component of the cytochrome c oxidase, the last enzyme in the mitochondrial electron transport chain which drives oxidative phosphorylation.
sp Q9Y4B6 DCAF1_HUMAN	DDB1- and CUL4-associated factor 1	Acts both as a substrate recognition component of E3 ubiquitin-protein ligase complexes and as an atypical serine/threonine-protein kinase, playing key roles in various processes such as cell cycle, telomerase regulation and histone modification.
sp Q16698 DECR_HUMAN	2,4-dienoyl-CoA reductase [(3E)-enoyl-	Auxiliary enzyme of beta-oxidation. It participates in the

Protein	Name	Function
	CoA-producing], mitochondrial	metabolism of unsaturated fatty enoyl-CoA esters having double bonds in both even- and odd-numbered positions in mitochondria.
sp Q01780 EXOSX_HUMAN	Exosome component 10	Putative catalytic component of the RNA exosome complex which has 3'->5' exoribonuclease activity and participates in a multitude of cellular RNA processing and degradation events.
sp P23142 FBLN1_HUMAN	Fibulin-1	Incorporated into fibronectin-containing matrix fibres. May play a role in cell adhesion and migration along protein fibres within the extracellular matrix (ECM).
sp Q8TAE8 G45IP_HUMAN	Growth arrest and DNA damage-inducible proteins-interacting protein 1	Acts as a negative regulator of G1 to S cell cycle phase progression by inhibiting cyclin-dependent kinases.
sp Q2TB90 HKDC1_HUMAN	Hexokinase HKDC1	Catalyses the phosphorylation of hexose to hexose 6-phosphate, although at very low level compared to other hexokinases. Involved in glucose homeostasis and hepatic lipid accumulation.
sp Q9BW19 KIFC1_HUMAN	Kinesin-like protein KIFC1	Minus end-directed microtubule-dependent motor required for bipolar spindle formation.
sp P05771 KPCB_HUMAN	Protein kinase C beta type	Calcium-activated, phospholipid- and diacylglycerol (DAG)-dependent serine/threonine-protein kinase involved in various cellular processes such as regulation of the B-cell receptor (BCR) signalosome, oxidative stress-induced apoptosis, androgen receptor-dependent transcription

Protein	Name	Function
		regulation, insulin signaling and endothelial cells proliferation.
sp Q9Y4Y9 LSM5_HUMAN	U6 snRNA-associated Sm-like protein LSm5	Plays role in pre-mRNA splicing as component of the U4/U6-U5 tri-snRNP complex that is involved in spliceosome assembly, and as component of the pre-catalytic spliceosome (spliceosome B complex).
sp Q86UE4 LYRIC_HUMAN	Protein LYRIC	Down-regulates SLC1A2/EAAT2 promoter activity when expressed ectopically. Activates the nuclear factor kappa-B (NF-kappa-B) transcription factor.
sp Q96S90 LYSM1_HUMAN	LysM and putative peptidoglycan-binding domain-containing protein 1	Enables protein binding.
sp Q9NQX4 MYO5C_HUMAN	Unconventional myosin-Vc	May be involved in transferrin trafficking. Likely to power actin-based membrane trafficking in many physiologically crucial tissues.
sp Q9H1E3 NUCKS_HUMAN	Nuclear ubiquitous casein and cyclin-dependent kinase substrate 1	Chromatin-associated protein involved in DNA repair by promoting homologous recombination (HR).
sp P50479 PDLI4_HUMAN	PDZ and LIM domain protein 4	Suppresses SRC activation by recognizing and binding to active SRC and facilitating PTPN13-mediated dephosphorylation of SRC 'Tyr-419' leading to its inactivation. Inactivated SRC dissociates from this protein allowing the initiation of a new SRC inactivation cycle. Involved in reorganization of the actin cytoskeleton.

Protein	Name	Function
sp O00541 PESC_HUMAN	Pescadillo homolog	Component of the PeBoW complex, which is required for maturation of 28S and 5.8S ribosomal RNAs and formation of the 60S ribosome.
sp P50336 PPOX_HUMAN	Protoporphyrinogen oxidase	Catalyses the 6-electron oxidation of protoporphyrinogen-IX to form protoporphyrin-IX.
sp P48634 PRC2A_HUMAN	Protein PRRC2A	May play a role in the regulation of pre-mRNA splicing.
sp Q15397 PUM3_HUMAN	Pumilio homolog 3	Inhibits the poly(ADP-ribosyl)ation activity of PARP1 and the degradation of PARP1 by CASP3 following genotoxic stress.
sp Q6DKI1 RL7L_HUMAN	60S ribosomal protein L7-like 1	Structural constituent of ribosome, involved in RNA binding.
sp Q13084 RM28_HUMAN	39S ribosomal protein L28, mitochondrial	Structural constituent of ribosome, involved in RNA binding.
sp P62841 RS15_HUMAN	40S ribosomal protein S15	Structural constituent of ribosome, involved in RNA binding, DNA binding, MDM2/MDM4 family protein binding, ubiquitin ligase inhibitor activity.
sp Q9NP81 SYSM_HUMAN	Serine—tRNA ligase, mitochondrial	Catalyses the attachment of serine to tRNA(Ser).
sp O15164 TIF1A_HUMAN	Transcription intermediary factor 1-alpha	Transcriptional coactivator that interacts with numerous nuclear receptors and coactivators and modulates the transcription of target genes.
sp Q08AM6 VAC14_HUMAN	Protein VAC14 homolog	Scaffold protein component of the PI(3,5)P2 regulatory complex which regulates both the synthesis and turnover of phosphatidylinositol 3,5-bisphosphate (PtdIns(3,5)P2).
sp QWIWA0 WDR75_HUMAN	WD repeat-containing protein 75	Ribosome biogenesis factor. Involved in nucleolar processing of pre-18S ribosomal RNA.

Protein	Name	Function
		Required for optimal pre-ribosomal RNA transcription by RNA polymerase I.

Supplementary Table S4: List of unique proteins in empty vector transfected cells

Protein	Name	Function
sp Q96IU4 ABHEB_HUMAN	Protein ABHD14B	Has hydrolase activity towards p-nitrophenyl butyrate (in vitro). May activate transcription.
sp Q6ZN18 AEBP2_HUMAN	Zinc finger protein AEBP2	Acts as an accessory subunit for the core Polycomb repressive complex 2 (PRC2), which mediates histone H3K27 (H3K27me3) trimethylation on chromatin leading to transcriptional repression of the affected target gene.
sp P43652 AFAM_HUMAN	Afamin	Functions as carrier for hydrophobic molecules in body fluids. Essential for the solubility and activity of lipidated Wnt family members.
sp Q8TD16 BICD2_HUMAN	Protein bicaudal D homolog 2	Acts as an adapter protein linking the dynein motor complex to various cargos and converts dynein from a non-processive to a highly processive motor in the presence of dynactin.
sp Q8TDN6 BRX1_HUMAN	Ribosome biogenesis protein BRX1 homolog	Required for biogenesis of the 60S ribosomal subunit.
sp Q08554 DSC1_HUMAN	Desmocollin-1	Component of intercellular desmosome junctions. Involved in the interaction of plaque proteins and intermediate filaments mediating cell-cell adhesion.
sp O75477 ERLN1_HUMAN	Erlin-1	Component of the ERLIN1/ERLIN2 complex which mediates the

Protein	Name	Function
		endoplasmic reticulum-associated degradation (ERAD) of inositol 1,4,5-trisphosphate receptors (IP3Rs).
sp Q5T3I0 GPTC4_HUMAN	G patch domain-containing protein 4	Involved in the regulation of cell growth and nucleolar structure.
sp P07203 GPX1_HUMAN	Glutathione peroxidase 1	Protects the haemoglobin in erythrocytes from oxidative breakdown.
sp P02008 HBAZ_HUMAN	Haemoglobin subunit zeta	The zeta chain is an alpha-type chain of mammalian embryonic haemoglobin.
sp P02042 HBD_HUMAN	Haemoglobin subunit delta	Involved in oxygen transport from the lung to the various peripheral tissues.
sp Q9Y3E1 HDGR3_HUMAN	Hepatoma-derived growth factor-related protein 3	Enhances DNA synthesis and may play a role in cell proliferation.
sp Q9NP66 HM20A_HUMAN	High mobility group protein 20A	Plays a role in neuronal differentiation as chromatin-associated protein.
sp P19013 K2C4_HUMAN	Keratin, type II cytoskeletal 4	Involved in cytoskeleton organization, epithelial cell differentiation and negative regulation of epithelial cell proliferation.
sp Q8N1N4 K2C78_HUMAN	Keratin, type II cytoskeletal 78	Protein with an intermediate filament domain. Keratins are the major structural proteins in epithelial cells.
sp Q13554 KCC2B_HUMAN	Calcium/calmodulin-dependent protein kinase type II subunit beta	Calcium/calmodulin-dependent protein kinase that functions autonomously after Ca ²⁺ /calmodulin-binding and autophosphorylation, and is involved in dendritic spine and synapse formation,

Protein	Name	Function
		neuronal plasticity, and regulation of sarcoplasmic reticulum Ca(2+) transport in skeletal muscle.
sp Q16626 MEA1_HUMAN	Male-enhanced antigen 1	May play an important role in spermatogenesis and/or testis development.
sp Q9UHG2 PCS1N_HUMAN	ProSAAS	May function in the control of the neuroendocrine secretory pathway.
sp A2A3N6 PIPSL_HUMAN	Putative PIP5K1A and PSMD4-like protein	Has negligible PIP5 kinase activity. Binds to ubiquitinated proteins.
sp P35813 PPM1A_HUMAN	Protein phosphatase 1A	Enzyme with a broad specificity. Negatively regulates TGF-beta signaling through dephosphorylating SMAD2 and SMAD3, resulting in their dissociation from SMAD4, nuclear export of the SMADs and termination of the TGF-beta-mediated signaling.
sp P06702 S10A9_HUMAN	Protein S100-A9	S100A9 is a calcium- and zinc-binding protein which plays a prominent role in the regulation of inflammatory processes and immune response.
sp Q5PRF9 SMAG2_HUMAN	Protein Smaug homolog 2	Has transcriptional repressor activity. Overexpression inhibits the transcriptional activities of AP-1, p53/TP53 and CDKN1A.
sp Q9H4B7 TBB1_HUMAN	Tubulin beta-1 chain	Tubulin is the major constituent of microtubules.
sp Q5QJE6 TDIF2_HUMAN	Deoxynucleotidyltransferase terminal-interacting protein 2	Regulates the transcriptional activity of DNNT and ESR1.

Protein	Name	Function
		May function as a chromatin remodelling protein.
sp Q96EK4 THA11_HUMAN	THAP domain-containing protein 11	Transcriptional repressor that plays a central role for embryogenesis and the pluripotency of embryonic stem (ES) cells.
sp Q86VY4 TSYL5_HUMAN	Testis-specific T-encoded-like protein 5	Involved in modulation of cell growth and cellular response to gamma radiation probably via regulation of the Akt signaling pathway.
sp Q9H832 UBE2Z_HUMAN	Ubiquitin-conjugating enzyme E2 Z	Catalyses the covalent attachment of ubiquitin to other proteins.
sp P16989 YBOX3_HUMAN	Y-box-binding protein 3	Binds to the GM-CSF promoter. Seems to act as a repressor. May have a role in translation repression.

Supplementary Table S5 : List of proteins differentially abundant between wild-type transfected and non-transfected cells

Fold Change	Protein	Name	Function
Less Abundant			
-1.8566911	sp Q9Y3U8 RL36_HUMAN	60S ribosomal protein 36	Component of the large ribosomal subunit.
-1.6788144	sp Q86Y82 STX12_HUMAN	Syntaxin-12	SNARE that acts to regulate protein transport between late endosomes and the trans-Golgi network. The SNARE complex containing STX6, STX12, VAMP4 and VTI1A mediates vesicle fusion
-1.121847	sp Q15637 SF01_HUMAN	Splicing factor 1	Necessary for the ATP-dependent first step of spliceosome assembly. Binds to the intron branch point sequence (BPS) 5'-UACUAAC-3' of the pre-mRNA. May act as transcription repressor.
-1.0410199	sp Q9Y520 PRC2C_HUMAN	Protein PRRC2C	Required for efficient formation of stress granules.
-0.74689996	sp P38159 RBMX_HUMAN	RNA-binding motif protein, X chromosome	RNA-binding protein that plays several roles in the regulation of pre- and post-transcriptional processes. Implicated in tissue-specific regulation of gene transcription and alternative splicing of several pre-mRNAs.
-0.6849414	sp P23588 IF4B_HUMAN	Eukaryotic translation initiation factor 4B	Required for the binding of mRNA to ribosomes

Fold Change	Protein	Name	Function
-0.5337738	sp P53999 TCP4_HUMAN	Activated RNA polymerase II transcriptional coactivator p15	General coactivator that functions cooperatively with TAFs and mediates functional interactions between upstream activators and the general transcriptional machinery. May be involved in stabilizing the multiprotein transcription complex. Binds single-stranded DNA.
-0.50896925	sp P37837 TALDO_HUMAN	Transaldolase	Transaldolase is important for the balance of metabolites in the pentose-phosphate pathway.
-0.37183204	sp P78406 RAE1L_HUMAN	mRNA export factor	Plays a role in mitotic bipolar spindle formation. Binds mRNA. May function in nucleocytoplasmic transport and in directly or indirectly attaching cytoplasmic mRNPs to the cytoskeleton.
-0.3331039	sp P62826 RAN_HUMAN	GTP-binding nuclear protein Ran	GTPase involved in nucleocytoplasmic transport, participating both to the import and the export from the nucleus of proteins and RNAs
-0.30670425	sp Q01518 CAP1_HUMAN	Adenylyl cyclase-associated protein 1	Directly regulates filament dynamics and has been implicated in a number of complex developmental and morphological processes, including mRNA localization and the establishment of cell polarity.

Fold Change	Protein	Name	Function
More Abundant			
0.33976412	sp P31939 PUR9_HUMAN	Bifunctional purine biosynthesis protein ATIC	Bifunctional enzyme that catalyzes the last two steps of purine biosynthesis
0.35881603	sp Q07866 KLC1_HUMAN	Kinesin light chain 1	Kinesin is a microtubule-associated force-producing protein that may play a role in organelle transport. The light chain may function in coupling of cargo to the heavy chain or in the modulation of its ATPase activity.
0.37648672	sp P11586 C1TC_HUMAN	C-1-tetrahydrofolate synthase, cytoplasmic	This protein is involved in the pathway tetrahydrofolate interconversion, which is part of One-carbon metabolism.
0.38646522	sp P27708 PYR1_HUMAN	CAD protein	This protein is a 'fusion' protein encoding four enzymatic activities of the pyrimidine pathway (GATase, CPSase, ATCase and DHOase).
0.3885932	sp P62495 ERF1_HUMAN	Eukaryotic peptide chain release factor subunit 1	Directs the termination of nascent peptide synthesis (translation) in response to the termination codons UAA, UAG and UGA.
0.41403818	sp P69905 HBA_HUMAN	Hemoglobin subunit alpha	Involved in oxygen transport from the lung to the various peripheral tissues.
0.42103648	sp P50395 GDIB_HUMAN	Rab GDP dissociation inhibitor beta	Regulates the GDP/GTP exchange reaction of most Rab proteins by inhibiting the dissociation of GDP from them, and the

Fold Change	Protein	Name	Function
			subsequent binding of GTP to them.
0.4262979	sp P10768 ESTD_HUMAN	S-formylglutathione hydrolase	Serine hydrolase involved in the detoxification of formaldehyde.
0.43407574	sp Q9UBB4 ATX10_HUMAN	Ataxin-10	Necessary for the survival of cerebellar neurons. Induces neuritogenesis by activating the Ras-MAP kinase pathway. May play a role in the maintenance of a critical intracellular glycosylation level and homeostasis.
0.43839556	sp Q9Y3I0 RTCB_HUMAN	RNA-splicing ligase RtcB homolog	Catalytic subunit of the tRNA-splicing ligase complex that acts by directly joining spliced tRNA halves to mature-sized tRNAs by incorporating the precursor-derived splice junction phosphate into the mature tRNA as a canonical 3',5'-phosphodiester. May act as an RNA ligase with broad substrate specificity and may function toward other RNAs.
0.50248647	sp P02786 TFR1_HUMAN	Transferrin receptor protein 1	Cellular uptake of iron occurs via receptor-mediated endocytosis of ligand-occupied transferrin receptor into specialized endosomes. Acts as a lipid sensor that regulates mitochondrial fusion by regulating activation of the JNK pathway.

Fold Change	Protein	Name	Function
0.5164809	sp P35998 PRS7_HUMAN	26S proteasome regulatory subunit 7	Component of the 26S proteasome, a multiprotein complex involved in the ATP-dependent degradation of ubiquitinated proteins.
0.5284708	sp P0DN79 CBSL_HUMAN	Cystathionine beta-synthase-like protein	Hydro-lyase catalyzing the first step of the transsulfuration pathway, where the hydroxyl group of L-serine is displaced by L-homocysteine in a beta-replacement reaction to form L-cystathionine, the precursor of L-cysteine. This catabolic route allows the elimination of L-methionine and the toxic metabolite L-homocysteine. Also involved in the production of hydrogen sulfide, a gasotransmitter with signaling and cytoprotective effects on neurons.
0.53512836	sp P23381 SYWC_HUMAN	Tryptophan--tRNA ligase, cytoplasmic	Regulates ERK, Akt, and eNOS activation pathways that are associated with angiogenesis, cytoskeletal reorganization, and shear stress-responsive gene expression.
0.54786944	sp Q99873 ANM1_HUMAN	Protein arginine N-methyltransferase 1	Arginine methyltransferase that methylates (mono and asymmetric dimethylation) the guanidino nitrogens of arginyl residues present in proteins such as ESR1, histone H2, H3 and H4, ILF3, HNRNPA1,

Fold Change	Protein	Name	Function
			HNRNPD, NFATC2IP, SUPT5H, TAF15, EWS, HABP4 and SERBP1
0.57735336	sp Q14141 SEPT6_HUMAN	Septin-6	Filament-forming cytoskeletal GTPase. Required for normal organization of the actin cytoskeleton. Involved in cytokinesis.
0.58534056	sp P14324 FPPS_HUMAN	Farnesyl pyrophosphate synthase	Key enzyme in isoprenoid biosynthesis which catalyzes the formation of farnesyl diphosphate (FPP), a precursor for several classes of essential metabolites including sterols, dolichols, carotenoids, and ubiquinones.
0.59459674	sp Q9BT78 CSN4_HUMAN	COP9 signalosome complex subunit 4	Component of the COP9 signalosome complex (CSN), a complex involved in various cellular and developmental processes. The CSN complex is an essential regulator of the ubiquitin (Ubl) conjugation pathway.
0.6055922	sp P21912 SDHB_HUMAN	Succinate dehydrogenase [ubiquinone] iron-sulfur subunit, mitochondrial	Iron-sulfur protein (IP) subunit of succinate dehydrogenase (SDH) that is involved in complex II of the mitochondrial electron transport chain and is responsible for transferring electrons from succinate to ubiquinone (coenzyme Q).

Fold Change	Protein	Name	Function
0.61219233	sp P17174 AATC_HUMAN	Aspartate aminotransferase, cytoplasmic	Biosynthesis of L-glutamate from L-aspartate or L-cysteine. Important regulator of levels of glutamate, the major excitatory neurotransmitter of the vertebrate central nervous system. Acts as a scavenger of glutamate in brain neuroprotection.
0.61734223	sp P33992 MCM5_HUMAN	DNA replication licensing factor MCM5	Acts as component of the MCM2-7 complex (MCM complex) which is the putative replicative helicase essential for 'once per cell cycle' DNA replication initiation and elongation in eukaryotic cells.
0.6257046	sp P54577 SYYC_HUMAN	Tyrosine--tRNA ligase, cytoplasmic	Catalyzes the attachment of tyrosine to tRNA(Tyr) in a two-step reaction: tyrosine is first activated by ATP to form Tyr-AMP and then transferred to the acceptor end of tRNA(Tyr).
0.71930486	sp P33176 KINH_HUMAN	Kinesin-1 heavy chain	Microtubule-dependent motor required for normal distribution of mitochondria and lysosomes.
0.72144926	sp P31930 QCR1_HUMAN	Cytochrome b-c1 complex subunit 1, mitochondrial	Component of the ubiquinol-cytochrome c oxidoreductase, a multisubunit transmembrane complex that is part of the mitochondrial electron transport chain which drives oxidative phosphorylation.

Fold Change	Protein	Name	Function
0.7647878	sp P49257 LMAN1_HUMAN	Protein ERGIC-53	Mannose-specific lectin. May recognize sugar residues of glycoproteins, glycolipids, or glycosylphosphatidyl inositol anchors and may be involved in the sorting or recycling of proteins, lipids, or both.
0.8274879	sp P22695 QCR2_HUMAN	Cytochrome b-c1 complex subunit 2, mitochondrial	Component of the ubiquinol-cytochrome c oxidoreductase, a multisubunit transmembrane complex that is part of the mitochondrial electron transport chain which drives oxidative phosphorylation.
0.88206655	sp Q06203 PUR1_HUMAN	Amidophosphoribosyl-transferase	This protein is involved in step 1 of the subpathway that synthesizes N(1)-(5-phospho-D-ribosyl)glycinamide from 5-phospho-alpha-D-ribose 1-diphosphate. This subpathway is part of the pathway IMP biosynthesis via de novo pathway, which is itself part of Purine metabolism.
0.8948843	sp P01023 A2MG_HUMAN	Alpha-2-macroglobulin	Is able to inhibit all four classes of proteinases by a unique 'trapping' mechanism.
0.913311	sp P52788 SPSY_HUMAN	Spermine synthase	Catalyzes the production of spermine from spermidine and decarboxylated S-

Fold Change	Protein	Name	Function
			adenosylmethionine (dcSAM).
0.93997234	sp Q15631 TSN_HUMAN	Translin	DNA-binding protein that specifically recognizes consensus sequences at the breakpoint junctions in chromosomal translocations, mostly involving immunoglobulin (Ig)/T-cell receptor gene segments. Seems to recognize single-stranded DNA ends generated by staggered breaks occurring at recombination hot spots. Exhibits both single-stranded and double-stranded endoribonuclease activity. May act as an activator of RNA-induced silencing complex (RISC) by facilitating endonucleolytic cleavage of the siRNA passenger strand.
0.9789583	sp P35222 CTNB1_HUMAN	Catenin beta-1	Key downstream component of the canonical Wnt signaling pathway.
1.062929	sp O94905 ERLN2_HUMAN	Erlin-2	Component of the ERLIN1/ERLIN2 complex which mediates the endoplasmic reticulum-associated degradation (ERAD) of inositol 1,4,5-trisphosphate receptors (IP3Rs) such as ITPR1.
1.1214811	sp Q15126 PMVK_HUMAN	Phosphomevalonate kinase	Catalyzes the reversible ATP-dependent phosphorylation of mevalonate 5-phosphate to produce mevalonate diphosphate and ADP, a key step in the mevalonic

Fold Change	Protein	Name	Function
			acid mediated biosynthesis of isopentenyl diphosphate and other polyisoprenoid metabolites.
1.1282995	sp O43172 PRP4_HUMAN	U4/U6 small nuclear ribonucleoprotein Prp4	Plays role in pre-mRNA splicing as component of the U4/U6-U5 tri-snRNP complex that is involved in spliceosome assembly, and as component of the precatalytic spliceosome (spliceosome B complex).
1.1322798	sp Q14165 MLEC_HUMAN	Malectin	Carbohydrate-binding protein with a strong ligand preference for Glc2-N-glycan. May play a role in the early steps of protein N-glycosylation.
1.2741292	sp O94925 GLSK_HUMAN	Glutaminase kidney isoform, mitochondrial	Catalyzes the first reaction in the primary pathway for the renal catabolism of glutamine. Plays a role in maintaining acid-base homeostasis. Regulates the levels of the neurotransmitter glutamate, the main excitatory neurotransmitter in the brain.
1.4723604	sp P15927 RFA2_HUMAN	Replication protein A 32 kDa subunit	Plays an essential role both in DNA replication and the cellular response to DNA damage.
1.7921993	sp O95251 KAT7_HUMAN	Histone acetyltransferase KAT7	Catalytic subunit of histone acetyltransferase HBO1 complexes, which specifically mediate acetylation of histone H3 at 'Lys-14' (H3K14ac),

Fold Change	Protein	Name	Function
			thereby regulating various processes, such as gene transcription, protein ubiquitination, immune regulation, stem cell pluripotent and self-renewal maintenance, and embryonic development.
2.1607912	sp Q6DKJ4 NXN_HUMAN	Nucleoredoxin	Functions as a redox-dependent negative regulator of the Wnt signaling pathway, possibly by preventing ubiquitination of DVL3 by the BCR(KLHL12) complex.
2.1607912	sp O95782 AP2A1_HUMAN	AP-2 complex subunit alpha-1	Component of the adaptor protein complex 2 (AP-2). Adaptor protein complexes function in protein transport via transport vesicles in different membrane traffic pathways.
2.7564037	sp P49589 SYCC_HUMAN	Cysteine--tRNA ligase, cytoplasmic	Catalyzes the ATP-dependent ligation of cysteine to tRNA(Cys).

Supplementary Table S6 : List of proteins differentially abundant between mutant transfected and non-transfected cells

Fold Change	Protein	Name	Function
Less Abundant			
-4.788916	sp P62249 RS16_HUMAN	40S ribosomal protein S16	Structural constituent of ribosome
-2.5582538	sp Q9BYD1 RM13_HUMAN	39S ribosomal protein L13, mitochondrial	Structural constituent of ribosome
-1.3551227	sp Q13505 MTX1_HUMAN	Metaxin-1	Involved in transport of proteins into the mitochondrion.
-1.1169671	sp Q9Y3B7 RM11_HUMAN	39S ribosomal protein L11, mitochondrial	Structural constituent of ribosome
-1.0647981	sp Q9Y263 PLAP_HUMAN	Phospholipase A-2-activating protein	Plays a role in protein ubiquitination, sorting and degradation through its association with VCP.
-0.853262	sp P78406 RAE1L_HUMAN	mRNA export factor	Binds mRNA. May function in nucleocytoplasmic transport and in directly or indirectly attaching cytoplasmic mRNPs to the cytoskeleton.
-0.8214491	sp Q9C0B1 FTO_HUMAN	Alpha-ketoglutarate-dependent dioxygenase FTO	RNA demethylase that mediates oxidative demethylation of different RNA species and acts as a regulator of fat mass, adipogenesis and energy homeostasis.
-0.69306874	sp P25705 ATPA_HUMAN	ATP synthase subunit alpha, mitochondrial	Mitochondrial membrane ATP synthase produces ATP from ADP in the presence of a proton gradient across the membrane which is

Fold Change	Protein	Name	Function
			generated by electron transport complexes of the respiratory chain.
-0.63297874	sp P35268 RL22_HUMAN	60S ribosomal protein L22	Structural constituent of ribosome.
-0.6043899	sp Q01518 CAP1_HUMAN	Adenylyl cyclase-associated protein 1	Directly regulates filament dynamics and has been implicated in a number of complex developmental and morphological processes, including mRNA localization and the establishment of cell polarity.
-0.57859886	sp P62826 RAN_HUMAN	GTP-binding nuclear protein Ran	GTPase involved in nucleocytoplasmic transport, participating both to the import and the export from the nucleus of proteins and RNAs.
-0.5629891	sp P00505 AATM_HUMAN	Aspartate aminotransferase, mitochondrial	Catalyzes the irreversible transamination of the L-tryptophan metabolite L-kynurenine to form kynurenic acid (KA). As a member of the malate-aspartate shuttle, it has a key role in the intracellular NAD(H) redox balance. Is important for metabolite exchange between mitochondria and cytosol, and for amino acid metabolism.
-0.5335376	sp P37837 TALDO_HUMAN	Transaldolase	Important for the balance of metabolites in the

Fold Change	Protein	Name	Function
			pentose-phosphate pathway.
-0.46492887	sp P05141 ADT2_HUMAN	ADP/ATP translocase 2	ADP: ATP antiporter that mediates import of ADP into the mitochondrial matrix for ATP synthesis, and export of ATP out to fuel the cell.
-0.45635405	sp P62913 RL11_HUMAN	60S ribosomal protein L11	Component of the ribosome, a large ribonucleoprotein complex responsible for the synthesis of proteins in the cell.
-0.44090268	sp P33993 MCM7_HUMAN	DNA replication licensing factor MCM7	Acts as component of the MCM2-7 complex (MCM complex) which is the putative replicative helicase essential for 'once per cell cycle' DNA replication initiation and elongation in eukaryotic cells.
-0.4202304	sp P61247 RS3A_HUMAN	40S ribosomal protein S3a	Structural constituent of ribosome.
-0.3888929	sp P54819 KAD2_HUMAN	Adenylate kinase 2, mitochondrial	Catalyzes the reversible transfer of the terminal phosphate group between ATP and AMP. Plays an important role in cellular energy homeostasis and in adenine nucleotide metabolism.
-0.3642355	sp P50454 SERPH_HUMAN	Serpin H1	Binds specifically to collagen. Could be involved as a chaperone in the biosynthetic pathway of collagen.

Fold Change	Protein	Name	Function
-0.3314769	sp P14618 KP YM_HUMAN	Pyruvate kinase PKM	Glycolytic enzyme that catalyzes the transfer of a phosphoryl group from phosphoenolpyruvate (PEP) to ADP, generating ATP.
-0.32553142	sp P02545 LMNA_HUMAN	Prelamin-A/C	Lamins are components of the nuclear lamina, a fibrous layer on the nucleoplasmic side of the inner nuclear membrane, which is thought to provide a framework for the nuclear envelope and may also interact with chromatin.
-0.29833755	sp P12236 ADT3_HUMAN	ADP/ATP translocase 3	ADP: ATP antiporter that mediates import of ADP into the mitochondrial matrix for ATP synthesis, and export of ATP out to fuel the cell.
-0.29114786	sp P39019 RS19_HUMAN	40S ribosomal protein S19	Required for pre-rRNA processing and maturation of 40S ribosomal subunits.
-0.26152506	sp P50991 TCPD_HUMAN	T-complex protein 1 subunit delta	Component of the chaperonin-containing T-complex (TRiC), a molecular chaperone complex that assists the folding of proteins upon ATP hydrolysis.
-0.25640583	sp P00558 PGK1_HUMAN	Phosphoglycerate kinase 1	Catalyzes one of the two ATP producing reactions in the glycolytic pathway via the reversible conversion of 1,3-

Fold Change	Protein	Name	Function
			diphosphoglycerate to 3-phosphoglycerate.
-0.2428719	sp P49368 TCPG_HUMAN	T-complex protein 1 subunit gamma	Component of the chaperonin-containing T-complex (TRiC), a molecular chaperone complex that assists the folding of proteins upon ATP hydrolysis.
-0.23416811	sp P15880 RS2_HUMAN	40S ribosomal protein S2	Structural constituent of ribosome.
-0.23386714	sp P07741 APT_HUMAN	Adenine phosphoribosyltransferase	Catalyzes a salvage reaction resulting in the formation of AMP, that is energetically less costly than de novo synthesis.
-0.22591352	sp Q15233 NONO_HUMAN	Non-POU domain-containing octamer-binding protein	DNA- and RNA binding protein, involved in several nuclear processes.
-0.19289137	sp P49736 MCM2_HUMAN	DNA replication licensing factor MCM2	Acts as component of the MCM2-7 complex (MCM complex) which is the putative replicative helicase essential for 'once per cell cycle' DNA replication initiation and elongation in eukaryotic cells.
-0.17863823	sp P04406 G3P_HUMAN	Glyceraldehyde-3-phosphate dehydrogenase	Has both glyceraldehyde-3-phosphate dehydrogenase and nitrosylase activities, thereby playing a role in glycolysis and nuclear functions, respectively.
More Abundant			
0.3297178	sp P50395 GDIB_HUMAN	Rab GDP dissociation inhibitor beta	Regulates the GDP/GTP exchange reaction of

Fold Change	Protein	Name	Function
			most Rab proteins by inhibiting the dissociation of GDP from them, and the subsequent binding of GTP to them.
0.3308436	sp Q9NPH2 INO1_HUMAN	Inositol-3-phosphate synthase 1	Key enzyme in myo-inositol biosynthesis pathway that catalyzes the conversion of glucose 6-phosphate to 1-myo-inositol 1-phosphate in a NAD-dependent manner.
0.33607486	sp P08133 ANXA6_HUMAN	Annexin A6	May associate with CD21. May regulate the release of Ca ²⁺ from intracellular stores.
0.34007517	sp P33176 KINH_HUMAN	Kinesin-1 heavy chain	Microtubule-dependent motor required for normal distribution of mitochondria and lysosomes.
0.40956342	sp P26639 SYTC_HUMAN	Threonine--tRNA ligase 1, cytoplasmic	Catalyzes the attachment of threonine to tRNA(Thr) in a two-step reaction.
0.5068129	sp P35637 FUS_HUMAN	RNA binding protein FUS	DNA/RNA-binding protein that plays a role in various cellular processes such as transcription regulation, RNA splicing, RNA transport, DNA repair and damage response.
0.62208825	sp Q06203 PUR1_HUMAN	Amidophosphoribosyl-transferase	Involved in a subpathway of IMP biosynthesis via de novo pathway, which is itself part of Purine metabolism.

Fold Change	Protein	Name	Function
0.71757966	sp P30046 DOPD_HUMAN	D-dopachrome decarboxylase	Tautomerization of D-dopachrome with decarboxylation to give 5,6-dihydroxyindole (DHI).
0.7993137	sp Q9P0L0 VAPA_HUMAN	Vesicle-associated membrane protein-associated protein A	May play a role in vesicle trafficking.
1.0460628	sp O15498 YKT6_HUMAN	Synaptobrevin homolog YKT6	Vesicular soluble NSF attachment protein receptor mediating vesicle docking and fusion to a specific acceptor cellular compartment. Functions in endoplasmic reticulum to Golgi transport.
1.2047311	sp O94925 GLSK_HUMAN	Glutaminase kidney isoform, mitochondrial	Catalyzes the first reaction in the primary pathway for the renal catabolism of glutamine. Plays a role in maintaining acid-base homeostasis. Regulates the levels of the neurotransmitter glutamate, the main excitatory neurotransmitter in the brain.
1.2580171	sp P15927 RFA2_HUMAN	Replication protein A 32 kDa subunit	As part of the heterotrimeric replication protein A complex, binds and stabilizes single-stranded DNA intermediates, that form during DNA replication or upon DNA stress.

Fold Change	Protein	Name	Function
1.3545654	sp P43307 SSRA_HUMAN	Translocon-associated protein subunit alpha	TRAP proteins are part of a complex whose function is to bind calcium to the ER membrane and thereby regulate the retention of ER resident proteins. May be involved in the recycling of the translocation apparatus after completion of the translocation process or may function as a membrane-bound chaperone facilitating folding of translocated proteins.
1.3545654	sp Q9BPX5 ARP5L_HUMAN	Actin-related protein 2/3 complex subunit 5-like protein	May function as component of the Arp2/3 complex which is involved in regulation of actin polymerization and together with an activating nucleation-promoting factor (NPF) mediates the formation of branched actin networks.
1.3843683	sp Q12874 SF3A3_HUMAN	Splicing factor 3A subunit 3	Involved in pre-mRNA splicing as a component of the splicing factor SF3A complex.
1.7049654	sp Q9H3P7 GCP60_HUMAN	Golgi resident protein GCP60	Involved in the maintenance of Golgi structure by interacting with giantin, affecting protein transport between the endoplasmic reticulum and Golgi.

Fold Change	Protein	Name	Function
1.9275721	sp Q9UPQ0 LIMC1_HUMAN	LIM and calponin homology domains-containing protein 1	Actin stress fibers-associated protein that activates non-muscle myosin IIa, negatively regulating cell spreading and cell migration.
2.0022073	sp Q92600 CNOT9_HUMAN	CCR4-NOT transcription complex subunit 9	Component of the CCR4-NOT complex which is one of the major cellular mRNA deadenylases and is linked to various cellular processes including bulk mRNA degradation, miRNA-mediated repression, translational repression during translational initiation and general transcription regulation.
2.020335	sp P17096 HMGA1_HUMAN	High mobility group protein HMG-I/HMG-Y	HMG-I/Y bind preferentially to the minor groove of A+T rich regions in double-stranded DNA. It is suggested that these proteins could function in nucleosome phasing and in the 3'-end processing of mRNA transcripts. They are also involved in the transcription regulation of genes containing, or in close proximity to A+T-rich regions.
2.0204513	sp P61011 SRP54_HUMAN	Signal recognition particle 54 kDa protein	Binds to the signal sequence of presecretory protein when they

Fold Change	Protein	Name	Function
			emerge from the ribosomes and transfers them to TRAM (translocating chain-associating membrane protein).
2.0311487	sp Q9Y2B0 CNPY2_HUMAN	Protein canopy homolog 2	Positive regulator of neurite outgrowth by stabilizing myosin regulatory light chain (MRLC).
2.0645323	sp P63172 DYLT1_HUMAN	Dynein light chain Tctex-type 1	Acts as one of several non-catalytic accessory components of the cytoplasmic dynein 1 complex that are thought to be involved in linking dynein to cargos and to adapter proteins that regulate dynein function. Plays a role in neuronal morphogenesis.
2.173147	sp Q12769 NU160_HUMAN	Nuclear pore complex protein Nup160	Functions as a component of the nuclear pore complex (NPC).
2.1889472	sp P49840 GSK3A_HUMAN	Glycogen synthase kinase-3 alpha	Constitutively active protein kinase that acts as a negative regulator in the hormonal control of glucose homeostasis, Wnt signaling and regulation of transcription factors and microtubules.
2.3445802	sp Q15274 NADC_HUMAN	Nicotinate-nucleotide pyrophosphorylase [carboxylating]	Involved in a subpathway that is part of the NAD(+) biosynthesis pathway, which is itself

Fold Change	Protein	Name	Function
			part of Cofactor biosynthesis.
2.3445802	sp Q9H223 EHD4_HUMAN	EH domain-containing protein 4	ATP- and membrane-binding protein that probably controls membrane reorganization/tubulation upon ATP hydrolysis. Plays a role in early endosomal transport.
2.3649187	sp Q9UGV2 NDRG3_HUMAN	Protein NDRG3	Function unclear. May function as a tumour suppressor and may also play important roles in the development of neurological and electrophysiological diseases.
2.3983614	sp Q9HDC9 APMAP_HUMAN	Adipocyte plasma membrane-associated protein	May play a role in adipocyte differentiation.
2.4703662	sp P29762 RABP1_HUMAN	Cellular retinoic acid-binding protein 1	Cytosolic CRABPs may regulate the access of retinoic acid to the nuclear retinoic acid receptors.
2.5580409	sp Q92609 TBCD5_HUMAN	TBC1 domain family member 5	May act as a GTPase-activating protein (GAP) for Rab family protein(s). Required for retrograde transport of cargo proteins from endosomes to the trans-Golgi network (TGN). Involved in regulation of autophagy.

Supplementary Table S7 : List of proteins differentially abundant between mutant transfected and wild-type transfected cells

Fold Change	Protein	Name	Function
Less Abundant			
-2.4344592	sp O95782 AP2A1_HUMAN	AP-2 complex subunit alpha-1	Component of the adaptor protein complex 2 (AP-2). Adaptor protein complexes function in protein transport via transport vesicles in different membrane traffic pathways.
-1.7803267	sp P30876 RPB2_HUMAN	DNA-directed RNA polymerase II subunit RPB2	DNA-dependent RNA polymerase catalyzes the transcription of DNA into RNA using the four ribonucleoside triphosphates as substrates.
-1.5180521	sp P52788 SPSY_HUMAN	Spermine synthase	Catalyzes the production of spermine from spermidine and decarboxylated S-adenosylmethionine (dcSAM).
-1.335764	sp Q9BTY7 HGH1_HUMAN	Protein HGH1 homolog	Chaperone-mediated protein folding
-1.0895904	sp P60763 RAC3_HUMAN	Ras-related C3 botulinum toxin substrate 3	Plasma membrane-associated small GTPase. In its active state binds to a variety of effector proteins to regulate cellular responses, such as cell spreading and the formation of actin-based protrusions including lamellipodia and membrane ruffles.
-1.0788805	sp Q7L1Q6 BZW1_HUMAN	Basic leucine zipper and W2 domain-containing protein 1	Enhances histone H4 gene transcription but does not seem to bind DNA directly.

Fold Change	Protein	Name	Function
-1.0704813	sp O43172 PRP4_HUMAN	U4/U6 small nuclear ribonucleoprotein Prp4	Plays role in pre-mRNA splicing as component of the U4/U6-U5 tri-snRNP complex that is involved in spliceosome assembly, and as component of the precatalytic spliceosome (spliceosome B complex).
-0.79752356	sp Q05193 DYN1_HUMAN	Dynamin-1	Microtubule-associated force-producing protein involved in producing microtubule bundles and able to bind and hydrolyze GTP. Most probably involved in vesicular trafficking processes. Involved in receptor-mediated endocytosis.
-0.62357765	sp P21912 SDHB_HUMAN	Succinate dehydrogenase [ubiquinone] iron-sulfur subunit, mitochondrial	Iron-sulfur protein (IP) subunit of succinate dehydrogenase (SDH) that is involved in complex II of the mitochondrial electron transport chain and is responsible for transferring electrons from succinate to ubiquinone (coenzyme Q).
-0.5995171	sp P36871 PGM1_HUMAN	Phosphoglucomutase-1	This enzyme participates in both the breakdown and synthesis of glucose.
-0.45797586	sp P35659 DEK_HUMAN	Protein DEK	Involved in chromatin organization.
-0.41750172	sp P62873 GBB1_HUMAN	Guanine nucleotide-binding protein G(I)/G(S)/G(T) subunit beta-1	Guanine nucleotide-binding proteins (G proteins) are involved as a modulator or transducer in various transmembrane signaling systems. The beta and gamma

Fold Change	Protein	Name	Function
			chains are required for the GTPase activity, for replacement of GDP by GTP, and for G protein-effector interaction.
-0.34489024	sp P31939 PUR9_HUMAN	Bifunctional purine biosynthesis protein ATIC	Bifunctional enzyme that catalyzes the last two steps of purine biosynthesis.
-0.2783318	sp P11177 ODPB_HUMAN	Pyruvate dehydrogenase E1 component subunit beta, mitochondrial	The pyruvate dehydrogenase complex catalyzes the overall conversion of pyruvate to acetyl-CoA and CO ₂ , and thereby links the glycolytic pathway to the tricarboxylic cycle.
-0.24159154	sp P49368 TCPG_HUMAN	T-complex protein 1 subunit gamma	Component of the chaperonin-containing T-complex (TRiC), a molecular chaperone complex that assists the folding of proteins upon ATP hydrolysis.
-0.13958682	sp Q04837 SSBP_HUMAN	Single-stranded DNA-binding protein, mitochondrial	In vitro, required to maintain the copy number of mitochondrial DNA (mtDNA) and plays crucial roles during mtDNA replication that stimulate activity of the replisome components POLG and TWNK at the replication fork.
More Abundant			
0.29401335	sp P16104 H2AX_HUMAN	Histone H2AX	Variant histone H2A which replaces conventional H2A in a subset of nucleosomes. Histones thereby play a central role in transcription regulation, DNA repair, DNA

Fold Change	Protein	Name	Function
			replication and chromosomal stability.
0.3704586	sp P63220 RS21_HUMAN	40S ribosomal protein S21	Structural constituent of ribosome.
0.38168684	sp P55060 XPO2_HUMAN	Exportin-2	Export receptor for importin-alpha. Mediates importin-alpha re-export from the nucleus to the cytoplasm after import substrates (cargos) have been released into the nucleoplasm.
0.43802047	sp P62140 PP1B_HUMAN	Serine/threonine-protein phosphatase PP1-beta catalytic subunit	Protein phosphatase that associates with over 200 regulatory proteins to form highly specific holoenzymes which dephosphorylate hundreds of biological targets. Protein phosphatase (PP1) is essential for cell division, it participates in the regulation of glycogen metabolism, muscle contractility and protein synthesis. Involved in regulation of ionic conductance and long-term synaptic plasticity.
0.5287636	sp P53999 TCP4_HUMAN	Activated RNA polymerase II transcriptional coactivator p15	General coactivator that functions cooperatively with TAFs and mediates functional interactions between upstream activators and the general transcriptional machinery. May be involved in stabilizing the multiprotein transcription complex.

Fold Change	Protein	Name	Function
0.53964293	sp P38159 RBMX_HUMAN	RNA-binding motif protein, X chromosome	RNA-binding protein that plays several roles in the regulation of pre- and post-transcriptional processes. Implicated in tissue-specific regulation of gene transcription and alternative splicing of several pre-mRNAs.
0.63821447	sp P35637 FUS_HUMAN	RNA-binding protein FUS	DNA/RNA-binding protein that plays a role in various cellular processes such as transcription regulation, RNA splicing, RNA transport, DNA repair and damage response.
0.82862306	sp Q9P0L0 VAPA_HUMAN	Vesicle-associated membrane protein-associated protein A	May play a role in vesicle trafficking.
0.8773641	sp P30046 DOPD_HUMAN	D-dopachrome decarboxylase	Tautomerization of D-dopachrome with decarboxylation to give 5,6-dihydroxyindole (DHI).
0.9104095	sp Q9H814 PHAX_HUMAN	Phosphorylated adapter RNA export protein	A phosphoprotein adapter involved in the XPO1-mediated U snRNA export from the nucleus.
0.9281879	sp Q15637 SF01_HUMAN	Splicing factor 1	Necessary for the ATP-dependent first step of spliceosome assembly.
0.96657825	sp P35527 K1C9_HUMAN	Keratin, type I cytoskeletal 9	Plays a role in keratin filament assembly.
1.0312784	sp Q9H307 PININ_HUMAN	Pinin	Transcriptional activator binding to the E-box 1 core sequence of the E-cadherin promoter gene.
1.2384619	sp P98179 RBM3_HUMAN	RNA-binding protein 3	Cold-inducible mRNA binding protein that enhances

Fold Change	Protein	Name	Function
			global protein synthesis at both physiological and mild hypothermic temperatures.
1.2384619	sp P62851 RS25_HUMAN	40S ribosomal protein S25	Structural constituent of ribosome.
1.3642771	sp P62753 RS6_HUMAN	40S ribosomal protein S6	Component of the 40S small ribosomal subunit.
1.4416274	sp P62917 RL8_HUMAN	60S ribosomal protein L8	Component of the large ribosomal subunit.
1.8834004	sp P51784 UBP11_HUMAN	Ubiquitin carboxyl-terminal hydrolase 11	Protease that can remove conjugated ubiquitin from target proteins and polyubiquitin chains. Inhibits the degradation of target proteins by the proteasome.
2.2395134	sp P07858 CATB_HUMAN	Cathepsin B	Thiol protease which is believed to participate in intracellular degradation and turnover of proteins.
2.3365922	sp Q8ND24 RN214_HUMAN	RING finger protein 214	Involved in protein ubiquitination.
2.888747	sp P17096 HMGA1_HUMAN	High mobility group protein HMG-I/HMG-Y	HMG-I/Y bind preferentially to the minor groove of A+T rich regions in double-stranded DNA. It is suggested that these proteins could function in nucleosome phasing and in the 3'-end processing of mRNA transcripts. They are also involved in the transcription regulation of genes containing, or in close proximity to A+T-rich regions.

Supplementary Table S8 : List of proteins differentially abundant between empty vector transfected and non-transfected cells

Fold Change	Protein	Name	Function
Less Abundant			
-2.650073	sp O14949 QCR8_HUMAN	Cytochrome b-c1 complex subunit 8	Component of the ubiquinol-cytochrome c oxidoreductase, a multisubunit transmembrane complex that is part of the mitochondrial electron transport chain which drives oxidative phosphorylation.
-2.5518029	sp Q10713 MPPA_HUMAN	Mitochondrial-processing peptidase subunit alpha	Substrate recognition and binding subunit of the essential mitochondrial processing protease (MPP), which cleaves the mitochondrial sequence off newly imported precursors proteins.
-1.7825811	sp P24928 RPB1_HUMAN	DNA-directed RNA polymerase II subunit RPB1	DNA-dependent RNA polymerase catalyzes the transcription of DNA into RNA using the four ribonucleoside triphosphates as substrates. Largest and catalytic component of RNA polymerase II which synthesizes mRNA precursors and many functional non-coding RNAs.
-1.4472072	sp Q9C0B1 FTO_HUMAN	Alpha-ketoglutarate-dependent	RNA demethylase that mediates oxidative demethylation of

Fold Change	Protein	Name	Function
		dioxygenase FTO	different RNA species, such as mRNAs, tRNAs and snRNAs, and acts as a regulator of fat mass, adipogenesis and energy homeostasis.
-0.8712561	sp Q15149 PLEC_HUMAN	Plectin	Interlinks intermediate filaments with microtubules and microfilaments and anchors intermediate filaments to desmosomes or hemidesmosomes.
-0.8128491	sp P13861 KAP2_HUMAN	cAMP-dependent protein kinase type II-alpha regulatory subunit	Regulatory subunit of the cAMP-dependent protein kinases involved in cAMP signaling in cells.
-0.5686383	sp P53004 BIEA_HUMAN	Biliverdin reductase A	Reduces the gamma-methene bridge of the open tetrapyrrole, biliverdin IX alpha, to bilirubin with the concomitant oxidation of a NADH or NADPH cofactor.
-0.49464598	sp Q92499 DDX1_HUMAN	ATP-dependent RNA helicase DDX1	Acts as an ATP-dependent RNA helicase, able to unwind both RNA-RNA and RNA-DNA duplexes.
More Abundant			
0.2042159	sp P06733 ENOA_HUMAN	Alpha enolase	Glycolytic enzyme the catalyzes the conversion of 2-phosphoglycerate to phosphoenolpyruvate

Fold Change	Protein	Name	Function
0.48937234	sp P63279 UBC9_HUMAN	SUMO-conjugating enzyme UBC9	Involved in the pathway protein sumoylation, which is part of Protein modification
0.4961204	sp P55010 IF5_HUMAN	Eukaryotic translation initiation factor 5	Catalyzes the hydrolysis of GTP bound to the 40S ribosomal initiation complex with the subsequent joining of a 60S ribosomal subunit.
0.509079	sp Q9BY32 ITPA_HUMAN	Inosine triphosphate pyrophosphatase	Pyrophosphatase that hydrolyzes the non-canonical purine nucleotides to their respective monophosphate derivatives.
0.56471723	sp P30049 ATPD_HUMAN	ATP synthase subunit delta, mitochondrial	Mitochondrial membrane ATP synthase produces ATP from ADP in the presence of a proton gradient across the membrane which is generated by electron transport complexes of the respiratory chain.
0.5949262	sp P61160 ARP2_HUMAN	Actin-related protein 2	ATP-binding component of the Arp2/3 complex, a multiprotein complex that mediates actin polymerization upon stimulation by nucleation-promoting factor (NPF).
0.6654975	sp P68871 HBB_HUMAN	Hemoglobin subunit beta	Involved in oxygen transport from the lung to the various peripheral tissues.

Fold Change	Protein	Name	Function
0.77291125	sp P35250 RFC2_HUMAN	Replication factor C subunit 2	The elongation of primed DNA templates by DNA polymerase delta and epsilon requires the action of the accessory proteins proliferating cell nuclear antigen (PCNA) and activator 1. This subunit binds ATP.
0.9915015	sp P01008 ANT3_HUMAN	Antithrombin-III	Most important serine protease inhibitor in plasma that regulates the blood coagulation cascade.
1.1482236	sp P37840 SYUA_HUMAN	Alpha-synuclein	Neuronal protein that plays several roles in synaptic activity such as regulation of synaptic vesicle trafficking and subsequent neurotransmitter release.
1.4167656	sp O00303 EIF3F_HUMAN	Eukaryotic translation initiation factor 3 subunit F	Component of the eukaryotic translation initiation factor 3 (eIF-3) complex, which is required for several steps in the initiation of protein synthesis.
1.5193136	sp Q15773 MLF2_HUMAN	Myeloid leukemia factor 2	Regulation of transcription.
1.5193136	sp P61086 UBE2K_HUMAN	Ubiquitin-conjugating enzyme E2 K	Accepts ubiquitin from the E1 complex and catalyzes its covalent attachment to other proteins.
1.9315825	sp P29762 RABP1_HUMAN	Cellular retinoic acid-binding protein 1	May regulate the access of retinoic acid to the

Fold Change	Protein	Name	Function
			nuclear retinoic acid receptors.
2.3856065	sp Q92600 CNOT9_HUMAN	CCR4-NOT transcription complex subunit 9	Component of the CCR4-NOT complex which is one of the major cellular mRNA deadenylases and is linked to various cellular processes including bulk mRNA degradation, miRNA-mediated repression, translational repression during translational initiation and general transcription regulation.
2.527652	sp Q16864 VATF_HUMAN	V-type proton ATPase subunit F	Subunit of the peripheral V1 complex of vacuolar ATPase essential for assembly or catalytic function. V-ATPase is responsible for acidifying a variety of intracellular compartments in eukaryotic cells.
2.527652	sp P49753 ACOT2_HUMAN	Acyl-coenzyme A thioesterase 2, mitochondrial	Acyl-CoA thioesterases are a group of enzymes that catalyze the hydrolysis of acyl-CoAs to the free fatty acid and coenzyme A (CoASH), providing the potential to regulate intracellular levels of acyl-CoAs, free fatty acids and CoASH. The enzyme is involved in enhancing the hepatic fatty acid oxidation in mitochondria.

Fold Change	Protein	Name	Function
3.0763242	sp P19525 E2AK2_HUMAN	Interferon-induced, double-stranded RNA-activated protein kinase	IFN-induced dsRNA-dependent serine/threonine-protein kinase that phosphorylates the alpha subunit of eukaryotic translation initiation factor 2 (EIF2S1/eIF-2-alpha) and plays a key role in the innate immune response to viral infection.
3.1480145	sp Q9P013 CWC15_HUMAN	Spliceosome-associated protein CWC15 homolog	Involved in pre-mRNA splicing as component of the spliceosome.
3.4633446	sp Q9H910 JUPI2_HUMAN	Jupiter microtubule associated homolog 2	Nicotinic Acid Adenine Dinucleotide Phosphate (NAADP) binding protein required for NAADP-evoked intracellular calcium release.

Appendix III: American College of Medical Genetics (ACMG) Variant Characterization

	Benign		Pathogenic			
	Strong	Supporting	Supporting	Moderate	Strong	Very Strong
Population Data	MAF is too high for disorder <i>BA1/BS1</i> OR observation in controls inconsistent with disease penetrance <i>BS2</i>			Absent in population databases <i>PM2</i>	Prevalence in affecteds statistically increased over controls <i>PS4</i>	
Computational And Predictive Data		Multiple lines of computational evidence suggest no impact on gene /gene product <i>BP4</i> Missense in gene where only truncating cause disease <i>BP1</i> Silent variant with non predicted splice impact <i>BP7</i>	Multiple lines of computational evidence support a deleterious effect on the gene /gene product <i>PP3</i>	Novel missense change at an amino acid residue where a different pathogenic missense change has been seen before <i>PM5</i> Protein length changing variant <i>PM4</i>	Same amino acid change as an established pathogenic variant <i>PS1</i>	Predicted null variant in a gene where LOF is a known mechanism of disease <i>PVS1</i>
Functional Data	Well-established functional studies show no deleterious effect <i>BS3</i>		Missense in gene with low rate of benign missense variants and path. missenses common <i>PP2</i>	Mutational hot spot or well-studied functional domain without benign variation <i>PM1</i>	Well-established functional studies show a deleterious effect <i>PS3</i>	
Segregation Data	Non-segregation with disease <i>BS4</i>		Co-segregation with disease in multiple affected family members <i>PP1</i>	Increased segregation data →		
De novo Data				<i>De novo</i> (without paternity & maternity confirmed) <i>PM6</i>	<i>De novo</i> (paternity & maternity confirmed) <i>PS2</i>	N/A
Allelic Data		Observed in <i>trans</i> with a dominant variant <i>BP2</i> Observed in <i>cis</i> with a pathogenic variant <i>BP2</i>		For recessive disorders, detected in <i>trans</i> with a pathogenic variant <i>PM3</i>		N/A
Other Database		Reputable source w/out shared data = benign <i>BP6</i>	Reputable source = pathogenic <i>PP5</i>			
Other Data		Found in case with an alternate cause <i>BP5</i>	Patient's phenotype or FH highly specific for gene <i>PP4</i>			N/A

N/A: not applicable

(Richards et al., 2015)

Appendix IV: Ethical Approvals



Approval Letter Progress Report

18/07/2022

Project ID: 7506

Ethics Reference No: 2002C/059

Project Title: Genetic analysis of inherited Parkinson's Disease and other related movement disorders

Dear Prof JA Carr

We refer to your request for an extension/annual renewal of ethics approval dated 28/06/2022 11:33.

The Health Research Ethics Committee reviewed and approved the annual progress report through an expedited review process.

The approval of this project is extended for a further year.

Approval date: 02 July 2022

Expiry date: 01 July 2023

Kindly be reminded to submit progress reports two (2) months before expiry date.

Where to submit any documentation

Kindly note that the HREC uses an electronic ethics review management system, *Infonetica*, to manage ethics applications and ethics review process. To submit any documentation to HREC, please click on the following link: <https://applyethics.sun.ac.za>.

Please remember to use your Project Id 7506 and ethics reference number 2002C/059 on any documents or correspondence with the HREC concerning your research protocol.

Please note that for studies involving the use of questionnaires, the final copy should be uploaded on Infonetica.

Yours sincerely,

Ms Brightness Nxumalo

Coordinator: Health Research Ethics Committee 2 (HREC 2)

National Health Research Ethics Council (NHREC) Registration Number:
REC-130408-012 (HREC1)•REC-230208-010 (HREC2)

Federal Wide Assurance Number: 00001372
Office of Human Research Protections (OHRP) Institutional Review Board (IRB) Number:
IRB0005240 (HREC1)•IRB0005239 (HREC2)

The Health Research Ethics Committee (HREC) complies with the SA National Health Act No. 61 of 2003 as it pertains to health research. The HREC abides by the ethical norms and principles for research, established by the World Medical Association (2013), Declaration of Helsinki; Ethical Principles for Medical Research Involving Human Subjects; the South African Department of Health (2006), Guidelines for Good Practice in the Conduct of Clinical Trials with Human Participants in South Africa (2nd edition); as well as the Department of Health (2015), Ethics in Health Research: Principles, Processes and Structures (2nd edition).

The Health Research Ethics Committee reviews research involving human subjects conducted or supported by the Department of Health and Human Services, or other federal departments or agencies that apply the Federal Policy for the Protection of Human Subjects to such research (United States Code of Federal Regulations Title 45 Part 46); and/or clinical investigations regulated by the Food and Drug Administration (FDA) of the Department of Health and Human Services.



05/01/2022

Project ID: 13196

Ethics Reference No: S20/01/005 PhD

Project Title: Investigation of Neurexin 2 as a Candidate for Parkinson's Disease

Dear Ms K Cuttler

We refer to your request for an extension/annual renewal of ethics approval dated 14/12/2021.

The Health Research Ethics Committee reviewed and approved the annual progress report through an expedited review process.

The approval of this project is extended for a further year.

Approval date: 23 February 2022

Expiry date: 22 February 2023

Kindly be reminded to submit progress reports two (2) months before expiry date.

Where to submit any documentation

Kindly note that the HREC uses an electronic ethics review management system, *Infonetica*, to manage ethics applications and ethics review process. To submit any documentation to HREC, please click on the following link: <https://applyethics.sun.ac.za>.

Please remember to use your Project Id 13196 and ethics reference number S20/01/005 PhD on any documents or correspondence with the HREC concerning your research protocol.

Please note that for studies involving the use of questionnaires, the final copy should be uploaded on Infonetica.

Yours sincerely,

Melody E Shana
Coordinator: Health Research Ethics Committee 1

*National Health Research Ethics Council (NHREC) Registration Number:
REC-130408-012 (HREC1)•REC-230208-010 (HREC2)*

*Federal Wide Assurance Number: 00001372
Office of Human Research Protections (OHRP) Institutional Review Board (IRB) Number:
IRB0005240 (HREC1)•IRB0005239 (HREC2)*

The Health Research Ethics Committee (HREC) complies with the SA National Health Act No. 61 of 2003 as it pertains to health research. The HREC abides by the ethical norms and principles for research, established by the [World Medical Association \(2013\)](#), [Declaration of Helsinki: Ethical Principles for Medical Research Involving Human Subjects](#); the [South African Department of Health \(2006\)](#), [Guidelines for Good Practice in the Conduct of Clinical Trials with Human Participants in South Africa \(2nd edition\)](#); as well as the [Department of Health \(2015\)](#), [Ethics in Health Research: Principles, Processes and Structures \(2nd edition\)](#).

The Health Research Ethics Committee reviews research involving human subjects conducted or supported by the Department of Health and Human Services, or other federal departments or agencies that apply the Federal Policy for the Protection of Human Subjects to such research (United States Code of Federal Regulations Title 45 Part 46); and/or clinical investigations regulated by the Food and Drug Administration (FDA) of the Department of Health and Human Services.



REC: Biological and Environmental Safety (Annual Progress Report)

Feedback Letter: *Approved*

22 November 2021

PI: Ms K Cuttler

REC: BES Reference #: BEE-2021-13149

Title: Investigation of Neurexin 2 as a Candidate for Parkinson's Disease

Dear Ms K Cuttler

Your response to stipulations, with BEE-2021-13149 was reviewed by the Research Ethics Committee: Biological and Environmental Safety (**REC: BES**) via committee review procedures and was approved. Please note that this clearance is only valid for a period of twelve months. Ethics clearance of protocols spanning more than one year must be renewed annually through submission of a progress report, up to a maximum of three years.

Approval Date: **22 November 2021 - 21 November 2022**

Please remember to use your REC: BES reference number: # BEE-2021-13149 on any documents or correspondence with the REC: BES concerning your research protocol.

If you have any questions or need further help, please contact the REC: BES office at 021 808 9003.

Visit the Division for Research Developments website www.sun.ac.za/research for documentation on REC: BES policy and procedures.

Sincerely,

Mr. Winston Beukes Coordinator: Research Ethics (Biosafety)

E: applyethics@sun.ac.za (Ethics Help-Desk)